INTERNATIONAL WORKSHOP ON VOLCANISM & VOLCANIC HAZARDS IN IMMATURE INTRAPLATE OCEANIC ISLANDS

LA PALMA, 15-18 SEPTEMBER, 1997

PROGRAMME AND ABSTRACTS

PUERTO NAOS, LA PALMA
CANARY ISLANDS, SPAIN, 1997

INTERNATIONAL WORKSHOP

September 15-18

VOLCANISM AND VOLCANIC HAZARDS IN IMMATURE INTRAPLATE OCEANIC ISLANDS

PROGRAMME AND ABSTRACTS

PREFACE

We welcome you sincerely on behalf of the Consejo Superior de Investigaciones Científicas (Spain), the Volcanic Studies group of the Geological Society of London (UK), the CEA-CNRS (France), the University of Las Palmas de Gran Canaria (Spain) and the Consejería de Política Territorial of the Canarian Government.

The general subject of the workshop will be volcanism and volcanic hazards in immature intraplate oceanic islands. The scientific programme will emphasise the different aspects of the growth, evolution and mass-wasting destructive processes in this specific type of islands, as well as their effects on the environment.

This scientific programme will include oral sessions, with some extended keynote talks. A poster presentation with a brief oral introduction will be held at the end of each day's sessions.

We would like to express our sincere gratitude to the Cabildo de La Palma and Cabildo de El Hierro for their interest and support.

Organising Committee

Edited: Consejo Superior de Investigaciones Científicas (Estación Volcanológica de Canarias) and Depto. de Física-Geología (Universidad de Las Palmas de Gran Canaria)

CSIC
CONSEJO SUPERIOR
DE INVESTIGACIONES CIENTIFICAS
(Estación Volcanológica de Canarias)

DEPARTAMENTO DE FISICA
Universidad de Las Palmas de Gran Canaria

PROGRAMME

PROGRAMME

MONDAY, SEPTEMBER 15TH

9.30 Registration and coffee
10.10 Introductory remarks

Session A-1: Geochronology

Chair: José Antonio Canas, Instituto Geográfico Nacional, Spain.

10.30 Keynote talk: Growth and destruction of Gran Canaria: Evidence from land studies, bathymetry, offshore seismic studies and drilling during ODP Leg 157.
Hans-Ulrich Schmincke, GEOMAR, Kiel, Germany.

11.30 Unspiked K-Ar dating of recent volcanic rocks from El Hierro and La Palma.
Hervé Guillou, Juan Carlos Carracedo and Simon Day.

12.00 Cosmic rays exposure dating in the Canary Islands.
Paul Harrop and Grenville Turner.

12.30 A palaeomagnetic study of the El Golfo collapse scarp section, El Hierro, Canary Islands: Volcanological and tectonic implications.
Nadia Szeremeta, Carlo Laj, Hervé Guillou, Katherine Kissel, Sylvain Houard and Juan Carlos Carracedo.

13.00 Dating pyroclastics by thermoluminescence
Manfred Frechen and Ulrich Schweitzer.

Session A-2: Geochemistry & magmatic plumbing

Chair: Chris Stillman, Trinity College, Dublin.

14.30 Keynote talk: Seamounts in the western Pacific: Lessons in the construction and erosion of oceanic intraplate volcanoes.
Hubert Staudigel, IGPP-UCSD, La Jolla CA, USA

15.30 Petrology, geochemistry and geochronology of Maupiti Island, (Society Archipelago). French Polynesia.
Silvain Blais, Gérard Guille, Hervé Guillou and René Maury.

16.00 Magmatic underplating and crustal magma accumulation beneath the Canary Island Archipelago, as evidenced by fluid inclusions.
Thor Hansteen, Andreas Klügel and Hans-Ulrich Schmincke.

16.30 Rates of magma ascent and depths of magma reservoirs beneath La Palma (Canary Islands).
Andreas Klügel, Thor Hansteen, Hans - Ulrich Schmincke and Peter Sachs.

17.00 Products of the 1993 submarine eruption off Socorro Island, Mexico.
Claus Siebe and Jean Christophe Komorowski.

17.30 Poster presentations

(brief oral introductions for posters in sessions A-1 and A-2):

1. Biologically Mediated Alteration of Volcanic Ash in Seawater: Litho- bio- and hydrosphere interaction.
   Hubert Staudigel, E,. Verdurmen, R.A. Chanstain and A. Yayanos

2. How to establish a Geochemical Earth Reference.
   Hubert Staudigel, Francis Albarede, Henry Shaw and William M. White.

3. The boron isotope geochemistry of ocean island basalts from sites of active intraplate volcanism on the Pitcairn and Society hotspots, South - Central Pacific
   Susanne Barth, Marc Chaussidon and Colin Devey.

4. Petrological and geochemical studies of individual eruptions on La Palma: the importance of detailed mapping and stratigraphic control in petrogenetic studies: Simon Day, Phil Gravestock and Juan Carlos Carracedo.

5. Peridotite xenoliths, olivine - pyroxene megacrysts and cumulates of the Bandama volcanic complex (Gran Canaria, Canary Islands): genesis in the oceanic lithosphere: Jose Mangas, Roberto Clocchiatti, Francisco José Pérez Torrado and D. Massare.

6. Alkali basalt - trachyte association from Raiatea island (Society archipelago, French Polynesia): Silvain Blais, Gérard Guille, René Maury, Hervé Guillou and Catherine Chauvel.

7. Geochronological, structural and morphological constraints on the genesis and evolution of the Canary Islands.
   Juan Carlos Carracedo, Simon Day, Hervé Guillou, Eduardo Rodríguez Badiola, José Antonio Canas and Francisco José Pérez Torrado.

8. The feeding system of the historical eruptions in Tenerife: Maria Carmen Solana, Chris Kilburn and Alfredo Aparicio.

9. Resediment syn-eruptive macroglobular basaltic peperites: lithofacies, textural characteristics and possible significance in immature intraplate oceanic islands:
   Domingo Jimeno and Cristina Segura

18.15 - 19.30 Poster and discussion board session.

Tuesday 16th September.
Session B-1: Volcano structure, instability and lateral collapses 1.

Chair: Herve Guillou, Centre des Faibles Radioactivitès, CEA-CNRS.

9.30 Keynote talk: Rift zones and dyke swarms
George Walker, Cheltenham & Gloucester College of Higher Education, U.K.

10.30 The episodic growth and partial destruction of pre - shield-lava Fuerteventura.
Chris Stillman.

11.00 Eruptive chronology and paleomagnetism of the Taburiente volcano, La Palma.
Jan Wijbrans, Lisa Tauxe and Hubert Staudigel .

11.30 Late (Quaternary) shield-stage volcanism in La Palma and El Hierro, Canary Islands.
Juan Carlos Carracedo, Simon Day and Hervé Guillou.

12.00 - 12.30 Coffee

12.30 Growth and destruction by lateral collapse of the Roque Nublo oceanic island stratovolcano, Gran Canaria, Canary Islands.
Francisco José Pérez Torrado, Simon Day and Juan Carlos Carracedo.

13.00 Intrusion of the Miocene cone sheet dike swarm of Gran Canaria (Canary Islands): a case study of subvolcanic intrusive growth of an oceanic island.
Carsten Schirnick, Paul van den Bogaard and Hans - Ulrich Schmincke.

Session B-2: Volcano structure, instability and lateral collapses 2.

Chair: Bill McGuire, Greig Fester Centre for Hazard Research, University College London.

14.30 Macroscopic, microscopic and magnetic flow indicators in dykes, with implications for velocity and strain profiles.
Gidon Baer.

15.00 Deformation associated with dike emplacement in sedimentary, plutonic and volcanic rocks.
Ram Weinberger.

15.30-16.00: Tea.

16.00 Keynote talk: Growth and collapse of Hawaiian volcanoes
Robin Holcomb, U.S. Geological Survey, Seattle.

17.00 Poster presentations

(brief oral introductions for posters in sessions B-1 to B-3)

1. The constructive and destructive first stages of the Canadas edifice (Tenerife, Canary Islands): Eumenio Ancochea, María José Huertas, Juan Coello, JoséMaría Fúster, Jean Marie Cantagrel and Elisa Ibarrola.

2. Island uplift and tilting generated by isostatic rebound after giant landslides.
John Smith and Paul Wessel.

3. Fault rocks, gouge breccia intrusions and groundwater in oceanic island volcanoes. Simon Day.

4. Revision of the site and the eruptive history of the 1677 eruption of La Palma: geological and archaeological evidence: Juan Carlos Carracedo, Simon Day, Hervé Guillou, Eduardo Rodríguez Badiola and Felipe Jorge Pais Pais.

5. 222Rn flux at Cañadas caldera, Tenerife (Canary Islands): Maria Candelaria Martin and Vicente Soler.

17.30 - 19.00 Poster and discussion board session.

Wednesday 17th September.

Session B-3: Volcano structure, instability and lateral collapses 3.

Chair: John Smith, SOEST, University of Hawaii, USA.

9.30 **Keynote Talk: Is Palaeomagnetism ☐ useful, ☐ useless, ☐ irritating (*) in volcanological studies?**
(*) please check one

Hervé Guillou, John Sinton and Juan Carlos Carracedo and Carlo Laj
Centre des Faibles Radioactivitès, CEA/CNRS, Gif-sur-Yvette , France

10.30 Growth, collapse and subsidence of Wailau Volcano, East Molokai, Hawaii.
Robin Holcomb, Bruce Nelson and Juan Carlos Carracedo.

11.00 A palaeomagnetic study of movement in the Hilina fault system, south flank of Kilauea volcano, Hawaii.
Colleen Riley, Jim Diehl and Bill Rose.

11.30 - 12.00 Coffee

12.00 Recognising incipient instability and lateral collapse precursors in steep - sided oceanic island volcanoes.
Simon Day, Juan Carlos Carracedo, Hervé Guillou, Francisco José Pérez Torrado, Joao Fonseca, Sandra Heleno da Silva and Phil Gravestock.

12.30 An evaluation of flank instability triggered by laterally and vertically propagating intrusions.
Derek Elsworth and Simon Day.

Session C-1: Oceanic island volcanoes & offshore sedimentary sequences.

Chair: Hubert Staudigel, Scripps Inst. Oceanography, UCSD-IGPP, La Jolla CA, USA

14.30 **Keynote talk: The history of debris avalanches, debris flows and turbidites in the Canary basin: a remote record of the evolution of the Canary Islands.**
Phil Weaver and Douglas Masson, Southampton Oceanography Centre, Southampton, U.K.

15.30 Volcano instability on the submarine south flank of Kilauea, Hawaii..
John Smith, Alexander Malahoff and Alexander Shor.

16.00 Landsliding on the Canary Islands: the missing submarine sediment record.
Miguel Canals, Barbara Alibés, Roger Urgeles and Belen Alonso.

16.30. Drilling the clastic apron of Gran Canaria (ODP Leg 157): Submarine transportation and deposition of "Syn-ignimbrite" tephra sediment flows resulting from sea-bound hot ash flows: Maria Sumita and Hans -Ulrich Schmincke.

17.00 Introductions to poster presentations, sessions C-1 and D-1.

1. Stratigraphic constraints on the timing and emplacement of the Alika giant Hawaiian submarine landslide: Gary McMurtry, Emilio Herrero - Bervera, J. Resig, M.Cremer, John Smith, C. Sherman and M.E. Torresan.

2. The Canary Debris Flow: source area morphology and failure mechanisms.
Doug Masson and Phil Weaver.

3. Debris avalanche deposits on the submarine flanks of the Canary Islands.
Doug Masson, Phil Weaver and Tony Watts.

4. The El Golfo Debris Avalanche, Canary Deris Flow and b turbidite – the result of a single slope failure west of the Canary Islands.
Doug Masson and Phil Weaver.

5. Genesis of the Roque Nublo ignimbrites, Gran Canaria, Canary Islands.
Francisco José Pérez Torrado, Joan Martí, Simon Day and José Mangas.

6. A possible tsunami deposit on Fuerteventura, Canary Iskands.
Simon Day and Juan Carlos Carracedo.

7. Civil protection in the face of volcanic crises in Spain.
José Sansón Cerrato.

17.30 – 19.00 Poster and discussion board session.

Thursday 18th September.

Session D-1: Hazards and volcano surveillance.

Chair: Robin Holcomb, U.S. Geological Survey, Seattle WA, USA

9.30 Geophysical monitoring of the Fogo Volcano, Cape Verde Islands.
Joao Fonseca, Sandra Heleno da Silva, Antonio Berberan, Inocencio Barros and Manuela Ramos.

10.00 Volcano-tectonic interpretation of the seismicity associated with the 1995 eruption on Fogo, Cape Verde Islands.
Sandra Heleno da Silva, Joao Fonseca and Simon Day.

10.30 Time and spatial clustering properties of the Etna Region seismicity during 1981-1991.
Valerio De Rubeis, Patrizia Tosi, Alessandro Zenari, Maria Serafina Barbaro and Sergio Vinciguerra.

11.00 Establishing baseline ground deformation studies in La Palma, Canary Islands, using GPS.
Jane Moss.

11.30 Coffee

12.00 The 1990-95 eruption of Unzen volcano, Japan, and its products.
Yasuo Miyabuchi and Akira Shimizu.

12.30 Intrinsic and scattering seismic wave attenuation in the Canary Islands.
José Antonio Canas, Arantxa Ugalde, Luis Pujades, Juan Carlos Carracedo, Vicente Soler and María José Blanco.

13.00 Keynote talk:Monitoring flank instabilities at active volcanoes.
Bill McGuire and Jane Moss, Greig Fester Centre for Hazard Research, University College London, U.K..

14:00 Closing remarks

16.00 Practical demonstration of geodetic deformation monitoring methods.

21.00 Farewell dinner offered by the Cabildo of La Palma

ABSTRACTS

Growth and destruction of Gran Canaria: Evidence from land studies, bathymetry, offshore seismic studies and drilling during ODP Leg 157

Hans-Ulrich Schmincke*, Mari Sumita* and Thomas Funck**
**Abteilung Vulkanologie und Petrologie, GEOMAR, Wischhofstr.1*
D-24148 Kiel, Germany. e-mail: hschmincke@geomar.de
***Department of Oceanography, Dalhousie University*
Nova Scotia, Canada

Introduction and summary

We present a summary of constructive and destructive processes during the evolution of Gran Canaria and adjacent islands based on land and marine data. Intrusive activity far outweighs extrusive activity in the formation of the voluminuous islands and may be the major process in causing vertical uplift. Volcanic material is supplied to the large sedimentary aprons peripheral to the islands chiefly during periods of explosive volcanic activity, especially entry of ash flows into the sea and flank collapses. Sector collapses of the islands and the resulting slumps, debris avalanches and debris flows are not confined to the basaltic shield stage because of the construction of large composite volcanoes with a significant percentage of evolved lavas, clastics and domes. Sector slumping of the submarine sedimentary aprons is common. The submarine morphology is further modified by growth of volcanoes on the submarine flanks of the islands. Subaerial and submarine erosion are more pronounced on the windward sides.

ODP Leg 157 (1994)

The ages, types and compositions of volcaniclastic sediments, physical properties and downhole logs obtain during Ocean Drilling Program (ODP) Leg 157 at Sites 953 (68 km northeast of Gran Canaria) and 954 (34 km mortheast GC) north and 955 (56 km southeast GC) and 956 (45 km southwest GC) south of Gran Canaria with a cumulative penetration of almost 3000 m and an overall recovery rate of 75 %, correlate well compositionally and stratigraphically to major volcanic and non-voclanic phases on the island (Fig.1). The growth and destruction of the island is characterized by three major periods of volcanic activity separated by erosional intervals.

Shield stage of Gran Canaria

The highest rate of volcaniclastic sedimentation (>150 m/m.y.) corresponds to the mid-Miocene basaltic late seamount stage of Gran Canaria, the lowermost deposits drilled being thick, graded hyaloclastite tuffs and debris flows, dominated by poorly vesiculated altered sideromelane clasts, suggesting eruption at water depth of more than 500 m. Almost 500 m of basaltic hyaloclastite tuffs, hyaloclastite lapillistones and lithic breccias were drilled at Holes 953C, 954B and 956B.

The vertical and lateral growth and changes in eruptive activity of the shield volcano is well reflected in the lithological and compositional contrasts within and between the sections drilled at Hole953C and Hole956B. These deposits represent mostly moderate to shallow water (<<ca. 500 m) eruptions, transition to the emergence and the fully subaerial island stage. Most of the basaltic volcaniclastic deposits are interpreted to have been deposited as debris flows resulting from destabilization of hyaloclastites generated during voluminous moderate (< 500 m?) to shallow water explosive volcanic activity and temporarily accumulated prior to episodic failure and transfer to the deep basins, fragmentation of subaerial lava flows that entered the sea and collapse of lava deltas and by flank collapse. About 16 debris flow units in Hole 953C range in thickness from ca. 1 to 50 m. Most are composed of well-sorted massive lapillistone to coarse hyaloclastite tuff. the top 5 to 10 % or so show laminar bedding to minor cross-bedding. Several types of coarse breccias at Hole 953C consist of basalt clasts of diverse composition, angularity and vesicularity and some contain pillow rind fragments. Only the upper of 3 debrites at Site 956 and underlying turbidites consist dominantly of highly vesicular formerly glassy ash to lapilli-sized clasts.

Breccias, lapillistones and tuffs containing increasingly vesicular shards, record the transition from shallow submarine to emergent. The erosion of the older subaerial shield basalts in eastern Gran Canaria is reflected in hundreds of thin fine-grained turbidites at Site 953 while submarine activity contained in the southwest (Site 956). These very thin turbidite beds, 1-40 cm thick, deposited prior to the first ignimbrite-related ash deposit at Hole 953C, are composed of variable amounts of dominantly silt- to sand sized tachylitic and lesser amounts of vesicular to blocky altered shards and are interpreted to represent chiefly erosionally fragmented scoria cones and lava flows. The upper 20 m of the basaltic shield sequence at Hole 956B are considered to record the youngest basaltic shield volcano activity in western Gran Canaria while largely epidastic material was supplied to Hole 953C in the northeast indicating migration of shield volcano activity on Gran Canaria from east to west.

Flank collapse during the shield stage

A lithic-rich debris flow deposit (Site 956), at least 80 m thick, overlain by 2 m of amphibole, phlogopite, apaptite and Cr-spinel-rich sandstones is interpreted to have been generated by major collapse of southwestern Gran Canaria prior to eruption of the Horgazales basalts, thereby triggering tsunami wavers dislocating beach sands on La Gomera or Fuerteventura, where older syenites and mafic plutonic rocks may have been exposed at this time, and transported them with the retreating wave to the basin between the islands. Two major sector collapses along the west coast, and one along the northern coast, inferred from the coastal morphology, are believed to have formed at the end of the shield-building phase. One is synchronous with the formation of the 20 km diameter Miocene Tejeda Caldera. High volcaniclastic and biogenic sedimentation rates around Gran Canaria (>50 m/Ma) tend to cover and bury major landslide blocks, however. We tentatively interpret the slope break at a depth of 600 m as the transition between subaerial and subaqueous chilled lavas at the end of the shield-building phase. The subsidence caused by the volcanic load (30,000 km^3) on the lithosphere may thus amount to no more than 600 m.

Subaerial felsic activity

A precisely dated (13.9 Ma) rhyolitic to basaltic syn-ignimbrite turbidite separates the basal hyaloclastites at 3 Sites from 50-100 m. thick, dominantly rhyolitic volcaniclastic turbidites correlated to the Mogan Group (14-13.3 Ma) and 130 to 250-m-thick, dominantly trachyphonolitic volcaniclastic turbidites correlated to the Fataga Group (13.3-9.5 Ma). Near-unique mineral phases or assemblages, glass, feldspar, amphibole and clinopyroxene and bulk rock compositions represent robust criteria for unequivocally correlating at least 7 synignimbrite volcaniclastic turbidites between three sites, which are 160 km (Sites 953 and 956) and 170 km (Sites 953 and 955) apart from each other (see abstract Sumita & Schmincke). Broad concentric deposition of turbidites composed of granulated ignimbrites south of the island contrasts with the more channelized submarine sediment transport off northeastern Gran Canaria. Tholeiitic to alkali basaltic, blocky, fresh sideromelane shards in many volcaniclastic turbidites are interpreted to represent the parent magmas to the rhyolites and phonolites which were erupted on the lower submarine flanks below the level of the low density magma column synchronously with the subaerial eruption of highly evolved ignimbrites.

The major volcanic gap

At all four sites, the accumulation rate based on intergrated bio-and magnetostratigraphy is at a minimum (ca. 20 m/m.y.) during the major nonvolcanic phase on Gran Canaria between ca. 9 and 5 Ma, indicating that the rate of supply of volcanogenic sediment to the apron closely corresponds in time to major volcanic phases, particularly to shallow submarine and subaerial pyroclastic activity. Several canyons on the island can be traced down the submarine flanks to a depth 3.5 km, indicating that at least deeper portions below the level of subsidence were eroded by mass flows continuing seaward from the subaerial canyons. Erosion differed significantly throughout the entire 16 million year history of the island between the wind-exposed, more strongly erupted northern versus the dry, leeward southern side of the island and this is reflected in the higher abundance of epiclastic sediments in Site 953. Offshore south to southeastern Gran Canaria, several canyons have fed a major sediment fan.

The Roque Nublo debris avalanches and debris flows

Two or 3 major debris flow avalanche events occurred during the late Fataga volcanic phase and are also reflected in the flank deposits drilled. Major debris avalanches generated by collapse of the Pliocene Roque Nublo skatocone are known to have entered the sea in northwestern, northeastern and southern Gran Canaria based on land outcrops. They are represented by coarse breccias in sites 953, 954 and 956 and by the major seismic reflector in the sedimentary apron around the island suggesting that the land volume must at least be doubled. Moreover, a 9.5-km wide volcaniclastic mound in the southern apron is interpreted to represent deposits of the Roque Nublo debris avalanche.

How stable are the Canary Islands?

Our land and marine data show that Gran Canaria has been remarkable stable with respect to sea level since about 14 Ma. Nearly horizontal seismic reflectors whose Late Miocene to Recent age has been verified by drilling north of Gran Canaria can be traced to northern Tenerife. This and other lines of evidence are incompatible with the model proposed by Watts and Masson (1995) that Tenerife has subsided by at least 2500 m since its formation as based on the interpretation of the morphology of submarine canyons to have formed originally subaerially. We think that formation of submarine canyons by sediment mass flows is common around the Canary Islands. Other factors that influence the submarine morphology are flank collapses generating major debris avalanches and debris flows such as north and south of Tenerife and late Pleistocene offshore volcanic activity such as north of the Teno Massif and on the southern flank of Tenerife and northeastern flank of Gran Canaria.

Unspiked K-Ar dating of Recent volcanic rocks from El Hierro and La Palma

H Guillou[1], JC Carracedo[2] and S Day[3]

[1]Centre des Faibles Radioactivit'es, CEA-CNRS, Gif-sur-Yvette, France; [2]Estación Volcanológica de Canarias, CSIC, La Laguna, Tenerife, Canary Islands, Spain; [3]Cheltenham and Gloucester College of Higher Education, Cheltenham, U.K.

1. Introduction

Volcanic islands are formed by a competition between constructive and destructive processes, which can be highly episodic. The precise reconstruction of the volcanic history of El Hierro and La Palma may be a key factor in the understanding of the origin and development of structural features common to Canarian and other volcanic islands such as three armed rift structures and giant gravitational collapses (Carracedo, 1994). Such a reconstruction involved a multi-disciplinary approach. In this study we present results of the combined use of magnetostratigraphy and high-resolution, highly-accurate radiometric dating.

To date rocks as young as those in the western Canaries (<< 1 ma), one must avoid the effects of mantle-derived (excess) ^{40}Ar and be able to detect and analyse very small amounts (<<1%) of radiogenic ^{40}Argon ($^{40}Ar^{*}$). The ^{40}Ar-^{39}Ar incremental heating method has been successfully applied to date low K content, young basalts (300-850 ka) from the East Pacific Rise (Duncan and Hogan, 1994). An alternative method of conventional K-Ar dating (the unspiked method of Cassignol et al., 1978) has proven successful in dating very young subaerial, K-rich volcanic rocks, some as young as <10 ka (Gillot and Cornette, 1986), but also recent tholeiitic subaerial rocks from Kilauea (Guillou et al, 1997a) as well as recent submarine rocks from the Loihi seamount (Guillou et al, 1997b).

We have utilised the unspiked technique to date some young to very young volcanic rocks of La Palma and El Hierro.

2. Selection of the geochronometers and analytical procedure

Samples from El Hierro.- Eighteen samples from El Hierro were selected for K-Ar age determinations on the basis of their positions in a well - defined magnetostratigraphy (Guillou et al. 1996). The rocks have been collected almost entirely in the north-eastern part of the island, where four different magnetozones have been identified and mapped. When possible, samples were collected in stratigraphic order in continuous sections, in boreholes and in the El Golfo collapse escarpment. This enabled us to verify the geological significance of the results obtained and also the accuracy of the dating technique, particularly in the youngest parts of the studied sequences.

Samples From La Palma:

Samples from La Palma were collected from two of the youngest large volcanoes that together form the southern part of the island. These samples represent the later stages of the evolution of the island. One set was collected in continuous sections in the collapse scarp of the Cumbre Nueva volcano, as in El Hierro: a particular objective of this work was to define the age of the Cumbre Nueva giant lateral collapse. The other set was collected using the results of the highly detailed mapping of the active Cumbre Vieja volcano in the south of the island (Carracedo et al., this volume) to establish stratigraphic constraints on the relative ages of the samples and in relation to the sea - level changes used by these authors to subdivide the polygenetic Cumbre Vieja volcano. We have produced radiometric ages from rocks of the cliff - forming series and of the younger scree and platform - forming series, whose development is related to these sea - level changes. This approach allowed sampling to take place across the entire extent of the Cumbre Vieja volcano. A particular objective of the mapping and radiometric dating work has been to define the ages of the different structural elements of the volcano, especially the reconfiguration of the volcanic rift zones in response to the development of volcano flank instability (Day et al., this volume).

Dating technique.- Only rocks without visible traces of alteration were selected for analysis.. Both K and Ar measurements were performed on the microcrystalline groundmass which is considered to be representative of the phase that has crystallised during the solidification of the lavas. Phenocrysts and xenocrysts, which may carry excess 40Ar, were removed using heavy liquids of appropriate densities, and magnetic separations. Potassium was analysed by atomic absorption and flame emission spectrophotometry. The isotopic composition of Ar and Ar content were determined using an unspiked K-Ar technique (Cassignol et al, 1978).

3. Results and Discussion

El Hierro.- Magnetic stratigraphy and mapping show the presence of four consecutive magnetozones (R1, N1, R2, N2), all of which were sampled. The oldest age, 1.12±0.02 Ma, comes from the steeply-dipping lavas of the El Tiñor volcanic edifice (R1 magnetozone) near Puerto de La Estaca. A similar age of 1.11± 0.01 Ma was obtained for the same formation 2.5 km to the south west (Barranco del Balo). The youngest emission vents of the El Tiñor volcanic edifice (R1 magnetozone), the Ventejis volcanic group, gave two ages of 1.05±0.02 and 1.04±0.02 Ma. The subhorizontal lavas of the San Andres plateau, corresponding to N1 magnetozone, yield an age of 1.04±0.01 Ma. The late xenolith-rich lavas from the El Tiñor edifice (R2 magnetozone) emission gave the youngest age: 882 ±13 ka. Magnetic polarity profiles carried out in the 1100 m vertical escarpment of El Golfo (N2 magnetozone) yielded only normal polarities and corrrespond to sample age from 545 ±11 ka to 176±3 ka.The sample ages are completely consistent with their stratigraphic positions. The ages of lavas from the presently - active triple rift system range from 158±4 ka to 11±7 ka.

Two independently calibrated polarity time scales are available. The first one (GPTS) is calibrated using conventional radiometric datings (K-Ar and 40Ar-39Ar methods). The second one is astronomically calibrated (APTS) using solar insolation periodicities observed in seawater O-isotopic curve (Shackletone et al, 1990; Hilgen 1991). In our results, all the recent lavas corresponding to the rift volcanism and to the El Golfo volcanic edifice are normal polarity and ranges in age from 15 ± 2 ka to 545 ka. Whatever the considered time scale, APTS or GPTS, this time period is a normal polarity period (the Brunhes normal chron), except for some very short excursions, such as the "Laschamp" or the "Blake" events that have not been detected.

The youngest dated lava which is related to the Ventejis eruptive centre, is 884 ± 13 ka, and has a reverse polarity. The second one, which is 1.04 ± 0.01 Ma has a normal polarity. These ages restrict the upper Jaramillo boundary in agreement with the aforementioned time scales.

The four oldest samples, with ages ranging from 1.04 ± 0.02 Ma to 1.12 ± 0.02 Ma show reverse polarities. These ages, very close to lower Jaramillo boundary, are consistent only with the APTS ; they lessen the duration of the Jaramillo subchron proposed by Izett and co-workers (1994) who extended this event to 1.11 Ma. The paleomagnetic and radiometric results obtained here constrain the lower limit of the Jaramillo event to an age of 1.04 ± 0.02 Ma, which is slightly younger than the APTS age (1.07).]

La Palma .- Samples from the Cumbre Nueva edifice range in age from 770 ± 3 to 566 ± 5. Their ages are again entirely consistent with their stratigraphic order. The samples straddle the Brunhes - Matuyama limit, which forms a useful magnetostratigraphic marker within this volcano. The youngest age of the sequence (566 ± 5) constrains the time of occurrence of the lateral collapse which destroyed the south-western flank of this volcano.

Dated lavas from the younger, historically active Cumbre Vieja volcano yield ages from 125 ka to 4 ka. The stratigraphic units (cliff- forming and platform - forming lavas) defined using the coastal morphology and inferred to be related to sea - level changes during the last glacial maximum (Carracedo et al. this volume) are shown by this to be of chronostratigraphic significance. The bulk of the cliff - forming series was formed in a period of very rapid growth between about 125 ka and 80 ka. This was the period of most intense subaerial activity in the history of the Cumbre Vieja volcano. The rest of the cliff-forming series was emplaced in a longer period (80 - 20 ka) of less intense activity. All of the platform-forming lavas are less than about 20 ka old. Those erupted from the NW and NE rift zones are between about 10 and 20 ka old, and these zones now appear to be extinct. All the rocks younger than about 10 ka have been erupted either from the N-S trending rift zone or from east - west trending fissures on the western slope of the island. The precise K-Ar dating described here has been of great importance in defining the time of onset of instability of the western flank of the Cumbre Vieja (Day et al., this volume).

References

Carracedo J. C. 1994. The Canary Islands: An example of structural control on the growth of large oceanic-island volcanoes. J. Volcanol. Geotherm. Res., 60, 3-4: 225-241.

Carracedo, J.C., Day, S., Guillou, H., Rodríguez Badiola, E., Canas, J.A. and Pérez Torrado, F. J., Geochronological, structural and morphological constraints in the genesis and evolution of the Canary Islands (this volume).

Cassignol, C., Cornette, Y., David, B. and Gillot, P.Y., 1978. Technologie K-Ar. CEN, Saclay. Rapp. CEA R-4802, 37 pp.

Day, S.J., Carracedo, J.C., Guillou, H., Pérez Torrado, F.J., Fonseca, J.F.B.D., Heleno da Silva, S.I.N. and Gravestock, P., Recognising incipient instability and lateral collapse precursors in steep-sided oceanic island colcanoes (this volume, b).

Duncan, R.A. and Hogan, L.G., 1994. Radiometric dating of young MORB using the 40Ar-39Ar incremental heating method. Geophys. Res. Lett., 18: 1927-1930.

Gillot, P.Y. and Y. Cornette, 1986. The Cassignol technique for K-Ar dating, precision and accuracy: examples from the late Pleistocene to recent volcanics from southern Italy. Chem. Geology, 59: 205-222.

Guillou H, Turpin L., Garnier F., Charbit S., and Thomas D.M. -Unspiked K-Ar dating of Pleistocene tholeiitic basalts from the deep core SOH4, Kilauea, Hawaii. Chemical Geology, in press.

Guillou H., Garcia M.O. and Turpin L.- Unspiked K-Ar dating of young volcanic rocks from Loihi and Pitcairn hot spot seamounts. J. Volcan. Geoth. Res, in press.

Guillou, H., Carracedo, J.C., Pérez Torrado, F. and Rodríguez Badiola, E., 1995. K-Ar ages and magnetic stratigraphy of a hotspot-induced, fast grown oceanic island: El Hierro, Canary Islands. J. Volcanol. Geotherm. Res., 73: 41-155.

Guillou, H., Carracedo J. C. and Day, S.J., Unspiked K-Ar dating of volcanic rocks from El Hierro and La Palma, western Canary Islands (this volume).

Hilgen F.J., 1991. Astronomical calibration of Gauss to Matuyama sapropels in the Mediterranean and implication for the Geomagnetic Polarity Time Scale. Earth & Planetary Sci. Lett., 104: 226-244.

Izett G.A.and Obradovich J.D., 1994. 40Ar/39Ar age constraints for the Jaramillo subchron and the Matuyama-Brunhes geomagnetic boundary. J. Geophys. Res., 99 : 2925-2934.

Shackleton N.J., Berger A. and Peltier W.R., 1990. An alternative astronomical calibration of the lower Pleistocene timescale based on ODP site 677. Trans. of the Roy. Soc. of Edin : Earth Sciences, 81, 251-261.

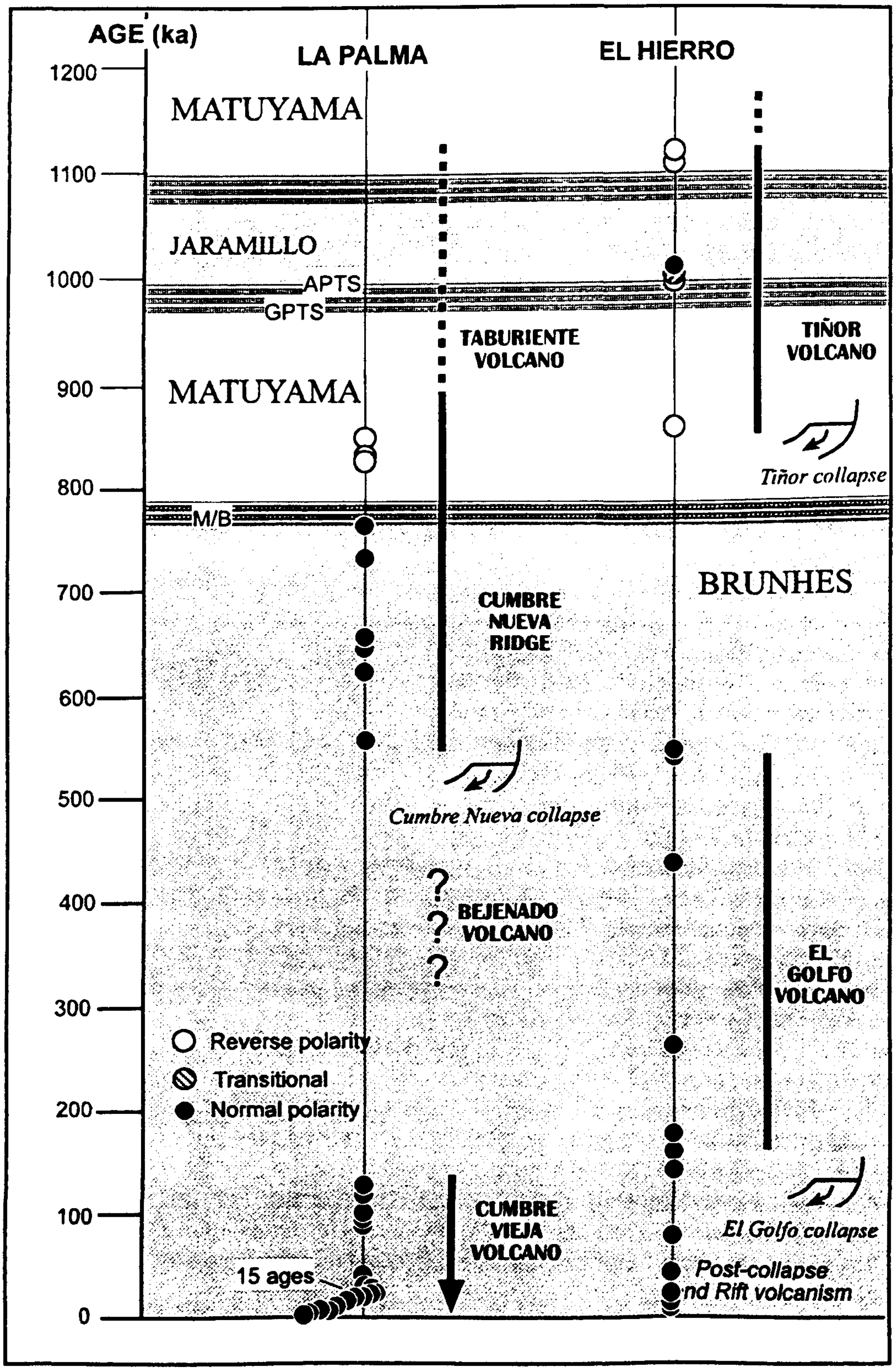
AGE (ka)
LA PALMA
EL HIERRO
1200
1100
1000
900
800
700
600
500
400
300
200
100
0
MATUYAMA
JARAMILLO
APTS
GPTS
MATUYAMA
M/B
BRUNHES
TABURIENTE VOLCANO
TIÑOR VOLCANO
Tiñor collapse
CUMBRE NUEVA RIDGE
Cumbre Nueva collapse
BEJENADO VOLCANO
EL GOLFO VOLCANO
Reverse polarity
Transitional
Normal polarity
CUMBRE VIEJA VOLCANO
El Golfo collapse
15 ages
Post-collapse
nd Rift volcanism

Cosmic Ray Exposure Dating in the Canary Islands

Paul Harrop
University of Manchester, UK

High energy cosmic rays that penetrate the Earth's magnetic field and atmosphere generate cosmogenic nuclides in near surface rocks. This phenomena is the basis for cosmic ray surface exposure dating. When fresh material, for example during a lava flow, is exposed at the Earth's surface, cosmogenic nuclides start to build up in the exposed surface of the rock. Since the production rates of several useful cosmogenic nuclides have been well constrained, the abundance of a particular cosmogenic nuclide is a measure of the duration of surface exposure of the rock provided no significant erosion has occurred. For a lava flow that has remained exposed continuously (not covered by subsequent deposits or flows), then the exposure age is equivalent to the eruption age.

Another important property unique to cosmic ray exposure dating is the ability to *directly* date major collapse events (land slips and volcanic subsidence) common on volcanic islands. The frequency and spatial distribution of such catastrophic events has tremendous importance for the assessment of future risk to human life and property.

Cosmic ray exposure dating, in particular using the ^{3}He and ^{21}Ne cosmogenic nuclide pair, has great potential in Quaternary active volcanic regions. The rarity of ^{3}He in nature (~1 atom in 10^{15} in crustal igneous rocks; Mamyrin & Tolstikhin, 1984) and its high production rate in surface exposed rocks make it capable of dating very young surfaces (<1000 years) as well as very old ones (up to several millions of years). The upper limit of the dating technique is limited only by the length of time a surface can remain exposed without significant erosion or burial. ^{3}He-^{21}Ne cosmic ray exposure dating is particularly valuable in areas where conventional dating techniques are difficult to apply. For example, ^{14}C dates are rare in regions where vegetation is sparse and is also limited to a maximum of 25 ka when it reaches equilibrium between production and decay. Similarly K-Ar and ^{40}Ar-^{39}Ar dating techniques are difficult to apply in rocks that are under 100 ka, and also require the presence of K-rich minerals such as sanidine.

Due to the mobility of cosmogenic ^{3}He in minerals, accurate surface exposure dating in warm climatic regions is restricted to rocks containing highly retentive minerals such as olivine and pyroxene. However, ^{21}Ne exposure dating can be applied to most common minerals and may be analysed in the same sample as the ^{3}He to derive an independent exposure age and also to monitor any diffusive loss of ^{3}He over time. Hence the combination of ^{3}He and ^{21}Ne has the potential to date most exposed volcanic rocks older then 1000 years.

^{3}He and ^{21}Ne cosmic ray exposure dating has previously been successfully applied to many Quaternary volcanic centres such as Hawaii (Kurz, 1986; Kurz *et al.*, 1990; Marti & Craig, 1987, Craig & Poreda, 1986); USA (Cerling, 1990; Poreda & Cerling, 1992), Massif Central in France (Cerling & Craig, 1994) and Reunion Island (Staudacher & Allegre, 1993). Many of these studies have thrown new light on the chronology of Quaternary volcanic complexes previously inaccessible by the ^{14}C and K-Ar dating techniques. In addition, the production rates of ^{3}He and ^{21}Ne have been tightly constrained by measuring their abundances in lava flows dated using the ^{14}C technique.

The Canary Islands offthe west coast of the African continent are the site of ongoing volcanic activity, the causes of which are not clear. Furthermore, because of the very limited historical record of the islands, and the difficulties associated with dating young lavas, details of the timing of all but the most recent and the most ancient activity is very uncertain. The ongoing study by the author has two main aims. The first aspect is to focus on the frequency of major collapse events (land slips and cauldron subsidence) in the Canary Islands. This will be achieved using a combination of ^{3}He-^{21}Ne

cosmic ray exposure and laser ^{40}Ar-^{39}Ar dating on pre- and post-collapse eruptives tightly enveloping the collapse event, and more importantly, clirectly dating the collapse event using ^{3}He-^{21}Ne cosmic ray exposure dating of the fault wall. This will greatly increase our knowledge of the frequency of catastrophic collapse events in the Canary Islands with inferences to other volcanic islands that have experienced similar processes. Secondly, due to the poor chronological control of the Canary Islands, selected volcanics will be dated using both cosmic ray exposure and high resolution laser ^{40}Ar-^{39}Ar dating to complete the volcanic chronology of the Canary Islands between existing historical records and early Quaternary and Tertiary K-Ar dated volcanics.

A pilot study (Harrop, 1996) has concentrated on the late Quaternary geological history of the eastern Canary Islands. The timing of a catastrophic caldera collapse event was the main focus on Tenerife. Exposure and K-Ar dating (Martí *et al.*, 1994) of volcanics enveloping the collapse event, and also direct dating of the fault wall using cosmogenic ^{3}He has constrained the collapse event to between 21 and 179 ka. However, the lower limit of 21 ka may be significantly lower than the true age of the collapse due to erosion on the fault wall. Mean ^{3}He exposure ages of 15.7 ± 0.7 and 15.4 ± 0.5 ka were obtained for the two Montana Mostaza lava flows - the oldest exposed eruptions post dating the Las Canadas collapse event - indicating that there was no significant hiatus between the two eruptions.

References

Cerling T. E. (1990) Dating geomorphologic surfaces using cosmogenic ^{3}He. *Quaternary Research* **33**, 148-156.

Cerling T. E. and Craig H. (1994) Cosmogenic ^{3}He production rates from 39°N to 46°N latitude, western USA and France. *Geochimica et Cosmochimica Acta* **58**.

Craig H. and Poreda R. J. (1986) Cosmogenic ^{3}He in terrestrial rocks: the summit lavas of Maui. *Proceedings of the National Academy of .Science, USA* **83**, 1970- 1974.

Harrop, P.J. (1996) Dating recent surface processes using cosmic ray generated ^{3}He in rocks. *Unpublished PhD thesis*, Manchester, U.K.

Kurz M. D. (1986) Cosmogenic helium in a terrestrial igneous rock. *Nature* **320**, 435-439.

Kurz M. D., Colodner D., Trull T. W., Moore R. B., and O'Brien K. (1990) Cosmic ray exposure dating with in situ produced cosmogenic ^{3}He: results from young Hawaiian lava flows. *Earth And Planetary Science Letters* **97**, 177- 189.

Mamyrin B. A. and Tolstikhin I. N. (1984) *Helium Isotopes m Nature*. Elsevier.

Marti, J., Mitjavila, J. and Arana, V. (1994) Stratigraphy, structure and geochronology of the Las Cañadas Caldera (Tenerife, Canary Islands). *Geology Magazine* **131**, 715-727.

Marti K. and Craig H. (1987) Cosmic-ray-produced neon and helium in the summit lavas of Maui. *Nature* **325**, 335-337.

Poreda R. J. and Cerling T. E. (1992) Cosmogenic neon in recent lavas from the Western United States. *Geophysical Research Letters* **19**(18), 1863-1866.

Staudacher T. and Allègre C. J. (1993) Ages ofthe second caldera of Piton de la Fournaise volcano (Reunion) determined by cosmic ray produced ^{3}He and ^{21}Ne. *Earth And Planetary Science Letters* **119**, 395-404.

A Paleomagnetic study of a volcanic sequence in the Island of El Hierro (Canary Islands): geomagnetic, volcannologic and tectonic implications

Nadia Szeremeta[1], Carlo Laj[1], Catherine Kissel[1], Hervé Guillou[1], Silvain Houard[1] and Juan Carlos Carracedo[2]

[1]*Centre des Faibles Radioactivit'es, CEA-CNRS, Gif-sur-Yvette, France*
[2]*Estación Volcanológica de Canarias, CSIC , La Laguna, Tenerife, Canary Islands, Spain;*

We have conducted a paleomagnetic study of a volcanic sequence comprising 68 flows in the Island of El Hierro (Canary Islands). This sequences is located in the northwestern part of the island and outcrops in the El Golfo embayement, along the Camino de la Pena, between the altitudes of 85 and 700 m.

Thin lava flows are commonly present in the upper part of the section, while more massive pyroclastic and trachytic flows are present in the middle part. Middle size flows are encountered in the bottom part. Usually successive flows are separated by well visible scorias or ashes or sometimes red levels.

Sampling started at the top of the section and extended downward to an altitude of 295 m. Sampling was not pursued below this altitude because the sequence is largely covered by piedmont deposits and is also characterized by intensive dyke intrusions. A total of 557 cores (i.e. 7-10 cores per flow), were drilled and oriented using most of the time magnetic and sun compasses.

Radiometric (K/Ar) dating conducted with an unspiked technique (Guillou et al, this conference), brackets the sequence between 448±8 ka and 133±4 ka, so that the section belongs entirely to the Brunhes chron. Intermediate ages of 261±6 ka, 176±3 ka, and 1158±4 ka were obtqined at altitudes 505 m, 585 m and 620 m respectively.

Thermal and af stepwise demagnetizations most generally isolate the same stable component of magnetization. Consistent paleomagnetic directions were obtained from samples from the same flow, with an OC95 confidence angle generally smaller than 6. Normal polarities were observed throughout the section, as expected for the Brunhes period.

The results, shown in figure I as an inclination/declination plot as a function of stratigraphy, yield information on three different aspects:

I) The data contribute to a better evaluation of the geomagnetic secular variation at Hierro for the Brunhes period (only old data, not really well constrained in time, were available so far (A. Abdel-Moneme et al., 1972). Rapid fluctuations are observed in both declination/ inclination records, and the scatter of the Virtual Geomagnetic Poles (VGP) is consistent with data from sites at different geographical localities. It is also consistent with MacFadden's model of geomagnetic secular variation. The VGPs generally lie <<over the geographic pole>> according to the Wilson's <<far sited effect>>.

2) A correlation analysis of the paleomagnetic results may improve the accuracy of the estimates of the extrusion process, between the <<tie points>> corresponding to the radiometric datings. Indeed, serial correlation between successive flows indicates that these flows have all recorded the same geomagnetic signal, implying that they were emitted in a very short time (bursts of activity). A calculation based on a recent publication (McElhinny et al, 1996) shows that in this section serial correlation extends at most over 2-3 successive flows. This is a strong indication that there have been no major bursts of volcanic activity during the edification of the sequence. The hypothesis that the extrusion rate (in flows per unit time) has been at first order constant between the datings, is thus sustained this analysis. This allows to calculate that the

average rate was about l flow/ 4.8 ka in the lower part, 1 flow/17 ka between 261 and 176 ka, 1 flow/9ka between 176 and 158 ka and finally I flow/l.l ka at the top of the section.

3) Finally, the data also indicate that in the lower part of the section, declination values are systemaically clockwise rotated with respect to the N-S axis (Figure 2). This deviation would suggest that a rotation of the section by about 20ø, may have occurred around 261 ka. The present data are, however, much too scarce to make this suggestion more than a speculation. Many additional data are needed to firmly establish the existence of the rotation, to establish whether it is a local tectonic phenomenon or whether it also affects the entire island, or even other neibouring islands.

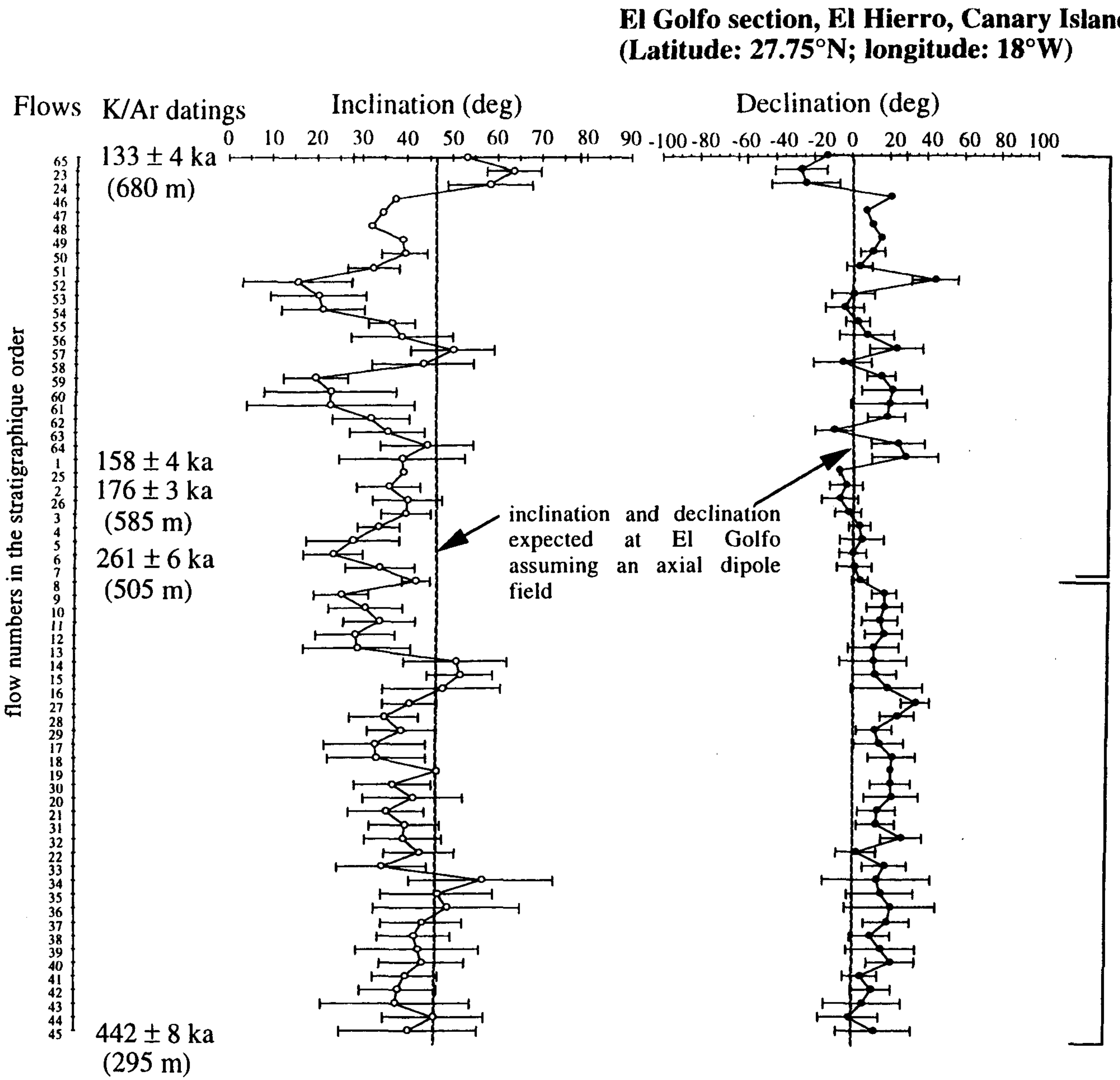

Figure 1: Declination, inclination VGP latitudes and longitudes records obtained from the El Golfo section.

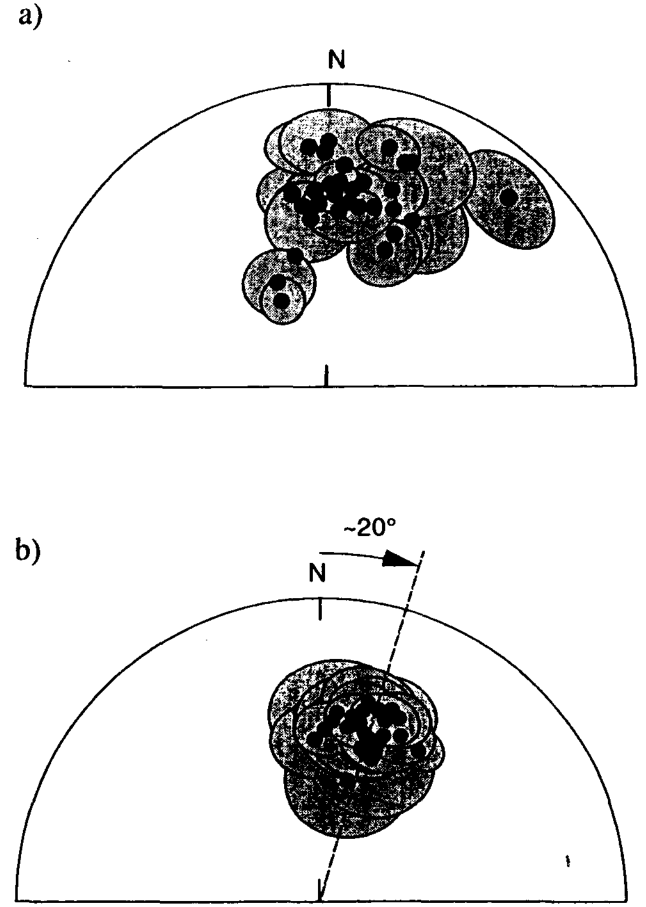

Figure 2: Stereographic projection of the paleomagnetic directions obtained for the upper part (a) and the lower part (b) of the section.

Dating Pyroclastics by Thermoluminescence

Manfred Frechen[1] and Ulrich Schweitzer[2]

[1] *Centre for Environmental Change & Quatemary Research, CGCHE*
Francis Close Hall, Swindon Road, Cheltenham, GL50 4AZ, U.K. (MFrechen@chelt.ac.uk)
[2] *Geologisches Institut, Universitat zu Koln, Zulpicher Str. 49a, D-50674 Koln, Germany*

Since the early days of thermoluminescence (TL) and Optical Stimulated Luminescence (OSL) dating, various attempts have been made to determine the cooling or eruption age of volcanic material. The dating of lava and pyroclastic deposits has its own set of problems like anomalous fading, low signal background ratio and the disequillibrium in the uranium series. To overcome these difficulties and to prove the capability of thermoluminescence for dating of volcanic material systematic investigations have been carried out to investigate TL and OSL properties of various types of proximal and distal air fall tephras, pyroclastic flow deposits and hyaloclastites. The indirect approach has been successful in dating aeolian sediments above and below the tephra horizons to bracket the eruption age by the deposition age of the sediments. These techniques are used as routine dating methods for eolian sediments younger than 100,000 (300,000) years as demonstrated for the Eltville Tephra and Laacher See Pumice in the West and East Eifel Volcanic Field, Germany. The combined OSL and TL age estimates are in agreement with the geological estimates for which independent age control is available. The second and direct approach is more difficult due to the above mentioned problems. Extensive fading experiments have been carried out for pumice of the Thera Pyroclastic Formation on Santorini island, Greece. The results of the Minoan and lower Pumice seem to be consistent with other independent chronological estimates (Schweitzer, unpublished PhD thesis). Dating results of Hekla ash H3 and unexpected old TL ages for hyaloclastites of the Krafla Volcanic System in Northern Iceland suggests that either the geological estimates are not reliable or that this class of volcanics has some unrecognized cause of inaccurate TL ages (Frechen et al. in press). By selecting suitable material which is free of complicating factors, reliable physical ages can be achieved for volcanic material.

The extensive dating study indicates that volcanic glass from both proximal and distal tephra has the potential to yield accurate TL ages and thus eruption ages up to 100,000 (500,000) years depending mainly on the annual dose rate and complicating factors such as poor reproducibility of TL, a low signal background ratio and anomalous fading.

The TL dating of volcanic glass up to 200,000 yr is still in an experimental stage but promising results have been determined for hyaloclastites from the Krafla Volcanic System, and from pumice of the Thera Pyroclastic Formation and the East Eifel Volcanic Field.

Seamounts in the Western Pacific: Lessons in the Construction, and Erosion of Oceanic Intraplate Volcanoes

H. Staudigel[1], A.A.P. Koppers[2] and J.R. Wijbrans[2]

[1]*Scripps Institiution of Oceanography, UCSD, La Jolla, CA 92093-0225 [hstaudigel@ucsd.edu]*
[2]*Dept. Earth Sciences, Free University Amsterdam,De Boelelaan 1085 1081HV Amsterdam*

The marine geology, geochemistry and geochronology of submarine island flanks, seamounts and guyots provide valuable insights into plate motion, the long-term history of hot spots and the evolution of OIV's in terms of their construction and mass wasting. We studied a series of Western Pacific seamounts and guyots using Seabeam bathymetry, dredging, geochemistry and geochronology, using Vlinder Guyot (116°55'N 154°20E) to illustrate the main features.

Vlinder bathymetry suggests multiple phases of magmatism followed by rejuvenated volcanism and flank collapse. Vlinder has a flat top at about 1500m water depth, shaped like a butterfly, approximately 40km by 50km wide. Four rift zones extend from this summit platform with azimuths and length of rifts of 347°/43km, 025°/40km, 239°/30km and 176°/50km. The NW rift zone displays a down-rift branch that points back towards the main volcano, identifying this part of the rift as an independent volcanic edifice that may have been active prior to the main volcanic activity at Vlinder. A satellite guyot on the SE rift ("Oma Vlinder") falls on the extension of the concave elevation profile of the main summit, suggesting that both were drowned by the same erosion and subsidence event. The otherwise very flat summit platform displays a central, symmetric volcanic cone of 500 m height above the main shelf of the guyot, suggesting about 20-30 Myrs lithospheric subsidence between drowning of Vlinder and its rejuvenated volcanism. Thus, bathymetry suggests multiple phases of shield building volcanism and a posterosional, rejuvenated stage of volcanism.

The main summit platform of Vlinder displays characteristic extensions at the emerging points of the rift zones. Major scars from submarine land slides are found around the main summit, in particular near the emerging points of rift zones. These emerging points mark the transition of intrusive/extrusive acitvity of the central summit to the rift zone. We suggest that this portion of the seamount may be more susceptible to be de-stabilized because of the superposition of two distinct intrusive mechanisms: radial tilt is caused by central intrusions (as in the Seamount Series on La Palma) and rift zone extension that is caused by expansion of the upper portion of the rift zone. These processes together result in over-steepened flanks of the main summit and subsequent slope failure. A similar preference for the origin of landslides can be found in other oceanic volcanoes, such as the SW rift of Mauna Loa.

40Ar/39Ar geochronology of seven mineral separates and two groundmass samples from major fault scarps and deeper flanks of the seamount provides information on the origin of the guyot and its volcanic history. Ages between 92-102 Ma suggest that Vlinder can be back-tracked to the South Pacific Isotope and Thermal Anomaly (SOPITA), without a corresponding modern hot spot. The source region characteristics of Vlinder track seamounts are consistent with an origin in the SOPITA, including its long lasting "enriched" character (87Sr/86Sr = 0.7028 - 0.7053; 143Nd/144Nd = 0.51232 - 0.51285; 206Pb/204Pb = 17.85 -18.84 ; 207Pb/204Pb = 15.55 - 15.70; 208Pb/204Pb = 37.87- 38.71). Ages of neighboring seamounts and guyots suggest an age progression and azimuth consistent with the Musicians/Lines trend. Vlinder displays two major shield building volcanic episodes, an early phase at 100-102 Ma on the Western flank of the main summit, 92-95 Ma in two eastern locations on a steep fault scarp in the northern portion and on Oma Vlinder. These data show that the main shield of Vlinder was formed over a time period of at least ten million years, possibly in two distinct volcanic phases, apparently shifting from the West to the East, whereby the NW represents the oldest portion of the seamount.Complex magmatic histories of OIV's such as at Vlinder appear to be rather common and show that meaningful geochronologic analysis of seamounts has to include careful structural analysis of volcano morphology, combined with detailed dredging and multiple 40Ar39Ar ages.

Petrology, geochemistry and geochronology of Maupiti island (Society archipelago, French Polynesia)

Sylvain Blais[1], Gérard Guille[2], Hervé Guillou3, and René C. Maury4

[1]Géosciences Rennes, CNRS-UPR4661, Université de Rennes 1, 35042 Rennes Cédex, France.
[2]CEA, DASE LDG, B.P. 12, 91680 Bruyères le Chatel, France.
[3]URA CNRS 1278, U.B.O., BP 809, 29275 Brest, France.
[4]Centre des Faibles Radioactivités, 91198 Gif-sur-Yvette, France

Located at about 470 km N. W. of the hot spot generating the Society archipelago islands (French Polynesia), Maupiti is with a 2,5 km diameter, the smallest island of the archipelago. Situated at the middle of a huge lagoon enclosed inside a nearly continuous coral rim, the volcanic structure culminates at 370 m and corresponds to an evolution stage preceding the atoll formation.

Maupiti is the oldest island of the archipelago. Effectively, the end of the volcanic acrivity period is about 4 Ma (Duncan and Mc Dougall, 1976; Diraison, 1991). The age is perfectly coherent with a drift speed model of about 11 cm/y for the Pacific plate. The island morphology is made of a main structure largely notched by erosion and of a secondary unit, located south - west part of the island and constitued by pyroclastic matenals of variable size. As usually met in the Polynesian islands, there is no important collapsed structure; however, the existence in the north - west area of the island of outcrops of coarse grained rocks can suggest the existence of a caldeira.

The most important aspect of the island is that it is composed by the stacking of metric pahoehoe type lava flows of basaltic composition. Only the summit flows are slightly differenciated (hawaites); on the other hand, the most extreme differenciated types of the alcalines series (trachytes and phonolites) are absent. The volcanic structure is cut by many dykes in the general N. 70° direction and correspond, for some of them, to mugearites or even benmoreites.

Magmatic underplating and crustal magma accumulation beneath the Canary Island Archipelago as evidenced by fluid inclusions.

Thor H. Hansteen, Andreas Kluegel and Hans-Ulrich Schmincke

GEOMAR, Abt. Vulkanologie und Petrologie, Wischhofstraße 1-3, D-24148 Kiel, Germany
Phone (49) 431 -600-2135, Fax (49) 431 -600-2924 E-mail: thansteen@geomar.de

Fluid inclusions in ultramafic and mafic parageneses (gabbroic to ultramafic xenoliths; olivine phenocrysts in basaltic rocks) from Gran Canaria and La Palma (Canary Islands) have been investigated. Samples include olivine phenocrysts, harzburgite and dunite xenoliths from Holocene basanitic volcanic centers on Gran Canaria, and dunite, pyroxenite to amphibolite cumulates, and MORB-type gabbro xenoliths from the 1949 San Juan eruption on La Palma. We have further compiled existing fluid inclusion data from Miocene transitional shield basalts from Gran Canaria and from olivine gabbroic and ultramafic xenoliths from Hierro and Gomera [1 -3].

Densities of CO_2-dominated fluid inclusions in ultramafic and mafic parageneses from Gran Canaria, La Palma, Hierro and Gomera show striking similarities. Most commonly, each rock type shows one or more density maxima which correspond to the following depths: 1) within the spinel stability field in the upper mantle, 2) at the Moho or in the lower crust, 3) within the upper crust. Some harzburgite, lherzolite and dunite xenoliths, and olivine phenocrysts in basanite, contain texturally early fluid inclusions corresponding to minimum depths of origin within the spinel peridotite field at 1.2 to 0.8 GPa, indicating fluid oversaturation for the Canary Island basanite magmas at these or higher pressures [4]. Overlapping pressure estimates between texturally early fluid inclusions in peridotite xenoliths and those in olivine phenocrysts from the host basanites additionally indicate magma reservoirs at such pressures within the mantle, and a possible link between those reservoirs and mechanisms of xenolith entrainment (Fig. 1). The occurrence of clinopyroxene and spinel as primary inclusions in olivine from the Gran Canaria basanites further suggests that these minerals were simultaneous liquidus phases at mantle pressures. The combined evidence implies crystal fractionation and entrapment of fluid inclusions at depths corresponding to those of xenolith entrainment.

Texturally late and partly decrepitated fluid inclusions in harzburgite, lherzolite and dunite xenoliths from Gran Canaria and Hierro give pressures of 400 to 300 Mpa, i.e. clo.se to the Moho. Inclusions in olivine from transitional shield basalts (Gran Canaria) and in MORB-type gabbro xenoliths (La Palma) show pressures corresponding to the lower core of the islands at about 300 MPa, and additionally to high levels of the magma plumbing system at about 100 MPa. Texturally early inclusions in dunite and olivine-bearing pyroxenite to amphibolite xenoliths from La Palma give a well-defined pressure range of 200 to 350 MPa. The combined data indicate intermittent ponding of basaltic magmas at Moho or lower crustal depths and additionally at a higher level, strongly suggestive of two main accumulation levels beneath each island. This suggests magmatic underplating as an ubiquitous process, and the existence of lower crustal magma reservoirs, beneath each of the islands. Additional magma accumulation may occur at various depths, ranging from the lower crust through high levels of the respective core complexes. The ranges of pressures observed probably represent local variations within the magma plumbing system specific to each island. We propose that mush zones containing variable fractions of cumulate crystals and mafic melts occur within the lower crust of the islands. This is compatible with a prevailing open texture and abundant glass in the ultramafic cumulate xenoliths from La Palma and Gran Canaria.

Magmas entering the crust from the upper mantle may reach a level of neutral buoyancy (LNB) close to Moho depths. Beneath a volcanically active ocean island, theconditions required for a LNB can probably be met at two different levels, one in the lower and one in the upper crust, as has been proposed for Hawaii [5,6]. Alternatively, a crystal mush zone with an overall density higher than basanite magma can, due to its largely liquid properties, have a strong braking effect on propagating dikes and thus represent a magma trap, without the conditions for a LNB being fulfilled in the lower crust. In either way, magmas entering the lower crust within the active magma plumbing system are expected to get pooled, and will propagate along zones of weakness if sufficiently replenished. Resulting sill-like bodies can act as short term reservoirs until a new magma pulse enters, or until significant crystallization and buildup of a fluid overpressure occurs. Hydraulic fracturing may then cause the magma to move to higher levels along a new pathway or a pre-existing zone of weakness. We suggest that short-time accumulation of primitive magmas within horizontally foliated lithologies close to Moho depths is the rule rather than the exception beneath the Canary Islands. Magma ponding times are specific to each island and can be estimated from zoned peridotite xenoliths. They range from days or weeks for Hierro and Gran Canaria, to months or years for La Palma [7].

Whilst sub-Moho processes can still be recognized in texturally early fluid inclusions from Gran Canaria and Hierro peridotites, those in La Palma peridotites and Gran Canaria shield basalts appear to have lost most of their original depth information. We suggest an almost complete re-equilibration of fluid inclusions as a consequence of exceptionally prolonged crustal storage in these cases.

Comparable fluid inclusion data from primitive mafic rocks in other tectonic settings, including Iceland and continental rift systems (Hungary, South Norway; [8,9])indicate that magma accumulation close to Moho depths shortly before eruption is not restricted to oceanic intraplate volcanoes. Short-time lower crustal residence of ascending mafic magmas probably also occurs in MOR and continental rift settings. Such limited lower crustal ponding and crystallization prior to eruption may be common, independent upon the tectonic setting.

References

[1] Gurenko AA, et al. (1996) Contrib Mineral Petrol 124: 422-435
[2] Hansteen TH, et al. (1991) Contrib Mineral Petrol 107: 242-254
[3] Frezzotti ML, et al. (1994) Eur J Mineral 6: 805-817
[4] Mangas J, et al. (1996) IAVCEI Abstracts, 72
[5] Ryan MP (1988): J Geophys Res 93: 4213-4248.
[6] Ryan MP (1995) Abstract, EOS Suppl, S287.
[7] Kluegel A, et al. (1997) Submitted to Terra Nova.
[8] Neumann E-R, et al. (1988) Contrib Mineral Petrol 98: 184-193
[9] Szabo Cs, Bodnar RJ (1996) Petrology 4: 240-249

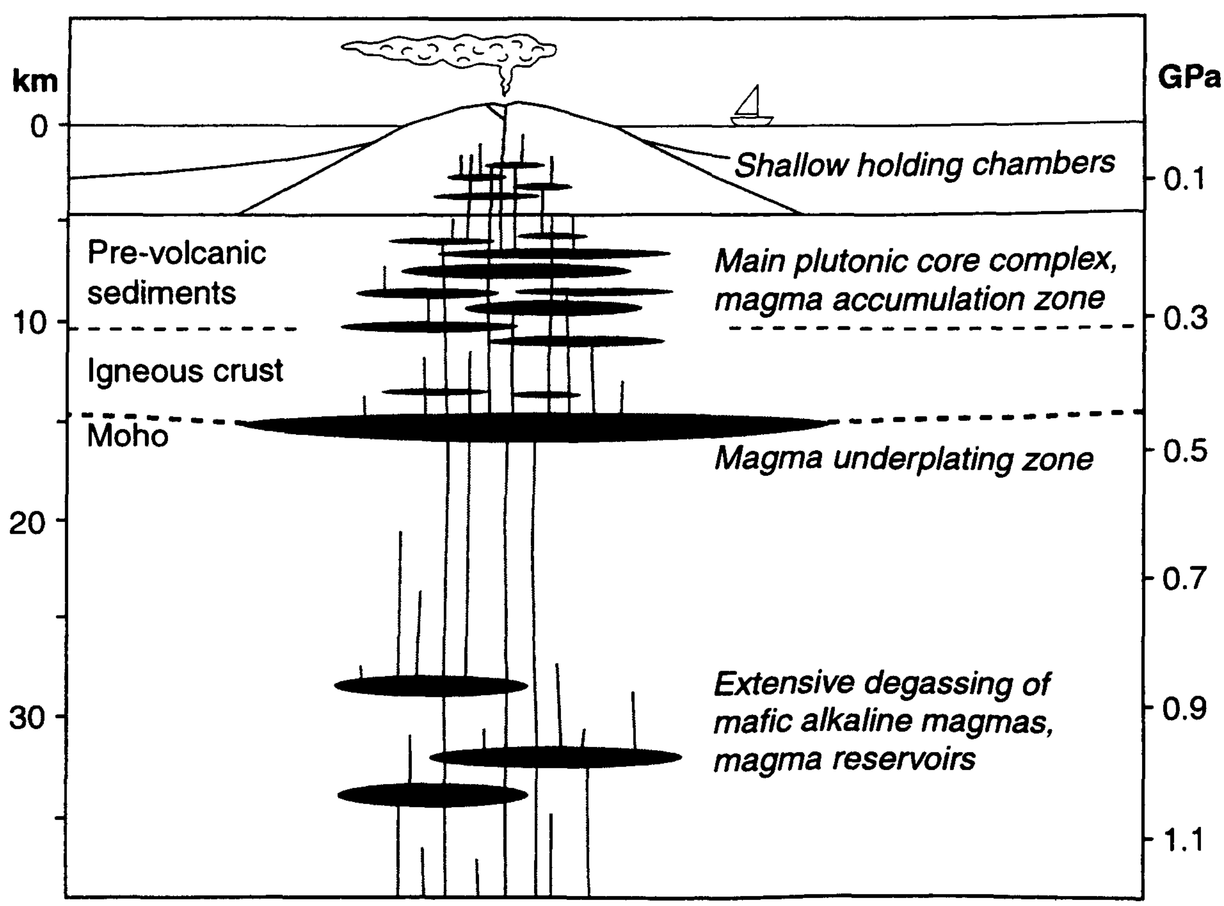
km
0
10
20
30
GPa
0.1
0.3
0.5
0.7
0.9
1.1
Shallow holding chambers
Pre-volcanic sediments
Main plutonic core complex, magma accumulation zone
Igneous crust
Moho
Magma underplating zone
Extensive degassing of mafic alkaline magmas, magma reservoirs

Rates of magma ascent and depths of magma reservoirs beneath La Palma (Canary Islands)

Andreas Kluegel, Thor H. Hansteen, Hans-Ulrich Schmincke, Peter M. Sachs
GEOMAR Forschungszentrum, Abt. Vulkanologie und Petrologie,
Wischhofstr. 1-3, D-24148 Kiel, Germany
Phone (49) 431-600-2140, Fax (49) 431-600-2924
E-mail: akluegel@geomar.de

Historic eruptions on La Palma, occurring along the Cumbre Vieja forming the southern third of the island, show many similarities: they typically began after a prolonged period of earthquakes, are chemically and mineralogically zoned, and erupted alkaline basalts commonly carrying crustal and mantle xenoliths during the final eruptive phase [1]. In order to calculate magma ascent rates and residence times in magma reservoirs beneath the island, we studied peridotite xenoliths from the 1949 and 1971 eruptions and from the >3 ka old San Antonio volcano [2]. The results place constraints on the present magma transport and storage system of the fast growing Cumbre Vieja volcano.

Xenolith properties. The xenoliths are spinel harzburgites and spinel dunites, interpreted as fragments of the upper mantle as indicated by their mineralogical and chemical composition [3]. Along most of their surface, all xenoliths show clinopyroxene-rich selvages towards the magma with prevailing cumulate textures documenting prolonged magma contact (Fig. 1). Some peridotite fragments are embedded in clinopyroxene-amphibole-rich cumulates. The selvages are accompanied by 1-3 mm wide diffusion zones along the peridotite rims where olivine is enriched in Fe, Mn, Ca, and depleted in Mg, Ni. Xenolith surfaces lacking selvages, and fractures filled with basaltic glass, generally show no or narrow diffusion zones (<20 mm). Wide and narrow diffusion zones both result from element exchange between peridotite and basaltic melts. Calculations based on a model of Fe-Mg interdiffusion document that wide zones formed over a period of 0.2 to 6 years, whereas narrow zones formed in less than 4 hours. Microthermometry of primary CO_2-dominated fluid inclusions gives pressure estimates of 200-450 MPa (7-15 km depth) for recrystallized peridotite olivines, and 200-340 MPa (7-12 km depth) for selvages [5]. Preliminary data for primary and secondary CO_2 inclusions in ultramafic cumulate xenoliths (olivine amphibolites and -pyroxenites) abundant in many eruptions give similar values of 200-300 MPa (7-10 km depth). These depths correspond to the lower crust, as the Moho is situated at 13-15 km depth under the central Canary Islands [6].

Implications. The calculated diffusion times imply that mantle xenoliths were in contact with magma months to years prior to the eruption. This period partly corresponds with the onset of seismic precursors of an eruption [4]. In comparison, the transfer time for a magma rising continuously from the inferred source region of the peridotites to the surface is much less than 2-4 days, derived from calculated xenolith settling rates of up to 0.2 m/s [4]. The considerable discrepancy between contact times and transfer rates, and the presence of cumulates around peridotite fragments and within selvages, strongly suggest that the ascending magmas stagnated in one or more reservoirs en route to the surface. The reservoirs are located in the lower crust at 7-12 km depth as indicated by fluid inclusions in selvages, cumulates, and wide diffusion zones.

Model of magma ascent. We propose a simplified model of the multi-stage magma ascent and storage beneath La Palma (Fig. 2).

1. Peridotite wall rock of the upper mantle is fragmented by, and entrained into, rising magma batches months to years prior to an eruption. The xenoliths are carried to the crust within hours to days at magma ascent velocities exceeding 0.2 m/s.
2. The host magma ponds in sill-like reservoirs or pockets within the crust where mantle xenoliths become sedimented. Diffusion zones, selvages, and cumulates form during a period of months to years. The host magma may differentiate and new magma batches may pond or become added. This stage may represent the filling of the inferred N-S trending rift zone in the south of La Palma [7].

3. Eventually, increasing pressure in the crustal magma reservoirs causes the propagation of dikes towards the surface and along the rift zone. This is indicated by seismic precursors occurring months to years prior to an eruption, where the seismic foci apparently moved southward along the rift zone in some cases [4].

4. After the eruption commences, only a few sedimented xenoliths are entrained into the rising magma. Most xenoliths are carried to the surface near the end of the eruption when the magma reservoirs become flushed, commonly at peak eruption intensity. This final ascent occurs within hours and causes further xenolith fragmentation as documented by young fractures showing narrow diffusion zones.

References

[I] Hernández-Pacheco A, Valls MC (1982), Arquipelago, Rev. Univ. Azores, C. Nat., 3, 83-94.
[2] Carracedo JC, et al (1996), Estudios Geol., 52, 103-114.
[3] Wulff-Pedersen E, Neumann ER, Jensen BJ (1996), Contrib. Mineral. Petrol., 125, 113-139.
[4] Kluegel A, Hansteen TH, Schmincke HU (1997), submitted to Terra Nova.
[5] Hansteen TH, Kluegel A, Schmincke HU (1997), submitted to Contrib. Mineral. Petrol.
[6] Banda E, et al (1981), Earth Planet. Sci. Lett., 55, 11-24.
[7] Carracedo JC (1994), J. Volc. Geotherm. Res., 60, 225-241.

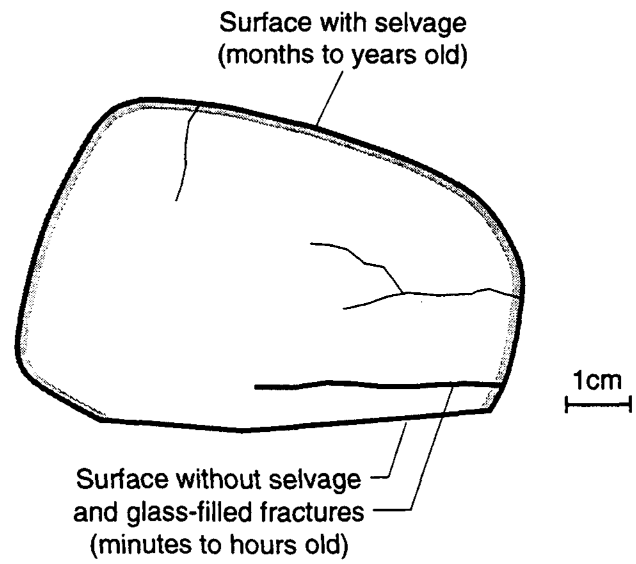

Fig. 1: Sketch depicting characteristic morphology of a peridotite xenolith.

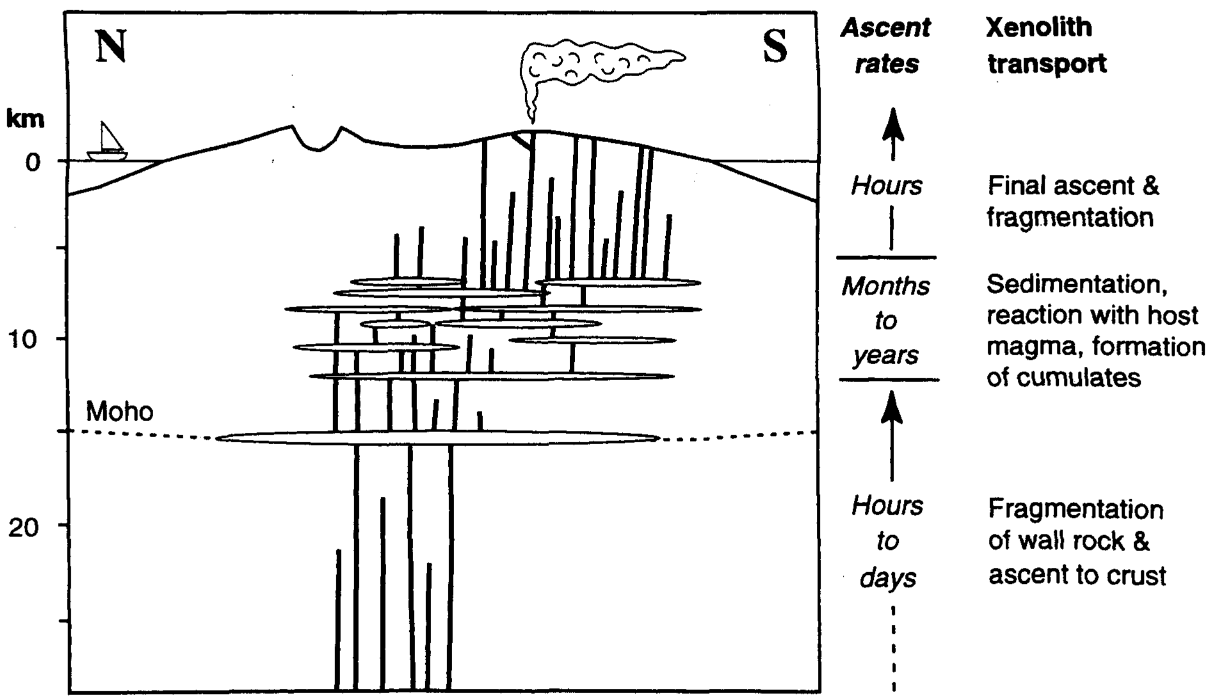

Fig. 2: Simplified model of magma ascent and storage beneath La Palma.

Products of the 1993 submarine eruption, off Socorro Island, Mexico

Claus Siebe[1] and Jean-Christophe Komorowski[2]

[1]*Instituto de Geofisica, Universidad Nacional Aut6noma de Mexico, Coyoacan, C.P. 04510, Mexico, D.F., Mexico.*

[2] *Institut de Physique du Globe de Paris, 4 Place Jussieu, Tour 14-24, B89, 75252 Paris Cedex 05, France*

Products of an underwater eruption near Socorro Island in the NE Pacific were observed directly on January 29, 1993, ten days after precursors were first recorded by hydrophones. Eruptive activity was noticed from ships as small steam plumes rising from the sea at an area centered at 18° 45' N, 111° 08' W, 2.4 km NW of Punta Tosca and 4.6 km SSW of Cape Henslow on Socorro Island. The observed steam was produced by 1-3 m large blocks of hot, dark-grey, highly vesiculated basalt rising buoyantly to the surface from two submarine vents at 210 and 30 m depth. Tens of blocks accompanied by bubbles could be observed rising to the surface in irregular pulses.

These scoriaceous blocks remained floating at the surface until they would crack into smaller pieces by thermal contraction emitting hissing noises from vapourizing seawater in contact with the hot interior of the blocks. Steam jets several m in height were produced and occasionally blocks were propelled laterally by the steam jet. Depending on vesicularity and permeability, blocks remained floating and drifting with the surface current for 1-15 minutes before sinking back. Floating rocks covered an area of about 6000 m^2. Buoyant scoria and reticulite are indicative of volatile (mostly CO_2) supersaturation and exsolution in the magma prior to rapid quenching, which inhibits loss of volatiles by bubble escape. A high-velocity ascent of low viscosity magma in a relatively narrow conduit is also required to prevent substantial gas escape and allow formation of reticulite. The buoyant scoria was probably ejected by intermittent lava fountaining at fixed vents as a result of changes in eruption velocities. Between January and July 1993 floating biocks of scoria and reticulite were collected on several occasions from the surface of the sea for chemical and mineralogical analyses revealing that the composition of the emitted lava did not change through time. Blocks of basalt (SiO_2 = 45-47 %) were highly vitric and vesicular with tabular anorthite phenocrysts up to 3 mm in length and minor grains of forsteritic olivine. REE and trace element composition of these rocks suggest an anomalous mantle source for the erupted alkali basalt lava.

Biological mediated alteration of volcanic ash in seawater: Litho- Bio- and Hydrosphere interaction

H. Staudigel[1], E. Verdurmen[1], R.A. Chastain[2], A. Yayanos[2], H. de Baar[3] and W.B. Bourcier[4]

[1]*Center for Isotope Geology, Netherlands Research School of Sedimentology, Vrije Univ. Amsterdam, stau@geo.vu.nl*

[2]*Scripps Institution of Oceanography, La Jolla CA 92093-0202*

[3]*Netherlands Institute for Ocean Research, Texel, NL.*

[4]*Lawrence Livermore National Laboratories, Livermore CA 94550*

Mantle-derived volcanic glass is introduced into the oceans as ash from subaerial volcanism, and various occurrences of volcanic glass from submarine eruptions. The abundance of glass in the oceanic realm is high and it was shown that their alteration results in major geochemical fluxes. The kinetics of glass alteration glass may be significantly enhance biologically enhanced through local increase in pH at their colonizing surfaces and through utilization of dissolved glass components. We designed a flow-through reactor for the (biologically controlled) interaction of basaltic glass and seawater and carried out a series of experiments to begin understanding the relationships between biological activity and the alteration process of volcanic glass in seawater. Experimental conditions simulated near-surface seawater physical and microbial conditions in the context of a sterile control.

These experiments show that biologically mediated alteration of volcanic glass is more effective than abiotic dissolution. Observed accumulation rates in biotic experiments suggest that the dissolution rates of Si is more than twice the sterile rate and isotopic analysis of fresh and altered glasses suggest that biotic exchange is about twice the sterile rate. Observation of siliceous deposits within the glass packing and the water reservoir of our flow-through reactor establishes a connection between the dissolution of volcanic ash and the deposition of biogenic silica such as in most chert deposits.

Trace element abundance patterns in altered glass show the enrichment of Ba (enrichedby 85 %), U (48%), Rb (22%), La (15%), Ce (18 %) and Sr (17 %).

These experiments demonstrate that biological activity plays a role in the global geochemical pathways of many elements, whereby mantle components can rapidly become portions of the biosphere, hydrosphere or oceanic crust. Global fluxes related to this process require more reliable estimates of the abundance of volcanic ash in the oceans.

How to establish a geochemical earth reference model?

Hubert Staudigel[1], Francis Albarede, Henry Shaw and William M. White

The rise of Earth System Science and the resulting need to view individual geochemical, geophysical and geological data sets in the context of the whole, dynamic Earth has resulted in the need for a Geochemical Earth Reference Model (GERM). A GERM should represent the current consensus of the geochemical and geophysical community of the definition of major geochemical reservoirs, their chemical inventory, and the fluxes between them. Such reference models have been used very successfully in other geoscience disciplines, such as whole-Earth geophysics. Typically, the availability of such a reference model is a necessary requirement for major advances in the understanding of a system, and the refinement of the less well constrained portions of the model follows inevitably from its use by a broad community.

As a basis for discussions with the scientific community, we established a strawman GERM on the Internet (http://www-ep.es.llnl.gov/germ/germ-home.html) that illustrates our current ideas. The World Wide Web is an ideally suited vehicle for this undertaking because of its flexibility and wide accessibility. A tentative division of Earth reservoirs has been established and an initial set of editors identified who will take responsibility for shaping a community consensus and in contributing their understanding of a given reservoir. The long-term goal of this work is to provide elemental and isotopic abundance information for all elements in a complete set of geochemical reservoirs for the Earth. Abundance data for all reservoirs will be accompanied by estimates of the potential ranges and uncertainties, relevant literature references, and explanations of the means by which the estimates were made.

Establishment of a GERM will require contributions from the broad community of earth scientists and active participation is encouraged. The effort will require a time and management structure not unlike that of a scientific journal. We envision the Internet GERM home page primarily as a compilation of referenced data that is operated like a journal, wherein editors can "publish" compiled information and establish a community consensus.

GERM-home page: http://www-ep.es.llnl.gov/germ

The Boron Isotope Geochemistry of Oceanic Island Basalts From Sites of active Intraplate Volcanism on the Pitcairn and Society Hotspots, South-Central Pacific

Susanne Barth[1], Marc Chaussidon[1] & Colin W. Devey[2]

[1]*Centre National de la Recherche Scientifique, Centre de Recherches Petrographiques et Geochimiques, CNRS-CRPG, BP 20, F-54501 Vandoeuvre-les-Nancy Cedex, France.*

[2]*Geologisch-Palaontologisches Institut, Universitat Kiel, D-24118 Kiel, Gerrnany.*

**At present: Institut fur Geologie und Palaontologie, Universitat Tubingen, D-72076 Tubingen, Gerrnany.*

ABSTRACT

Boron isotopic compositions and B concentrations of submarine lavas from sites of active intraplate volcanism on the Pitcaim and Society hotspots in French Polynesia, containing among the most extreme "enriched mantle" signatures of EM-I and EM-II type, respectively, show considerable variations that are unique among oceanic island basalts [1-5]. Systematic correlations between $\delta^{11}B$ and most major and trace element concentrations indicate that the magmas have experienced significant shallow-level assimilation and fractional crystallization processes. Boron isotope systematics are shown to be a sensitive tracer for constraining late-stage magma evolutionary processes of mantle-derived magmas.

INTRODUCTION

Intraplate ocean island volcanoes are produced by upwelling of diapirs ("plumes") from deep reservoirs of the Earth's mantle which has been shown to contain several isotopically and chemically distinct components (see [6] for recent review). Boron isotope geochemistry holds considerable promise as a new tracer for providing intrinsic insight into mantle geochemistry and the evolution of the oceanic crust. Boron is an ubiquitous element that is highly concentrated in the continental crust (~ 10-13 ppm, [7] and references therein), seawater (4.5 ppm [8]), and altered oceanic crust (up to > 100 ppm, mean ~ 5 ppm [9]) compared to the primitive mantle (0.1-0.3 ppm [4,10]). The relatively large mass difference between the two stable isotopes of boron, ^{10}B and ^{11}B, leads to a wide range of boron isotope variations in surface material (total $\delta^{11}B$ range ≈ 90 ‰ [11,12]; for δ notation see below). At magmatic temperatures, however, the isotopes of boron, an incompatible element in mantle processes [13], are not significantly affected by fractionation [14] and, therefore, should reflect primary magmatic source compositions.

We have analyzed oceanic island basalts from sites of active intraplate volcanism on the Pitcairn and Society hotspots in French Polynesia which represent among the most extreme "enriched mantle" signatures of EM-I and EM-II type [15], respectively, as deduced from chemical and radiogenic (Sr-Nd-Pb) isotope constraints [16-18]. In contrast, oxygen isotope data [19] yielded no unequivocal evidence for recycled material in the plume sources since the reported variations may, at least to some extent, be considered as analytical artifacts [20]. Our boron isotope and B concentration data detemnined on fresh submarine glasses from several Pitcairn and Society Seamounts, along with complementary major element analyses performed on the same rock samples, are reported by Barth et al. [1,2] and summarized below.

GEOLOGICAL SETTING

The Pitcairn and Society Seamounts are part of several volcanic chains in the south-central Pacific. The Pitcairn Seamounts are located to the east-southeast of Pitcairn Island and are thought to represent the present-day expression of the Pitcairn hotspot that formed the Pitcairn - Gambier - Duke of Gloucester linear island chain. The Society superswell comprises several submarine volcanoes which are located to the east-southeast of the peninsula of Tahiti and are to be considered as the result of hotspot volcanism presently active at the end of the 300 km long Society Island archipelago.

EXPERIMENTAL

Boron isotope ratios ($^{11}B/^{10}B$) and B concentrations of fresh submarine glasses from the Pitcairn and Society Seamounts were measured by Secondary Ion Mass Spectrometry (SIMS) on a Cameca ims-3f ion microprobe at the CNRS-CRPG institute in Vanoeuvre-lès-Nancy (France). Boron isotope compositions are given as $\delta^{11}B$ values (in per mil) such that

$$\delta^{11}B = \{ [(^{11}B/^{10}B_{\text{Sample}}) / (^{11}B/^{10}B_{\text{NIST SRM-951 Standard}})] - 1 \} \times 10^3$$

relative to a a NIST SRM-951 boric acid standard value of 4.04558 [21]. The $\delta^{11}B$ values were detennined at ± 1.5 %O (1 sigma) and the B contents at ± 10 % (1 sigma). Analytical details of the applied SIMS technique are reported by Chaussidon et al. [22]. Major element concentrations were measured by electron microprobe at the University of Vandoeuvre-lès-Nancy.

RESULTS AND DISCUSSION

The variations in boron isotopic compositions and B concentrations are enormous in the Pitcairn ($\delta^{11}B$ = -10.0 to -5.6 ‰, B = 1.5 to 3.9 ppm) and Society (-14.8 to -0.6 ‰, 1.3 to 6.4 ppm) volcanic suites [1,2], exceeding those previously reported for oceanic island basalts [3-5] . The boron isotope variations cannot be considered as a result of post-emplacement alteration of the glass since (1) neither macroscopic nor microscopic signs of alteration are visible in the glass, and (2) exchange with seawater ($\delta^{11}B$ = +39.5 ‰, B = 4.5 ppm [8]) would have produced unrelated $\delta^{11}B$ versus immobile trace element pattems, instead of systematic trends.

Pronounced systematic correlations of the $\delta^{11}B$ values with almost all major and trace element concentrations are observed as a unique feature of the Pitcairn and Society lavas. The variations in major and trace element concentrations, and in particular in MgO, indicate the impoltance of low-pressure crystal fractionation. Such crystal fractionation at magmatic temperatures will, however, leave the boron isotope ratio largely unaffected [14]. Hence, the pronounced covariations indicate that the boron isotope systematics of the Pitcairn and Society magmas are controlled by shallow-level assimilation and fractional crystallisation processes involving material which has probably experienced variable degrees of water-rock interaction. In conclusion, boron isotope systematics are a sensitive tracer for constraining late-stage magma evolutionary processes of mantle-derived magmas.

Acknowledgements
Collection of the samples was funded by BMFT grants to P. Stoffers. who is thanked for kind provision of the samples. We are indebted to D. Mangin and J.-M. Claude † for technical assistance with ion and electron microprobe measurements, respectively. This work was supported by a postdoctoral NATO fellowship provided by the DAAD (Deutscher Akademischer Austauschdienst) to S.B. A travel grant provided by the DFG (Deutsche Forschungsgemeinschaft) to S.B. allowed participation in this International Conference and is gratefully acknowledged.

References

[1] Barth, S., Chaussidon, M. & Devey, C.W. (submitted).
[2] Barth, S., Devey, C.W. & Chaussidon, M. (submitted).
[3] Chaussidon, M. & Jambon, A. *Earth Planet. Sci. Lett.* **121**, 277-291 (1994).
[4] Chaussidon, M. & Marty, B. *Science* **269**, 383-386 (1995).
[5] Gurenko, A.A. & Chaussidon, M. *Chem. Geol.* (in press).
[6] Hof nann, A.W. *Nature* **385**, 214-229 (1997).
[7] Leeman, W.P. & Sisson, V.B. in *Reviews of Mineralogy, Boron: Mineralogy, Petrology and Geochemistry*, E.S. Grew and L.M. Anovitz, Eds. (Mineralogical Society of America, Washington, 1996), Vol. **33**, pp. 645-707.
[8] Spivack, A.J. & Edmond, J.M. *Geochim. Cosmochim. Acta* **51**, 1033-1043 (1987).
[9] Smith, H.J., Spivack,, A.J., Staudigel, H. & Hart, S.R. *Chem. Geol.* **126**, 119-135 (1995).
[10] McDonough, W.F. & Sun, S,.S. *Chem. Geol.* **120**, 223-253 (1995).
[11] Barth, S. *Geol.Rundsch.* **82**, 640-651 (1993).
[12] Palmer, M.R. & Swihart, G.H. in *Reviews of Mineralogy, Boron: Mineralogy, Petrology and Geochemistry*, E.S. Grew and L.M. Anovitz, Eds. (Mineralogical Society of America, Washington, 1996), Vol. **33**, pp. 709-744.
[13] Chaussidon, M. & Libourel, G. *Geochim. Cosmochim. Acta* **57**, 5053 (1993).
[14] Palmer, M.R., London, D., Morgan VI, G.B. & Babb, H.A. *Chem. Geol.* **101**, 123-129 (1992).
[15] Zindler, A. & Hart, S. A. *Rev. Earth Planet. Sci.* **14**, 493-571 (1986).
[16] Devey, C.W., Albarede, F., Cheminee, J.-L., Michard, A., Muhe, R. & Stoffers, P. *J. Geophys. Res.* **95**, 5049-5066 (1990).
[17] Woodhead, J.D. & Devey, C.W. *Earth Planet. Sci. Lett.* **116**, 81-99 (1993).
[18] Hemond, Ch., Devey, C.W. & Chauvel, C. *Chem. Geol.* **115**, 745 (1994).
[19] Woodhead, J.D., Greenwood, P., Harmon, R.S. & Stoffers, P. *Nature* **362**, 809-813 (1993).
[20] Eiler, J.M., Farley, K.A., Valley, J.W., Stolper, E.M., Hauri, E.H. & Craig, H. *Nature* **377**, 138-141 (1995).
[21] Palmer, M.R. & Slack, J.F. *Contrib. Mineral. Petrol.* **103**, 434-451 (1989).
[22] Chaussidon, M., Robert, F., Mangin, D., Hanon, P. & Rose, E. *J. Geostand. Geoanalysis* (in press).

Petrological and geochemical studies of individual eruptions on La Palma: the importance of detailed mapping and stratigraphic control in petrogenetic studies.

Day, S.J.[1,2], Gravestock, P.[2] & Carracedo, J.C. [2,3]

[1] *Greig Fester Centre for Hazard Research, Department of Geological Sciences, University College London, Gower Street, London WC1E 6BT, Great Britain.*
[2] *Department of Geography & Geology, Cheltenham & Gloucester College of Higher Education, Francis Close Hall, Swindon Road, Cheltenham GL50 4AZ, Great Britain.*
[3] *Estacion Volcanologica de Canarias, Instituto de Productos Naturales, CSIC, Aptdo. Correos 195, 38206 La Laguna, Tenerife, Spain.*

Most studies of oceanic island volcanic suites do not consider compositional variation within the products of single eruptions. Perhaps the most extreme example of such variation is in the 1730-36 eruption of Lanzarote, Canary Islands (part of the "post - erosional" activity on Lanzarote), which produced a range of rock compositions from nephelinite through to olivine tholeiite (Carracedo et al. 1992). Here we consider variations within historic eruptions of the intensely active "shield - building - stage" Cumbre Vieja volcano, La Palma, which typically last 1 - 2 months. The two eruptions we have investigated to date are the 1949 and 1585 eruptions, but the same methodology is applicable to other historic and sub - historic eruptions. The first task is detailed mapping of the vent areas of the eruption and reconstruction of a detailed eruptive history, also using eyewitness accounts if these are available. A precisely located suite of samples from all stages of the eruption is then collected. Each sample is assigned a <u>sequence number</u>, defined as:

Sequence Number = 1 + (number of samples known to be older than the sample).

Using sequence numbers defined in this way expresses as precise an order of eruption as is justified by the mapping: note that some samples may have the same sequence number.

The 24th June - 4th August 1949 eruption of the Cumbre Vieja (Bonelli Rubio 1950) is of particular interest since it produced incipient instability of the western flank of the volcano, marked by intense seismicity and the appearance on July 1st or 2nd 1949 of surface ruptures associated with an inferred detachment fault under the western flank of the volcano (Day et al., this volume). It is of great interest to know how these structural events are related to the magmatic evolution of the eruption. A simplified map of the eruption vents and the proximal areas of lava flows is shown in Fig. 1. Three phases of magmatic activity are recognised:

1. Early activity at the crest of the Cumbre Vieja ridge: eruption of mixed lithic breccia and juvenile spatter from the Duraznero vent (24th June - 6th July). Formation of the surface ruptures of the incipient detachment fault took place in this period but does not seem to have produced any immediate changes in the style of eruptive activity.
2. Fissure eruption at the San Juan eruptive centre from 8th July to 26th July. This eruptive centre appears to have initially taken the form of small scoria cones or hornitos spaced out along a 600 m long array of en echelon fissures, which erupted a'a lavas and lapilli. Soon after the start of the eruption, however, the fissure system extended further downslope to produce additional en echelon fissures, while the upper part of the fissure system collapsed to produce an elongate sinuous trough up to 100 m wide and 30 m deep. Explosions associated with the collapses produced mixed spatter - coarse lithic breccia cones

around the vents which were then breached. The bulk of the San Juan lava flows, which eventually reached the coast, were erupted from vents on the floor of this trough. During this period there was no magmatic activity at the crest of the Cumbre Vieja, but violent phreatic explosions on 12th July produced the Hoyo Negro pit crater.

3. Renewed activity at Duraznero (July 30th - August 4th): a N-S trending fissure erupted lava and spatter in intense Strombolian activity, producing a welded spatter blanket around the vent, distal lapilli deposits and mainly clastogenic lavas which descended the eastern flank of the volcano.

Petrological and geochemical data for samples collected from products of all three phases of the eruption indicate that they form two successive groups, as follows:

Group I rocks were erupted in the first phase of activity on the summit ridge and from the San Juan vents up until the collapse of the eruptive fissure system. The last Group I sample (Sequence Number = 8) was taken from the mixed spatter and lithic ejecta deposit formed at the time of the collapse around one of the new, lower vents. These rocks contain abundant large augite phenocrysts, sparse olivine phenocrysts and sparse, small gabbroic xenoliths and pyroxene and feldspar xenocrysts.

Group II rocks were erupted both from the San Juan vents, in the latter part of the second phase of activity, and from the Duraznero vents in the last phase of the eruption. These rocks have olivine and pyroxene phenocrysts (the former more abundant than in the Group I rocks) and a sparse but varied xenolith population which includes dunites, Cr - diopside wehrlites and augite - rich pyroxenites and alkali amphibolites as well as gabbros and partially fused syenites. The gabbroic xenoliths include foliated two - pyroxene gabbros, inferred to be from the oceanic crust.

Selected geochemical plots for these rocks are shown in Fig. 2. The Group I rocks are relatively evolved tephrites which are characterised by an extremely homogenous composition, suggesting derivation from a single unzoned magma body which crystallised olivine pyroxenite cumulates. In contrast the Group II rocks are basanites with more varied compositions. Some Group II rocks were contaminated by mixing with Group I magma but a general feature of this group is a wider variation in composition (especially in incompatible element ratios). We infer that rather than being derived from a single magma body the Group II magmas were stored in a plexus of small partially isolated magma bodies (dykes or vein complexes). The xenolith populations suggest that the Group I magma reservoir was within the oceanic crust whilst the Group II magma bodies were within the oceanic lithosphere. The lack of correlation between the erupted magma compositions and the phases of the eruption implies that both groups ascended through a single conduit from which the feeders of the various surface vents branched off at relatively shallow depth, consistent with the interpretation that the distribution and orientation of these vents reflects near -surface, instability - related deformation (Day et al., this volume).

The 1585 Jedey eruption is even more complex than the 1949 eruption. Although it lasted little more than a month, at least 12 discrete vents developed along a set of three en echelon fissures. The central fissure was characterised by eruption of basanitic, intermediate hybrid and phonolitic magmas which formed two large partially emergent cryptodomes; while the other two fissures only erupted basanitic magmas. Our studies of this eruption are presently at an early stage but they indicate that the basanitic magmas ascended from mantle depths and intersected and reactivated a small shallow phonolitic magma body.

References.

BONELLI RUBIO, J.M. 1950. *Contribucion al estudio de la erupcion del Nambroque o San Juan (Isla de La Palma).* Madrid, Instituto Geografico y Catastral, 25 pp.

CARRACEDO, J.C., RODRIGUEZ BADIOLA, E. & SOLER, V. 1992. The 1730 - 1736 eruption of Lanzarote, Canary Islands: a long, high - magnitude basaltic fissure eruption. J. Volc. Geotherm. Res. 53, 239 - 250.

Fig. 1. Faults and vents of the 1949 eruption of the Cumbre Vieja volcano, La Palma, with dates of activity. Map based on data from Bonelli Rubio (1950) and detailed mapping by S.J. Day.

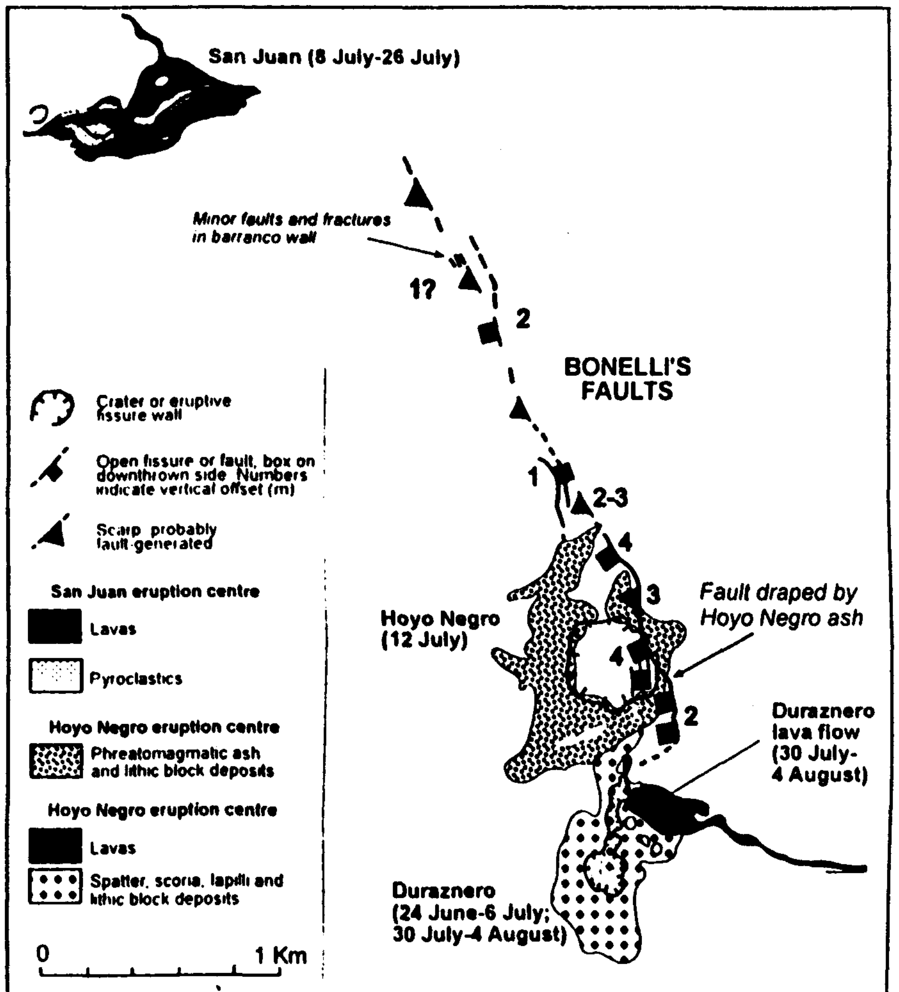

Fig. 2. Plots of compositional data against sequence number (see text for definition of sequence number) for rocks of the 1949 eruption. Note sharp compositional change at time of collapse of the early San Juan vents (sequence number = 9).

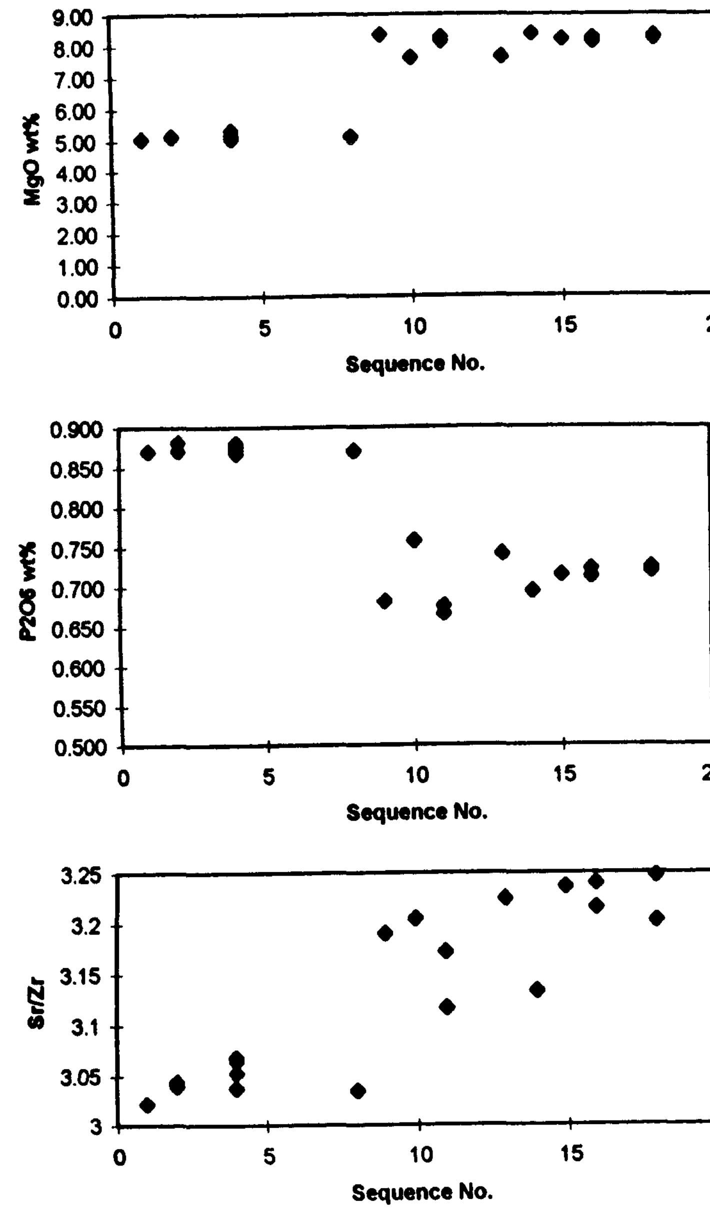

Peridotite xenoliths, olivine-pyroxene megacrysts and cumulates of the Bandama Volcanic Complex (Gran Sanarla, Spain): genesis in the oceanic lithosphere

Mangas, J. (1); Clocchiatti, R. (2); Perez-Torrado F.J. (1) and Massare, D. (2)

(1) Departamento de Fisica-Geologia. U.L.P.G.C. Apdo. 550, 35080 Las Palmas de Gran Canaria, Spain.

(2) Laboratoire Pierre Sue, C.E. de Saclay, 91191 Gif sur Yvette Cedex, France.

Geologic information on the deeper parts of the oceanic lithosphere is difficult to obtain directly. Mantle and crustal xenoliths carried to the surface by basaltic melts represent one very important source of such information. Thus, our research is based on the study of 18 samples of peridotite xenoliths and olivine-pyroxene phenocrysts, megacrysts and cumulates from pyroclastic deposits of Bandama volcanic complex (Gran Canaria), and 2 samples of lava flows associated to this complex. We have combined data from the volcanological study and the electron microprobe and microthermomertric analysis of minerals, and melt and fluid inclusions, and the bulk-rock analysis of these samples to define some characteristics of magmatism which gave rise to the Bandama volcanoes.

Gran Canaria island is at the centre of the Canary Archipielago. Geophysical data indicate the occurrence of an oceanic-type basement underneath the island modified by massive intrusions with a Moho depth of 13 kms (Fig. 1). Magmatic activity of this island began in the Miocene with an episode of submarine volcanism and their subaerial volcanism have been divided over three main episodes: Old Cycle (Miocene, 14.5-8.5 Ma), Roque Nublo Cycle (Pliocene, 5.5-2.7 Ma) and Recent Cycle (Plio-Quaternary, 2.9-Present).

The quaternary volcanic complex of Bandama is some 10 Kms to the southwest of the city of Las Palmas de Gran Canaria and is made up of a volcanic caldera (La Caldera de Bandama) and a strombolian cone (El Pico de Bandama). Bandama eruption began in the area of La Caldera with a strombolian episode which produced deposits of fall and a basanite lava flow. Later, the magma in the counduit mixed periodically with groundwater, producing both phreatomagmatic eruptions with base surge deposits and strombolian eruptions with fall deposits. Although the volcanism episodes were to continue in the area around La Caldera, most of these manifestations were centred around the NW area of the fisure, producing the strombolian cone known as the Pico Bandama, abundant deposits of fall in the surrounding areas and an intracanyon flow. The genesis of La Caldera is posterior to El Pico and was produced as a result of the last effusive-explosive eruptions and the eventual collapse of the volcanic cone located to the SE of the fissure. Around the wall of La Caldera, the materials to be found from the floor to the roof, are the following: a) phonolites and conglomerates of Miocene age; b) ignimbrites from the Roque Nublo Cycle and c) pyroclast deposits and a lava flow of the Bandama volcanic complex.

Lava flows of Bandama have thick below 5 m. and these show basanite composition (SiO_2 41.8% and sum of the alkalis 3.8%) and porphyritic texture with phenocrysts and microcrysts of olivine, pyroxene and oxide (spinel and ilmenite) with sizes under 2 cm. Micro~robe analvsis of these minerals reveal olivine Fo_{70-89} (Ni/Ca ratio: 0.3-2.2) and clinopyroxene Wo_{40-52}, En_{27-54}. Spinel appear as subordinate minerals and as inclusions in phenocrysts and have Cr203 content between 36.4 and 40.2%. These analysis show variations of composition between the cores and rims of some phenocrysts and reveal different crystal generations.

Phreatomagmatic eruptions form base surge and explosive breccia rich in lithics (such as phonolites, tephrites and alkaline basalts) deposits with spectacular volcanic-sedimentary structures (imbricated channels, sand waves, bomb impacts, etc.). However, the strombolian volcanism is characterized by the presence of fall deposits, containing peridotite xenoliths and olivine-pyroxene megacrysts and cumulates with sizes under 7 cms. Microprobe analysis of these minerals show:

- phenoscrysts and megacrysts of olivine Fo_{77-89} (Ni/Ca: 0.5-2.2 and spinel with Cr_2O_3: 34-36.3%), clinopyroxene Wo_{34-52}, En_{33-51} (spinel with Cr_2O_3: 20.8-23.4%) and kaersutite (destabilized to fassaite -- Wo_{54-57}, En_{31-34}--, rhönite, olivine and subsaturated melt).

- Olivine-clinopyroxene cumulates (dunite, werhlite, clinopyroxenite with olivine, clinopyroxenite) with olivine Fo_{80-87} (Ni/Ca: 0.6-2.1 and spinels with Cr_2O_3: 14-31.2%) and clinopyroxene Wo_{39-51}, En_{36-55} (spinels with Cr_2O_3: 10-16.1 %) .

- Peridotite xenoliths (dunite and Iherzolite) with olivine Fo_{83-89} (Ni/Ca: 1-20 and spinels with Cr_2O_3: 13.2-32.8%), orthopyroxene Fo_{84-85} (spinels with Cr_2O_3: 31.3%) and clinopyroxene Wo_{40-44}, En_{48-50}.

Melt inclusion study in olivine from fall deposits and lava flows show SiO_2 content: 35-44%, sum of alkalis: 4.1 -7% and high values of S and Cl (<5,500 and <980 ppm, respectively). The melt inclusion compositions are different from the lava whole rock and the intersticial melt. The melting temperatures (Tm) of melt inclusions range between 1,060 and 1,260°C.

Microthermometric study of melt and fluid inclusions in olivine and clynopyroxe shows pure, or almost pure, CO_2 trapped in the gas bubble. These carbonic fluids reveal a wide range of Th of CO_2 (-39 to 31 °C) in liquid, indicating minimun depths of mineral formations (at Tm: 1200°C) between 12-18 Km for olivine-pyroxene megacrysts, 4.5-27 Km for olivine-pyroxenes cummulates, 10.5-25 km for peridotite xenoliths, and 7.5-33 Km for olivine phenocrysts of lava flows (Fig. 1).

The minerals which make up the megacrysts, cumulates and xenoliths of Bandama reveal reaction rims with the lava which are reequilibrated with the magma. These minerals display textural, mineralogical, microthermometric and chemical composite characteristics from the ratio to minerals of the lava flow and thus we can conclude that those minerals were originated under different conditions.

From the aforementioned data, we can conclude that the magma which gave rise to the Bandama volcanic complex ascended from upper mantle to the surface (-33 km to 0.5 km), trapping peridotite xenoliths, olivine-pyroxene megacrysts and cumulates of different origins from the upper mantle and the oceanic crust (-27 to -4.5 km) (Fig. 1).

Gran Canaria Island

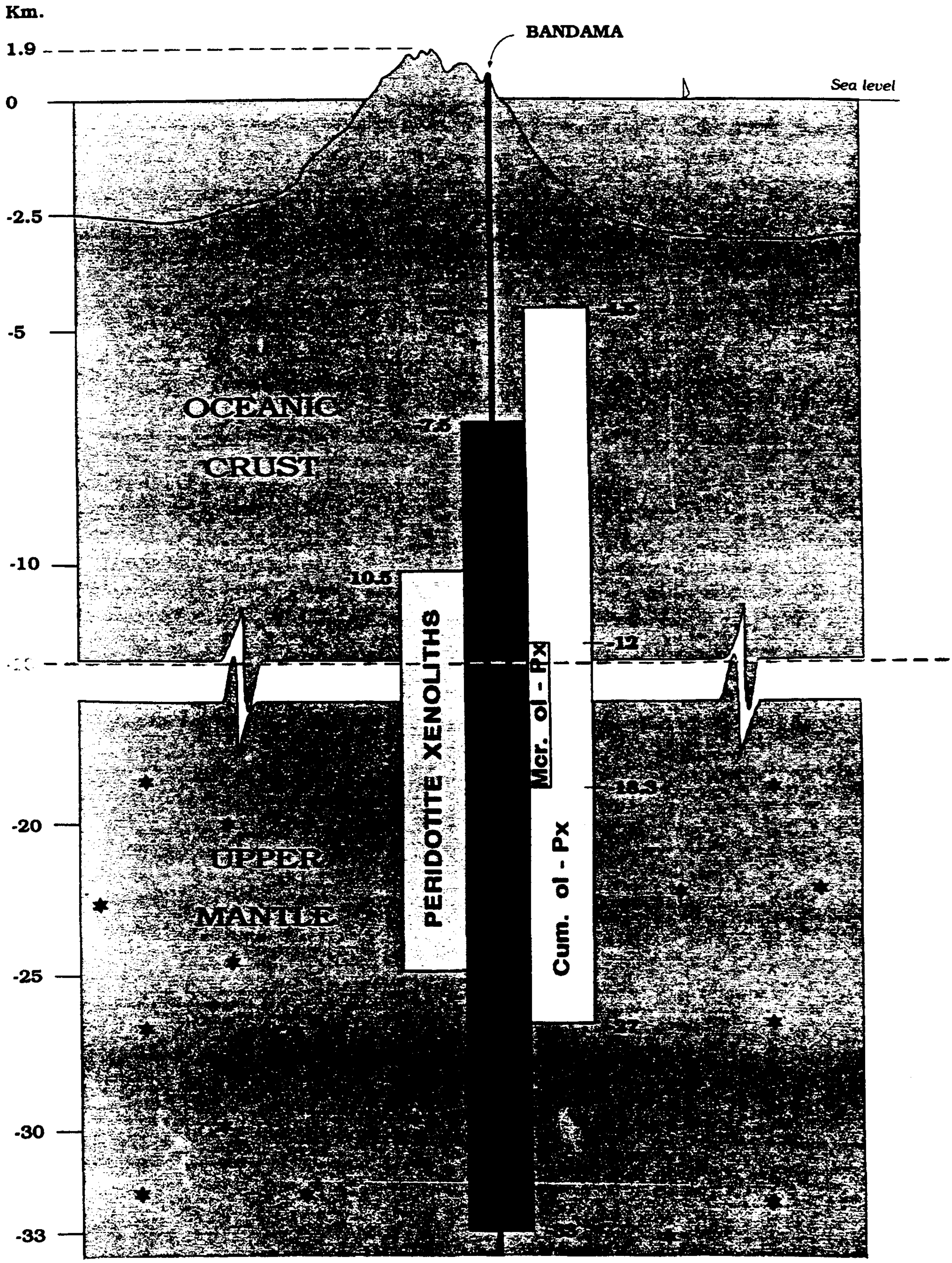

Figure 1. Interpretative scheme of depth calculated by CO_2-rich fluid inclusions trapped in olivine and pyroxene from lava flows, peridotite xenoliths and megacrysts of Bandama.

Alkali basalt - trachyte association from Raiatea island (Society archipelago, French Polynesia)

Sylvain Blais[1], Gerard Guille[2], René C. Maury[3], Hervé Guillou[4] and Catherine Chauvel[1]

[1]*Geoscienccs Rennes, CNRS-UPR4661, Uyniversité de Rennes 1, 35042 Rennes Cédex, France.*
[2]*CEA, DASE LDG, B.P 12, 91680 Bruyéres le Chatel, France.*
[3]*URA CNRS 1278, U.B.O, BP 809, 29275 Brest, France.*
[4]*Centre des Faibles Radioactivités, 91198 Gif-su-Yvette, France.*

Raiatea island lies 350 km NW of the present Society hot spot. It consists of two coalesent structures: the shield volcano in the south and the trachyte - capped Temehani ridge in the notth.

The shield volcano consits in a 1000 m thick pile of lava flows of exclusively basaltic composition. These alkali basalts were emplaced as metic lava flows during the main effusive volcanic phase (2.7 to 2.5Ma). The collapsed central part ofthe shield volcano, the Faaroa caldera has a mean diameter of 8 km and is opened eastward.

The Temehani ridge is a N-S trending plateau overlying the northern slopes of the shield volcano, and consists in trachytic lava flows. Four trachytic domes occur to the east of the Temehani ridge. They probably were emplaced along a fracture subparallel to the ridge. Trachytic lava flows and domes have similar chemical and mineralogical compositions.

Chemical analyses show that an important gap exist between alkali basalts and trachytes. However, major and trace element variations are consistent with an origin of the trachytes by crystal fractionation.

New K-Ar datings were obtained on the groundmass of fresh (L.O.I. <2%) basaltic and trachytic lavas. The results range from 2.75 to 2.52 Ma for the basaltic flows and from 2.54 to 2.44 Ma for both the trachytic flows and from 2.54 to 2.44 Ma for both the trachytic flows and the trachytic plugs. There is therefore no significant time between the emplacement of the latest basalts and that of the trachytes, which erupted after the shield building event.

Geochronological, structural and morphological constraints in the genesis and evolution of the Canary Islands

*J.C. Carracedo[1,2], S. Day[2], H. Guillou[3], E. Rodríguez Badiola[4], J.A. Canas[5] and F. J. Pérez Torrado[6]

[1]*Estación Volcanológica de Canarias, CSIC, La Laguna, Tenerife, Canary Islands, Spain*
[2]*Cheltenham & Gloucester College of Higher Education, Cheltenham, U.K. and Greig Fester Center for Hazard Research, University College London, UK.*
[3]*Centre des Faibles Radioactivités, CEA-CNRS, Gif sur Yvette, France*
[4]*Museo Nacional de Ciencias Naturales, CSIC, Madrid, Spain*
[5]*ETSICC, Universidad Politécnica de Cataluña, Spain*
[6]*Facultad de Ciencias del Mar, ULPGC, Las Palmas, Gran Canaria, Canary Islands*

1. Introduction

The Canarian Archipelago is a group of volcanic islands on a slow-moving oceanic plate, close to a continental margin. The cause of the archipelago is controversial: a hotspot or mantle plume, a zone of lithospheric deformation, a region of compressional block-faulting or a rupture propagating westwards from the active Atlas Mountains fold belt have been proposed by different authors. However, comparison of the Canarian Archipelago with the prototypical hotspot-related island group, the Hawaiian Archipelago, reveals that the differences between the two are not as great as had previously been supposed on the basis of older data.

Concrete evidence for the relative roles of regional tectonics and mantle plumes in the genesis of the islands may come from large-scale seismological and structural studies of the deep structure of the surrounding oceanic crust and lithosphere and from constraints provided by geochemical and isotopic features of the magmas involved. Notwithstanding, it is interesting to analyse, as we do here, the existing geological information from the islands themselves, especially the timing of eruptive activity in the islands and their morphological and structural features. This may help to establish some clear constraints that may narrow down the range of acceptable models for the genesis and development of the Canary Islands.

2. Age of the Canarian volcanism

The extensive K/Ar dating carried out in the Canary Islands, with about 400 K/Ar ages published from lava flows, gives a remarkable control of the subaerial volcanic history of this archipelago. The age of the earliest exposed volcanic rocks in each island as well as the periods of volcanic activity and alternating gaps are clearly defined (Fig. 1A).

However, detailed geochronological work using accurate dating techniques and cross-checking against palaeomagnetic reversals has proved that some previous ages of these islands have substantial errors, sometimes of several million years. Such errors are especially significant in the islands of La Palma and El Hierro, where most of the subaerial lavas are of Quaternary age (Guillou et al., 1996; this volume). Recent studies have shown that ages from stratigraphic sequences, consistent with the general volcanic stratigraphy and the corresponding polarities of the standard geomagnetic polarity time-scale, are the most reliable (Carracedo et al., this volume; Guillou et al., this volume).

Two groups of islands can nevertheless be defined using the published ages: 1) Lanzarote, Fuerteventura, Gran Canaria and La Gomera, with subaerial volcanism 12 ma or older and well-defined hiatuses in the volcanic activity, and 2) Tenerife, La Palma and El Hierro, with exposed volcanics 7.5 ma or younger and essentially uninterrupted volcanic histories.

The presence of a hiatus in volcanic activity occurs only in the older islands (Middle-Lower Miocene) of Lanzarote, Fuerteventura, Gran Canaria and La Gomera (Fig. 1A). In contrast, the volcanic activity has continued uninterrupted in the younger islands (Upper Miocene-Quaternary) of Tenerife, La Palma and El Hierro.

Similar interruptions are observed in the prototypical hotspot islands of the Hawaiian Archipelago, where they constitute a key stratigraphic feature separating the shield-stage volcanism from the post-erosional or rejuvenated-stage volcanism (Walker, 1990). We may conclude that, as in the Hawaiian Islands, the periods of volcanic quiescence allow the separation of the Canary Islands into different categories (Fig. 1B): a) the islands of Lanzarote, Fuerteventura and Gran Canaria, at present with post-erosional, rejuvenated-stage volcanism; b) the island of La Gomera, presently in the gap stage, and c) the islands of Tenerife, El Hierro and La Palma, in the pre-gap shield stage. This time-related division may be preferable to the generally used "eastern" and "western" subdivision of the Archipelago, since it recognises the anomalous location of the older island of La Gomera in the middle of the western Canaries group.

3. Contrasting structural features in the eastern and western Canaries?

Recently obtained onshore and offshore geological information in the younger islands of Tenerife, La Palma and El Hierro [Holcomb and Searle, 1991; Carracedo, 1994; Carracedo et al., this volume; Watts and Masson, 1995; Guillou et al., 1996; Guillou et al., this volume; Day et al., this volume) has revealed volcanological, structural and geomorphological features (triple-armed active rifts and giant landslides) typical of hotspot islands. These features are less evident in the older Canaries.

The apparent contrasting structural features observable in the younger and older Canaries may reflect only different stages of development of the islands. We consider the multiple rifts and giant landslides to be characteristic of the shield-stage of development, both in the Canaries and other intraplate oceanic islands of hotspot-related origin. These structures may be present in the older, post-erosional stage islands (Ancochea et al., 1996; Stillman, this volume). However, modifications during the erosional gaps, that in the Canary Islands are considerably longer than in most of the other archipelagos of similar origin, make their recognition difficult. At similar phases of evolution the islands appear to have similar structural features.

4. Has a hotspot generated the Canary Islands?

The association of the Canarian archipelago with an asthenospheric plume has been proposed repeatedly. In our model, the first volcanic manifestations of this hotspot would have been localised at the continental-oceanic boundary (COB) west of Fuerteventura. Sediment thickness at continental margins exceeding 10 Km should be a major factor in modifying the strength of the lithosphere, since lower overburden and conductivity of the sediments may be associated with significant weakening of the lithosphere. Volcanism may have propagated to the NE along the continental boundary, forming the Fuerteventura-Lanzarote ridge. The assumption that the Canarian archipelago progresses from Lanzarote to Fuerteventura and oceanwards seems inconsistent with the presently accepted geochronological and geological information, and probably reflects an unfounded link between the Canaries and the Atlas tectonism (Anguita and Hernán, 1975). The island of Fuerteventura is a lineation of volcanic complexes with similar oldest subaerial ages of about 20 ma (Ancochea et al, 1996), Lanzarote being simply a younger prolongation of Fuerteventura to the NE (parallel to the continental edge). Both islands are in fact separated by a narrow strait less than 100 m deep and form a single edifice. The initial spread of volcanism in the

Canaries would be, therefore, opposite in direction to the fracture propagating from the Atlas region postulated by Anguita and Hernán (1975).

Zones of high seismic attenuation (Canas et al., 1995) at the western end of the archipelago indicate the presence of an asthenospheric anomaly, and may be direct evidence of the presence of the plume.

5. Alternation of volcanic activity between El Hierro and La Palma?

The detailed and precise dating of volcanic activity on these two islands, which have been the most active in the Canarian archipelago in the last 1 Ma, suggests that periods of intense volcanism on one island coincides with periods of relative inactivity on the other (Fig. 2). This alternation suggests that both islands may have a common magma source in the asthenosphere. A period of intense activity on one island culminates in a giant lateral collapse which is followed by a switch in the location of the most intense volcanism to the other island. We speculate that the switch may be caused by the unloading effect of the collapse, which would place the rebounding lithosphere beneath into horizontal compression and suppress upward migration of magma.

References

Anguita, F. and Hernán, F., 1975. A propagating fracture model versus a hot spot origin for the Canary Islands. Earth & Planet. Sc. Lett., 27, 1: 11-19.

Ancochea, E., Brändle, J.L., Cubas, C.R., Hernán, F. and Huertas, M.J., 1996. Volcanic complexes in the eastern ridge of the Canary Islands: the Miocene activity of the island of Fuerteventura, J. Volcanol. Geotherm. Res., 70, 183-204.

Canas, J.A., Pujades, L.G., Blanco, M.J., Soler, V. and Carracedo, J.C., 1994. Coda-Q distribution in the Canary Islands. Tectonophysics, 246: 245-261.

Carracedo J. C. 1994. The Canary Islands: An example of structural control on the growth of large oceanic-island volcanoes. J. Volcanol. Geotherm. Res., 60, 3-4: 225-241.

Carracedo, J.C., Day, S.J., Guillou, H. and Gravestock, P., The later stages of the volcanic and structural evolution of La Palma, Canary Islands: The Cumbre Nueva and Cumbre Vieja Volcanoes (this volume).

Day, S.J., Carracedo, J.C., Guillou, H., Pérez Torrado, F.J., Fonseca, J.F.B.D., Heleno da Silva, S.I.N. and Gravestock, P. Recognising incipient instability and lateral collapse precursors in steep-sided oceanic island volcanoes (this volume).

Guillou, H., Carracedo, J.C., Pérez Torrado, F. and Rodríguez Badiola, E., 1995. K-Ar ages and magnetic stratigraphy of a hotspot-induced, fast grown oceanic island: El Hierro, Canary Islands. J. Volcanol. Geotherm. Res., 73: 41-155.

Guillou, H., Carracedo J. C. and Day, S.J., Unspiked K-Ar dating of volcanic rocks from El Hierro and La Palma, western Canary Islands (this volume).

Holcomb, R.T. and Searle, R.C., 1991. Large landslides from oceanic volcanoes. Marine Geotechnology, 10: 19-32.

Walker, G.P.L., 1990. Geology and volcanology of the Hawaiian Islands. Pacific Sc., 44: 315-347.

Watts, A. B., Masson, D. G. 1995. A giant landslide on the north flank of Tenerife, Canary Islands. J. Geophys. Res., 100: 24487-24498.

Stillman, C., The episodic growth and partial destruction of pre - shield-lava Fuerteventura (this volume).

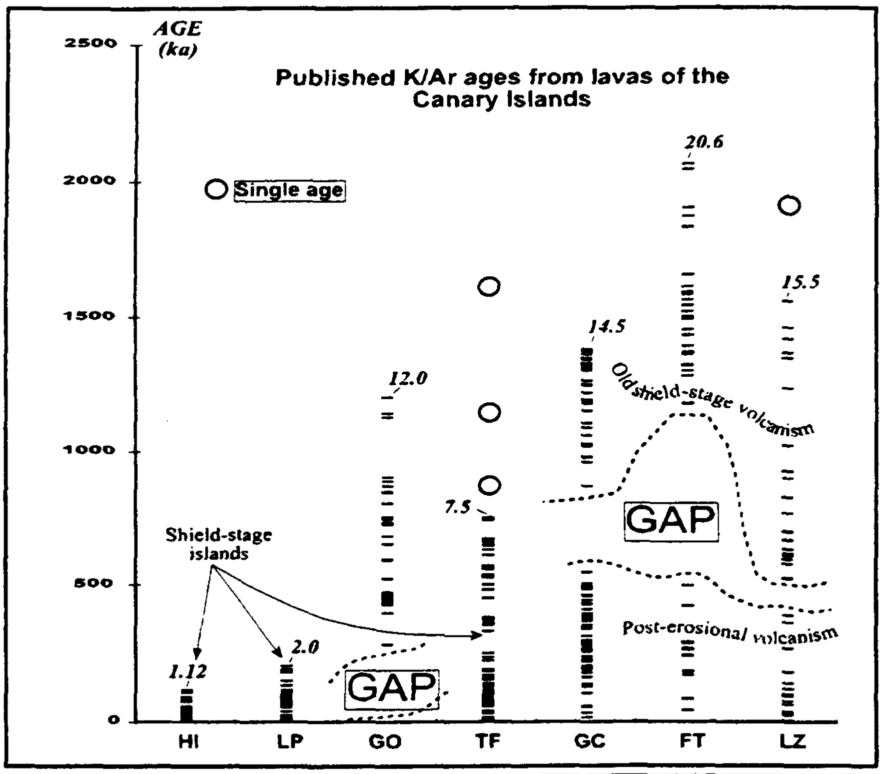

Fig. 1A

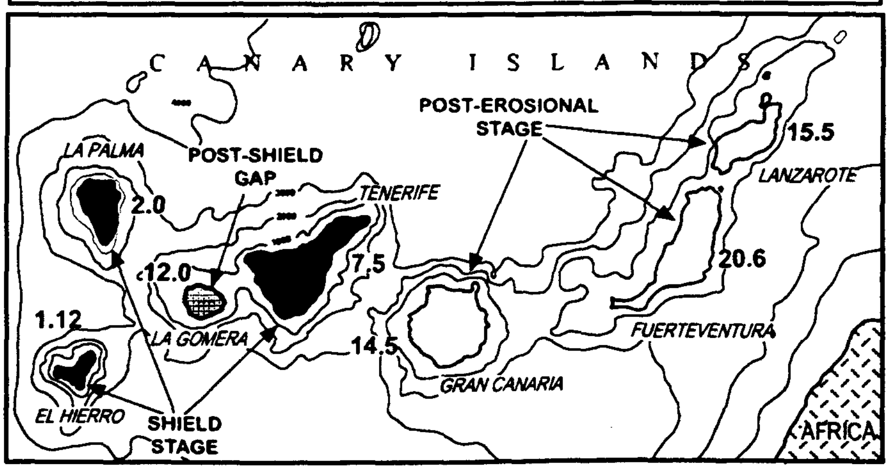

Fig. 1B

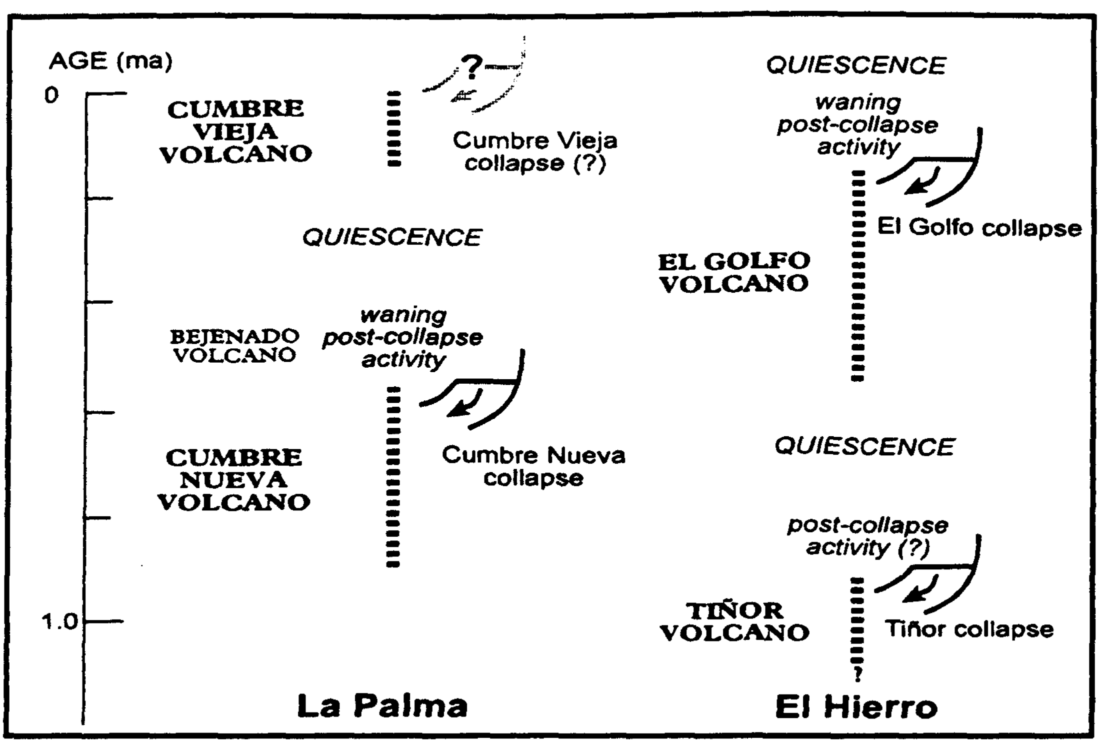

Fig. 2

The feeding system of the historical eruptions in Tenerife.

M.C. Solana[a], C.R.J. Kilburn[b], A. Aparicio[a]

[a]*Dpto, de Volcanologia, MNCN-CSIC, Madrid.*
[b]*Dpt. of Geological Sciences, UCL, London.*

Tenerife is the biggest of the volcanic Canary Islands. With a surface area of some 2,000 sq. km. it has shown a wide range of activity, from quiet lava effusions to caldera-forming eruptions. Studies of its historic activity suggest that the volcano is being fed by subcrustal reservoirs, from which magma ascent may be triggered by deep-seated instabilities, as much as 60 km below the floor of the Atlantic.

Tenerife rests on oceanic crust 11-20 ktn thick. Its main construct is the Teide-Pico Viejo stratovolcano, which rises 3,700 m above sea level (c. 6,700 m above the ocean floor) and 1,700 m above the floor of Las Cañadas caldera. The Teide-Pico Viejo complex lies close to the intersection of the island's dominant volcanotectonic lineaments (today apparent as ridges, or "dorsales"): La Esperanza (ENE-WSW) to the northeast and Teno (NW-SE) to the nordlwest.

Holocene volcanism has been mostly effusive, except for the subplinian eruption, 2,000 years ago, of Monta~a Blanca in the Teide-Pico Viejo complex. At least five eruptions have been recorded since European colonisation in the 15th Century (Fig. 1): Taoro (15th Century), the Siete Fuentes-Fasnia-Arenas (Arafo) sequence in 1704-1705, Garachico (1706), Chahorra (1798) and Chinyero (1909). All have been effusive with strombolian activity and, in some instances, also with extremely violent explosive episodes due to the interaction of magma with water in aquifers. The volumes erupted during each sequence lie in the range of 10-70 million cu.m. Apart from Taoro's activity, the eruptive vents have been located along one of the principal dorsal ridges. Guanche (the pre-Hispanic islanders) tradition and fragmentary accounts from the 15th-16th Centuries further suggest that persistent (perhaps strombolian) activity may have continued at the summit of El Teide until the 1600's.

The historic magmas belong to a differentiation sequence from basanite to phonolitic tephrite. The evolution towards phonolitic tephrites is accompanied by a decease in the size and number of phenocrysts, and also by the appearance of amphibole as a phenocryst phase. The basanites are porphyritic with 8-20 vol% olivine (Fo_{19-81}), 10-25% clinopyroxene (Di-Wo) and opaque phases (magnetite-ulvospinel), set in a matrix of acicular plagioclase (~0.3 mm long) and microcrystals of olivine, pyroxene and opaque minerals; the olivine and pyroxene phenoctysts are typically about 1mm across, and rarely larger than 3 mm. The tephrites are virtually aphyric with occasional phenocrysts of subidiomorphic pyroxene (Di-Wo) and less than 5% of a kaersutitic amphibole that normally displays well~developed reaction rims (sometimes penetrating the whole crystal) and which occasionally includes subidiomorphic olivines of mm size; common phenocryst dimensions are about 1 mm for pyroxene and 2 mm for amphibole. The tephritic groundmass consists of oriented, acicular plagioclase and amphibole (0.2-0.3 mm), together with opaque phases, in an essentially glassy matrix.

The acicular nature of groundmass plagioclase indicates disequilibrium growth, as might be expected from the rapid ascent of magma from its feeding reservoir. Barometric calculations from both bulk chemistry and phenocryst assemblages are consistent with crystallization depths of 35-65 km (1.1-2.0 GPa) for the basanites and 20-27 km (0.6-0.8 GPa) for the phonolitic tephrites. These values indicate subcrustal depths for Tenerife's historical magma reservoirs, the phonolitic magmas possibly evolving while trapped at the base of the crust.

Study of the 18th Century lavas has revealed chemical zoning for at least the early stages of individual eruptive sequences. During the 1760 Garachico eruption, the composition of newly-emerging magma changed with time from basanite to phonolitic tephrite; later eruptive stages effused both basanites and more-evolved magmas, but it has not yet been possible to determine the relative ages of these products. The key feature is that both eruptive sequences first emitted basanites with crystallization depths of about 60-65 km, followed by more evolved products with crystallization depths shallower by 10 km or more (to depths of 45-50 km in 1704-1705, and to 20-25 km in 1706).

Four simple situations can be envisaged for yielding the observed initial zonation of erupted magmas. Assuming Tenerife to be fed by a single zoned reservoir, a sufficiently forceful withdrawal might allow deeper magma to push its way through an outlet at the top of the chamber ahead of shallower magma, which can only escape later as the driving pressure declines. Alternatively, (a) the feeding fissure might extend from the side of a zoned magma chamber, allowing the early withdrawal of deep magma (Fig 2a), or (b) a batch of deep-level magma may penetrate the reservoir, traversing the chamber before its existing magma escapes (Fig. 2b). All these possibilities have been proposed for other volcanic systems. Applied to Tenerife, however, the required range of depths for the magma (say, 10-15 km) and volumes emitted (nominally 20-65 million cu.m.) suggest that, unless a much greater volume of magma was also intruded into the crust, the effective area of magma withdrawal was not more than a few hundred square metres. Qualitatively, the fluid dynamical requirements for such finger-like withdrawal of magma appear to be prohibitive.

The fourth interpretation (Fig. 2c) views the magmatic feeding zone as a collection of small magma bodies distributed over depths from 25 to 65 km below the ocean floor. Although each body has a potential to ascend, those at greater depths are more easily disturbed by local instabilities. As the deeper bodies ascend, they disturb nearby magma bodies, setting in motion a train of magma batches. Deeper magma appears first at the surface simply because it was originally the first magma batch to start moving.

Whichever interpretation is preferred, data from Tenerife's historical lavas suggest that eruptions have been fed by magma rapidly ascending from subcrustal levels. It cannot be assumed, therefore, that a renewal of activity will be preceded by a long interval of precursory phenomena. At the same time, geophysical surveys seeking to detect the magmatic system might be well-advised to focus on depths greater than 20-25 km below sea level.

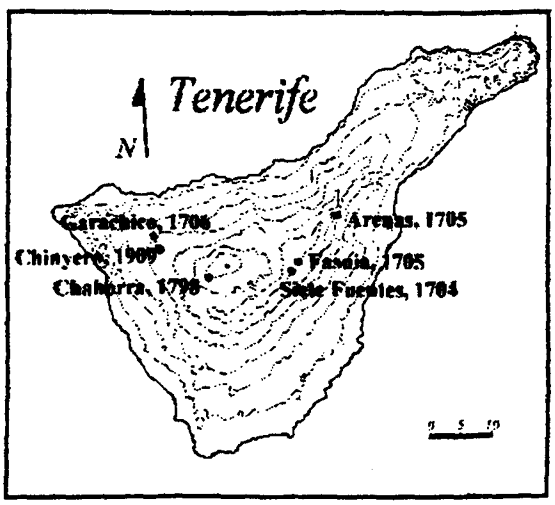

Fig. 1- ***Position and date of eruption of the historical volcanoes in Tenerife.***

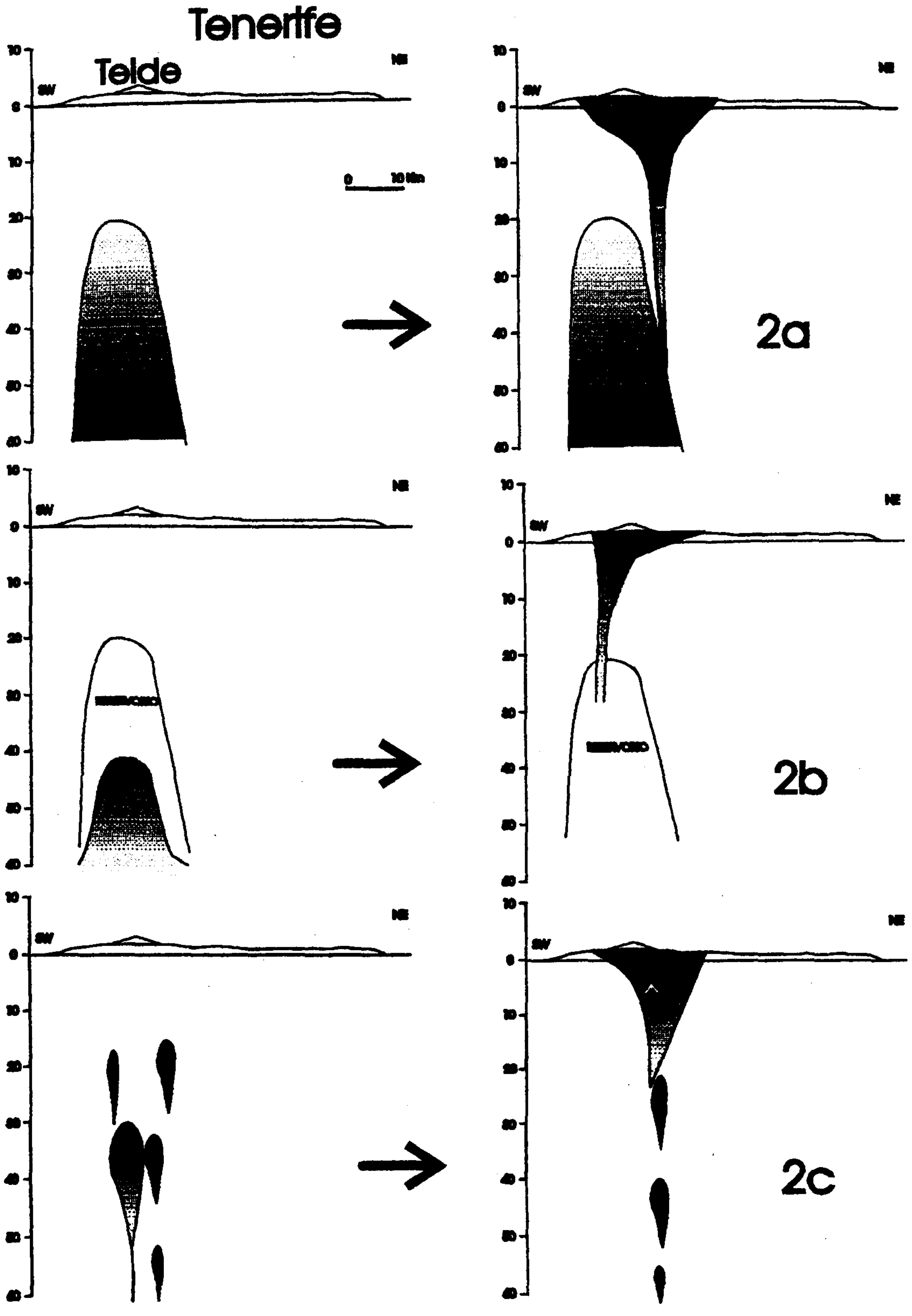

Fig. 2- *Three possibilities of magmatic feeding system for the historical eruptions in Tenerife. Note that, in all the cases, the shape and width of the reservoires are schematic.*

Resedimented syn-eruptive macroglobular basaltic peperites: lithofacies, textural characteristics and posible significance in immature intraplate oceanic islands

Domingo Gimeno and Cristina Segura

Dept. Geoquímica, Petrologia i Prospecció Geològica, Facultat de Geologia
Universitat de Barcelona. 08071 - BARCELONA - SPAIN

Peperites and peperitic facies are the product of magma-wet sediment interaction, and in most cases are produced in a shallow intrusive environment (a few meters to some tens of meters under the surface) (e.g., Kokelaar 1982; Busby-Spera & White 1987; Kano 1989; Hanson and Wilson 1993; and references therein). This interaction is mainly developed throughout fluidization of wet sediment, and is characterized by immiscibility (mingling, comingling) between magma and sediment.

A number of descriptions of intrusive pillows developed under a moderate pile of sediments exist (e.g. Snyder & Fraser, 1963; Kano 1991), sometimes being associated with peperitic facies (Branney and Suthren 1988; Assorgia and Gimeno 1994, etc.)

In order to clarify terminology, terms are used in the following manner: a/ intrusive pillow is a pillow or tubular-shaped body of magma growing from an igneous dyke or sill within wet, poorly consolidated sediment; b/ pillow, true pillow or pillow lava is a pillow-shaped or tubular-shaped body of magma growing in the magma-water or magma-ice interface, from dykes or lava flows; c/ peperite is a rock that consists of quenched and disrupted igneous material, mingled and comingled with the host sediment, that was previously fluidized in some degree.

We will focus on three examples from Miocene:

1.- The intrusive pillows and associated peperites of Guardia Marina beach in the Funtanazza trough (Central-western Sardinia island, Italy), made up of subalkaline basalts (Assorgia and Gimeno, 1994).
2.- The intrusive pillows and resedimented syn-eruptive macroglobular basaltic peperites of the E sector of Monte Arci volcanic center (Central Sardinia island, Italy) , that consist of calc-alkaline basalts with high alumina basalt affinity (Maccioni 1974, Beccaluva et al. 1974)
3.- The lava flows, resedimented syn-eruptive macroglobular basaltic peperites and minor associated intrusive pillows of Maçanet de la Selva sector (some 60 Km north of Barcelona, NE Spain), that consists of alkaline to transitional basalts (Araña et al. 1983, López Ruiz and Rodríguez Badiola 1985, Gimeno et al. in progress).

1.- At Guardia Marina volcanism developed in a beach environment, with some meter to some dozen to meters of water depth. Most of the outcrops show intrusive pillow with minor peperites associated, mainly of microglobular type (sensu Busby-Spera and White, 1987). Locally, pillows evolve to lateral digitations decimetric in size with associated peperites, and there exist stratiform expansions (some meter long, some decimeter thick) of densely packed microglobular peperites of unclear origin (intrusive or resedimented?).

2.- In the bottom of Monte Arci volcanic complex there exists a variety of basaltic submarine rocks, originated in a shallow shelf environment (some 100 m of water depth). In the SE sector of Monte Arci large (metric) intrusive pillows crops out showing well-developed glassy skin, clear margins and concentrical jointing, as well as marginal hyaloclastites included in the host, fluidized sediment. The hyaloclastites are interpreted as origined by peeling off of the glassy skin of intrusive pillow because of their evident fitting with the margin of pillows. In the W sector of Monte Arci sector, large amounts of resedimented basaltic massive hyaloclastites crop out, sometimes including large clasts of breccia pillow. In the NE sector, a singular set of sedimentary deposits occur. They are built of large clasts of glassy massive aphiric basalt floating in a fine-sized micritic limestone and palagonitic matrix. The strata are decimetric in thickness and look unorganized and matrix supported, with sedimentological characteristics assimilable to mass- and debris-flow deposits. The basalt clasts show irregular margins, with ameboidal, or even arborescent, margins and interdigitations with matrix. When observed closer, the basalt clasts have systematically borders including irregular drops of the matrix, in the same way that matrix contains, mainly around the clasts, irregular drops of basalt. We interpret these deposits like large-scale redeposited basaltic peperites, in the same way that Hanson and Wilson (1993) did with silicic ones. The large basaltic clasts might be considered macroglobular peperites and the milimetric or submilimetric drops of basaltic glass present in the matrix could be interpreted as microglobular peperites. We can suspect an origin for these deposits similar to the proposed by these authors, i.e. by lateral desestabilization of mounds mainly constituted by suboutcroping liquid magma intruding unconsolidated sediment. The misse-en-place of this magma in the mounds might be mainly like vertical feeder dikes and sills, giving place to intrusive pillows and peperites, and then been desestabilized and redeposited in the sedimentary environment while magma clasts preserved their plastic behaviour and hot temperature (capacity of subsequent reaction with sediments).

The Maçanet outcrops consists of a succession of basaltic lava flows that mainly constitutes the filling of a shallow lacustrine environment. Most of the observations have been done in the Asland quarry, placed west of the Maçanet village. The bottom of the quarry (june 1997) offers good ouccrops of massive alkaline basaltic lava flows, with good columnar jointing. These lava flows have some meter of thicknes and could be erupted in subaerial environment. A massive stratiform sedimentary deposit some meter thick is placed inmediately above of the aforementioned lava flows; it is constituted by massive and vesicular glassy (now devetrified and microcrystalline) clasts of basaltic rocks floating in a massive micritic matrix of limestone. The margin of basaltic clasts are similat to those described in NE Monte Arci sector (irregular, ameboidal, peperitic, etc.), the vesicles are systematically filled by micritic sediment, the matrix contains irregular drops of lava, and sometimes the basaltic clasts (massive or hignly vesiculated, indistinctely) are highly packed. The upper part of the quarry shows irregular massive lava flows (or domatic structures) and lacustrine micritic sediments. An irregular network of interconnected basaltic to basalt-andesitic sills and dikes intruded these sediments, giving up to macroglobular peperitic melanges and locally to intrusive pillows (best exposed in the quarry at may 1993). All the quarry has been subsequently intruded by vertical basaltic lava dikes. The massive deposit might be considered as resedimented macroglobular peperites and their origin in a similar way to the Monte Arci one.

These type of resedimented syn-eruptive volcaniclastic deposits have been scarsely described, even in recent books (see f.i. McPhie, Doyle and Allen 1993), and we can suspect that can be important both in continental lacustrine environments highly controled by tectonics (type Maçanet) and in shallow marine environments (f.i., in oceanic islands, in the transition from submarine emergent to shield building stage). If the percentual of non-volcanic clasts in the host sediments is poor this fact can higly difficult the recognition of these deposits in the fossil record.

References

Araña, V., Aparicio, A., Martín Escorza, C., García Cacho, L., Ortiz, R., Vaquer, R., Barberi, F., Ferrara, G., Albert, J. and Gassiot, X., 1983. El volcanismo neógeno-cuaternario de Cataluña: caracteres estructurales, petrológicos y geodinámicos. Acta Geol.Hispànica, 18-1, 1-17.

Assorgia, A., and Gimeno, D., 1994, Coeval genesis of pillow lava on the sea floor and under a thin cover of unlithified sediments (and associated formation of peperites). Geologie en Mijnbown, 72, 363-373.

Beccaluva, L., Maccioni, L., Macciotta, G. and Venturelli, G., 1974. Dati geologici e petrochimici sul massiccio vulcanico di Monte Arci (Sardegna). Memorie della Società Geologica Italiana, Supp. 2, XIII: 387-405, Pisa (Italy).

Branney, M.J., and Suthren, R.J. 1988. High-level peperitic sills in the English Lake district: distinction from block lavas, and implications for Borrowdale Volcanic Group stratigraphy. Geol.Journal, 23: 171-187.

Busby-Spera, C.J., and White, J.D.L., 1987. Variation in peperite textures associated with differing host-sediment properties. Bull.Volcanol., 49: 765-775.

Hanson, R.E., and Wilson, T.J., 1993. Large-scale rhyolite peperites (Jurassic, southern Chile), J.Volcanol.Geotherm.Res., 54: 247-264.

Kano, K.I., 1989. Interactions between andesitic magma and poorly consolidated sediments. examples in the neogene Shirahama Group, South Izu, Japan. J.Volcanol.Geotherm.Res., 37: 59-75.

Kokelaar, B.P., 1982. Fluidization of wet sediments during the emplacement of various igneous bodies. J.geol.Soc.London, 139: 21-33.

López Ruiz ,J. et Rodríguez Badiola, E., 1985, La región volcánica mio-pleistocena del NE de España. Estudios geol., 41, 105-126.

Maccioni, L., 1974. Nuovi rinvenimenti di lave a cuscino nel Miocene della Marmilla (Sardegna Centro-Occidentale). In: Paleogeografia del Terziario Sardo nell'Ambito del Mediterraneo Occidentale: 277-282, Rendiconti del Seminario della Facoltà di Scienze, University of Cagliari, Cagliari (Italy).

McPhie, J., Doyle, M. & Allen, R., 1993, Volcanic Textures: a guide to the interpretation of textures in volcanic rocks. Centre for Ore Deposits and Exploration Studies. University of Tasmania, Hobart, Tasmania, 198 pp.

Snyder, G.L., and Fraser, G.D., 1963. Pillowed Lavas. U.S.Geol.Surv. Prof. Paper, 454-B,C, p 1-23+1-7.

Rift zones and dyke swarms

George Walker
Cheltenham & Gloucester College of Higher Education, U.K.

The episodic growth and partial destruction of pre - shield-lava Fuerteventura.

C.J.Stillman

Trinity College Dublin. Ireland.

EXTENDED ABSTRACT

The island of Fuerteventura presents a rare opportunity to study the submarine development of one of the Canary Islands and the subsequent growth and denudation of the emergent volcanic edifice. In the central western region of the Island is exposed a "basal complex" representing the construction of a submarine volcanic edifice throughout the lengthy period from Upper Cretaceous/Palaeocene to Miocene. This is overlain by submarine to subaerial Miocene to Recent lavas and pyroclastic deposits which reveal a complex history of volcanic activity alternating with periods of quiescence and active erosion. It is clear that there have been major uplifts which have brou,ght the pre-Miocene basal complex to the present surface erosion level, as well as major collapses, and it is possible that these movements have been associated with major regional tectonic events on the African passive margin.

The construction of the Basal Complex commences with pillow lavas intercalated with sea-floor sediments overlain by emergent volcanics. the whole being intensely intruded by dykes. sills and high level plutons. These intrusions reveal a variety of ages rangillg trom 48 to 22Ma and appear to relate to a succession of.magmatic events. Subsequent Miocene volcanic activity is revealed by later dykes and apparently co-magmatic lava flows which b~lilt further volcanic edifices. Whilst much of the data on the basal complex used in this paper is the work of the author and colleagues, information on the younger volcanics is derived from more recent work ably collated by Ancochea et al (1996).

The oldest rocks ofthe "basal complex" consist of early Cretaceous terrigenous and calcareous clastic sediments and black shales, interpreted as part of a deep-sea fan constructed on the rifted margin of West Africa. Subsequent onset of calcareous pelagic deposition in Albian times was associated with strong uplift and localised submarine erosion of parts of the subjacent terrigenous clastic sequences. The earliest submarine volcanic rocks were then extruded after a hiatus of unknown duration. A thick pile of volcanic l-reccias and pillow lavas was constructed. The pre-volcanic and basal volcanic sequences are today very steeply tilted - in many cases inverted, in a structure apparently of tectonic origin, which pl eceded the dilation which controlled the emplacement of the main Eocene to Miocene dyke swarm This detormation must have taken place soon after the onset of volcanism.

It is not clear trom the exposed geological record whether the deformation was accompanied by significant erosion; indeed tollowing the tilting and overturning of the succession, there was continued submarine pillow lava effilsion with intercalated marine sediment deposition during a lengthy period of volcanism, up to early to middle Oligocene. However there is evidence that the island did emerge at a later stage of this igneous activity.

It is apparent that both the submarine and early emergent island volcano was t'onned during a period of extensional linear fissural volcanism, revealed in a complex dominated by a swarm of NNE-trending parallel dykes, in the axial zone of which total dilation exceeds 80%. The swarm has many of the features of a sheeted dyke swarm and is associated with small high-level plutons that appear to be co-magmatic with many of the dykes. Magmas were emplaced during a series of dilational episodes over a period of more than 22 million years. There is evidence that the dykes rose high into the edifice of a subaerial island, in a manner similar to the Koolau Dyke Swarm in the Hawaiian Islands . Many of these dykes have undergone hydrous metamorphism with extensive replacement of the original mineralogy by epidote, chlorite, and

sericite and the oxygen and hydrogen isotopes from these minerals show that they were in equilibrium with meteoric water. It is thus believed that these were emplaced in a subaerial island and the isotopes suggest that this island may have had an elevation as high as 2500m above sea level. The pattem of metamorphism suggests that the dykes themselves were both conduits for the c,irculating waters and the source of the heat that drove the hydrothermal system.

Evidence of emergence and active erosion of the island in the Oligocene is provided by inter-lava bioclastic and volcaniclastic sediments. These contain clasts of altered dyke lithologies and coarse and fine-grained basic igneous rocks of types similar to the plutonic rocks of the basal complex, suggesting unroofing of at least some of the plutons prior to the Oligocene sedimentation. An elevation of several thousand metres above sea level must have been achieved by the early Oligocene, before rapid erosion - possibly by combination of collapse and mass wasting - reduced the edifice to just below sea level. This material was probably redistributed in later submarine mass-flow movements; clasts ot similar plutonic material are reported in debris-flow deposits in the core taken from DSDP site 397. Though these are aged at 17.2 and 16.5Ma, they may well have been reworked from this soulce.

The Miocene marked the relaxation of the strong extensional dilation which had so far controlled the magmatic emplacement, permitting the construction of a number of individual volcanic structures. Early evidence ofthe relaxation is given by the Vega syenitic ring complex, dated at 18.7 and 21.4Ma. The subsequent history has been described in a number of papers and summed up by Ancochea et al (1996). These authors have shown that during the Miocene three major volcanic complexes were developed on or adjacent to the observed Basal Complex, and some of these edifices continued to build directly on the older successions. Though in many places the top of the Basal Complex is marked by deep weathering and erosion, in at least one case it is difficult to observe a significant break until later in the Miocene succession. The period or periods over which these Miocene edifices were reduced to the present level must be sought in the stratigraphy of the Miocene successions. Current rates of erosion are insufficient for the purpose. The present geomorphological form of the island indicates that recent erosion is controlled by a drainage pattern probably initiated on the elevated island but significantly modified by major topographic collapse structures. The erosion has generated deep barrancos and sharp-crested intervening 'cuchillos' tollowing this drainage pattern, but there is little evidence of mass wasting. On the other hand the major collapse structures (by whatever means they were generated) may well have been significant contributors to the movement of large mases of the island superstructure, perhaps generating the 'apron' seen in the bathymetric contours. Little evidence has so far been reported that a significant palt of the apron owes its origin to pyroclastic flows such as those on Gran Canaria. The central part ot the island is topographically dominated by the Central Depression, with hills to the west formed trom the Basal Complex and to the east and north from Miocene and younger volcanics. The depression formed probably by a major collapse in some cases subsequent to deep weathering of Basal Complex lithologies and before the deposition of Miocene formations such as the Malindraga Formation (Ancochea et al 1996). The flat plain of the depression is covered by a thick successsion ot sediments and sub-historic volcanoes. A minimum age of c. 1 8Ma for this collapse structure may be deduced from the age of the Malindrage Formation which was erupted after the depression had tol-lned. A second major collapse is probably recorded off the NW coast of the Jandía peninsula wl1ere the arcuate shape of the isobaths may denote a northward slide causing a depression almost 12 km wide and probably causing the Jandía escarpment, which has subsequently receded by erosion. The arcuate shape of this scarp may probably be controlled by the dominant dyke trends. If so the ages of the dykes (c. 1 5Ma) would give a maximum age for the collapse. In this case the larger part ot the volcano superstructure - the centre of which is believed to have been north of the present sl1ol-e line - must have subsided, presumably by some tectonic movement. In the north the existence ot the Ampuyenta Formation - an "agglomerate" composed mainly of fragments from lava flows l robably derived by erosion of an older subaerial edifice implies that this area did not undergo major delludatioll; the succeeding Miocene succession rests unconformably on the Ampuyenta Formation but is largely constructional with lava flows intercalated with sedimentary horizons. Throughout the subsequent events deposition has exceeded erosion such that the northern part of the island is dolllillated by low profile volcanoes down whose slopes flow the Recent to sub-historic lava flows. With the identification of the volcanic edifices and with adequate bathymetric information, it may ow be possible to compare the volume of the offshore apron with the quantity potentially removed from the island by mass wastage.

Eruptive Chronology and Paleomagnetism of the Taburiente Volcano, La Palma

J. Wijbrans [1], L. Tauxe[2] and H. Staudigel[2]

[1]*Dept. Earth Sciences Free University Amsterdam, De Boelelaan 1085m 1081HV Amsterdam [wijj@geo.vu.nl]*
[2]*Scripps Institiution of Oceano~raphy, UCSD, La Jolla, CA 92093-0225 [ltauxe@ucsd.edu] [hstaudigel@ucsd.edu]*

The Taburiente volcano is excellently exposed in the main, northern part of the island of La Palma. with its complex, intrusive core in the Caldera de Taburiente, the early submarine extrusive series in the seamount sequence in the Barranco de Las Angustias, and its extensive subaerial lavas of the "Coberta Sequence". The subaerial volcanics of the Taburiente volcano allow nearly complete sampling coverage in a large number of nearly vertical cliffs of up to 1400 m in the Caldera de Taburiente and between 200 and 600 m in numerous canyons radiating out from the center of the volcano exposing the major section of the volcano, from the Barranco de Las Angustias (SW) to Bco. del Agua (ESE). In addition, lavas can be sampled in a large number of several km long water adits that have been dug into the Taburiente volcano. cross - cutting the entire subaerial volcano. This unique exposure makes the Taburiente volcano one of the best exposed oceanic volcanoes.

The seamount series erupted between 3-4 Ma, based on foraminifera deposited in hyaloclastites. Subsequent to this, the seamount sequence was uplifted and tilted, eroded and finally covered with the subaerial lavas of the Coberta. Until recently, the onset of Coberta volcanism has been dated to about 1.7 Ma by Abdel-Monem et al. (1972). An additional 40Ar/39Ar age was given by Singer and Pringle (1996) for the Brunhes-Matuyama boundary (0.777 Ma) in a road section near La Galga identified by L. Tauxe (unpublished data).

We have carried out a paleomagnetic and geochronological (40Ar/39Ar) study of the Coberta Lavas. Paleomagnetic investigations on samples from 29 temporally discrete sites included step-wise alternating field and thermal demagnetization. Many sites had complicated multi-component magnetizations. A total of 17 sites had a minimum of five specimens with well defined characteristic directions and good within site agreement were deemed acceptable for the purposes of assessing the time averaged geomagnetic field at La Palma. The 6 normal (mean direction of 353.1/44.7 with an 95 of 10.6) and 11 reversed (mean of 181.1/-39.9 with an 95 of 8.8) sites suggest that the two polarity states are statistically antipodal, and indistinguishable from directions expected from an axial geocentric dipole. Volumetrically, the largest portion of the subaerial Taburiente volcano was formed in a reversed magnetic field.

The timing of volcanism was placed into an absolute geochronological framework by Ar/Ar geochronology. We sampled and dated the stratigraphically lowest and highest lavas, for several canyons ("Barrancos") around the Taburiente Volcano. The oldest ages were found for lavas in the bottom of barrancos at El Time (0.95 and 0.86 Ma), a barranco near Montaret (1.1 Ma), Los Tilos (0.85) and the Bco del Agua near Sta Lucia (1.13 Ma). These are all reversely magnetized. Slightly younger ages were found in normally magnetized, near-surface flows near Las Tricias (0.76 Ma) and other, near surface flows near Montaret (0.60 Ma and 0.85 Ma).

Our geochronological data suggest that the bulk of the Taburiente shield was formed in a rather narrow time interval between 1.2 and 0.6 Ma, even though the beginning of volcanism may have been prior to 1.7 Ma (Abdel-Monem, 1972) Myrs. From this, we infer three major stages of igneous activity, (1) the formation of the seamount sequence (within 3-4 Ma), (2) subsequent inrusive activity that lifted the seamount sequence up above sealevel some 2 km, and tilted it radially outward by 45°, and lastly (3) the subaerial phase (between 1.2-0.60 Ma). Volcanism obviously coninues to the present day along the southern rift zone of the volcano. Repeated phases of magmatic activity are common on the Canary Islands, as they are well documented on Gran Canaria, for example.

References

Abdel-Monem et al., 1972, Am.J.Sci., 272: p. 805-825.
Singer and Pringle, 1996, EPSL 139: 47-61.

Late (Quaternary) shield-stage volcanism in La Palma and El Hierro, Canary Islands

J.C. Carracedo[1], S. J. Day [2] and H. Guillou[3]

[1]*Estación Volcanológica de Canarias, CSIC,, La Laguna, Tenerife, Spain;*
[2]*Dept. Greig Fester Centre for Hazard Research, University College London, UK;*
[3]*Centre des Faibles Radioactivités, CEA-CNRS, France.*

1. Introduction

During the Quaternary, shield-stage volcanism mainly occurred in the western edge of the Canarian archipelago, in the islands of La Palma and El Hierro. In this period three main volcanic edificies were formed in La Palma: i) the late extension of the Taburiente volcano along a N-S rift (locally called the Cumbre Nueva (CN) ridge) formed the CN ridge (about 770±3 to 566±5 ka, Guillou et al., this volume), that was subsequently partially destroyed by a giant landslide possibly involving 180-200 km^3 of subaerial volcanics, ii) the Bejenado volcano, that partly filled the CN collapse embayment, and iii) the N-S elongated Cumbre Vieja (CV) volcano, that forms the southern half of La Palma and constitutes its last stage of growth, including all eruptive activity in the last 125 ka (see Fig 1). Coeval volcanism developed the entire subaerial island of El Hierro, forming two main edifices separated by two giant lateral collapses: i) the Tiñor volcano (1.12 ma to 882 ka, Guillou et al., 1996), and ii) the El Golfo volcano, that developed inside the previous collapse embayment from about 545 to 133 ka (Guillou et al., 1996). Since this last collapse, volcanism in El Hierro have been simultaneously active in the three arms of the island's rift system and have not yet produced a well-defined volcanic edifice as the previous Tiñor and El Golfo volcanoes.

Detailed field observations and mapping and high-precision dating of volcanic activity on these two islands (Guillou et al., 1996 and this volume) suggests that periods of intense volcanism on one island coincides with periods of relative inactivity on the other (Carracedo et al, this volume).

2. Late geological evolution of of La Palma

2.1 Last stage of growth and destruction of the Taburiente volcano: The Cumbre Nueva collapse

The CN ridge has developed on the southern flank of the larger and older Taburiente volcano (Fig. 1), that forms the northern part of La Palma and started to grow about 2 ma ago, according to Ancochea and co-workers (1994). Six new ages, extending from 770±3 to 566±5 ka, have been determined in lavas of the Taburiente main volcano and the CN ridge (Guillou et al., this volume). These samples are in stratigraphic sequences in the CN scarp (Fig. 2-A). The analysis of geomagnetic polarities in these sequences shows that the CN ridge lavas are of normal (Brunhes) polarity whereas the underlying main Taburiente volcano lavas present reverse (Matuyama) polarities in this part of the island, the contact between both edificies being a short duration palaeomagnetic discordance. There is no stratigraphic evidence to differentiate the CN ridge from the main Taburiente volcano.

The CN ridge may have reached more than 2 km in altitude and an area of about 300 km^2. In its latest stages of growth this volcano evolved to an unstable configuration and its west flank collapsed (Fig. 2-B). The embayment formed was subsequently filled by lavas of the Bejenado and CV volcanoes, resting unconformably on the embayment-filling deposits.

These deposits deposits do not outcrop. They are buried by the lavas of these volcanoes and the thick sedimentary sequence of El Time (Fig. 2). They can only be reached through boreholes drilled in the area of Los Llanos for underground water exploration.

The evolution of the CN collapse is summarised in Fig. 3.

Characteristics of the CN lateral collapse and genesis of the Caldera de Taburiente. The geometry and extent of the collapsed block can be estimated from field observations and the information obtained from the boreholes mentioned above: The volume was about 180-200 km^3. The age of the collapse is less than 566 ± 5 ka, from the age of one of the topmost lavas of the collapse scarp. The eastern perimeter of the block is an arc parallel to the present-day CN scarp, and is partially concealed by the CV volcano. The north-western boundary is interpreted as a strike-slip fault.

The present Caldera de Taburiente, probably the most spectacular feature of La Palma, is related to the CN collapse and the growth of the Bejenado volcano, as indicated in Fig 3. We interpret its location and trend as the result of the collapse event and subsequent erosional enlargement.

2.2 The CV volcano

Recent activity in La Palma is all in the south of the island, and has formed a large polygenetic volcano, the CV volcano. This is a 2000 m high ridge with a subaerial area of 220 km^2 and a subaerial volume of about 125 km^3. The volcano is mostly built of sequences of alkaline lavas (Day et al., this volume, a), but also contains a number of phonolite domes which are scattered over the volcano. There is no central crater complex: instead, the summit of the volcano is formed by a long north-south trending ridge. This ridge is formed by the main concentration of largely monogenetic volcanic fissures and vents, or volcanic rift zone. A number of historic eruptions (<500 years) have occurred in broadly E-W fissures on the western flank of the volcano.

Detailed mapping (1/5.000 in the zones of high vent concentration and 1/10.000 in the lavas draping the flanks of the volcano) has been carried out and 20 new high-precision radiometric dates of stratigraphically well-defined units within the volcanic sequence have been obtained (Guillou et al., this volume).

Sea-level changes and stratigraphy. The absence of elements to differentiate and correlate the different volcanic units, very similar in aspect, initially made it very difficult to define the stratigraphy of the volcano. The western flank of the CV volcano has undergone significant marine erosion, resulting in coastal subvertical cliffs which reach 700 m in height in some places. The presence of a period of relative inactivity and strong erosion made it possible to define stratigraphic units by their relationship to the coastal cliffs that have developed around the volcano: a cliff-forming series which is exposed in these cliffs and a scree-forming series, which is draped over the cliffs and forms the coastal lava platforms at their bases. The radiometric dating shows that these units have chronostratigraphic significance: cliff-forming lavas are older than about 20 ka, whereas scree-and platform-forming lavas are all younger. The boundary

Growth and progressive instability of the CV volcano. The oldest CV lava dated, at the base of the western cliff, gave an age of 123 ± 5 ka. The evolution of the CV volcano since that time is summarised in Fig. 4. The CV volcano developed very rapidly from about 125 ka to about 80 ka, controlled by a typical triple-armed volcanic rift structure (Fig. 4-A), but with a dominant N-S-trending rift (the CV ridge).

From about 80 ka to 20 ka, the rate of growth of the volcano decreased, although all three volcanic rift zones continued to be active (Fig. 3-B). The rate of addition of material was insufficient to keep pace with the rate of coastal erosion. This was the main period of formation of the coastal cliffs.

After about 20 ka the island began to grow again. At this time the NW volcanic rift seems to have been less active than the other two: this may be an early manifestation of the subsequent rift reorganisation (Fig. 3-C).

Since about 7 ka the distribution of volcanic vents on the CV has changed almost completely (Fig. 3-D). The NE-and NW-trending volcanic rifts have disappeared. Activity has been concentrated along the N-S rift, which has extended northwards. Most recently, eruptive fissures have developed on the western flank of the volcano. The reorganisation of the volcanic rift system on the volcano indicates that the stress field within it has changed greatly, resulting in an increasing instability of the volcano. Further evidence for a reconfiguration of the stress field within the CV is provided by the orientations of elongate volcanic vents and fissures (Day et al., this volume, b).

3. Geological evolution of of El Hierro

The volcanic history of El Hierro clearly exemplifies the intense interaction between volcano growth and lateral collapse episodes in the very early stages of subaerial development of an oceanic island. Fig. 5 shows schematically the main stages of the volcanic history of El Hierro.

Stages A, B and C correspond to the main phases of the Tiñor volcano development. Stage D illustrates the collapse of the volcano, probably soon after its last (Ventejís) eruptions (882 ± 13 ka, Guillou et al., 1996). Most of the volcanism during the Tiñor volcano growth was concentrated in the region of the younger NE rift: it is not clear whether the Tiñor volcano had a single dominant volcanic rift or whether the others have been removed by other collapses.

After a prolonged period of reduced activity (880 ka to 550 ka approximately), renewed intense activity began within the Tiñor collapse embayment. These produced a large volcanic edifice (the El Golfo volcano) between 545 and 176 ka (stage E). Initial activity was dispersed, with many monogenetic vents along the arms of a triple rift system erupting basic magmas (Lower El Golfo Series) but at a later stage activity became concentrated more centrally and magma compositions changed from basic to more evolved rocks, culminating in eruption of trachytic lavas and block - and - ash deposits from a central vent area. The El Golfo volcano buried the Tiñor edifice except in the north - east of the island.

During the growth of the El Golfo volcano, the San Andrés aborted collapse affected the eastern flank of the volcano, at the time of transition between Lower El Golfo and Upper El Golfo activity. The El Julan lateral collapse may also have occurred during growth of the El Golfo volcano (stage F) but the age of this structure is not well - constrained since it has been entirely buried by younger lavas.

Following the end of eruption of differentiated magmas (perhaps associated with the El Julan collapse?) volcanic activity continued but in a very different style. Basaltic lavas and associated scoria and lapilli were erupted from vents located in the three branches of the present - day rift system (WNW, SSE and NE rifts). This Rift volcanism filled the El Julan embayment, completely covering the collapse scar. Rift series activity also partly buried the San Andrés fault scarp. The earlier stages of rift series activity may have finally destabilised the NW flank of the El Golfo volcano and triggered the first giant collapse towards the N-NW (stage G). Following this collapse eruption rates declined sharply: in particular, the entire sequence in the central part of the El Julan embayment may predate the El Golfo collapse although further radiometric dating is required to confirm this.

After the El Golfo collapse, the embayment was greatly modified and enlarged by coastal erosion, with the development of a marine abrasion platform and several families of screes and alluvial fans, while activity continued on the other side of the island (such as the lavas around the Las Playas barranco). Falling sea level led to emergence of the abrasion platform and formation of a series of aeolian sand dunes. These dunes were subsequently buried by renewed volcanic activity in the embayment, from about 20 - 30 ka onwards, which produced a series of basaltic lavas that covered the abrasion platform. This pattern of a period of volcanic repose following collapse is typical of both La Palma and El Hierro (Carracedo et al., this volume).

Once the abrasion platform was covered the embayment - filling sequence appears to have extended out onto the submarine slope of the island forming a large unstable lava delta (stage H). Collapse of this lava delta may have produced the younger El Golfo collapse that is recorded in the offshore submarine sequences (Masson, 1996).

The present - day island of El Hierro is therefore the product of successive volcanoes accreted onto earlier edifices after lateral collapse has ended the preceding stage of growth.

References

Ancochea E., Hernán F., Cendrero A., Cantagrel J.M., Fúster J.M., Ibarrola E., Coello J., 1994. Constructive and destructive episodes in the building of a young oceanic island, La Palma, Canary Islands, and genesis of the Caldera de Taburiente. J. Volcanol. Geotherm. Res., 60, 3-4: 243-262.

Carracedo J. C. 1994. The Canary Islands: An example of structural control on the growth of large oceanic-island volcanoes. J. Volcanol. Geotherm. Res., 60, 3-4: 225-241.

Carracedo, J.C., Day, S., Guillou, H., Rodríguez Badiola, E., Canas, J.A. and Pérez Torrado, F. J., geochronological, structural and morphological constraints in the genesis and evolution of the Canary Islands (this volume).

Day, S.J., Gravestock, P. and Carracedo, J.C., Petrological and geochemical studies of individual eruptions on La Palma : The importance of detailed mapping and stratigraphic control in studies of magmatic rocks (this volume, a).

Day, S.J., Carracedo, J.C., Guillou, H., Pérez Torrado, F.J., Fonseca, J.F.B.D., Heleno da Silva, S.I.N. and Gravestock, P., Recognising incipient instability and lateral collapse precursors in steep-sided oceanic island colcanoes (this volume, b).

Guillou, H., Carracedo J. C. and Day, S.J., Unspiked K-Ar dating of volcanic rocks from El Hierro and La Palma, western Canary Islands (this volume).

Guillou, H., Carracedo J. C., Pérez Torrado, F. and Rodríguez Badiola, E. 1996. K-Ar ages and magnetic stratigraphy of a hotspot - induced, fast - grown oceanic island: El Hierro, Canary Islands. . *Journal of Volcanology and Geothermal Research* 73, 141 - 155.

Masson, D.G. 1996. Catastrophic collapse of the volcanic island of Hierro 15 ka ago and the history of landslides in the Canary Islands. Geology, 24- 3: 231-234.

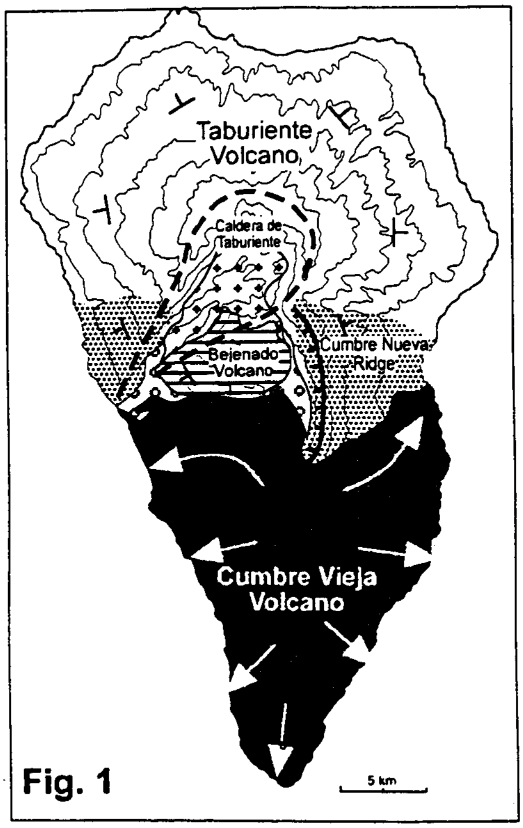

Fig. 1

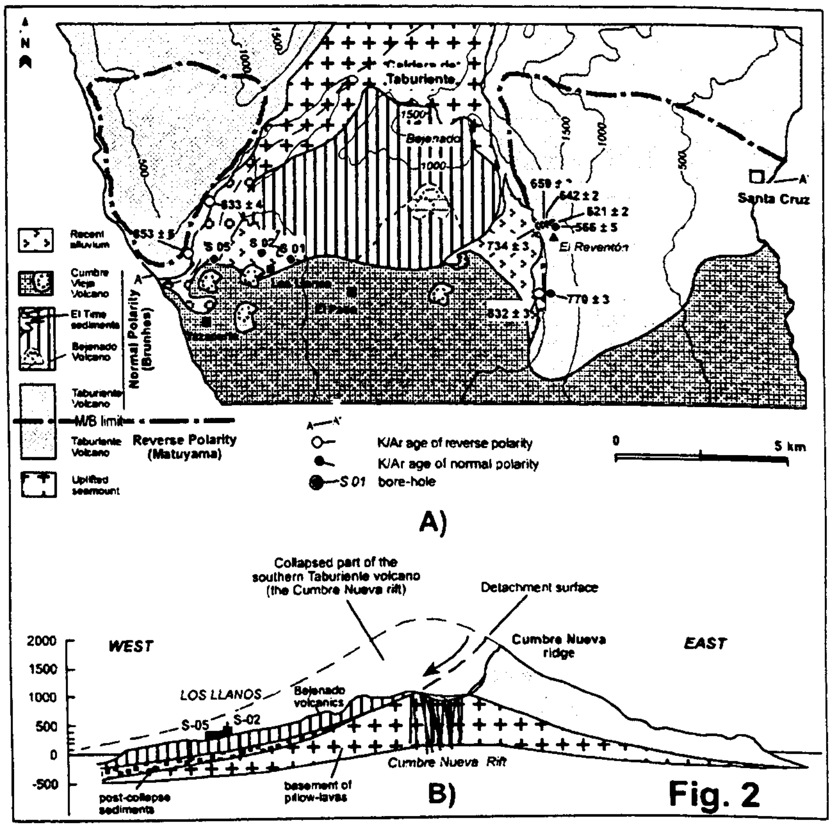

Fig. 2

Fig. 3

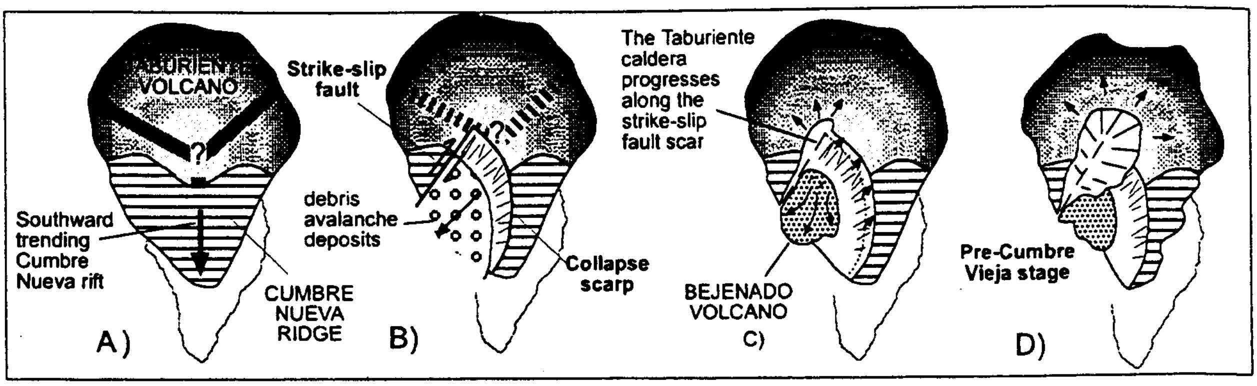

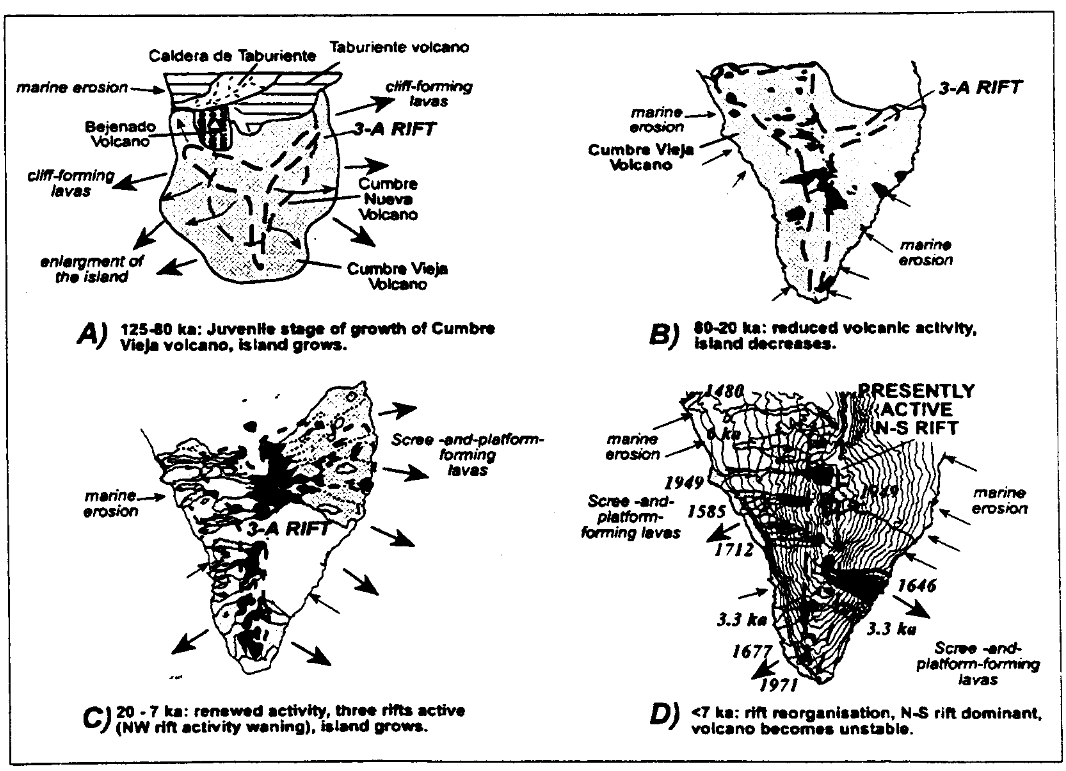

A) 125-80 ka: Juvenile stage of growth of Cumbre Vieja volcano, island grows.

B) 80-20 ka: reduced volcanic activity, island decreases.

C) 20 - 7 ka: renewed activity, three rifts active (NW rift activity waning), island grows.

D) <7 ka: rift reorganisation, N-S rift dominant, volcano becomes unstable.

Fig. 4

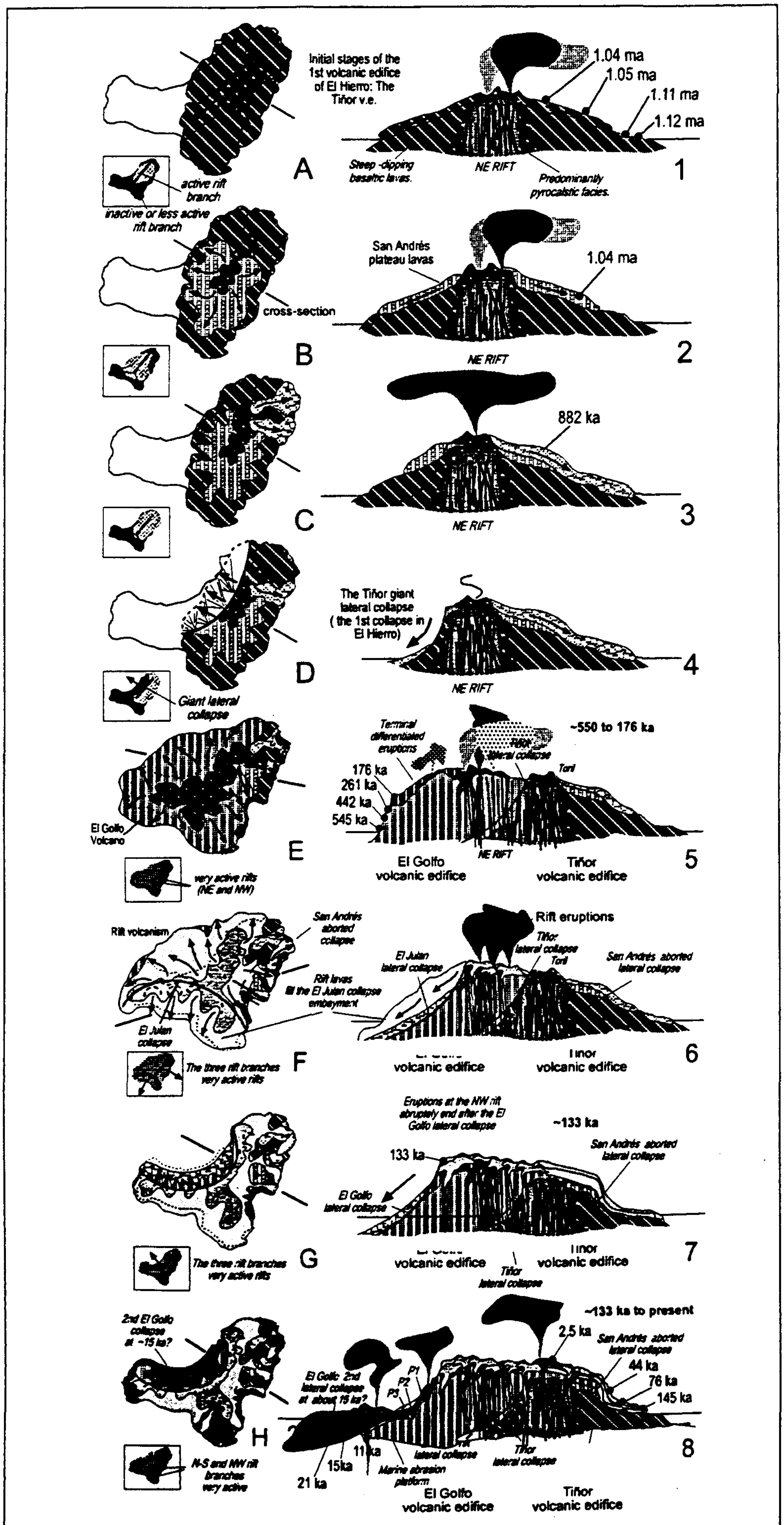
Initial stages of the 1st volcanic edifice of El Hierro: The Tiñor v.e.
1.04 ma
1.05 ma
1.11 ma
1.12 ma
A
active rift branch
inactive or less active rift branch
Steep-dipping basaltic lavas.
NE RIFT
Predominantly pyroclastic facies.
1
San Andrés plateau lavas
1.04 ma
cross-section
B
NE RIFT
2
882 ka
C
NE RIFT
3
The Tiñor giant lateral collapse (the 1st collapse in El Hierro)
D
Giant lateral collapse
NE RIFT
4
Terminal differentiated eruptions
~550 to 176 ka
176 ka
261 ka
442 ka
545 ka
El Golfo Volcano
E
very active rifts (NE and NW)
NE RIFT
El Golfo volcanic edifice
Tiñor volcanic edifice
5
Rift volcanism
San Andrés aborted collapse
Rift lavas fill the El Julan collapse embayment
El Julan collapse
The three rift branches very active rifts
F
Rift eruptions
El Julan lateral collapse
Tiñor lateral collapse
San Andrés aborted lateral collapse
volcanic edifice
volcanic edifice
6
Eruptions at the NW rift abruptly end after the El Golfo lateral collapse
~133 ka
133 ka
San Andrés aborted lateral collapse
El Golfo lateral collapse
The three rift branches very active rifts
G
volcanic edifice
volcanic edifice
Tiñor lateral collapse
7
2nd El Golfo collapse at ~15 ka?
~133 ka to present
2.5 ka
San Andrés aborted lateral collapse
44 ka
76 ka
145 ka
El Golfo 2nd lateral collapse at about 15 ka?
P1
P2
P3
H
N-S and NW rift branches very active
21 ka
15ka
11 ka
lateral collapse
Marine abrasion platform
Tiñor lateral collapse
El Golfo volcanic edifice
Tiñor volcanic edifice
8

Growth and destruction by lateral collapse of the Roque Nublo oceanic island stratovolcano, Gran Canaria, Canary Islands.

F. J. Pérez Torrado[1], S. J. Day[2,3] & J. C. Carracedo[4,2]

[1] *Dept. Fisica - Geologia, Universidad de Las Palmas de Gran Canaria, Gran Canaria, Spain.*
[2] *Dept. Geography & Geology, Cheltenham & Gloucester CHE, U.K.*
[3] *Greig Fester Centre for Hazard Research, University College London, U.K.*
[4] *Estación Volcanológica de Canarias, CSIC, La Laguna, Tenerife, Spain.*

The Roque Nublo volcano developed from about 5.5 Ma to 2.7 Ma on the island of Gran Canaria. Its growth followed an erosional hiatus after the end of intense volcanic activity of Miocene age (ca. 14.5 Ma to 8.5 Ma) in which the island first formed. It is therefore post - erosional in the Hawaiian sense, and had a lower eruption rate than most shield - building volcanoes. However, the Roque Nublo volcano had a much higher eruption rate than is typical of post - erosional volcanism. It therefore has many of the characteristics of shield - building oceanic island volcanoes, including development of a summit crater complex fed by a differentiated shallow magma system, a stratovolcano - type geometry and repeated lateral collapses.

The Roque Nublo Group, representing the products of the volcano, is divided into a number of formations (see key to Fig. 1). The oldest of these, the El Tablero formation, represents the first stages of post - erosional activity (from 5.5 to 4.6 Ma) before development of the stratocone. It consists of a number of monogenetic strombolian cones and lava flows scattered over the island, and so is more typical of post - erosional activity than the late activity. The main stratovolcano contains three extracrater formations, which form its flanks. These are the Riscos de Chapin (ca. 4.6 to 3.9 Ma; basanite and alkali basalt to trachyte and phonolite lavas with mino intercalated pyroclastic and epiclastic deposits); Tirajana (ca. 3.9 to 3.0 Ma; mainly pyroclastic and epiclastic rocks, with minor intercalated lavas); and Tenteniguada (ca. 3.9 to 2.7 Ma; phonolitic plugs and domes partly coeval with the other units) formations. The Riscos de Chapin formation represents an early effusive period of activity of the volcano, whilst later activity became almost entirely explosive, resulting in the rocks of the Tirajana formation. These two formations show strong radial variations (Figs. 1 & 2). The Riscos de Chapin lavas vary from entirely basic near the periphery of the volcano to a well - developed basaltic to trachytic differentiation sequence at the centre. The epiclastic rocks of the Tirajana formation (sediments and laharic breccias) are also found on the lower slopes of the volcano, whilst Tirajana formation sequences in the medial and proximal area are dominated by lithic - rich ignimbrites (see Pérez Torrado et al., *Genesis of the Roque Nublo Ignimbrites Gran Canaria, Canary Islands*, this volume for detailed discussion of these deposits). The Rincon de Tejeda formation represents an early intracrater sequence and consists of lacustrine sediments, lag breccias and agglutinates intruded by alkali gabbro plugs and a radial dyke swarm. The central area of the island also contain a number of younger extrusive and intrusive units, emplaced between the lateral collapses which affected the volcano: these are discussed below.

Unlike the continuous sequences characteristic of shield - building activity, the Roque Nublo Group contain within it a number of unconformities. These are especially prominent in the west and south of the island where intense pre - Roque Nublo erosion of the Miocene volcanic rocks produced a mountainous terrain with severa large canyon systems. These canyons, particularly the Barranco de Tejeda in the west and the Barranco de Tirajana in the south - east, were re - incised repeatedly during the growth of the Roque Nublo volcano and may have influenced its morphology and structural evolution.

In the later stages of its growth the Roque Nublo volcano underwent a series of lateral collapses to the south and west. The slopes of the volcano were steeper on these sides than in the north and east, probably as a result o erosion along the canyon systems originally formed in the Miocene, as noted above. Thus the directions o instability of the volcano may have been controlled by pre - existing drainage systems. The deeply - eroded remnants of debris avalanche deposits from these collapses occur as far south as the coast near Arguineguin, 25 km away from the source region (García Cacho et al., 1987, 1994; Mehl & Schmincke 1992), and as far west a the Mesa de Junquillo, 15 km from the source. The collapse structures themselves developed near the summit o the volcano and are partly preserved in the deeply - eroded region around Ayacata. The internal structures of the collapses are well - exposed in this region and provide much evidence regarding collapse mechanics. Detailed mapping has revealed that three collapse episodes occurred, separated by periods of erosion, edifice growth and intrusion emplacement, and pre - collapse deformation representing incipient instability. The mapping has also revealed the age relationships of the collapses to the in situ formations of the volcano. The previously - defined Ayacata formation (Pérez Torrado et al. 1995), defined as consisting of all the debris avalanche deposits, i therefore abandoned and the different debris avalanche units assigned member status within the other formations.

The first collapse produced massive, chaotic breccias: the Pargana member of the Tirajana formation. These, represent two or more relatively slow - moving viscous debris flows composed of homogenised, water - saturated matrix - rich breccia with blocks up to 1 km across. The unit also contains many peperitic basalt intrusion emplaced during and after debris flow movement. The Pargana member is limited in extent, indicating that the debris flows probably only reached several kilometres from the source. Much of the Pargana member was subsequently deformed and further displaced in the second and third collapses.

The second and third collapses, the Timagada and Montana del Aserrador collapses, are represented in the Ayacata area only by widespread occurrences of fault rocks and gouge breccia mtrusions, but can be correlated with debris avalanche deposits to the south and west by occurrences in the deposits of clasts from different groups of intrusions in the deposits. The debris avalanche deposits are therefore named the Timagada member o the Tirajana formation and the Montaña del Aserrador member of the El Montañon formation (see below). Each collapse seems to have begun with coherent sliding of blocks up to kilometres across on discrete fault surfaces Recognisable summit intrusive complexes of brecciated gabbro and porphyry, emplaced between the collapse episodes, occur within these collapse structures. These intrusive complexes have been transported south and west by distances of several kilometres by sliding on the basal fault surfaces of the collapses. Patterns of movement of the fault blocks, and marked asymmetry of the Timagada collapse structure in particular, have been deduced from slickenlines and tool marks on the fault surfaces. Only the lower parts of these block - sliding domains arq preserved in the Ayacata area; the upper parts appear to have disaggregated to form the debris avalanches.

After the Timagada collapse, deep erosion in the headwall region of the Barranco de Tejeda was followed by a resumption of activity within the collapse scar, producing the El Montanon formation which fills a palaeocanyon system. This formation generally resembles the proximal facies of the Tirajana formation, being dominated by lithic - rich ignimbrites with interbedded felsic agglutinates, epiclastic breccias and lavas. It can be correlated using clast populations in the ignimbrites with groups of intrusions in the Ayacata area, and may also be equivalent to the younger Tenteniguada domes and plugs to the east. The depth of the erosion (over 500 m) i, particularly remarkable in that age constraints indicate that the interval between the Timagada and Montaña de Aserrador collapses is a few hundred thousand years at most. Re - growth of the volcano must have also occurred in this interval. Both the rapid erosion and the subsequent collapse to the west are considered to reflect the importance of the pre - existing and repeatedly re - established Barranco de Tejeda canyon system.

References

Garcia Cacho, L., Anguita, F., Araña, V., Barberi, F., Diez - Gil, J.L., Ortiz, R. & Sbrana, A. 1987. Una nueva perspectiva de la Formación Roque Nublo (Gran Canaria) Bol. Geol. Min., 98, 859 - 863.

Garcia Cacho, L., Diez - Gil, J.L. & Araña, V. 1994. A large volcanic debris avalanche in the Pliocene Roque Nublo stratovolcano, Gran Canaria, Canary Islands. J. Volc. Geotherm. Res. 63, 217 - 229.

Mehl, K. & Schmincke, H.U. 1992. Multiple sector collapse of the Pliocene Roque Nublo stratocone on Gran Canaria (Canary Islands). III CGE y VIII CLG, Salamanca. Abstracts Y, 448 - 452.

Pérez Torrado, F.J., Carracedo, J.C. & Mangas, J. 1995. Geochronology and stratigraphy of the Roque Nublo Cycle, Gran Canaria, Canary Islands. J. Geol. Soc., London 152, 807 - 818.

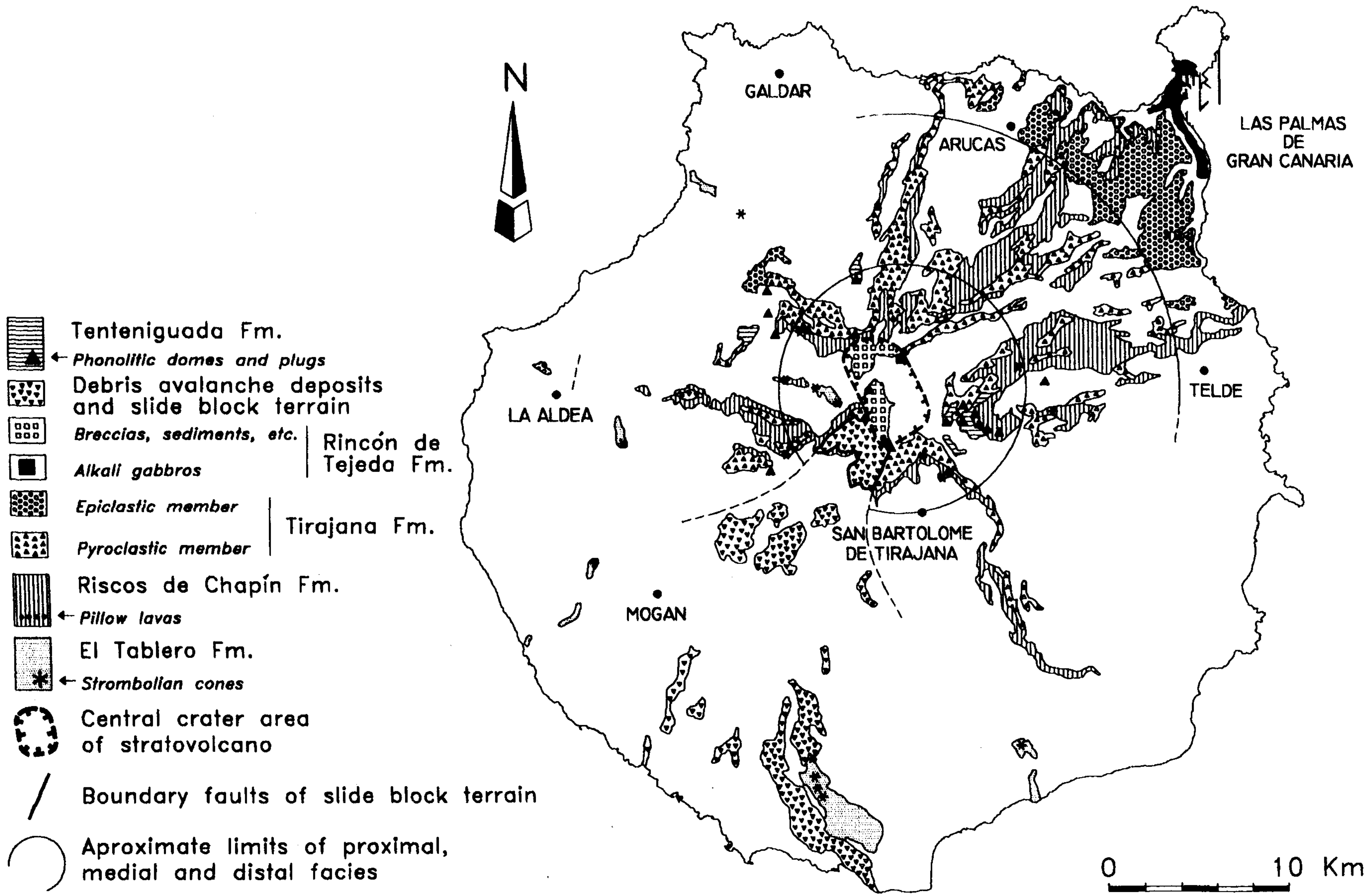

Figure 1.- Simplified map of the Roque Nublo group.

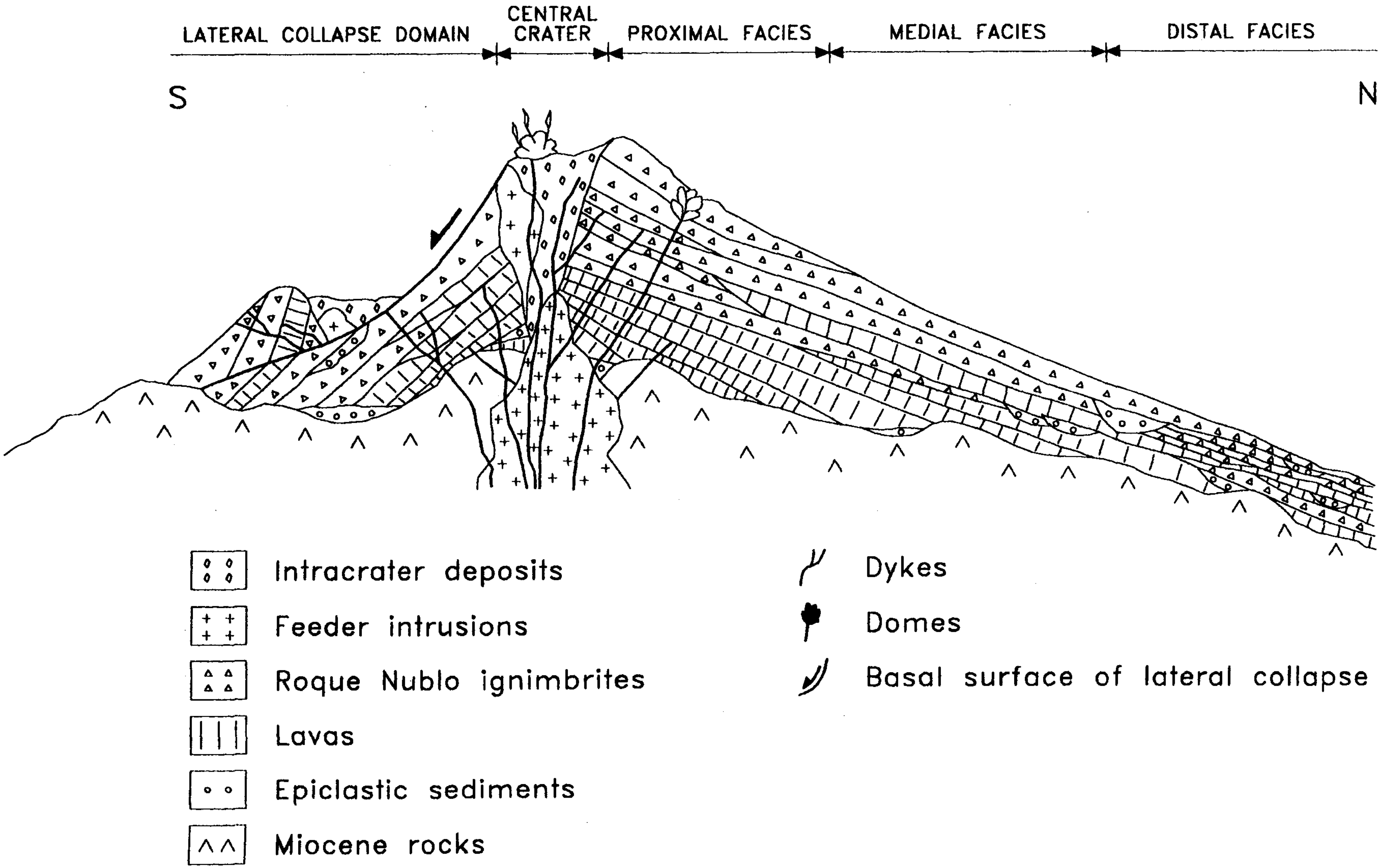

Figure 2.- Schematic cross – section through the Roque Nublo stratovolcano at a late stage in its development.

Intrusion of the Miocene cone sheet dike swarm of Gran Canaria (Canary Islands) - A case study of subvolcanic intrusive growth of an oceanic island.

Carsten Schirnick, Paul van den Bogaard, Hans-Ulrich Schmincke
GEOMAR Forschungszentrum, Abt. Vulkanologie und Petrologie
Wischhofstr. 1-3, D-24148 Kiel, Germany
E-mail: cschirnick@geomar.de

More than 1000 mainly trachytic to phonolitic cone sheet dikes and hypabyssal syenitic stocks form a 20 km wide and >1200 m high intrusive complex within the pyroclastic and epiclastic filling of the Miocene Tejeda caldera [1-3]. The complex is a concentric structure, roughly centered within the caldera fill, with a central area occupied by syenitic stocks and circumferential cone sheet dikes that dip towards the caldera center. Four concentric zones are distinguished based on the volume fractions of intrusive compared to older caldera-filling volcanic and volcaniclastic rocks: (1) a central 3-by-5 km diameter, low density dike zone dominated by >60 vol.% syenitic stocks and <20 vol.% dikes that intruded into volcaniclastic breccias (<20 vol.%); (2) an annular 3-4 km wide high density dike zone with >75 vol.% dikes and <5 vol.% syenite screens in intracaldera volcaniclastics (<20 vol.%); (3) an annular 2-3 km wide low density dike zone with <30 vol.% dikes (locally up to 60 vol.%) and <10 vol.% syenite screens and small syenitic laccoliths in volcaniclastic rocks; and (4) a marginal 1-3 km wide belt between zone 3 and the caldera margin, where <5 vol.% (locally <20 vol.%) dikes and sills intruded into volcanic rocks. Two generations of cone sheet dikes are distinguished based on distinct petrographies and relative intrusive ages: An older generation of alkali feldspar trachytes (~75 vol.%) and a younger generation of aegerine-bearing alkali feldspar trachytes to phonolites (~25 vol.%). Radial dikes, similar in composition to cone sheet dikes of either generation, occur in zones 2, 3 and 4 but are subordinate in number and volume (<l vol.%).

The structural attitudes of cone sheet dikes, based on measured plunge and dip of dike margins, are uniform throughout the intrusive complex and vary only on a local scale: The mode of dikes dips 44±10° (±1σ) inwards within 2-4 km distance from the center and 42±15° at 6-8 km distance; dip angles average 43±13° at the deepest exposed levels of the complex (<500 m asl) and 37±12° at higher levels (>1000 m asl). Plunge directions indicate a mutual axis of radial symmetry located in the center of the intrusive complex. Based on the structural data we infer an idealized geometry of a truncated cone for individual cone sheet dikes. The dike swarm forms a vertical stack of intrusive sheets as opposed to dikes converging in a single focus. The bulk volume of cone sheet dikes is approximately 100-300 km^3, based on the exposed dike volume as lower limit and a truncated cone with 4 km base diameter, 12 km top diameter and 3.7 km height representing the maximum dimensions of zone 2 cone sheet dikes as upper limit. The geometry of the complex, the subordinate volume of radial dikes and predominantly vertical offsets (70-90°) at individual cone sheet dikes indicate that the uplift of the hanging wall, i.e. the central caldera area, was near-vertical. A cumulative uplift of at least 2100-2800 m is estimated based on the average dike dip (43°) and dike density (>75 vol.%) in the 3-4 km wide high density dike zone.

Single crystal ages of alkali feldspar and biotite (*) phenocrysts, determined by laser probe $^{40}Ar/^{39}Ar$ analysis (quoted as mean apparent age at 1σ-level) indicate accumulation of >1000 m of volcanic and volcaniclastic deposits in the Tejeda caldera between 13.49±0.04 Ma and 11.96±0.03 Ma, concurrent with deposition of the extracaldera Upper Mogan to Middle Fataga Formations (13.63 to 11.36 Ma [4]). Cone sheet dikes (11.71±0.07 to 7.32±0.05 Ma) and syenites (12.2±0.3 Ma [5] to 8.94±0.03* Ma) intruded into the caldera fill concurrent with eruptive (12.43 to 12.33 Ma, 12.07 to 11.36 Ma, 10.97 to 9.85 Ma [4]) and non-eruptive intervals (9.85 to 8.84 Ma [4]) of the Fataga Group. Radiometric ages of individual dikes, i.e. the scattered occurrence of younger cone sheet dikes within the dike swarm and strikingly different ages of neighbouring intrusions in dike zones 2 and 3 (12.2±0.3 versus 7.32±0.05 Ma and 11.71±0.07 Ma versus 9.99±0.01 Ma) preclude a systematic concentric age progression with distance from the center of the complex.

Calculations based on simple Rayleigh-fractionation models indicate that the observed range of individual cone sheet dike compositions can be produced by up to ~85 wt.% fractionation of the assemblage alkali feldspar+biotite+FeTi-oxides+apatite from assumed parental trachytic melts having compositions similar to the least evolved cone sheet dikes. Compositions of alkali feldspar syenites, in contrast, are consistent with calculated mixed compositions of crystalline residual and incompletely extracted batches of fractionated melt. Rare kaersutite-bearing syenites and mafic enclaves in alkali feldspar syenites suggest that the parental trachyte melts were fractionated from mantle-derived alkali basalt.

Low fH_2O (< 70 bars at logfo2 = - 16.0 and 745 - 762°C), based on biotite-sanidine-magnetite equilibrium [6, 7], and high F-concentrations in biotites and apatites indicate that the evolved magmas were fluorine-rich and crystallized under highly water-undersaturated conditions, precluding volatile-saturation and retrograde boiling [8] as the driving forces of cone sheet dike formation. More likely, cone sheet dike formation in the Tejeda system was controlled by deformation processes initiated by the recurrent replenishment of a flat, laccolith-like shallow magma chamber. Magma supply exceeding the volume that could be compensated for by resurgent doming of the overlying caldera-fill resulted in the formation of cone-shaped fractures into which the fractionated melt was pressed, leaving a crystalline residual behind. Lateral extension and contraction of the magma chamber, stationary at shallow depth (<2300 m below sealevel), controlled the base diameter of the truncated-cone-fracture and consequently the dispersed but concentric intrusion of the cone sheet dike swarm: Lateral expansion of the magma chamber resulted in the formation of dike cones up to 14 km wide (at sealevel) as opposed to narrow dike cones resulting during stages of lateral contraction. The age range and abundance of cone sheet dikes indicates that cone sheet dike formation was a recurrent and nearly continuous process (ca 200 intrusive events per Ma) compared to discontinuous eruption of the trachyphonolitic ignimbrites and lavas of the Fataga Group (<20 eruptions per Ma), suggesting that the explosive eruptions reflect peak magma supply rates exceeding the balance of cone sheet dike formation and resurgent doming.

References

[1] H.-U. Schmincke (1967) *Bulletin of Volcanology* **31**, 153-162.

[2] F. Hernan and R. Velez (1980) *Estudios geológicos* **36**, 65-73.

[3] H. Ferriz and H.-U. Schmincke (1989) *European Science Foundation Meeting on Canarian Volcanism*; Lanzarote, Spain, 142-144.

[4] P. v. d. Bogaard and H.-U. Schmincke (in press) ODP *Scientific Results, College Station*, TX.

[5] I. McDougall and H.-U. Schmincke (1976) *Bulletin of Volcanology* **40**, 1-21.

[6] D. R. Wones and H. P. Eugster (1965) *American Mineralogist* **50**, 1228-1272.

[7] G. K. Czamanske and D. R. Wones (1973) *Journal of Petrology* **14**, 349-380.

[8] W. J. Phillips. *Tectonophysics* **24**, (1974) 69-84.

Macroscopic, microscopic and magnetic flow indicators in dykes, with implications for velocity and strain profiles

Gidon Baer
Geological Survey of Israel

INTRODUCTION

Dyke emplacement comprises several interrelated processes: (1) propagation of the leading fracture ahead of the dyke, (2) propagation of dyke-tip fluids, and (3) magma flow within the dyke. Dyke propagation directions are commonly determined by the geometry of its segments, whereas flow directions of dyke-tip fluids and initial magma flow directions may be determined by finger-like structures observed along the host rock walls or along the dyke exterior (e.g., Baer and Reches, 1987). Magma flow directions within the dyke are generally determined by the petrofabric and the anisotropy of magnetic susceptibility (AMS) of the dyke interior (e.g., Shelley, 1985, Ernst and Baragar, 1992). Previous studies have shown that the AMS ellipsoids may be controlled by the alignment of the other minerals in the rock (Stacey, 1960; Hargraves et al., 1991), however, the exact nature of these relations is still enigmatic. This study examines the relations between maximum available flow indicators in a single dyke. Within this framework, special attention is paid to the correlation between magnetic anisotropy and flow-induced strain indicators, such as deformed vesicles. This correlation may prove a useful tool for future strain analyses in flowing media.

FLOW INDICATORS

The analyzed dyke is found on the southern flanks of Mt. Etna. It belongs to the Zoccolaro swarm of post Trifoglietto II age (<25,000 years) (McGuire, 1983), and its intrusive center is inferred to be about 5 km north of the studied outcrop. The dyke intrudes friable pyroclastic rocks that have been eroded more easily than the dyke, thus leaving the dyke walls almost unweathered. The present analysis is limited to a 15 cm wide band at the margin of the dyke and a 10 cm wide band at the center of the dyke.

Oblique to subvertical elongate dyke-wall lobes are well exposed along the dyke contact, resembling in appearance ropy lava (pahoehoe) surfaces. This resemblance suggests that flow in the dyke was perpendicular to the long axes of the dyke-wall lobes. Elliptical (deformed) vesicles occupy a significant part of the dyke volume. Their long axes range in length from 1 to 5 mm, and their intermediate and short axes are 0.2-2 mm long. The 3-D vesicle orientations was studied in three mutually perpendicular planes (Fig. 1): (a) parallel to the dyke plane, (b) normal to the dyke plane and to the dyke-wall lobes; and (c) normal to the dyke plane and parallel to the dyke-wall lobes. Plane (b) shows the most pronounced vesicle orientation preference. In this plane their elongation is normal to the dyke-wall lobes. If we accept that the longest vesicle dimension aligns parallel to the flow direction, then the vesicles in the dyke also indicate flow perpendicular to the dyke wall lobes.

Dyke rock textures were examined by oriented thin sections along a profile taken at 2, 6, 13 and 41 cm away from the contact, also in the three mutually perpendicular planes described above (Fig. 1). In plane (a) (parallel to the dyke plane) a major fraction of the plagioclase crystals show basal sections, with almost no preferred orientation. Cubic magnetite grains (<5%) are irregularly scattered, showing no clear geometric relationships with the rock fabric. Plane (b) shows the most pronounced preferred orientation of plagioclase laths and vesicles. Magnetite grains are aligned in single- and multi-grain chains that are parallel to the general rock fabric. In plane (c) only very weak preferred orientation is observed in the dyke rock. Magnetite grains are generally irregularly scatterred, but in several places they are clustered in the interstices between the plagioclase laths. These relations show that plane (a) is the foliation (flow) plane of the dyke, as expected, and that the magnetic and petrographic fabric lineation (and thus also magma flow) are perpendicular to plane (c), i.e., also perpendicular to the dyke-wall lobes (Fig. 1).

ANISOTROPY OF MAGNETIC SUSCEPTIBILITY

Oriented cores for AMS analyses were taken in 5 profiles across the marginal band of the dyke and one profile in the central part of the dyke. The magnitudes and field orientations of the principal susceptibility axes were measured with a Sapphire Instrument SI-2 low-field magnetic susceptibility and anisotropy meter. To describe the observed magnetic anisotropy, the following parameters are measured: (I) Bulk (mean) susceptibility of the sample, $K=(K_I+K_2+K_3)/3$, where $K_1 \geq K_2 \geq K_3$ are the maximum, intermediate and minimum susceptibility axes respectively, and (2) total anisotropy, $H=100(K_I-K_3)/K$ (after Owens, 1974).

Bulk susceptibilities, K, range from 1.5×10^{-2} to 2×10^{-2} (SI units). The bulk susceptibility values gradually increase with the distance of the sample from the contact. Total anisotropy, H, ranges from 2.5% to 5.8% and shows significant variations across the profiles. H is highest at 3-6 cm from the contact and decreases towards the contact and towards the dyke center. Total anisotropy and bulk susceptibility profiles seem to be unrelated.

Maximum susceptibility (K_1) axes are clustered close to the dyke plane, and plunge on the average 20° to the southeast, which is the direction of the dyke-wall lobes. This agreement between K_1 axes and wall structures could suggest that K_1 axes indicate the direction of magma flow within the dyke, however, most K_3 axes are also in the dyke plane, rather than perpendicular to that plane, indicating an "intermediate" or "inverse" magnetic fabric (Rochette et al., 1992), in which K3 axes coincide with the long crystal axes and thus infer the flow direction. Single domain (SD) magnetites are a common cause for such magnetic fabrics (e.g., Potter and Stephenson, 1988), and indeed, normalized intensity curves (J/J_0) of 6 samples from distances between 3 and 41 cm from the contact, which were stepwise demagnetized in 5 or 10 mT increments indicate the presence of a significant proportion of SD grains in all the samples. This could explain the inverse fabric behaviour, namely, that K_1 axes are perpendicular. and K_3 axes are parallel to the flow direction, as determined by the vesicle and the petrofabric analyses (Fig. 1).

AMS-STRAIN RELATIONSHIP

Axial ratios of vesicles were measured to estimate the strain profile in the dyke. The vesicles are 3D ellipsoidal with 3 principal axes (Fig. 1): L_1 (maximum) - in the dyke plane, normal to the dyke-wall lobes; L_2 (intermediate) - in the dyke plane, parallel to the dyke-wall lobes; and L_3 (minimum) - normal to both dyke plane and dyke-wall lobes. The strain profile across the dyke is constructed from the harmonic means (Lisle, 1977) of L_1/L_3 ratios that were measured at each location. The highest strain (L_1/L_3=3.13) is found at 6 cm from the contact, decreasing to the contact (L_1/L_3=1.86) and to the center of the dyke (L_1/L_3=1.92).

A preliminary attempt to correlate flow-induced magnetic anisotropy with strain shows that the trends of the anisotropy and strain profiles across the dyke are similar: both are low close to the contact, highest at 3-6 cm from the contact and decrease toward the center of the dyke. The correlation between the two parameters is also fairly good (R=0.78). Regardless of the exact physical explanation of the AMS - strain relations, we believe that AMS measurements are promising as a tool for future strain determination. To demonstrate the dependence of AMS fabric on the position across a dyke, and thus its potential as a strain gauge, some AMS profiles across dykes from other sub-volcanic environments are shown. The trends along the various profiles suggest that: (1) the magnetic fabric is sensitive to the position across the dyke, and (2) different patterns of fabric variations could be the result of different flow profiles. Once strain and AMS are calibrated, these AMS profiles could be used for strain and velocity profile determination.

References

Baer, G. & Z. Reches 1987. Flow patterns of magma in dikes, Makhtesh Ramon, Israel. *Geology*, 15: 569-572.

Ernst, R.E. & W.R.A. Baragar 1992. Evidence from magnetic fabric for the flow pattern of magma in the Mackenzie giant radiating dyke swarm. *Nature*, 356: 511-513.

Hargraves, R.B., D. Johnson & C.Y. Chan 1991. Distribution Anisotropy: The cause of AMS in igneous rocks? *Geophys. Res. Lett.*, 18: 2193-2196.

Lisle, R.J., 1977. Estimation of the tectonic strain from the mean shape of deformed elliptical markers. *Geol. Mijnbouw*, 56, 140- 144.

McGuire, W.J., 1983. Prehistoric dyke trends on Mount Etna; implications for magma transport and storage. *Bull. Volcanol.*, 46, 9-22.

Owens, W.H. 1974. Mathematical model studies on factors affecting the magnetic anisotropy of deformed rocks. *Tectonophysics*, 24: 115- 131.

Potter, D.K. & A. Stephenson 1988. Single-domain particles in rocks and magnetic fabric analysis. *Geophvs. Res. Lett.*, 15: 1097- 1100.

Rochette; P., M. Jackson and C. Aubourg, 1992. Rock magnetism and the interpretation of anisotropy of magnetic susceptibility. *Rev. Geophysics*, 30, 209-226.

Shelley, D. 1985. Determining paleo-flow directions from groundmass fabrics in the Lyttelton radial dykes, New Zealand. *J. Vol. and Geotherm.* Res., 25: 69-79.

Stacey. F.D. 1960. Magnetic anisotropy of igneous rocks. *J. Geophys. Res.*, 65: 2429-2442.

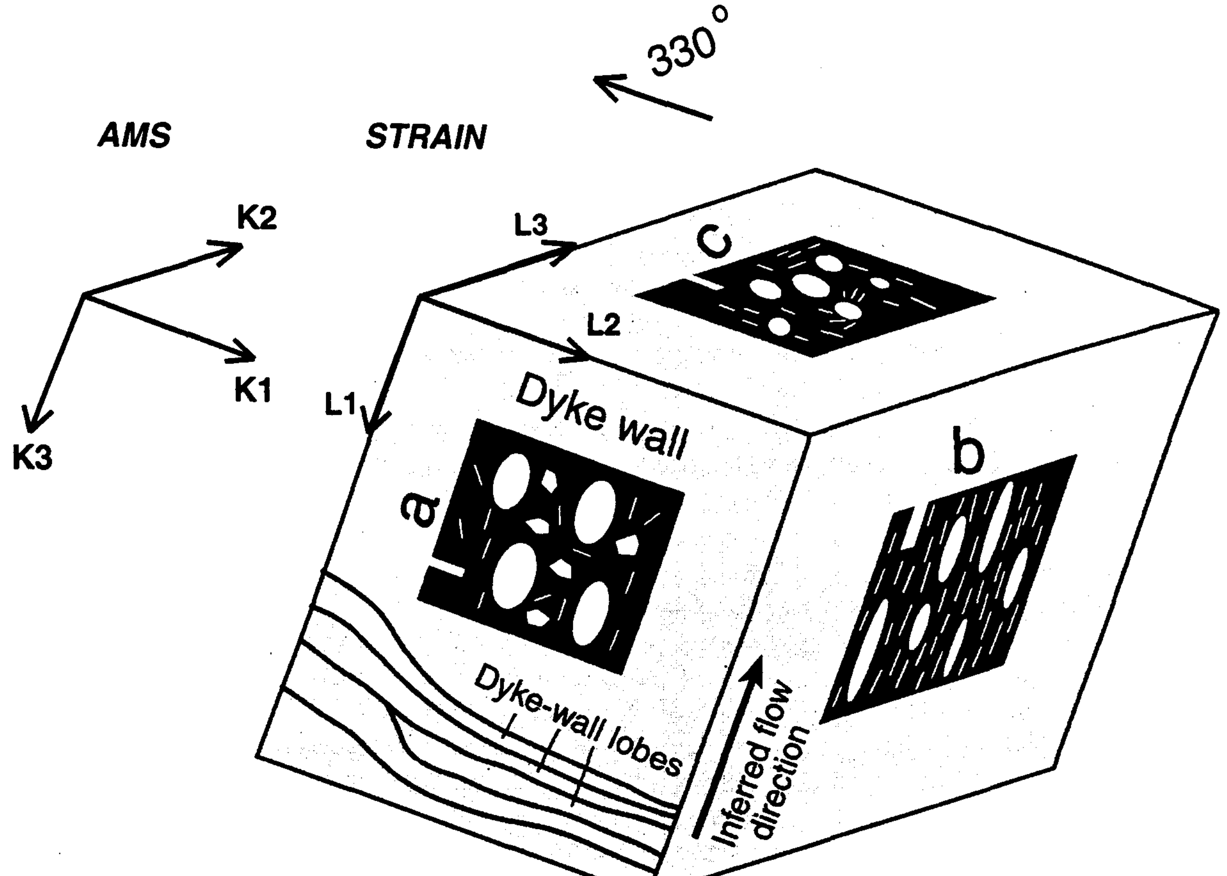

Figure 1. Schematic presentation of the spatial relations between the various flow indicators: dyke-wall lobes, petrofabric, deformed vesicles, and AMS. L and K denote the principal axes of vesicles and AMS respectively.

Host-rock deformation associated with dike emplacement in sedimentary, plutonic and volcanic rocks

Ram Weinberger

Geological Survey of Israel, 30 Malkhe Israel Street, Jerusalem 95501, Israel

The style and distribution of inelastic deformation around dikes help to better estimate the conditions during their emplacement. To understand the factors that govern the style of dike-related deformation, different host rocks in different geological environments were examined: sandstone, dolomite and shale in Makhtesh Ramon, Israel; granite rocks in the Sinai Peninsula, Egypt; and pyroclastic and basalt rocks in eastern Iceland. The present study demonstrates that dike-related shear fracturing is significantly more common than previously recognized, and includes shear features of various styles and scales: dike-subparallel deformation bands (lamellae of crushed detrital quartz grains) in sandstone; faults and folds in dolomite and shale layers; dike-parallel shear fractures in granite; and shear fractures and grabens in volcanic layers. The shear features are commonly observed adjacent to dike walls and rarely beyond dike tips. They are abundant within a few meters away from the dike walls, and are absent elsewhere away from the dikes. Shear offsets on the order of 1 mm to a few tens of cm are found along the dike contacts and at their tips. These observations strongly suggest that shear features form during dike propagation, near dike tips (in the dike "process zone"), and are subsequently juxtaposed along the dike walls.

Slickensided surfaces have been observed within failing bridges and displacements up to 1 m was recorded along faults associated with dyke segments; thus the segmentation may provide a source of seismicity during dyke propagation. The width of the deformation zone around dikes provides a first order approximation for the process-zone size around dikes in sandstone, dolomite, and shales in Makhtesh Ramon. The process-zone is up to several meters in size (<6 m), and is three orders of magnitude smaller than the dike half-length (>6000 m), but is of the same order of magnitude as the segment length. Dikes within other host-rock types and geological environments produce a wide range of process-zone sizes (0-50 m). However, the dike length could not be constrained, impeding further analysis of the dike-length to process-zone-size ratio. The width of the deformation zone is related to the average dike thickness, and varies along the dike length often in a periodic manner (Figure).

Distinguishable patterns of deformation are commonly observed near dike segments. The role of segment-propagation paths (straight or curved), of segment geometry (dike offset-to-thickness and overlap-to-thickness ratios) on the pattem of defommation was deduced separately. Segments that followed straight propagation path in granite are typically associated with bending and fracturing of the bridge, whereas segments that follow curved propagation paths in granite are typically associated with rotation of the bridge. If dike offset-to-thickness and overlap-to-thickness ratios are smaller than one, segments that propagated along curved paths in sandstone are typically associated with a fan-like pattem of defommation bands; if dike offset-to- thickness and overlap-to-thickness ratios are larger than one, similar segments are typically associated with a net-like pattem of deformation bands.

The mechanical constraints on the width of the dike-related defommation zones were examined under linear-elastic-fracture-mechanics (LEFM) assumptions, and compared with the observations from Makhtesh Ramon (1) to evaluate the applicability of the theoretical analysis; (2) to constrain the pemlitted values of variables such as the host-rock stiffness and the driving pressure gradient. The distance from the dike tip of potential joints increases with dike half-height and with the square of the driving pressure, and decreases with the square of the tensile strength plus the remote stress component perpendicular to the dike plane.

However, the actual distance of potential joints can get much shorter due to pore pressure effects, and cannot easily get much larger than the length of the dike tip cavity. The distance from the dike tip of potential shear defommation increases with dike half-height and with the square of the driving pressure, and decreases with the square of the shear resistance to band fommation. This distance is less than the length of the dike tip cavity for reasonable values of the host-rock shear resistance to band formation. The analysis also showed that the potential deformation zone width is parabolically related to the dike thickness. Measuring the deformation zone width, the average dike thickness and height, one can calculate the ratio between the host-rock stiffness to the shear resistance needed to fomm a defommation band. Comparison with the observations from Makhtesh Ramon shows the applicability of the theoretical analysis, and suggests that the defommation bands fomm near the laterally advancing front of the dike subparallel to the dike planes. The permitted values of the host-rock stiffness and the driving pressure gradient were obtained.

The stress and damage (deformation) fields of interacting dike segments were examined under the damage mechanics model. This model differs from the approach of previous studies in two major aspects: (1) the host material is non-linear with effective elastic properties that depend upon the damage distribution; (2) the fracturing process is explicitly controlled by the damage evolution. The fracturing process was illustrated by simulating growth of two echelon dike segments subjected to uniform driving pressure while propagating in a damaged material. The simulation results illustrate the stress-dependency of the distributed damage (i.e., different remote differential stresses enhance different damage distribution). In addition, the results showed the sensitivity of the damage distribution to the arrangement of the segments, the mutuality of segment propagation, and variations in the physical properties of the host material. Symmetric and asymmetric distributions of damage were produced by changing the applied stress and by controlling the segment-tip growth. The increasing tendency for hom growth is indicated for high twist angles and shear-stress magnitudes. The damage pattems yielded are satisfactorily correlated with the field observations, and constrain the stress state during dike emplacement. A single dike growth was simulated within an infinite medium, applying the damage mechanics model. The model assumed that a hydraulic connection is maintained between the reservoir and the dike, and pressure variations in the reservoir immediately vary the pressure at the dike tip. The model illustrated that an increase of magma pressure in the reservoir enhances a larger defommation zone than that associated with the background magma pressure, leaving a "signature" in the host rock. Hence, variations in the magma pressure in the reservoir appear to be a viable mechanism for the fommation of the observed variations in the width of the dike generated deformation zone.

Acknowledgments:

This study is part of R.W's Ph.D. dissertation at the Hebrew University, Jerusalem under the supervision of Gidon Baer, Amotz Agnon, Gadi Shamir, and Zvi Garfunkel. I am grateful to Vladimir Lyakhovsky and Moshe Eyal for their contribution to the study.

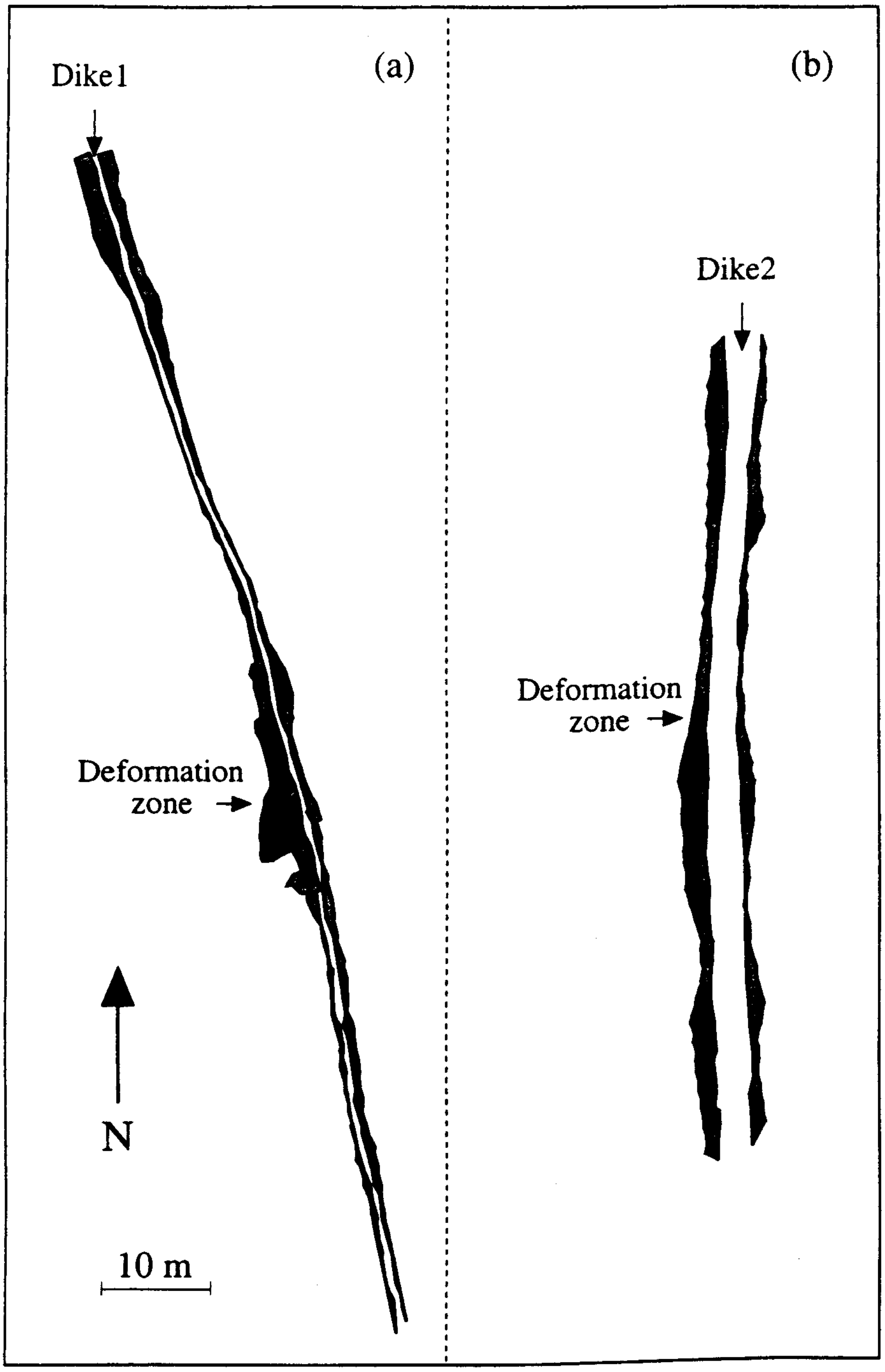

Maps of dikes and their associated deformation zones. Deformation zone width (DZW) is defined as the distance between the furthest deformation band on either side of the dike, measured perpendicular to the walls. The DZW varies along the dike length often in a periodic manner.

Growth and Collapse of Hawaiian Volcanoes

Robin T. Holcomb
University of Washington

The discovery of enormous landslides littering the seafloor around the Hawaiian Islands has led to significant reinterpretation of several Hawaiian volcanoes and new views of volcano development.

The volcanoes that have received particular attention include Wailau of East Molokai, Waianae of West Oahu, and the Island of Kauai. These are especially amenable to stratigraphic study because each recorded reversals of the geomagnetic field during its growth and was subsequently incised deeply by erosion. Although they are similar in having lost their unbuttressed flanks to large-scale landsliding during their post-shield stage of development, their intact remnants display different degrees of structural complexity.

East Molokai appears to be the simplest, with evidence so far for just one deep caldera filled by a simple stratigraphic sequence differing from that in the flanks of the volcano.

Waianae displays a more complicated succession of nested calderas filled by magnetically contrasting sequences of lava.

Kauai is a complex of three shield fragments, each shield having grown against the flank of an older neighbor and then losing its unbuttressed flank in a giant landslide. A sequence of thick, horizontal lava flows that was formerly interpreted as filling one large caldera near the center of Kauai instead accumulated in a topographic saddle between the three volcanoes.

Other Hawaiian volcanoes are more difficult to study because they apparently did not record geomagnetic reversals or are younger and less eroded. Nevertheless, comparisons with the better-studied shields lead to intriguing speculations about possible complexities of several other volcanoes too. Those complexities are potentially valuable for studies of landslides and magma evolution, and they should be testable by use of magnetostratigraphy, isotopic geochemistry, and radiometric dating.

The constructive and destructive first stages of the Cañadas Edifice (Tenerife, Canary Islands)

E. Ancochea[a]; M.J. Huertas[a]; J. Coello[b]; J.M. Fuster[a]; J. M. Cantagrel[c] & E. Ibarrola[a].

[a]Dpto. Petrología y Geoquímica. Fac.C.Geológicas. Univers. Complutense. 28040 Madrid, Spain
[b]Dpto. Edafología y Geología. Universidad de La Laguna. 38204 Tenerife, Spain.
[c]Dpto. Geologie, U.R.A. 10. Univ. Blaise Pascal-CNRS. 5, rue Kessler. 63038 Clermont-Ferrand, France.

During the last 3 Ma the Tenerife central zone has been occupied by shield or central composite volcanoes, collectively named the Cañadas Edifice. In this zone, the oldest visible materials; the Cañadas I Edifice are 3.5 Ma old. They appear in the Cañadas Wall and in the southern flanks of the Cañadas Edifice, in the bottom of deep radial ravines and in water galleries (Ancochea et al.,1990 and 1995).

The zone of the Cañadas Wall with the largest surface outcrop of the materials of the Cañadas I phase is a complex sector (LA; figure) in which two lithological units can be distinguished. The Angostura Basaltic Unit, with a visible thickness of about 150 m, is formed by a succession of basaltic or trachybasaltic lava flows characterized by the presence of plagioclasic hialobasalts with abundant breccia structures. Their ages vary between 3.34 to 2.99 Ma. The Angostura Trachytic Unit (2.77 to 2.66 Ma) is formed by massive, yet fractured, trachytic rocks as well as salic pyroclasts. In another Cañadas Wall sector (BT, figure) a thick series outcrops (Boca de Tauce Unit), dipping to the SW. It is formed mainly of basalts or plagioclasic hialobasaltic breccias with similar composition, position and age (3.00 Ma) to the Angostura Units.

In the outward SE flank of the Cañadas Caldera (TA, figure), there are a series of deep radial ravines exposing a series of lava flows dipping to the SE. The series is composed of more than 350 m of basalts interspersed with some salic rocks and ages: 3.69 to 3.43 Ma. In another ravine to the S of Cañadas Edifice (PA, figure), underneath 2.2 Ma lava flows, there is another series of brecciod plagioclasic basalts which can be correlated with all those mentioned above. In an external radial gorge to the west (TA, figure), massive and pyroclastic trachytes are frequently cut by dykes. A horizontal water gallery that penetrates under them cuts brecciated plagioclasic hialobasalts analogous to those outcropping in the Cañadas Wall.

Finally, a drill hole made in the NW of the Cañadas Wall (CH, figure), after penetrate several hundreds of meters of more recent salic lava flows, arrives to plagioclasic hialobasalts which represent the NW extension of the Cañadas Edifice.

The dips of the lava flows denote a source situated in the central part of the island, unable to be determined precisely without additional data. The height of the edifice formed in this first phase must have been over 2300 m (the height of the outcrops in Cañadas Wall).

In the Cañadas I materials, or in the older materials of the Old Basaltic Series, there are dykes of very different directions which reasonably must correspond to different centers. If one eliminates those that are coherent with the patterns of dykes of posterior units, the remaining directions converge in a zone situated to the S of Guajara (figure) which could be the approximate position of the emission center. Assuming an edifice almost circular in shape with its center approximately in the above mentioned convergence zone of the dykes, its dimensions would be of almost 19 km in diameter and 3000 m in height.

After the first phase of activity of the Cañadas Edifice, an important destructive period took place which is manifest by the existence of large debris-avalanche deposits. This deposits appear essentially in the Roques de Garcia sector (RG, figure) that dissects the Cailadas Caldera, as well as in the Cailadas Wall in the lower section of the Llano de Ucanca. In both cases, these breccia are cut by dykes of the Cañadas II Edifice, indicating that each was indeed formed before that edifice. On the other hand, there is a breccia to the N in the Tigaiga Massif, in the water galleries and under materials which has an age of 2.2 Ma (Ibarrola et al., 1993). This unit was formed, for the most part, by debris avalanche episodes.

Where the debris avalanche deposits do not occur in the Cañadas Wall or in the southern exterior part of the Cañadas Caldera, the lower levels of Cañadas II Edifice (2.35-2.0 Ma) lean on the Cañadas I materials, indicating an interruption in the volcanic deposits in this sector.

The debris-avalanche deposits outcropping mostly in the north of the Cailadas Edifice, and the fact that most of the outcrops are located to the S of the Cañadas Edifice (figure), indicates the existence of a sudden destruction of the edifice to the North by flank-failure mechanism. This deposits can be seen in their proximal zone in the Cañadas Wall itself (Roques de Garcia breccia) and in the most distal zones in the N flank of the Cañadas Edifice I (Tigaiga Breccia).

In the galleries of the valley of La Orotava there is another breccia (Coello and Bravo, 1989). This Orotava breccia appear at a higher stratigraphic level than the one just mentioned and has an age under 0.73 Ma. In one of the galleries of this valley, Carracedo (1975) dated a phonolitic flow interbedded between both the breccias, giving 2.3 Ma, which is analogous to the Tigaiga Breccia age. Possibly, the Tigaiga Breccia formed a detachment level which favoured the landslide that formed the valley of La Orotava and the Orotava Breccia itself.

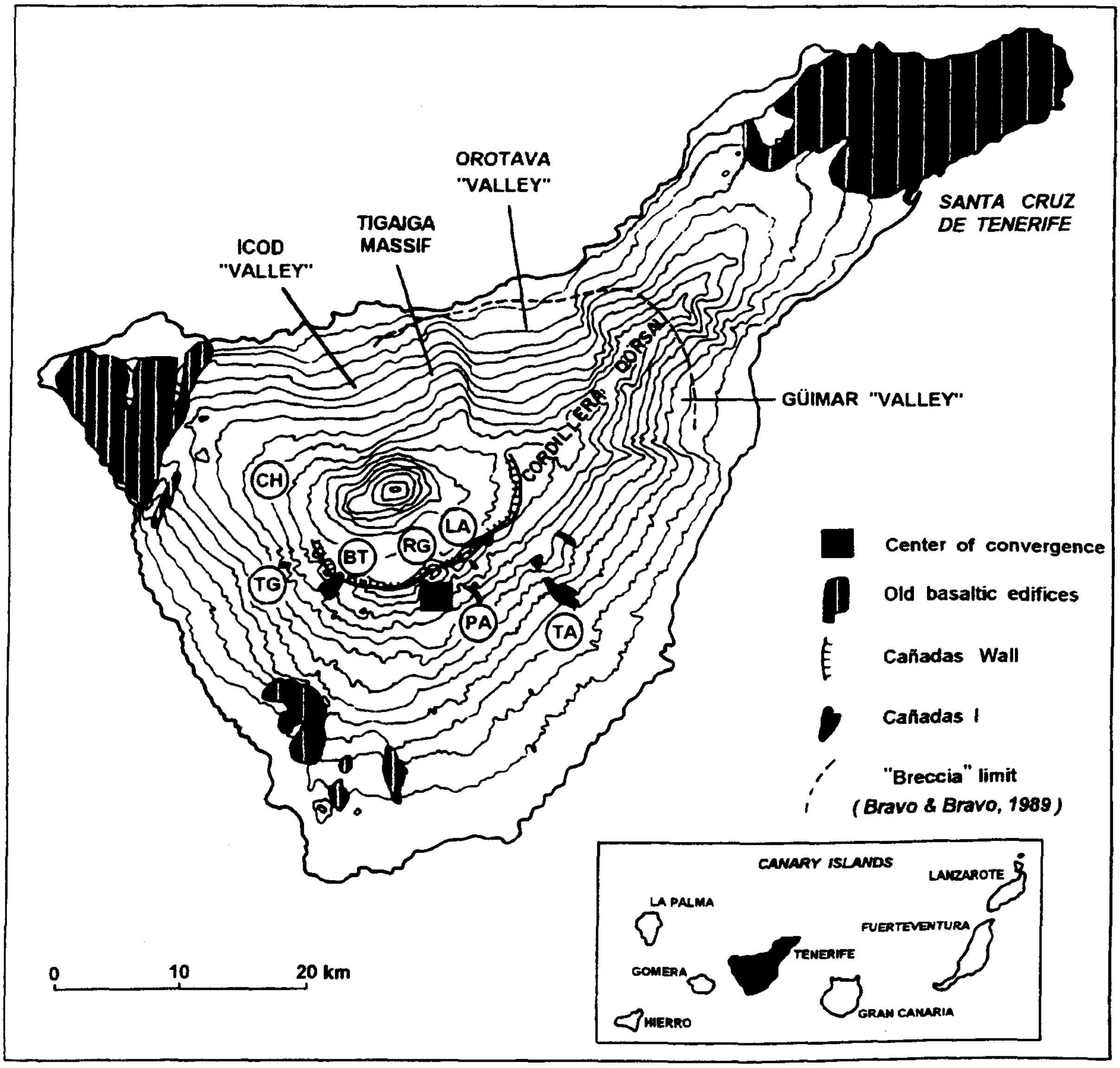
OROTAVA
"VALLEY"
TIGAIGA
MASSIF
ICOD
"VALLEY"
SANTA CRUZ
DE TENERIFE
CORDILLERA DORSAL
GÜIMAR "VALLEY"
CH
LA
RG
BT
TG
PA
TA
Center of convergence
Old basaltic edifices
Cañadas Wall
Cañadas I
"Breccia" limit
(Bravo & Bravo, 1989)
0
10
20 km
CANARY ISLANDS
LANZAROTE
LA PALMA
FUERTEVENTURA
TENERIFE
GOMERA
GRAN CANARIA
HIERRO

ISLAND UPLIFT AND TILTING GENERATED BY ISOSTATIC REBOUND AFTER GIANT LANDSLIDES

John R. Smith and Paul Wessel
Univ. Hawaii, SOEST, 2525 Correa Rd., Honolulu, HI 96822
jrsmith@soest.hawaii.edu and wessel@soest.hawaii.edu.

Early studies established the relationship between subsidence and volcanic load on the Hawaiian Ridge, whereby the volcanic construction of the Hawaiian Islands, by the hot spot plume, and their subsequent load upon the Cretaceous-age oceanic crust down-bows this crust causing the islands to sink. This subsidence, noted to be 2.4 mm/yr at Hilo relative to a "stable" Honolulu, is rapid and has caused most Hawaiian volcanoes to descend 2-4 km since reaching sea level, while the bases have subsided 5-8 km. Between one-half to two-thirds of the volcanic construction is suspected to be offset by this subsidence. Processes which could reduce the subsidence effect and/or cause uplift include unloading caused by erosion or riding up the flexural bulge caused by the younger volcanoes as each volcano travels offthe hot spot as the Pacific tectonic plate moves northeast at ~10 cm/yr.

The purpose if this paper is to model the unloading effects (redlstrlbutlon of mass) due to these debris avalanches and slumps, and depict the change to the flexural curve beneath the island chain. Such effects are analogous to glacial rebound; the isostatic readjustment caused by melting of glacial shields on continental regions. However, the landslide case is somewhat different because the shedded material is still present on the ocean floor near the island. With the debris avalanches, the material may be thinly spread over a broad area, while the slide blocks resulting from slumping appear to be shifted slightly seaward over time, resting intact adjacent to, and comprising part of, the volcano's base.

Three-dimensional numerical modeling experiments were devised to examine how this mass redistribution affects the isostatic flexural curve. Dimensions and estimated volumes of landslide deposits were obtained from the literature. By implementing approximate sizes of a pre-slide Oahu and Hawaii Islands, the relative percentages of the edifice mass required to generate the emplaced deposits were determined. A debris avalanche of 10-40% of pre-slide Oahu is required to account for the 1200-5000 km^3 Nuuanu event deposit, while only ~1% of pre-slide Hawaii is necessary to generate the 200-800 km^3 Alika I and II avalanche deposits.

Trials were run using 25, 30, and 40 km plate thicknesses. The island uplift resulting from the Nuuanu slide was calculated to be in excess of 100 m (25 km plate) with greater uplift directly over the failed flank, causing the edifice to tilt away from the calved-off portion. The landslide deposit depresses the plate several meters beneath the debris field itself. Smaller slides originating from a larger edifice (Alika I and II) do not produce as much flexural response (~20 m uplift for a 25 km plate).

The effects of slow moving, intact slumps where the failed blocks remain relatively close to the island pedestal were examined for the case of the Hilina slump? comprising approximately 10% of the Hawaii Island edifice. Perhaps more significant than the comparable uplift to the 10% Nuuanu case, is the +100 m of downwarp beneath the massive slumped foot.

These experiments have not yet considered the viscoelastic effect which may constrain the time frame for flexural response. The landslide rebound process, especially in the case of a relatively large slide or slump, should be considered as an added component to the evolutionary course of oceanic islands.

Fault rocks, gouge breccia intrusions and groundwater in oceanic island volcanoes.

S.J. Day
Dept. of Geography & Geology, Cheltenham & Gloucester College of Higher Education, U.K.

Greig Fester Centre for Hazards Research
University College London, U.K.

Seismic and geodetic evidence clearly demonstrates the importance of brittle deformation in oceanic island volcanoes, and especially in the development of volcano flank instability. The mechanics of oceanic island deformation can therefore be expected to be profoundly influenced by the properties of the faults on which this deformation takes place, and in particular of the fault rocks produced along the active slip zones. Despite this, few previous accounts exist of fault rocks in old, deeply eroded collapse structures (perhaps the most notable previous studies are those in the Roque Nublo collapse structures of Gran Canaria (Garcia Cacho et al. 1987; Mehl & Schmincke 1992)) and none at all of fault rocks in younger, more shallowly eroded, and active collapse structures. Furthermore, no analysis of the mecharlical properties of those fault rocks which have been identified has been carried out, in contrast to the intensive studies of tectonic faults in non - volcanic areas (see Scholz 1990 for a review) and at mid - oceanic ridge plate boundaries (see Gudmundsson 1995 for a review). This lack of study of fault rocks in oceanic island volcanoes reflects, in part, a lack of surface exposure of such rocks. Regions such as the actively - deforming south flank of Kilauea volcano, Hawaii, are characterised by gaping fissures at the surface (which must link down into faults at depth) and fault scarps (*pali*) entirely draped by younger lavas. The intense activity of the Hawaiian volcanoes and also of many other active oceanic island volcanoes greatly reduces the potential for surface exposure of fault rocks, exposed by erosion or exhumed from depth by continued slip in the fault zones. However, recent investigations in the Canary Islands by the author have revealed a number of fault rock exposures, even in recently active volcanoes: it seems likely that similar exposures exist in other volcanoes but have not been identified as such. Accordingly, emphasis is placed in this contribution upon the appearance of these rocks at outcrop, and how field and petrographic observations can be used to study the mechanics of the faults in which they formed.

The most extensive exposures of fault rocks in the Canary islands are in the deeply - eroded Roque Nublo collapse structures in central Gran Canaria. Detailed mapping has revealed the presence of three separate, superimposed collapse structures in the area around Ayacata (Torrado et al., this volume). Of these the second and third to form consist of faulted domains bounded by shallowly - inclined basal detachments and steeply - inclined to vertical headwall and sidewall faults. Within the allochthonous faulted domains deformation is largely coherent and confined to narrow fault zones and clastic breccia intrusions separating blocks of essentially undeformed pre - existing rock which are up to a few kilometres across and several hundred metres thick. These blocks have slid for distances of up to several kilometres on the shallowly - inclined (< 10^o) basal detachment faults. This remarkable mobility is comparable to that of thrust sheets in tectonic fold belts, especially in view of the fact that many of the faults are well under a metre thick and thus a fraction of the thickness predicted by normal fault thickness - displacement relationships (Forslund & Gudmundsson 1992; Gudmundsson 1995; Walsh & Watterson 1988).

At outcrop the faults in the Roque Nublo collapse structures are characterised by grooved and slickenlined bounding surfaces at the margins: these structures may be incised into the wall rock or in thin layers of cohesive cataclastic material adhering to the wall rocks. They provide important information on the overall movement field during the collapses (Torrado, Day & Carracedo, this volume), especially when tool marks and "roche moutonee" - like erosional structures around hard clasts in the wall rock indicate slip sense as well as slip direction. Such surfaces are commonly well - preserved under overhangs produced by erosion of the softer materials which occupy the bulk of the fault zone. These consist of a variety of mainly weakly indurated gouge - like cataclasites ranging from streaky banded clays (some with recognisable intensely deformed pumiceous and other clasts) to homogenous clay matrix - rich breccias to homogenous lithic - rich breccias, all produced by abrasion of the wall rocks during faulting. The clast populations in these breccias are extremely varied even when the immediately adjacent wall rocks are formed by homogenous rock units, indicating vigorous mixing of materials in the fault zones. The homogenous breccias commonly form sheet - like to irregular intrusions, intruded both along the faults and as gouge breccia dykes and vein complexes in the host rocks. These homogenous breccia intrusions were produced by fluidisation of the cataclasites: the clayey nature of the matrix indicates that this fluidisation was aided by the presence of large amounts of water. The low - viscosity fluidised material would have been at lithostatic pressure or even super - lithostatic pressure. This is confirmed by the almost perfectly random orientation of the faults and gouge breccia intrusions, which include many subhorizontal sheets, coupled with the coherent deformation field measured using the slip directions and slip senses indicated by the fault surface structures noted above. By analogy with the Rubey & Hubbert (1959) model for movement on thrust faults the very high fluid pressure on the faults would have allowed the very large movements on the basal and sidewall detachment faults of the collapse structures.

In strong contrast to the faults of the Roque Nublo collapse structures are those of the San Andres aborted collapse structure on the island of El Hierro (Day et al., in press; Carracedo et al., this volume). The main fault of this structure, which bounds a displaced block some 10 km long and at least 4 km wide and 1 km thick that has slid seaward by some hundreds of metres, has a single main slip plane and fault rock sheet. This has been preserved at a number of places on and at the foot of a 300 m high fault scarp, largely as a result of burial under screes which are now being eroded away. The fault rocks which are exposed therefore formed within 300 m or less of the palaeosurface. In the best - preserved outcrops the fault zone consists of a sheet of indurated cataclasite, a few tens of centimetres thick, on the footwall side of the slip surface. The cataclasite grades from a relatively coarse fault breccia through an ultracataclasite zone to a thin layer, less than a centimetre thick, of pseudotachylyte (frictional melt rock) at the fault surface itself. The structure of this fault zone resembles that of basal slip surfaces in certain very large non - volcanic landslides in mountainous areas (Erismann 1979; Masch et al. 1983): these are the only other settings in which pseudotachylyte has formed so close to the surface. There is no evidence for the presence of syn - deformational aqueous fluids (in the form of alteration or veining) and indeed the occurrence of frictional melt rock is most easily explained if it is assumed that the fault surface was dry during movement (Lachenbruch 1980). The persistence of large frictional forces during slip on the San Andres fault system may account for the cessation of movement on this unique aborted lateral collapse structure.

A third group of faults which may be associated with a Canarian collapse structure occur in the upper part of the pre - collapse sequence in the headwall of the Orotava collapse structure on Tenerife. Numerous minor faults, running parallel to the trend of the collapse structure, cut lavas and pyroclastic units (including various lapilli and pumice beds). In these pyroclastic units the faults are marked by thin (< 1 cm thick) bands of unlithified powdery crushed rock. These resemble crush bands developed in high - porosity sandstones (Woodcock & Underhill 1987; Weinberger et al. 1995). A feature of such bands is that they show slip - hardening behaviour, which may account for the large number of faults and the small displacements in the Orotava headwall area. Their development reflects the high porosity and unlithified particulate nature of the pyroclastic rocks in this sequence. Initially similar rocks which have been altered or lithified show very different behaviour, exemplified by fumarolically indurated lithic - lapilli deposits on top of the 1585 lava dome at Jedey on La Palma, in which cohesive fault rocks formed within two metres of the surface.

This survey of fault rocks in the Canaries indicates that an important part in the development and behaviour of faults and fault rocks in oceanic island volcanoes is played by groundwater. In addition to promoting instability through the mechanical and thermal pore fluid pressurisation effects identified by, *inter alia*, Elsworth & Day (this volume), the presence of abundant pore fluids will promote the development of highly pressurised, fluidised fault gouges and therefore sustained sliding of kilometre - scale blocks on low - angle basal detachment surfaces. Conversely, internal deformation or sliding between blocks may permit escape of these pressurised fluids into gouge breccia intrusions and arrest motion of the lower parts of sliding masses while the escaping fluids may promote disaggregation of the upper regions into debris avalanches: these are closely associated with the collapse structures in Gran Canaria (Torrado et al., this volume). The complete arrest of the intact sliding block in the San Andres fault system may be the result of a lack of sufficient pore water within the deforming region for these processes to occur.

It is therefore important to understand the distribution of pore fluids, principally in the form of meteoric groundwater and seawater, within oceanic island volcanoes. In active volcanoes water tables can be mapped in wells and water drainage tunnels (Canarian *galerias*) where these are abundant; but a variety of geophysical methods may be more generally applicable. In old collapse structures palaeo - water tables can be mapped using alteration patterns: in the Guimar edifice of Tenerife, low - temperature zeolite - facies alteration is pervasive below the palaeo - water table whilst localised but high - temperature fumarolic alteration occurs above the palaeo - water table. Differing degrees of alteration in different groups of dykes indicate that the mapped palaeo - water table is that which was present immediately prior to the collapse of the Güimar edifice.

References.

Day, S.J., Carracedo, J.C.. & Guillou, H. 1997. Age and geometry of an aborted rift flank collapse: the San Andres fault system, El Hierro. Canary Islands. *Geological Magazine* 134 (4): 523-537.

Erismann, T.H. 1979. Mechanisms of large landslides. *Rock Mechanics* 12, 15 - 46.

Forslund. T. & Gudmundsson, A. 1992. Structure of Tertiary and Pleistocene normal faults in Iceland. *Tectonics* 11, 57 - 68.

García Cacho, L., Anguita, F., Araña, V., Barberi, F., Diez - Gil, J., Ortiz, R. & Sbrana, A. 1987. Una nueva perspectiva de la Formación Roque Nublo (Gran Canaria). Bol. Geol. Min., 98, 859 - 863.

Gudmundsson, A. 1995. Infrastructure and mechanics of volcanic systems in Iceland. *Journal of Volcanology and Geothermal Research* 64, 1 - 22.

Lachenbruch, A.H. 1980. Frictional heating, fluid pressure, and the resistance to fault motion. *Journal of Geophysical Research* 85, 6097 - 6112.

Masch, L., Wenk H.R. & Preuss, E. 1985. Electron microscopy study of hyalomylonites ---- evidence for frictional melting in landslides. *Tectonophysics* 115, 131 - 160.

Mehl, K. & Schmincke, H.U. 1992. Multiple sector collapse of the Pliocene Roque Nublo Stratocone on Gran Canaria (Canary Islands). III Congreso Geologico Espana y VIII Congreso Latinoamericano Geologia, Salamanca. Abstracts 1 448 - 452.

Rubey, W.M. & Hubbert, M.K. 1959. Role of fluid pressure in mechanics of overthrust faulting. I: Mechanics of fluid - filled porous solids and its application to overthrust faulting. *Bulletin of the Geological Societv of America* 70, 115- 166.

Scholz. C.H. 1990. *The Mechanics of Earthquakes andfaulting*. Cambridge, U.K.; Cambridge University Press. 439 pp.

Walsh, J.J. & Watterson. J. 1988. Analysis of the relationship between displacement and dimensions of faults. *Journal of Structural Geology* 10, 238 - 217.

Woodcock, N.H. & Underhill. J.R. 1987. Emplacement - related fault patterns around tlle Nortllern Granite, Arran, Scotland. *Bulletin of the Geological Society of America* 98, 515 - 527.

Weinberger, R., Baer, G., Shamir, G. & Agnon, A. 1995. Deformation bands associated with dyke propagation in porous sandstone, Makhtesll Ramon, Israel. In: Physics and Chemistry of Dykes. Baer & Heimann (eds.) Publ. Balkema, Rottcrdam. P. 95 - 112.

Revision of the site and the eruptive history of the 1677 eruption of La Palma, Canary Islands, by cross-analysis of contemporary accounts and detailed geological and archaeological observations

J.C. Carracedo[1,2], S. Day[2], H. Guillou[3], E. Rodríguez Badiola[4] and F.J. Pais Pais[5]

[1]*Estación Volcanológica de Canarias, CSIC, La Laguna, Tenerife, Canary Islands, Spain*
[2]*Cheltenham & Gloucester College of Higher Education, Cheltenham, U.K*
[3]*Centre des Faibles Radioactivites, CEA-CNRS, Gif sur Yvette, France*
[4]*Museo Nacional de Ciencias Naturales, CSIC, Madrid, Spain.*
[5]*University of La Laguna, Tenerife, Canary Islands, Spain*

The 1677 volcanic eruption, located close to the town of Fuencaliente at the south end of La Palma, has long been associated with the large volcanic cone of San Antonio, an emission centre showing relatively high energy phreatomagmatic phases which would have devastated the town of Fuencaliente had they occurred in 1677. However, detailed geological observations (Fig. 1), radiometric dating and a reinterpretation of available eye-witness accounts prove the San Antonio emission centre to be a preexisting volcano related to an eruption that occurred several thousand years earlier. This conclusion is also consistent with the recent discovery of pre-Hispanic aboriginal (Guanche) relics in a cave on the flank of the San Antonio cone (Fig. 2). The true 1677 eruption was of a much smaller magnitude and occurred from a small strombolian vent and a cluster of aligned spatter vents on either side of the San Antonio volcano. 75-125 x 106 m3 of lavas from these spatter vents covered an area of 4.5 x 106 m2 and formed a wide coastal platform with 1.6 x 106 m2 of new land gained from the sea. This modest magnitude eruption is in better accord with the negligible damage caused to the area reported in the contemporary accounts.

Archaeological studies in the area show the presence on the flanks of the San Antonio cone of well-preserved remains of the pre-Hispanic inhabitants (the benahoaritas) in the form of dwellings and pottery. This archaeological evidence confirms the presence of this cone at least 184 years before the occurrence of the 1677 eruption.

This revision of the 1677 eruption and its magnitude is relevant for the precise reconstruction of the recent volcanism of La Palma and the correct definition of volcanic hazards in the island. It exemplifies, as well, the importance of detailed geological work as a necessary step in the accurate interpretation of contemporary accounts. Oral tradition regarding the site and nature of eruptions can become confused with remarkable rapidity: a similar misidentification of eruption sites to that which has occurred at Fuencaliente has affected recent accounts in the scientific literature of an eruption which occurred on Fogo island (Cape Verde archipelago) in 1951.

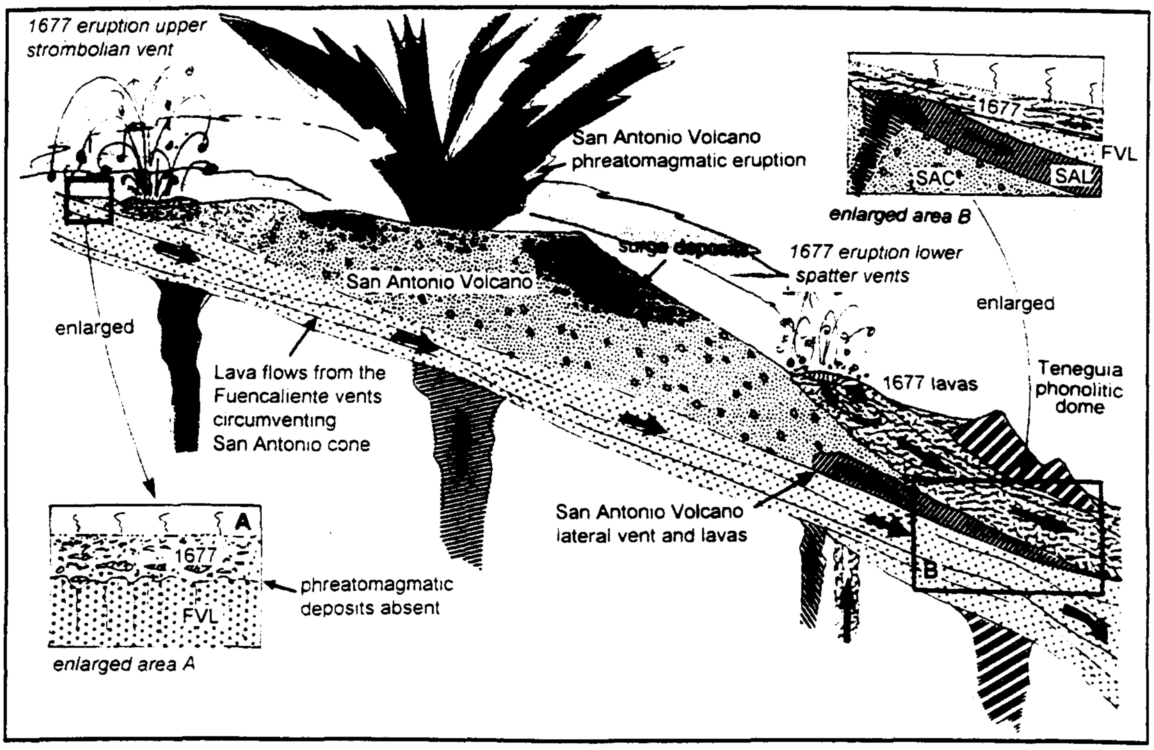

Fig. 1.- Schematic drawing showing the main stratigraphic and volcanological evidences excluding the San Antonio volcano as part of the 1677 eruption. *FVL*: Fuencaliente volcanic group lavas (> 3.2 ka). *SAC*: San Antonio cone. *SAL*: San Antonio lavas.

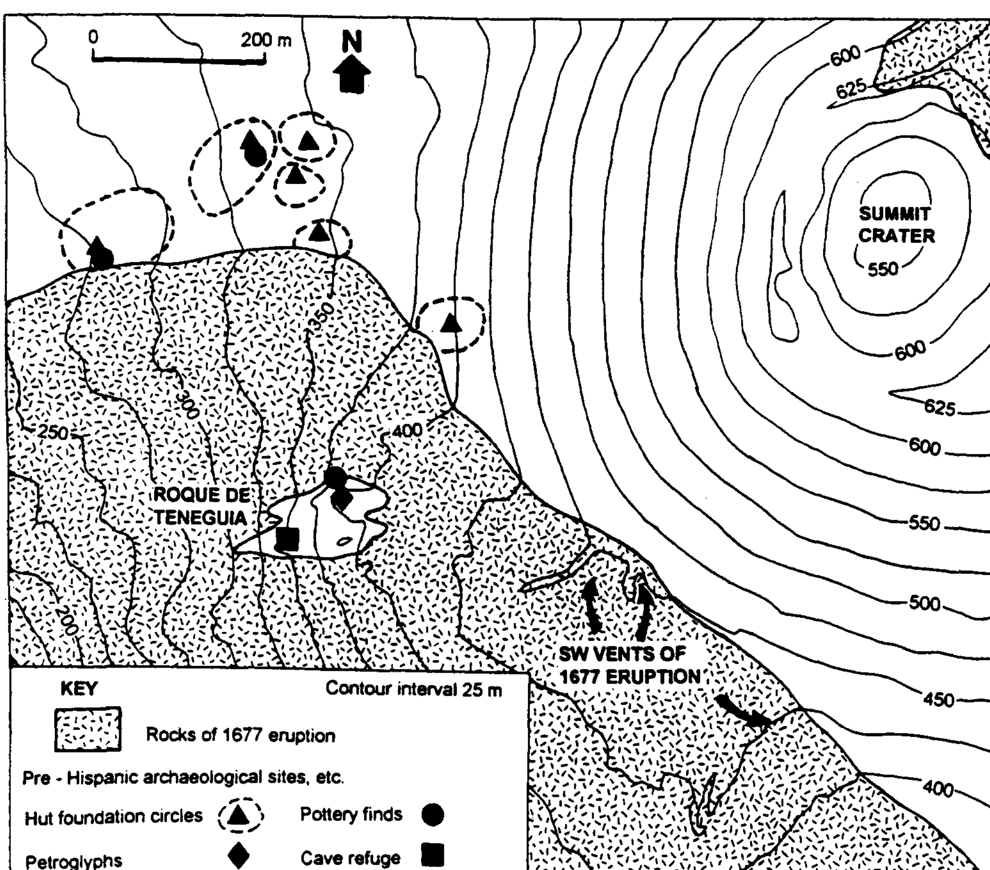

Fig. 2.- Mapping of the pre-Hispanic archaeological remains in the San Antoio volcano area shows that the guanches dwelt on the lavas of the San Antonio Volcano. The guanche dwellings, shown in the map. were partially covered by the 1677 lavas. This is sound, non-geological evidence supporting the San Antonio as a volcano pre-dating the 1677 eruption.

222Rn flux at Cañadas caldera, Tenerife (Canary Islands)

Martin, M.C.(*) and Soler, V. (**)

(*) Geology and Soil Science, University of La Laguna, Tenerife, (Canary Islands)

(**) Volcanological Station of the Canary Islands - CSIC, Tenerife, (Canary Islands)

Tenerife Island is a volcanic complex with a documented activity continuing since the Miocene into historic times. Present day residual volcanic activity is manifested by fumaroles (Teide volcano), anomalous high temperature zones (up to 50 °C), microseismicity and cold distal gas emissions.

High radon concentrations in the underground environment (galleries) have been reported in relation to the volcanic structure of Tenerife (Soler et al; 1991). To study the radon concentration and its temporal behaviour in the deep subsoil of the island, a radon monitoring programme has been carried out during 1994-95 at three wells. Vertical profiles were measured at two of the boreholes to study the radon concentration gradient alon.~ the pipe.

Radon measurements were done using Solid State Nuclear Track Detectors (SSNTD) with integration time of one month, supplied and analysed by Landauer Inc. and by gamma spectrometry ($NaI_{(Tl)}$ detector) of ^{214}Bi and ^{214}Pb in activated charcoal canisters, with inte~ration time of 3-4 days.

1. <u>Mña. Majua well</u>, located inside the Canadas Caldera at 400 m from Teide volcano. The well is 505 m deep and is cased along the entire pipe. The water table is presently located at 445 m. From this depth to the bottom the casing is perforated. CO_2 concentration above the water is about 12 % vol. Along most of the length of the well high Rn values were found. Close to the surface (0 m) 284 pCi/l are measured, with higher values (874-1051 pCi/l) between 50 and 300 m. Anomalous ^{238}U or ^{226}Ra contents have not been detected in underground waters from Tenerife (Catalan et al, 1993), thus the high radon activities measured at Mña. Majua well, point to a highly active radon flux coming from depth. CO_2 volcanic emissions could be acting as carrier gas for radon transport to surface.

2. <u>Guaza well</u> is located at the tip of the southern ridge of the island. The water table is at 130 m but there is no available information on casing nor on CO_2 content. In this well a radon monitoring at 120 m depth during one year was carried out. During the observation period, the Rn levels were low, ranging from 101 to 161 pCi/l.

3. <u>Güimar well</u>, located in the Guimar Valley. The water table is at 98 m and also, there is no available information on casing nor on CO_2 content. The profile along the pipe shows a radon level almost constant, with values of 23-25 pCi/l from the surface to above the water table.

The detected radon concentrations close to the surface at Güimar and especially at Mña. Majua wells (23 and 284 pCi/l at 0 m respectively) are much higher than the normal content in air (< 1 pCi/l). This behaviour is interpreted in this work to be due to the existence of an active radon tlux along the entire pipe, coming from exsolved radon from underground water. enhanced by CO_2 emissions.

The temporal variation of radon at Güimar and Guaza wells (where the radon level is quite low), shows a seasonal pattern and a positive correlation with atmospheric temperature. This indicates that in this wells Rn flux is influenced by meteorological parameters. On the other hand, at, Mña. Majua well, where the overall radon concentration is very high, this correlation is less clear, exhibiting relatively strong time variations, which are not correlated with atmospheric variables. These fluctuations probably reflect changes in subsurface geophysical processes at depth or different inputs of volcanic CO_2 into the svstem.

At this stage, it has so far proved impossible to infer any relation between radon emission variations and seismic activity in the area, due to the low time resolution of the method used for Rn measurements (one month integration time) and to the low level of seismic activity in the area. However, there is evidence of active radon flux within the studied area, that is clearly related to the volcanic system. Thus, an improved radon monitoring programme seems to be a promising tool for volcanic surveillance at Tenerife, and specifically at Teide volcano.

Acknowledgements: This work was been supported by the Canarian Government, DGECD project n. 92/142. Access to wells and logistic support afforded by the Consejo Insular de Aguas de Tenerife are gratefully acknowledged. We are indebted to the Observatorio Meteorológico de Sta. Cruz de Tenerife for the meteorological data.

References

Catalan, A. Bayo, O.; Garcia-Yanes, M. Martín, R. and Hernández-Armas, J. (1993). Caracterización radiológica de aguas de Canarias. Com. IX Congr. Nac. De Física Médica. 22-24 sept. 1993, Tenerife, Spain.

Soler, V., Carracedo, J.C, Coello, J., De la Nuez, J., Martín, C. and Badiola, E. Radon in galleries related to volcanic activity in the island of Tenerife, Canary Islands. Int. Conf. Active Volcanoes Risk Mitigation, Naples, 1991 (Abstract).

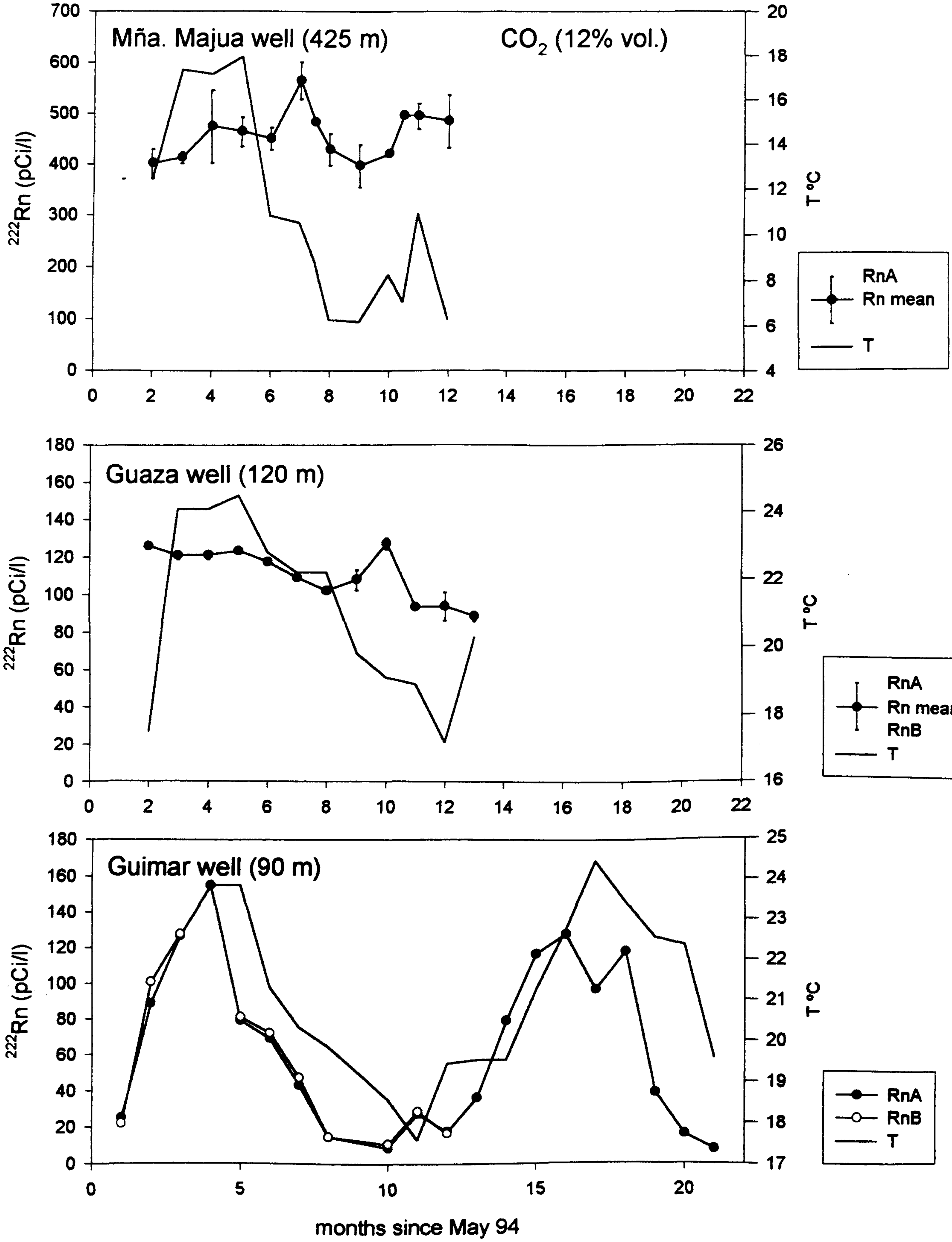

Mña. Majua well (425 m)
CO_2 (12% vol.)
^{222}Rn (pCi/l)
T °C
RnA
Rn mean
T
Guaza well (120 m)
^{222}Rn (pCi/l)
T °C
RnA
Rn mean
RnB
T
Guimar well (90 m)
^{222}Rn (pCi/l)
T °C
RnA
RnB
T
months since May 94

Keynote Talk: Is Palaeomagnetism □ useful, □ useless, □ irritating (*) in volcanological studies? (*) please check one

Hervé Guillou[1], John Sinton[2] and Juan Carlos Carracedo[3] and Carlo Laj[1]

[1] Centre des Faibles Radioactivitès, CEA/CNRS, Gif-sur-Yvette , France; [2]Department of Geology, University of hawaii, 96813, USA; [3]Estación Volcanológica de Canarias, Consejo Superior de Investigaciones Cientificas, La Laguna, Tenerife, Canary Islands, Spain.

The use of Palaeomagnetism — especially geomagnetic reversals— can be considered _IRRITATING, since this method, which is basically statistical in nature, requires intensive sampling and tedious laboratory measurements, and is, in the opinion of some, USELESS.

However, in our work in the Hawaiian Islands and the Canarian archipelago, we have found this a very USEFUL method in stratigraphic work, decisively helping to define correlatable magnetostratigraphic units in pre-Brunhes volcanic formations, as well as in providing USEFUL constraints to improve the reliability and accuracy of radiometric ages. Work in the Waianae Volcano (Oahu, Hawaii) by Presley and co-workers (1997), and in the islands of Molokai and Kauai (Holcomb et al., 1977) contributed to the reconstruction of their volcanic histories and to the definition of important structural and volcanic features (Holcomb, 1997, Holcomb et al., 1996).

Analogous intensive work carried out in recent years in the western Canaries (Tenerife, La Palma and El Hierro) using detailed geological mapping, magnetostratigraphy and precise, unspiked K-Ar dating (Guillou et al., 1996; Guillou et al., 1997; Carracedo et al., 1997; Wijbrans et al., 1997) attest the usefulness of the combined use of these methods in volcanic terrains. Palaeomagnetism is also a very USEFUL method in the reconstruction of major tectonic events affecting volcanic formations, as illustrated in the near-vertical rotation of parts of the Hilina fault system (Riley et al., 1997) and near-horizonatl rotation in the Tiñor volcano in El Hierro (Szeremeta et al., 1997).

References

Carracedo, J.C., Day, S.J. and Guillou, H., 1977b. Late (Quaternary) shield-stage volcanism in La Palma and El Hierro, Canary Islands. Internat. Workshop immature oceanic islands, La Palma, 1977. Vol. Abstr: 61-66.

Guillou H., Carracedo J.C., Pérez Torrado F. and Rodríguez Badiola E., 1996. K-Ar ages and magnetic stratigraphy of a hotspot-induced, fast grown oceanic island : El Hierro, Canary Islands. J. Volcanol. Geotherm. Res. 73: 141-155.

Guillou, H., Carracedo, J.C. and Day, J.C., 1977. Unspiked K-Ar dating of recent volcanic rocks from El Hierro and La Palma. Internat. Workshop on Immature oceanic islands, La Palma, 1977. Vol. Abstr: 13-16.

Holcomb, R.T., 1997. Growth and Collapse of Hawaiian Volcanoes. Intern. Works. immat. oceanic isl., Abstr:79.

Holcomb, R., Nelson, B., Ten Brink, U., Carracedo, J.C. and McGee, D., 1966. Extent and depth of landsliding on the submarine north flank of Molokai, HI. GSA Cordilleran, Kona, Hawaiian Islands.

Holcomb, R.T., Nelson, B. and Carracedo, J.C., 1977. Growth, collapse and subsidence of Wailau Volcano. East Molokai, Hawaii. Internat. Workshop on Immature oceanic islands, La Palma, 1977. Vol. Abstr: 94-96.

Presley, T.K., Sinton, J.M. and Pringle, M., 1997. Postshield volcanism and catastrophic mass wasting of the Waianae Volcano, Oahu, Hawaii. Bull. Volcanol., 58: 597-616.

Riley, C.M.,. Diehl, J.F and W.I. Rose., 1977. A paleomagnetic study of movement in the Hilina fault system, south flank of Kilauea Volcano, Hawaii. Internat. Workshop on Immature oceanic isl, La Palma, 1977. Abstr: 96.

Szeremeta, N., Laj, C., Guillou, H., Kissel, C., Houard, S. and Carracedo, J.C., 1997. A palaeomagnetic study of the El Golfo collapse scarp section, El Hierro, Canary Islands: Volcanological and tectonic implications. Internat. Workshop on Immature oceanic islands, La Palma, 1977. Vol. Abstr: 19-21.

Wijbrans, J., Tauxe, L.and Staudigel, H., 1977. Eruptive chronology and paleomagnetism of the Taburiente volcano. La Palma. Internat. Workshop on Immature oceanic islands, La Palma, *1977. Vol. Abstr*: 59-60.

Growth, Collapse and Subsidence of Wailau Volcano, East Molokai, Hawaii

Robin T. Holcomb[1], Bruce K. Nelson[2] and Juan Carlos Carracedo[3]

[1]School of Oceanography, University of Washington, Seattle, WA 98195-7940. U.S.A.
[2]Department of Geological Sciences, University of Washington, Seattle, WA 98195-1310, U.S.A.
[3]Estacion Volcanologica de Canarias, Instituto de Productos Naturales (CSIC), La Laguna, Tenerife, Canary Islands, SPAIN

Wailau (also called East Molokai) is the shield volcano comprising the eastern two-thirds of Molokai. It overlaps the collapsed northeast flank of the Maunaloa shield volcano of west Molokai and is overlapped by the small rejuvenated-stage shield of the Kalaupapa Peninsula as well as the Lanai and West Maui shield volcanoes. Its stratigraphic relations and radiometric dates indicate that Wailau grew between about 2.0 and 1.5 Ma. Only a small part of Wailau is presently exposed on Molokai; the shield grew largely beneath the sea and has subsided nearly 2 km since it ceased growing. In addition to having most of its south flank covered by younger volcanoes, much of its north flank has been removed. In addition, GLORIA side-scan sonar mapping offshore to the north has revealed a giant submarine debris avalanche having a volume greater than 1000 km^3 and extending northward more than 200 km from the island. This report summarizes our research on the growth of Wailau and collapse of its north flank.

The structure and original shape of the volcano have been determined from study of its subaerial magnetostratigraphy. The oldest rocks exposed, along the north coast on the west side of Haupu Bay, are south-dipping tholeiitic basalt flows in a sequence ~200 m thick, having reversed magnetic polarity. Above that is a normal-polarity sequence 200-300 m thick that probably represents the Olduvai epoch of ~1.98-1.76 Ma; this sequence is exposed in cliffs of the north coast westward from Haupu Bay to Kalaupapa and eastward for a few kilometers from Papalaua Valley past Puahaunui Point. It is overlain in turn by 300 m of distinctively interlayered tholeiitic and alkalic basalts having reversed polarity and K/Ar ages greater than 1.5 Ma. The upper, chemically transitional rocks are exposed widely on all flanks of the volcano.

A different stratigraphic sequence occurs along the central north coast between Haupu Bay and Papalaua Valley, where the stacked magnetozones to east and west are replaced by a section more than 600 m thick of flat-lying to gently dipping tholeiitic-to-alkalic transitional basalt flows having normal polarity and age of about 1.55 Ma. This sequence is interpreted as caldera fill. The edge of the caldera -- with the caldera-filling flows ponded above talus along the caldera wall -- is exposed in seacliffs at the head of Haupu Bay and along an arcuate band in the lower slopes of Waiohookalo, Pelekunu and Wailau valleys.

Much of the lava and breccia near the caldera mar~in is hi~hly altered. Dikes are numerous in the breccia, rare in the caldera fill and of intermediate abundance in the lower units outside the caldera. A dense intrusive complex presumably underlies the caldera fill.

The caldera fill and upper flanks of the volcano are capped by postshield flows of mugearite with lesser amounts of hawaiite and trachyte; these flows have reversed polarity, and some have been dated at 1.49-1.35 Ma. At ~0.4 Ma rejuvenated-stage eruptions of normal-polarity alkalic basalt and basanite built a satellitic lava shield against the base of the coastal cliffs. That shield forms the Kalaupapa peninsula, which currently rises 123 m above sea level.

Using the sequence established from magnetostratigraphy and field relationships, we have also characterized the isotopic and chemical stratigraphy of the subaerial shield flanks and caldera fill. We have found a small but systematic trend toward less radiogenic Pb compositions with time from the tholeiitic through transitional alkalic sections. The exposed shield has a nearly constant Nd isotopic composition that is distinct from those of adjacent volcanoes.

Because the volcano in map view presently has the shape of a semi-ellipse and the filled caldera has the shape of a semi-circle, with the chord of each figure extending along the north coast, it appears that Ihe caldera was formerly circular and that the northern half of the volcano is now missing. Most workers agree that the removal of the north flank is related in some way to the giant debris avalanche offshore, but the exact nature of this relationship has been obscure. Moore et al. (1989) thought that the slide removed only a small fraction of the submarine flank -- far outside the caldera -- and that the upper flank was removed by later erosion. Other workers have suspected that the slide bisected the volcano directly.

Our work offshore has focused on three specific hypotheses:

Hypothesis #1. Sliding was restricted to the volcano's peripheral north flank -- more than 12 km from the present shoreline -- but penetrated downward at least 5 km to the base of the volcanic pile. Although the slide involved only the outer flank of the volcano, its volume was large because of its great depth of penetration. The northern half of the caldera was removed not by the landslide but by subsequent marine erosion, which undercut the headwall scarp at sealevel and caused the escarpment to retreat as the volcano continued to subside.

Hvpothesis #2. Sliding extended headward into the caldera, nearly to the present shoreline, but the slip surface was shallow, penetrating only 1-2 km beneath the surface of the volcano. The north flank was removed by this shallow slide, the upper northern half of the caldera complex sliding northward ~40 km to form part of a large block (25 km long by 10 km wide) whose flat surface is now about 3.5 km below sealevel. The slip surface is partially exposed upslope from the large block but is covered in other places by reefs and smaller slide blocks.

Hvpothesis #3. Sliding extended landward well into the caldera and also penetrated deeply into the volcanic pile, forming an extremely large proximal slump block in addition to the smaller slump blocks and distal debris avalanche; only the toe of the slump disaggregated to form an avalanche. The subaerial north flank of the volcano was removed not by erosion or translation but by relative subsidence of ~2 km and rotation of ~10ø to form the present submarine flank, modified slightly by marine erosion and reef growth.

We have tested these hypotheses by using deep-diving submersibles to examine stratigraphic sections and collect samples for comparison with subaerial lavas of Wailau. We used the three hypotheses to predict different rock units cropping out in the walls of submarine canyons and elsewhere on the submarine flank of the volcano.

If hypothesis #l were correct, the extra-caldera rocks exposed in submarine canyons should be stratigraphically lower than any now exposed on the island, probably having tholeiitic composition and reversed magnetic polarity. Intra-caldera rocks close to shore should consist of peripheral breccia and dikes beneath normal-polarity flows of transitional composition.

If hypothesis #2 were correct, the offshore slope between 300-2000 m depth should consist almost entirely of reef material accumulated atop the slip surface. Little volcanic rock should be exposed on the shallower parts of the volcano's submarine north flank, though the slip surface may be exposed to view in canyon walls. Rocks below the slip surface should represent deep parts of the volcano -- as in hypothesis #l -- and remnants of the caldera breccia or intrusive complex might be exposed. Parts of the caldera fill and alkalic cap should be preserved in the large slump block at 3500-4000 m depth about 30 km north of Molokai.

If hypothesis #3 were correct, stratigraphic units exposed in the shallow submarine flank should be similar to those still exposed on subaerial parts of the volcano. The extra-caldera rocks should include a layer of alkalic compositions and reversed polarity above interlayered alkalic and tholeiitic flows, and the intracaldera rocks should have a layer of alkalic composition and reversed polarity above lavas of transitional chemistry and normal polarity.

We first used the U.S. Navy DSRV Sea Cliff in September 1992 for two brief dives to depths of 1600-3700 m. During the first dive onto the large block 30 km offshore, we found tholeiitic basalt instead of the transitional and alkalic rocks predicted by hypothesis #2, leading us to reject that hypothesis. During the second dive into a submarine canyon ~12 km offshore we found outcrops of alkalic basalt low in the canyon wall. In Pb-isotopic composition the submarine samples are distinct from the tholeiitic rocks of the volcano but indistinguishable from lavas of the subaerial alkalic cap. This led us to favor hypothesis #3, that the submarine flows offshore belong to the thin alkalic cap and reached their present position through subsidence of a giant slump block without significant later erosion. We therefore concluded tentatively that slumping penetrated the volcano as far as its rift zones and to a depth of at least several kilometers, with the proximal slump block having rotated backward 5-10° as it subsided ~2 km.

Wanting to confirm this tentative conclusion with additional data from other sites, we used the University of Hawaii PISCES V submersible in August-September 1996 for eight dives to depths of 300-1900 m in order to examine more thoroughly the prominent escarpment at 1300-2000 m depth and walls of submerged canyons extending landward from it. Two dives climbed the escarpment, five sampled canyon walls nearby at depths of 1200- 1600 m, and one examined a canyon and submerged reef terrace farther inshore at depths of 300-800 m. We expected during these dives to find a sequence of lava flows like those on the present island but displaced downward ~2 km.

We were surprised, however, to find a submarine stratigraphy in which lava flows comprise only a part of a section that is quite different from any now exposed on the island of Molokai or elsewhere on the Hawaiian Islands. The 1300-m terrace landward of the escarpment consists, from bottom to top, of 3 layers: l) ~100 m of conglomerate composed of subangular to subround basalt clasts, interbedded with thin lava flows; 2) ~100 m of lava interbedded with thin conglomerates and sand, with a carbonate-rich layer 1-2 m thick separating mostly columnar basalts below from pillow basalts above; 3) ~100 m of palagonitized sand and silt, with no interbedded lavas. The upper unit is covered in some areas by pillow lava that drapes the escarpment and canyon walls; the pillows are obscured by pelagic sediment on gentle slopes but are free of sediment on steeper slopes. Much of the pillow lava originates from a submarine shield ~8 km northeast of the Kalaupapa Peninsula. The upper flank above 400 m depth is capped by a broad terrace consisting of younger reefs.

None of our original hypotheses predicted the stratigraphy that we eventually observed. Having reconsidered those hypotheses and their consequences, we now suggest that hypothesis #3 is correct but that the stratigraphic section observed in the submarine canyons entirely postdates the giant Wailau landslide. According to this interpretation, the observed submarine section accumulated atop a giant slump block that extended nearly to the present island. This block subsided >1 km but remained above sealevel at the end of sliding at ~1.5 Ma, being mantled initially by coarse debris eroded from the intact part of the volcano and then by lava flows during ~1.5-1.2 Ma. Alkalic eruptions continued as the block subsided below sealevel at ~1.3 Ma but ceased prior to deposition of fine sediments that were derived presumably by longshore drift from shoreline lava deltas during the growth of West Maui at ~1.2-1.0 Ma. We are now using trace-element and isotopic analyses and K/Ar dating to test this interpretation.

A PALEOMAGNETIC STUDY OF MOVEMENT IN THE HILINA FAULT SYSTEM, SOUTH FLANK OF KILAUEA VOLCANO, HAWAII

C.M. Riley, J.F. Diehl, and W.I. Rose
Michigan Technological University
Geological Engineering and Sciences, Houghton, MI USA 49931.
cmriley@mtu.edu

Slippage of the south flank of Kilauea Volcano in Hawaii is associated with catastrophic landslide events. The surface expression of this slippage is the Hilina Fault System with fault scarps as high as 500 m.. Paleomagnetic directions from lava flows exposed in the Hilina fault scarps at Puu Kapukapu and Keana Bihopa are used to determine the average rate of movement along a fault(s) separating the two sections. These data also help resolve problems in correlating Hawaiian ashes.

Fifty-six paleomagnetic sites in individual lava flows were collected at Keana Bihopa in the footwall block of the 500 m high Hilina Pali fault scarp. Specimens from 396 cores were demagnetized using alternating field demagnetization, and site-mean directions calculated. Paleomagnetic data for 42 sites in the 300 m high Puu Kapukapu section (the hanging wall block) were provided by the paleomagnetics group at the California Institute of Technology.

Site-mean directions from lava flows between the Mo'o Ash and the Middle Pohakaa Ash at Keana Bihopa and Puu Kapukapu indicates approximately 8° of backward tilt of the Puu Kapukapu section with respect to the Keana Bihopa section. Therefore, the fault(s) separating the two blocks must be listric. Systematic differences in inclination data suggests two distinct intervals of movement. Using basic slope stability analysis, the average rate of movement of the Puu Kapukapu block with respect to Keana Bihopa over the time interval represented by these lavas is 5 cm/yr which is equivalent to 1.5 Kalapana-size displacements every 100 years. The data also indicate that Puu Kapukapu has rotated 14.8° ± 8.5° counterclockwise about a nearby vertical axis with respect to Keana Bihopa.

Lastly, the similarity of waveform patterns between Puu Kapukapu and Keana Bihopa also confirms previous work correlating ash layers in the two sections. These waveform patterns can also be recognized in the inclination data from the Hilo Drill Core (HDC). However, the ash layer identified as the Pahala Ash in the HDC is not equivalent to the Pahala Ash in the Puu Kapukapu and Keana Bihopa sections. This ash is better correlated with the Upper Pohakaa Ash.

Recognising incipient instability and lateral collapse precursors in steep - sided oceanic island volcanoes.

Day, S.J.[1,2], Carracedo, J.C.[3,2], Guillou, H.[4], Pérez Torrado, F.J.[5], Fonseca, J.F.B.D.[6], Heleno da Silva, S.I.N.[6], & Gravestock, P.[2]

[1]*Greig Fester Centre for Hazard Studies, University College London, U.K.*
[2]*Dept. of Geography & Geology, Cheltenham & Gloucester College of Higher Education, U.K.*
3: Estación Volcanológica de Canarias, Tenerife, Spain.
[4]*Centre des Faibles Radioactivites, CEA - CNRS, Gif - sur - Yvette, France.*
[5]*Dept. de Ciencas del Mar, Universidad de las Palmas de Gran Canaria, Spain.*
[6]*Dept. de Fisica, Instituto Superior Tecnico, Lisboa, Portugal.*

Although Kilauea volcano, Hawaii is commonly regarded as the type example of an unstable oceanic island volcano, it is in many respects atypical of such volcanoes. The Hawaiian volcanoes are both larger and substantially less steep than many oceanic island volcanoes, with heights of up to 10 km above the ocean floor and slopes averaging 5 - 8°. In contrast, volcanoes such as the Cumbre Vieja, La Palma; Teide, Tenerife; and Pico do Fogo, Fogo rise 7 to 8 km above the surrounding ocean floor but have average slopes between 15° and more than 20°. The maximum average subaerial slope of Pico do Fogo is no less than 28°! The greater slope angles make these islands intrinsically less stable.

The south flank of Kilauea is also atypical in that it shows semi - continuous, partly incremental (co - seismic) seaward movement which continues through inter - eruptive periods (Swanson et al. 1976). This probably reflects the persistence of magma and ductile, high - temperature cumulates in the deeper parts of the Kilauean rift zones (Clague & Denlinger 1994). In contrast, studies of the Cumbre Vieja and Pico do Fogo volcanoes (see also McGuire and Moss, this volume) indicate that these volcanoes do not deform during inter - eruptive periods but show clear signs of instability before, during and after near - surface intrusion emplacement and volcanic eruptions. There is however no evidence for major deformation of these volcanoes, accumulated over numerous eruptions. Furthermore, examination of the San Andres fault system on the island of El Hierro indicates that there was at most a few tens of metres of slip on this fault system before sudden slip of about 300 metres in an aborted lateral collapse event (Day et al., 1997). These observations imply, therefore, that steep oceanic island volcanoes can become prone to catastrophic flank failure after only a little precursory deformation; but that such failure is only likely to occur during the course of eruptions or intrusion events. It is therefore important to recognise features that indicate that an oceanic island volcano is evolving towards, or already in, a state of potential catastrophic instability.

1. <u>Development of seaward - facing normal fault or non - magmatic dilational fissure systems, and associated oblique - or strike - slip accommodation faults, in surface outcrop</u>. The best evidence for the onset of flank instability on oceanic island volcanoes is provided by surface ruptures associated with fault systems within the flanks. Examples include the fault system formed along the crest of the Cumbre Vieja volcano during the 1949 eruption, with a maximum surface offset in excess of 4 m; and major "dry" fissures developed over a distance of several kilometres in the 1951 eruption of Pico do Fogo. These fault systems ruptured the surface during eruptions: a critical problem is therefore distinguishing them from faulting around the upper tips of dykes. Useful criteria include: (i) geometry: the normal fault system is asymmetric and seaward - facing (graben above dykes are more symmetrical) while the fissure system shows no axial subsidence; (ii) timing of formation: both the 1949 faults and the 1951 fissures developed well after the start of the eruptions, in periods not directly associated with emplacement or drain-back of magma; (iii) evidence for the absence of magma in the immediate subsurface, such as a lack of fumarolic activity.

2. <u>Seismological indicators of the development of seaward - facing fault systems in the sub - surface</u>. Whether flank fault systems associated with incipient lateral collapse have surface expressions or are "blind" (see below), their activity during eruptive episodes produces distinctive patterns of seismicity. During the 1949 eruption on La Palma, seismicity appears to have been most intense in a north - south elongated region at shallow depth (1 -2 km ?) beneath the western flank of the volcano, downslope from the eruptive vents (Fig. 1). This is interpreted as indicating the presence of a seaward - dipping detachment fault beneath this western flank which, together with the

surface - rupturing normal faults that define the fi~ture headwall, forms an incipient collapse structure. The seismicity on Fogo during the 1 95 1 eruption is not well - enough known to show whether a similar structure existed there but shallow seismicity during and after the 1995 eruption on Fogo (Heleno da Silva et al., this volume) may define part of a developing incipient collapse structure. A distinctive feature of seismicity associated with these incipient lateral collapse structures appears to be that it is at its most intense weeks to months after the start of the destabilising eruptions. This delay has important implications for the likely mechanism of destabilisation (Elsworth et al., this volume).

3. Volcanic rift reorganisation; corresponding re - arran~ements of subsurface dyke swarms in old, incised collapsed volcanoes. The majority of oceanic island volcanoes are characterised by the presence of discrete linear zones in which vents are concentrated ("volcanic rift zones"): these correspond to discrete feeder dyke swarms in the subsurface. The rift zones are defined both by the distribution of vents and by elongation directions of individual vents or groups of vents, which are controlled by the orientation ofthe underlying dykes (Tibaldi 1995). In many volcanic islands these rift zones radiate out from the summit of the volcano and define a triple - rift ("Mercedes Star") geometry, or more - or - less linear two - rift geometries governed by the buttressing effect of older volcanoes (as at Kilauea) or by regional tectonic stresses (as in the Azores and on Karthala). A distinctive precursor of lateral collapse appears to be reorganisation of these rift zones as the edifice becomes weakened and the magmatically- or regionally- controlled stress regime at depth becomes decoupled from the topographically - controlled near - surface stress regime. As dykes pass upwards from the one stress regime to the other they rotate into a new preferred orientation by progressive segmentation, producing en echelon groups of elongate vents. In old volcanoes which have been affected by lateral collapses and subsequently deeply incised these changes are manifested in late dyke and intrusion swarms with distinctive orientations and en echelon geometries: examples are provided by the Presa de los Hornos complex in the Roque Nublo volcano of Gran Canaria; dyke swarms in the Guimar edifice on Tenerife; and dyke swarms in the Monte Amarelo edifice on Fogo. Reorganisation of volcanic riflc zones into new geometries related to developing fault systems has occurred in the Cumbre Vieja volcano, La Palma over the past 7000 years or so (Fig. 2); and in the Pico do Fogo volcano within historic time. Surface rupture by the flank fault systems has occurred much more recently on both of these volcanoes and so it appears that incipient lateral collapses develop first as blind fault systems in the subsurface, and only breach the surface at a later stage.

Other changes, such as the abandonment of shallow magma bodies and an increase in the abundance of xenoliths from the deep crust and mantle lithosphere, as the magma feeding system is destabilised by the increasing instability of the volcano above, may also occur. Incipient, potentially catastrophic instability at steep oceanic island volcanoes can only be reliably identified by a combination of detailed geological mapping, highly precise geochronological work, and geophysical monitoring.

References.

BONELLI RUBIO, J.M. 1950. *Contribución al estudio de la erupción del Nambroque o San Jualn (Isla de La Palma)*. Madrid, Instituto Geográfico y Catastral, 25 pp.

CLAGUE, D.A. & DENLINGER, R.P. 1994. Role of olivine cumulates in destabilizing tlle flanks of Hawaiian volcanoes. sulletin of Volcanology, 56, 425 - 434.

DAY, S.J., CARRACEDO, J.C. & GUILLOU, H. 1997. Age and geometry of an aborted rift flank collapse; the San Andres fault system, El Hierro, Canary Islands. Geological Magazine, in press.

SWANSON, D.A., DUFFIELD, W.A. & FISKE, R.S. 1976. Displacement of the south flank of Kilauea volcano: the result of forceful intrusion of magma into the rift zones. United States Geological Survey Professional Paper 963.

TIBALDI, A. 1995. Morphology of Pyroclastic Cones and Tectonics. Journal of Geophysical Research 100, 24521 - 24535.

Fig. 1. Mercalli intensity contours of seismicity associated with the 1949 eruption of the Cumbre Vieja, La Palma, showing displacement of isoseisms to the west of the surface fault break and eruptive vents. After Bonelli (1950)

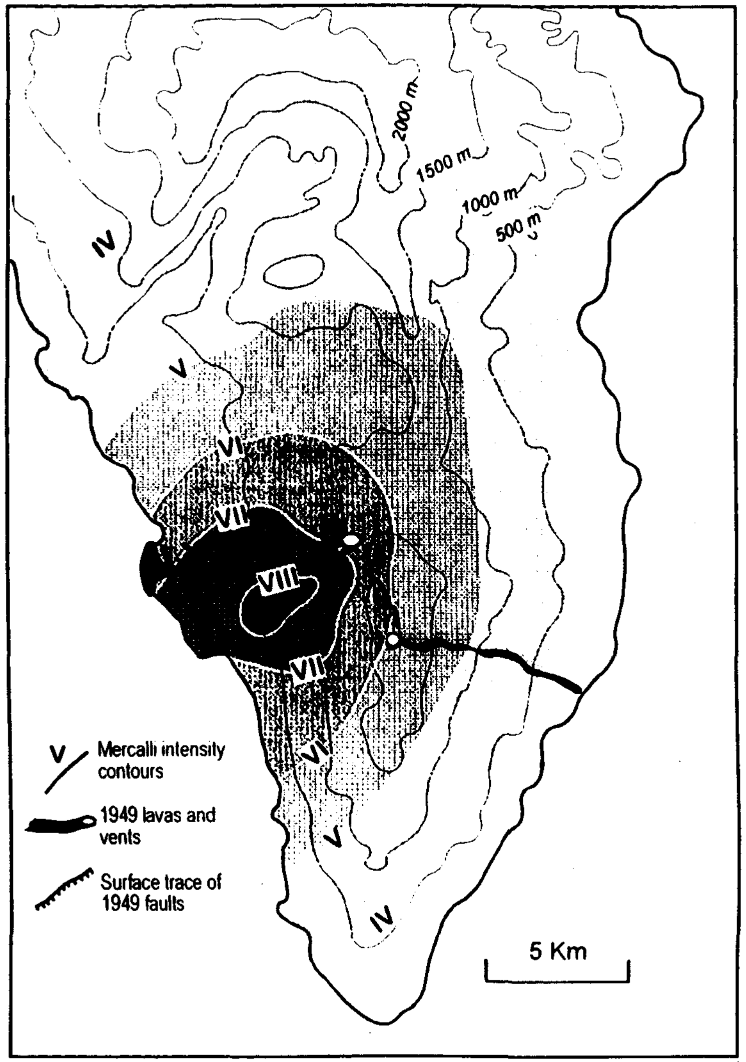

Fig. 2. Change in distribution and orientation of elongate volcanic vents in the central part of the Cumbre Vieja, La Palma, after about 7000 a B.P. Note en echelon groups of vents (all historic) on the western flank of the volcano.

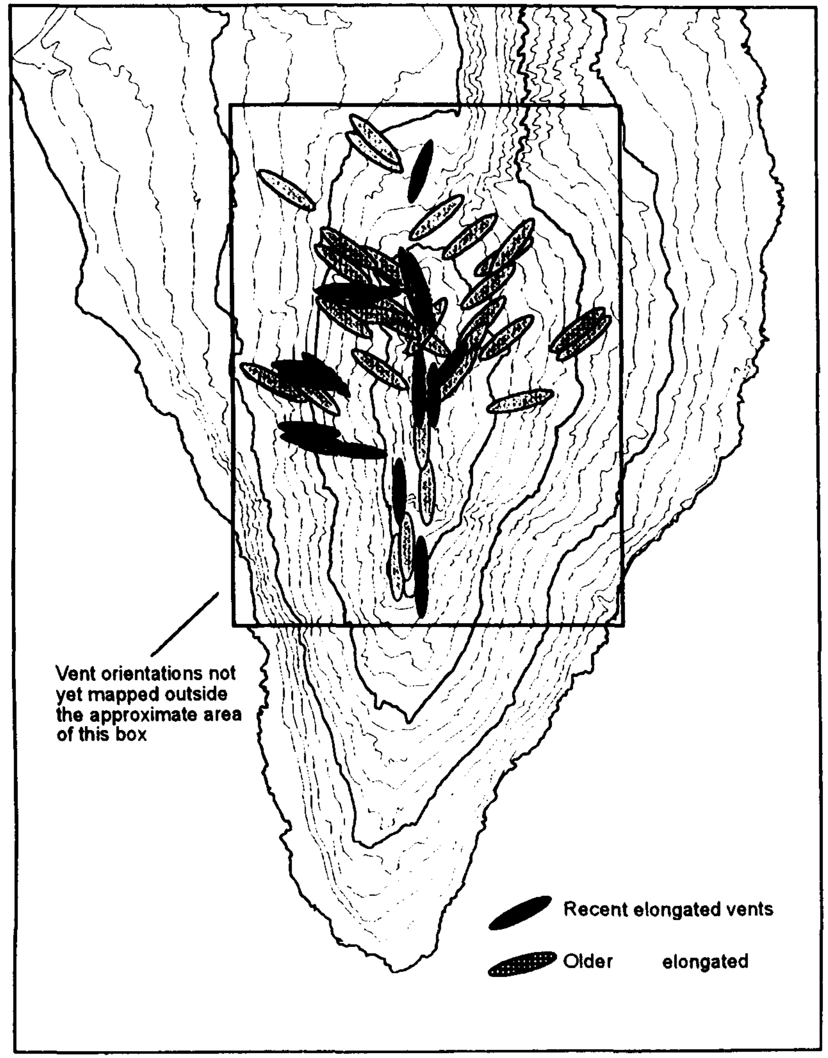

An Evaluation of Flank Instability Triggered by Laterally and Vertically Propagating Intrusions

Derek Elsworth[1] and Simon J. Day[2]

[1]*Department of Mineral Engineering, Pennsylvania State University, U.S.A.*

[2]*Department of Geography & Geology, Cheltenham & Gloucester College of Higher Education, U.K. and Greig Fester Centre for Hazards Research, University College London, U.K.*

Abstract

Large scale lateral collapses, with volumes of up to thousands of cubic kilometres, are a ubiquitous feature of oceanic island volcanoes in their most active, *shield-building*, stage of growth. The overall slopes of these volcanoes vary in angle from less than 5° to more than 20°. At the lower end of this range, in particular, the causes of these massive failures are enigmatic since the destabilising gravitational stresses generated on basal failure planes are much less than resisting frictional forces, for reasonable values of friction coefficients. Instability may be triggered by a reduction in strength on the decollement underlying a potential slide block through an increase in pore fluid pressures in the porous material comprising the volcanic edifice. Here we consider how a relatively small volume of magma, emplaced as a dyke or dykes in a volcanic rift zone, can destabilise a volcano flank through its effects on the pore fluid pressure exerted by groundwater or hydrothermal fluids. These effects are of two types: mechanical straining of the intergranular or fracture network pore space occupied by the fluids as the dykes are emplaced; and thermal straining caused by the continued flow of magma through long-lived dykes (particularly those feeding surface lava flows) and consequent heating of the surrounding rocks.

Both mechanical and thermal fluid pressurization mechanisms may be quantified. In this work, mechanical behavior is represented by a migrating volumetric dislocation, representing either the laterally or vertically migrating dyke geometries illustrated in Figures 1 (a) and (b). Mechanically induced fluid pressures may be evaluated either relative to intrusion rate, U, dyke thickness, w, fluid permeability and hydraulic diffusivity of the host rock, or through surrogate groupings of these parameters in the nondimensional groupings of dimensionless intrusion velocity, U_D, and dimensionless dyke thickness, w_D. For the same intrusional geometries (Figure 1), thermally induced pore fluid pressures are modulated by the differential magma temperature, fluid and skeletal modulii and thermal expansion coefficients, with migration rates controlled by thermal and fluid diffusivities. These parameters may be arranged into two unique nondimensional groupings and a diffusive time, to define pressure build-up following intrusion of a feeder dyke. With the induced pore fluid pressure field determined around the intruded dyke geometry, the destabilizing influence on a portion of the flank may be determined by isolating a potentially unstable block in a simple free-body, as illustrated in Figure 1 (c). Uplift forces resulting from the mechanically and thermally induced pore fluid pressure distributions may be evaluated, and used to resolve equilibrium of the block relative to translational failure on a basal failure plane.

Factor of safety, F, represents the ratio of forces resisting translational failure to those promoting failure. Where frictional resistance, alone, is assumed, the factor of safety may be divided by the friction coefficient for the flank material, $\tan f$ where values of $F/\tan f$ in the range 1 to 0.6 represent incipient failure for rocks of strengths typical to flank environments. The relative influence of upwelling versus lateral intrusion on destabilisation by mechanical pressurization is illustrated in Figure 2 for a spectum of failing block widths. For a volcano with a 1 km scarp height above sea level, the block widths of Figure 2 range from 0.1 km to 100 km. The upwelling intrusion remains at a depth of 2 km and has a width of 10 km. The potential destabilizing influence is clear, even for this relatively deep-seated intrusion that has not yet migrated to the surface. The destabilising effect is maximised where the upwelling intrusion intersects the surface (Figure 2) and exceeds that for a laterally migrating dyke, except for very large dyke intrusion lengths, where the magma push at the rear scarp exceeds the destabilising effects of narrow upwelling dykes. The sequencing and morphology of intrusion events are clearly important since either of these forms of intrusion are capable of independently initiating flank failure.

The destabilizing influence of thermal pressurization may also be evaluated for the upwelling dyke morphology. The destabilizing influence of a feeder dyke present along a 10 km section of the rear scarp is illustrated in Figure 3. For freely diffusive media, with parameters representing the minimum thermal effect in volcaniclastics, no discernible thermal pressurization results, even after one year. However, for thermal and mechanical parameters representative of the maximum effect (also for volcaniclastics), thermal effects are significant, and build in destabilizing-influence with time. These effects are of sufficient magnitude to trigger failure for the case of upwelling dykes.

Comparison of results from these models with the deformation associated with actual eruptions is made difficult by a lack of data relating to the values of critical variables in the models. Most importantly of all, the large-scale permeabilities of particulate and fractured volcanic materials are poorly known and highly variable. Correspondingly, these analyses are most useful as an indicator of important factors controlling the effects of dyke intrusion events upon the stability of oceanic island volcanoes. Besides highlighting the importance of understanding the permeability structure and hydrology of volcanoes, we have shown that orientation of intrusions and intrusion propagation direction will significantly change mechanical pressurisation effects. Day et al. (this volume) show that near-surface dyke propagation directions change from lateral to vertical as incipient instability develops in steep-sided islands, suggesting a possible positive feedback process. We have also shown that thermal pressurisation effects are strongest well after the start of an eruption: understanding the factors that control the duration of eruptions and relating these to measurable quantities (such as the amount of pre-eruptive inflation) will therefore be important in the prediction of future dyke-induced lateral collapses.

Indications of the importance of including pore fluid pressure effects in analysis of the stability of oceanic island volcanoes can be found in the patterns of flank deformation associated with certain recent eruptions. These are the 1949 eruption of the Cumbre Vieja volcano, La Palma (Canary Islands) (Day et al., this volume); the 1951 eruption on Fogo (Cape Verde Islands) (Day et al., this volume); and possibly also the 1995 eruption of Fogo (Heleno da Silva et al., this volume). The timing of deformation in all three eruptions suggests that it is primarily controlled by thermal pressurisation of pore fluids in the rocks around the magma conduits.

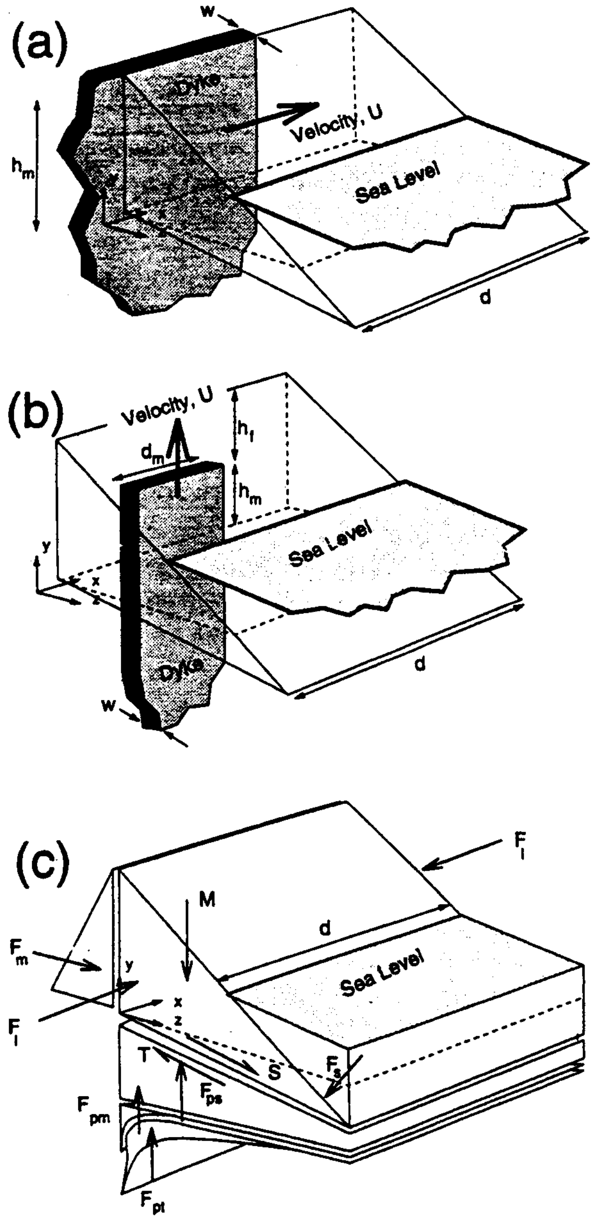

Figure 1: Intrusion geometries within a volcano flank, illustrating (a) laterally mobile and (b) vertically mobile dykes, injected at emplacement velocity, U, and of thickness, w. From the emplacement geometry, the equivalent forces acting on a potential slide block may be determined.These include uplift due to groundwater pressures, F_{ps}, magmastatic loading at the rear block scarp, F_m, and destabilizing uplift forces due to mechanically, F_{pm}, and thermally, F_{pt}, induced pore fluid pressures.

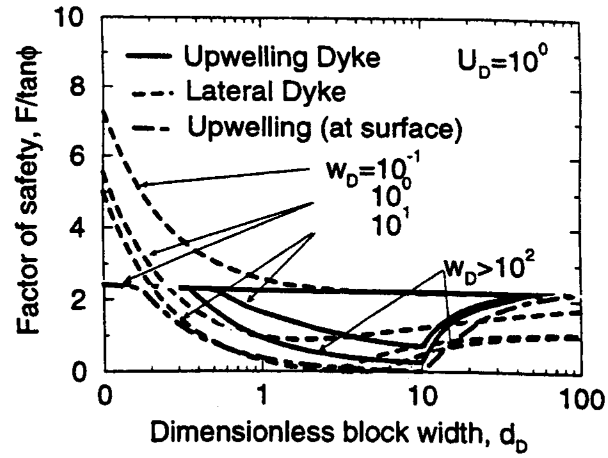

Figure 2: Nondimensional factors of safety for volcano flanks intruded by laterally and vertically propagating dykes where induced pore fluid pressures result from mechanical effects. Slope inclination is 24° with a water-table sloping from sea level at 12°. Nondimensional dyke thicknesses, w_D, are representative of intrusion into volcaniclastics. For the upward propagating dyke, and a backscarp height of 1 km above sea level, the advancing dyke tip is 2 km below the flank crest, and block widths range between 0.1 km and 100 km for a 10 km width dyke. Nondimensional block width, d_D, is the width of the failure block, d, normalized by the scarp height above sea level.

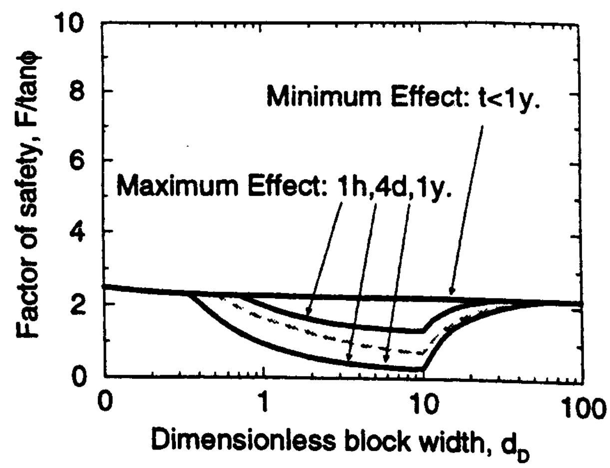

Figure 3: Nondimensional factors of safety for volcano flanks intruded by vertically propagating dykes where induced fluid pressures result from thermal effects. Anticipated maximum and minimum thermal effects are shown for time periods, since intrusion, of *1 hour, 4 days and 1 year*. Mechanical pressurization shown dashed (Figure 2).

The history of debris avalanches, debris flows and turbidites in the Canary basin - a remote record of the evolution of the Canary Islands

P.P.E. Weaver and D. G. Masson

Southampton Oceanography Centre, Empress Dock, Southampton, S014 3ZH., UK.

The Canary Islands are subject to catastrophic failure events which can erode substantial portions of individual islands. Hundreds of cubic kilometres of debris from these events are dumped on the lower island flanks as rock avalanche deposits containing kilometre size boulders. These avalanches can overload the sediments on the island flanks which may then collapse to form debris flows and turbidity currents which flow downslope toward the Madeira Abyssal Plain (MAP). Mapping of surface sediments in the Canary Basin, using GLORIA sidescan sonar and shallow seismics, has enabled us to trace the path of a single event which resulted from a failure on the island of El Hierro at around the end of the last ice age (between 13 and 17 thousand years ago). This event involved displacement of some 800 km^3 of rock and sediment, and affected over 100,000 km^2 of seafloor. The avalanche headwall is the 900 m onshore scarp of the El Golfo depression on El Hierro and the avalanche deposit extends to waterdepths of 3000 to 4000 m. The surface of the avalanche is covered by angular blocks of volcanic rock up to 1.2 km across and 200 m high. The Canary Debris Flow, initiated by the avalanche, originated at about 4000 m waterdepth on the western slopes of the islands of El Hierro and La Palma and travelled 600 km to the edge of the MAP. The associated turbidity current deposited a layer of mud across the MAP up to 4 metres thick.

The Canary Debris Flow was not a unique event. The scars left by a number of other failures can be seen on the south side of El Hierro, on Tenerife and on the western side of La Palma. The distribution of the deposits is, however, widespread and an enormous amount of work would be required to locate and study each event. The most convenient place to study the history of these major events is in the MAP where each one is recorded as a volcaniclastic turbidite and these are stacked on top of each other. Events which have occurred in the last 750,000 years have been studied by piston core analysis, whilst the deeper sequence was drilled in 1994 by the Ocean Drilling Program Leg 157. These core data show a regular but infrequent influx of volcaniclastic turbidites generated from the Canary Islands. The drilling data shows a history of volcaniclastic turbidites extending to beyond 17 million years, but with increased rates of deposition from about 7 million years to the present day. In the last million years 8 events were recorded. Calculations can be made of the total volume of volcaniclastic turbidites deposited on the MAP and these show the following trend:

92 km^3 per million years between 16 and 7 Ma;
200 km^3 per million years from 7 to 3.5 Ma;
318 km^3 per million years from 3.5 to 1.6 Ma;
471 km^3 per million years in the last 1.6 million years.

This increase in volume of mass wasted products may reflect increasing volcanism through time within the Canary Islands. It is likely that each new island passes through a very unstable stage during its youth, but instability may continue for several million years on each island. Thus Tenerife is still undergoing large scale mass wasting but Gran Canaria appears to be more stable. The drilling data shows increased pulses of volcaniclastic sediments coincident with the inception of each new island (Gran Canaria, Tenerife, El Hierro and La Palma), in each case lasting about 1 to 2 million years. One unexpected result of the drilling was the identification of a group of turbidites which appear to derive from the Canary Islands but lack a volcanic component. These turbidites include some of the largest volume events and are distributed irregularly in time. When compared with the age of inception of each Canary island it appears that an input of these turbidites immediately predates the inception of each island and lasts for about one million years. We postulate that such flows characterise the submarine growth stage of each island before fine grained volcanic sediment was contributed to the island flanks. Once the island became shallow enough for freatic volcanism, and especially following subaerial exposure and normal weathering, the island flank sediment would contain fine grained volcaniclastic debris thus generating volcaniclastic turbidites. Our model therefore predicts a submarine stage of island growth lasting about one million years followed by a relatively unstable subaerial stage of one to two million years followed by an interval of a few million years when some large scale mass wasting would still occur before the island became a more stable edifice.

Volcano instability on the submarine south flank of Kilauea, Hawaii

J.R. Smith, A. Malahoff, and A.N. Shor

Univ. of Hawaii, SOEST, 2525 Correa Rd., Honolulu, HI 96822,
jrsmith@soest.hawaii.edu, malahoff@soest.hawaii.edu, and sandy@soest.hawaii.edu.

Previous studies identified the south flank of Kilauea as the Hilina slump, an active landslide encompassing most of the volcano slope down to the Cretaceous-age seafloor. Analysis of SEA BEAM and HAWAII MR1 sonar data, seismic reflection prohles, and magnetic anomaly grids over the offshore continuation of Kilauea's south flank have recently been completed. These data allowed interpretation of surficial to deeper subsurface structure. This slope, comprised of the three active hot spot volcanoes Mauna Loa, Kilauea, and Loihi seamount, is the locus of the Hawaiian hot spot and is the site of frequent low intensity seismicity as well as episodic large magnitude earthquakes. Its subaerial portion is reported to creep seaward at approximately 10 cm/yr. The Hilina slump is the only large submarine landslide in the Hawaiian Archipelago thought to be active, and this study is the hrst to more highly resolve a particular slide feature.

The overall picture gained from these data sets is one of mass wasting of the neovolcanic terrain as it builds upward and seaward, though reinforcement by young and pre-Hawaii seamounts adjacent to the pedestal is apparent. Extensive lava delta deposits are formed by hyaloclastites (black sands) and detritus from recent lava flows into the sea. These deposits dominate the upper submarine slope offshore of Kilauea. Along the lower flanks of submarine volcanic rift zones are patches of hummocky topography suggesting failure by avalanching or more frequent sloughing off of material. The Hilina Pali fault system does not continue offshore as the same series of normal faults downthrown seaward. Instead, the offshore slump block is comprised of four distinct morphological sections, analogous to the Varnes (1978) rotational slump model. Based on results from the new high resolution offshore mapping the estimated area presently affected by Kilauea south flank slumping is roughly 2100 km^2, with an estimated volume of 10,000-12,000 km^3 equal to about 10% of the Hawaii Island subaerial and submarine volume.

Seaborne magnetic studies have yielded 23 normally polarized major magnetic anomalies located in three separate magnetic zones. Volcanic cones and rift zones still attached to their deep-seated volcanic roots, or dike systems, typically show high amplitude magnetic anomalies and usually some surface expression since they are usually fairly shallow. Conversely, volcanic cones and rift zone pieces separated from their dike systems by large scale ground movements and then transported downslope tend to show broader, less intense magnetic anomalies and little, if any, surface expression due to deeper burial over time. Both types of anomalies are observed on the Hawaii Island southeast flank, and are grouped into distinct zones. The in situ volcanic centers are located in two neovolcanic zones, one including the presently stable area around coastal Mauna Loa and Loihi submarine volcano, as well as along the submarine continuation of the East and Southwest Rift Zones of Kilauea volcano. These neovolcanic zones are separated by a neotectonic region corresponding to the entire Hilina slump feature, which is the mobile portion of the Kilauea south flank. It is composed of broad, low amplitude anomalies interpreted to result from detached, buried rootless volcanic blocks which may have slid into place during previous landsliding events. The magnetic anomaly interpretations are supported by the surface and near subsurface data sets. Several large blocks resting on the seafloor near the base of the island (roughly, the toe of the slump) may be somewhat similar in size and shape as the buried blocks farther upslope, as interpreted from the magnetic data.

Volcano building on the leading edge of the Hawaiian hot spot is a "two steps up, one step down" process where several scales of flank degradation are apparent. Loihi and Hohonu seamounts appear to buttress the south flank and form the lateral bounds of the failure "window", allowing counterclockwise rotation of the slump block through it. Thus, slope instabilities on the southeast flank of Hawaii Island suggest a complex interplay of neotectonic and neovolcanic activity in a mid-plate setting, and provide an active model for interpreting the processes causing structural collapse in the form of extensive submarine landslides within the Exclusive Economic Zone's of oceanic islands and seamounts throughout the world ocean.

Landsliding on the Canary Islands. The missing submarine sediment record

M. Canals[1], B. Alibes[1], R. Urgeles[1] and B. Alonso[2]

(1): Associate Unit on Marine Geosciences CSIC-UB. GRC Geociencies Marines, Universitat de Barcelona, Campus de Pedralbes, E-08071 Barcelona, Spain.

(2) Associate Unit on Marine Geosciences CSIC-UB. Grupo de Geologia Marina, Instituto de Ciencias del Mar, CSIC, P. Joan de Borbó s/n, E-08039 Barcelona, Spain.

Landslides on the Canary Islands

As far as new seafloor areas are explored and new data are acquired it becomes evident that the Canary Islands hold a long and complex history of subaerial and submarine landslides. Up to now, at least eight partly or totally submarine landslide deposits have been identified around the Canary Islands (Urgeles et al., 1997a). Volumetrically, the most important ones are the Orotova-Icod Debris Avalanche (Watts and Masson, 1995; Masson, 1996) north of Tenerife Island, and the Canary Debris Flow (Simm and Kidd, 1983; Kidd et al., 1985; Masson et al., 1992a; Weaver, 1994) and the El Golfo Debris Avalanche (Masson, 1996; Urgeles et al., 1997a) off the island of Hierro, where an smaller landslide, the El Julan has been also identified (Holcomb and Searle, 1991).

Source areas of the Orotova-Icod, El Golfo and El Julan Debris Avalanches are located on the island flanks. In contrast the source area of the Canary Debris Flow, together with its correlated turbidite b in the Madeira Abyssal Plain (MAP), is in the insular submarine slope, west of El Hierro, at 3200 m of water depth, as postulated by Urgeles et al. (1997a) from volumetric calculations and interpretation of detailed swath bathymetry mapping. Areal extent and volumes of these landslide deposits, as well as their ages, are indicated on Table 1.

Event	Area (km^2)	Volume (km^3)	Age (ka)
Orotova-Icod D.A.	≥5,500	≥1,000	650-350[1] /1,200-170[2]
Canary Debris Flow	6,000	400	17-10
El Golfo D.A.	2,600	150-180	136-21
El Julan D.A.	900	30-100	160

Table 1.- Landslide deposits around the Canary Islands for which area and volume are known with a reasonable confidency, together with their ages (data from various sources). (1): Age of the Orotava section; (2): Age of the Icod section.

These landslide deposits, together with some, less-studied ones, represent a total volume of about 2,000 km^3 which could be compared with the overall areas and volumes of the islands where they originate. Such kind of calculations have been made by Watts and Masson (1995) for the Orotova-Icod Debris Avalanche, which covers an areamore than twice the surface area of the island of Tenerife, and Urgeles et al. (1997a) for the landslides affecting the island of El Hierro which caused 4 to 5.2% of the whole edifice to slid.

Ages and occurrence of landslides have been also used to calculate the frequency of landslide events in the Canary Islands, which has been estimated at one event every 110,000 years (Masson, 1996; Urgeles et al., 1997a). Studies of the Hawaiian Ridge by Moore et al. (1989) reported, in contrast, a frequency of one event every 340,000 years. Landslides seem to occur in the late stages of the growth of oceanic islands (Watts and Masson, 1995), however the relationship between shield phases on individual islands and associated landslides is not direct (Schminke, 1994; Urgeles et al., 1997a).

Turbidite deposits on the Madeira Abyssal Plain

The Canary Islands are one of the source-areas of the turbidite deposits filling the Madeira Abyssal Plain, where four main turbidite types have been identified: organic, volcanic, calcareous and intermediate (de Lange et al., 1987). After organic-rich turbidites, volcanic-rich turbidites are volumetrically the second most important sediment type in the MAP, according to the calculations made by Weaver et al. (1997) and Alibes (1997). At all, about 1,800 km^3 of compacted volcanic-rich turbidites have accumulated during the last 16.6 Ma BP, it is Late-Middle Miocene (Weaver et al., 1997). Decompacted volumes are of about 2,800-3,000 km^3 after calculations by Weaver et al. (1997) and Alibés (1997).

Volcanic-rich turbidites are the only turbidite type in the MAP whose percentage has been clearly increasing with time in the various seismic units defined (Alibés, 1997; Rothwell et al., 1997). Percentual increases are particularly noticeable from Early Pliocene (5.3-3.4 Ma BP) to Late Pliocene (3.4-1.6 Ma BP) to Pleistocene (1.6-0 Ma BP), when volcanic-rich turbidites passed from 14% to 17.8% to 25.2% of the total decompacted volumes of sediment in the MAP (Alibés, 1997). The precedent figures can be expressed as decompacted volumes per unit time (Table 2).

Seismic unit	Age		Decompacted volume of volcanic-rich turbidites (km^3)	Decompacted volume accumulated per unit time(km^{3}x 100 ka)	Percenta ge of increase
A0	Pleistocene	1.6-0	771.7	48.2	31.7
A1.	Late Pliocene	3.4-1.6	659	36.6	16.6
A2	Early Pliocene	5.3-3.4	597.4	3 1.4	261
A3	Late and Middle Miocene	16.6-5.3	979.2	8.7	----

Table 2.- Decompacted volumes per unit time for the volcanic-rich turbidites in the Madeira Abyssal Plain based on previous volume calculations per turbidite type and seismic unit as defined by Alibés (1997).

It is to be noted that the former volumetric figures and those derived from them vs. age are minimum estimates since volcanic-rich turbidites have also accumulated in areas other than the MAP in the Canary Basin, and since the study area does not cover the totality of the MAP but essentially the area referred as the Great Meteor East (Alibés, 1997). From Table 2 it becomes apparent that the biggest percentual jump regarding volcanic-rich turbidites occurred during Early Pliocene times, and that the volume of volcanic-rich turbidites per unit time has been increasing from Middle Miocene times up to now.

Discussion and conclusions

Decompacted volumes of volcanic-rich turbidites in the MAP can be compared with the volumes of landslide deposits around the Canary Islands. The reported (Table 1) landslide deposits are on top of the sediment infill and most of them constitute the present day sea-floor or sub-seafloor. As a consequence, they should remain essentially non compacted or only very slightly compacted. Also, none of them is older than Pleistocene. The volume of the landslide deposits on Table I is, roughly, 2,000 km^3, while the Pleistocene decompacted volume of volcanic-rich turbidites is 771.7 km^3 (Alibés, 1997). Assuming the error margins in such a calculatior, it would mean that only about one third of the overall landslide volumes on the Canary Islands would effectively reach the MAP under the form of turbidity currents. This estimate agrees with the calculation made by Masson et al. (1992b) about the volume proportions of the Canary Debris Flow and the correlated turbidite b on the MAP.

Also, taking into account the ages of the shield phase of the various islands (Schminke, 1994), the sudden increase of volcanic-rich turbidites during Early Pliocene can be only explained by the intensification of landsliding from the islands, like Gran Canaria and Tenerife, which were already built at that epoch. And if our estimations are correct and could be extrapolated, about two thirds of the released volcaniclastic sediment volumes would have been deposited in relatively proximal areas, far from the MAP. The overall volume of Early Pliocene volcanogenic sediment could have been at least three times that accumulated in the MAP, it is some 1,800-2,000 km^3. The same calculations could be applied to all the seismic units and time intervals, from where much higher volumes than those in Table 2 would result.

The western island of La Palma was initiated in the Late Pliocene (≈ 3.4 Ma), and together with El Hierro, fully entered in the system only in Pleistocene times, which could explain both the maximum observed in the decompacted volume per unit time (Table 2) and the almost doubled percentage of increase (16.6 vs. 31.7 in Table

2) when comparing Early-Late Pliocene vs. Late Pliocene-Pleistocene. In addition, a sustained input from the older, eastern islands probably contributed to the volcanogenic sedimentation during Pliocene and Pleistocene times.

If these interpretations are correct, we should expect that older turbidites correlate with landsliding events in the older islands, like Gran Canaria and Tenerife, while younger turbidites could correlate with landslides in the much younger islands of La Palma and El Hierro but also with delayed landslides from the older islands.

Probable Late Miocene source areas for volcanic-rich turbidites are the slopes of Lanzarote or La Gomera islands, as inferred from geochemical data by Jarvis et al. (1997). A major change in the source areas for the turbidites on the MAP has been reported to occur at the beginning of the Late Pliocene, coinciding with the initiation of volcanism in the island of La Palma, cesation of activity on Gomera, a volcanic hiatus on Tenerife and the development of a large stratocone on Gran Canaria (Schminke, 1994; Jarvis et al., 1977). Chemical composition of the volcanic debris indicates the continued existence of multiple sources during Late Pliocene and Pleistocene, which would include more basic material from Tenerife, La Palma and, more recently, El Hierro, and a more fractionated volcaniclastic component from Gran Canaria and the easternmost islands of Lanzarote and Fuerteventura (Jarvis et al., 1997).

The differences between the age of the main shield phase of each individual island and the ages of the major reported landslides on each show great contrasts, from at least 10 Ma for Tenerife, to 0.8 Ma for La Palma and 0.3 Ma for El Hierro (Urgeles, 1997a). Since we don't find any convincing reason to accept a much more delayed landslide development in the older islands than in the younger ones, we should accept that most of the landslide deposits from Gran Canaria and Tenerife are still to be found provided they have not been cannibalized during the building episodes of the younger, eastern islands of the archipelago. Volcanic-rich turbidites do not appear in the MAP until 6.5-7 Ma BP and the Canary Islands have an history extending back at least to 20 Ma BP. Lebreiro et al. (1997) has hypothesized that turbidites shed from the older eastern islands of Lanzarote, Fuerteventura and Gran Canaria were trapped in a local basin which had filled by 6.5-6 Ma BP or, alternatively, that the birth of Tenerife broke the western margin of this local basin allowing turbidite currents to flow further west to the MAP (Lebreiro et al., 1997). Another possibility, recently highlightened by Urgeles et al. (1997b) after examination of the seismostratigraphy west of La Palma and El Hierro, could simply be a depocenter shift related to the prosecutive construction of new islands as observed for the islands of La Palma and El Hierro. The former reasonings support the interpretation that most (we have estimated it roughly at two thirds) of the landslide-derived sediment could have accumulated on relatively proximal areas, where they contributed to form the volcanic aprons and/or infill local basins far from the distal MAP.

Bibliography

Alibés, B. (1997).- Tesis Lic., Univ. Barcelona.

de Lange, G. J., Jarvis, I., Kuijpers, A. (1987).- in Weaver, P. P. E. and Thomson, J., eds., Geology and Geochemistry of Abyssal Plains, 31: 147- 165.

Holcomb, R.T., Searle, R.C. (1991).- Mar. Geotech., 10: 19-32.

Jarvis, I., Moreto, J., Gérard, M. (1997).- In H.U. Schmincke, P.P.E. weaver, J.V. Eirth, w.A. Duffield; eds., Proc. ODP, Sci. Results, 157, College Station TX (Ocean Drilling Program) (in press).

Kidd, R.s., Simm, R.W., Searle, R.C. (1985).- Mar. Petrol. Geol., 2: 210-221.

Lebreiro, S. M., Weaver, P.P.E. and Howe, R.W. (1997).- In H.U. Schmincke, P.P.E. Weaver, J.V. Firth, W.A. Duffield, eds., Proc. ODP, Sci. Results, 157, College Station TX (Ocean Drilling Program) (in press).

Masson, D.G. (1996).- Geology, 24: 231-234.

Masson, D.G., Hugget, Q.J., Weaver, P.P.E., Brunsden, D., Kidd, R.B. (1992a).- Landslide News, 6: 9-12.

Masson, D.G., Kidd, R.B., Gardner, J.V., Hugget, Q.J., Weaver, P.P.E. (1992b).- In C.W. Poag and P.C. de Graciansky, eds., Geological Evolution of Atlantic Continental Rises, van Nostrand Reinhold, New York, USA; p. 327-343.

Moore, J.G., Clargue, D.A., Holcomb, R.T., Lipman, P.W., Normark, W.R., Torressan, M.E. (1989).- J. Geoph. Res., 94: 14465 - 14484.

Rothwell, R G., Alibes, B. and Weaver, P.P.E. (1997).- In H.U. Schmincke, P.P.E. Weaver, J.V. Firth, W.A. Duffield, eds., Proc. ODP, Sci. Results, 157, College Station TX (Ocean Drilling Program) (in press).

Schminke, H.U. (1976).- In G. Kunkel, ed., Biogeography and ecology in the Canary Islands, The Hague (W. Junk); p. 67- 184.

Schminke, H.U. (1982).- In U. von Rad, K. Hinz, H. Sarntheim, E. Seibold, eds., Geology of the Northwest African Continental Margin, Springer-Verlag, New York, USA; p. 273-306.

Schminke, H.U. (1994).- Geological field guide of Gran Canaria (6th edition); Pluto Press, Kiel.

Schminke, H.U., Weaver, P.P.E., Firth, J.V. et al. (1995).- Proceedings of the ODP, Initial Reports, 157: College Station, TX (Ocean Drilling Program).

Simm, R.W., Kidd, R.B. (1983).- Geo-Mar. Lett., 3: 13-16.

Urgeles, R., Canals, M., Baraza, J., Alonso, B., Masson, D.G. (1997a).- J.Geoph. Res. (accepted).

Urgeles, R., Canals, M., Baraza, J., Alonso, B. (1997b).- Mar. Geol. (accepted).

Watts, A.B., Masson, D.G. (1995).- J. Geoph. Res., 100 (B2): 24487-24498.

Weaver, P.P.E. (1994).- Sedimentology, 41: 1025-1038.

Weaver, P. P. E., Jarvis, 1., Lebreiro, S.M., Alibes, B., Baraza, J., Howe, R.W. and Rothwell, R.G. (1997).- In H.U. Schmincke, P.P.E. Weaver, J.V. Firth, W.A. Duffield, eds., Proc. ODP, Sci. Results, 157, College Station TX (Ocean Drilling Program) (in press).

Drilling the clastic apron of Gran Canaria (ODP Leg 157): Submarine transportation and deposition of "Syn-ignimbrite" tephra sediment flows resulting from sea-bound hot ash flows .

Mari Sumita* and Hans-Ulrich Schmincke*

**Abteilung Vulkanologie und Petrologie, GEOMAR, Wischhofstr.1*
D-24148 Kiel, Germany: msumita@geomar.de

Between 14 and ca. 9 million years, several tens of 10-20 m thick, strongly welded peralkaline rhyolitic to trachyphonolitic ignimbrites pyroclastic flows were erupted from a 20 km ϕ caldera on the 40 km ϕ island of Gran Canaria (Canary Islands). Thicker (10-150 cm) ash layers in 200-450 m thick tephra sections drilled 60-90 km north and south of Gran Canaria (ODP Leg 157) are interpreted to have resulted from the entry of these hot ash flows into the sea as evidenced by glass and mineral chemical similarity to specific subaerial ignimbrites, compositional homogeneity and abundance of densely welded glassy ash and lapilli particles. The abundance of glass contrasts strongly with the subaerial source ignimbrites most having been thoroughly devitrified at high T. Most of the fragmentation generating major ash turbidites took place as successive dense hot (600-700°C) flow units entered the sea, and piled up as chaotically structured mounds of variably welded tuff that sourced the syn-ignimbritic ash and lapilli mass flows that entered the sediment basins.

Microprobe analysis of several thousand glass shards and phenocrysts allows to clearly distinguish between compositionally homogeneous ignimbrite-related and subsequent impure volcaniclastic tephra layers mixed with lithic erosional and biogenic skeletal shallow water to planktonic debris. Many coarse ash to fine lapilli-sized basal parts of syn-ignimbrite tephra layers are topped by well-sorted slightly graded ash layers composed of bubble wall and bubble junction shards. These may represent ash turbidites resulting from co-ignimbrite ash clouds that settled through the sea at some distance from the island and/or from pumice rafts. Most, however, may represent material from the bulk ash flow as it entered the sea with the finer ash fraction having concentrated in the more dilute part of the turbidite flow. The concentric sedimentation of the ash turbidites contrasts strongly with the channelized submarine transport systems that dominate periods of volcanic quiescence. Ash layers of clearly air-fall origin are almost absent among the several hundred tephra layers drilled.

Quench granulation may have been enhanced significantly by backwash waves advancing inland following tsunamis generated when major flow units rapidly and forcefully entered the ocean. Fragmentation was accellerated by steam eruptions probably generated by water pockets within the nearshore welded tuff mounds as well as by water that had entered cooling cracks in the hot mass. These processes may have continued for months as the hot sheets had formed coastal cliffs along the shores, quenching and brittle fracture generating glassy welded tuff particles.

A correlation between the drill sites and with the land has been achieved for the Mogan and Fataga Groups, for the boundaries between the Lower, Middle and Upper Mogan Formations, and of at least 6 synignimbrite tephra layers with distinct ignimbrites among the three widely spaced sites as well as to their source ignimbrite cooling units on land. The high precision ages of the land ignimbrites coupled with the high resolution correlation allow to calculate precise sedimentation rates in the interval between 14 and 13.3 million years which vary from 97m/m.y. to 142m/m.y. for Site 953, 43m/m.y. to 72m/m.y. for Site 955 and 54m/m.y. to 93m/m.y. for Site 956.

Stratigraphic constraints on the timing and emplacement of the Alika giant hawaiian submarine landslide

McMurtry, G. M., Herrero-Bervera. E., Resig, J., Cremer, M., Sherman, C., and Smith, J. R.

Soest, University of Hawaii, Honolulu
HI 96822, garym@soest.hawaii.edu

Previous work by J. Moore and others has found evidence for a series of giant waves that have impacted the coasts of Lanai? Molokai and other southern Hawaiian Islands, tentatively dated at 100+ and 200+ ka by U-series methods on uplifted coral clasts. Seafloor imaging and related work by P. Lipman and others off Hawaii Island has suggested the Alika phase 2 debris avalanche as the source of the 100 ka giant wave deposits, although its precise age has been elusive. More recently, M. Garcia described a basaltic sand bed in ODP site 842 (~300 km west of Hawaii) estimated at 100 ± 20 ka that is suggested to correlate with this or another large Hawaiian landslide.

Our approach to the timing and linkage of giant submarine landslides and paleo-tsunami deposits is a detailed stratigraphic survey of proximal pelagic deposits, beginning with a suite of seven piston, gravity and box cores collected in the vicinity of the Alika 2 slide. Methods comprise: U-series dating? including excess ^{230}Th and ^{210}Pb profiling, high-resolution paleomagnetic stratigraphy, visual and x-ray sediment lithology, and the petrology and geochemistry of the included turbidites and ash layers.

Results show sedimentation to vary by nearly three orders of magnitude, from 2.5 mm/ky in sediments on the abyssal plain 10 km from the toe ofthe slide to 1.4 mm/y in rough, hummocky topography within the Alika 2 debris field. Preliminary stratigraphic analysis indicates numerous smaller turbidites have deposited here since ca. 240 ka, and that slumping and rapid sediment infilling have continued within the slide area after ca. 100 ka.

Preliminary ages for the Alika 2 slide from investigation of two of the cores are: 100 ± 15 ka and 125 ± 24 ka (2σ) based on excess ^{230}Th dating; tentative ages for the Alika phase l and/or South Kona slide are 190 ± 27 and 242 ± 80 ka (2σ). Excess ^{230}Th profiling combined with paleomagnetic stratigraphy reveals the thickness of the turbidites. A ~60 cm thick turbidite l-2 km from the Alika 2 toe shows the predominant geochemical signature of a Mauna Loa source; U-series analyses of included planktonic forams as well as ^{40}Ar-^{39}Ar dating of the glasses are planned to better constrain its approximate 100 ka age. Results from the analysis of $\delta^{18}O$ data show that the forams lived somewhere between 113 - 127 ka, which corresponds to the last stage 5 interglacial period. We only have two dates, the one at 113 ka and the other at 127 ka. These dates are indeterminate because they are on either side of the hump that occurs in the $\delta^{18}O$ record.

The Canary Debris Flow: source area morphology and failure mechanisms.

D.G. Masson and P.P.E. Weaver

Southampton Oceanography Centre, Empress Dock, Southampton SO14 3ZH, UK

The Canary Debris Flow originated in 4000 m water depth on the western slopes of the Canary Islands, and travelled 600 km west, to the edge of the Madeira Abyssal Plain (1). The morphology of the source area of the debris flow has been mapped using GLORIA reconnaissance (2) and TOBI high-resolution (3) sidescan sonars. West of about 19° W, the seafloor is characterised by a strongly lineated downslope-trending fabric. This is interpreted as due to streams of debris separated by longitudinal shears. Multiple flow pulses are indicated by a series of asymmetrical lateral ridges which mark the northern boundary of the flow (4). East of 19° W, GLORIA data show only a weak fabric of irregular patches and alongslope lineaments. TOBI data show the patches to be coherent sediment blocks up to 10 km across, surrounded by debris flow material (5). These are interpreted as 'in situ' areas of seafloor sediment which have survived the slope failure and debris flow event rather than transported fragments of a failed sediment slab. TOBI data from the area of alongslope lineaments show a series of small faults downstepping to the west (6). This area of seafloor is interpreted as one of partial sediment failure, where the failure process became 'frozen' before total mobilisation of the seafloor sediments could occur. The slope failure which created the Canary Debris Flow appears to have been a 'slab slide', and the sequence of faults and the progressive downslope increase in the sediment disruption between the faults is inferred to show the breakup mechanism of the failing slab. Breakup probably occurred concurrently with failure. Immediately upslope from the debris flow source area, a characteristic rough blocky seafloor is interpreted as the surface of a debris avalanche derived from the slopes of the island of Hierro (7, 8, 9). The debris flow and avalanche appear to be simultaneous events, with failure of the slope sediments occurring while the avalanche deposits were still mobile enough to fill and disguise the topographic expression of the debris flow headwall (10). Loading of the slope sediments by the debris avalanche probably triggered the Canary Debris Flow.

Acknowledgement

Financial support from the Europoean Commission Marine Science and Tecnology (MAST II) programme is gratefully acknowledged (Sediment Transport on European Atlantic Margins [STEAM] project; grant MAS2-CT94-0083).

Debris avalanche deposits on the submarine flanks of the Canary Islands

D. G. Masson[1], P.P.E. Weaver[1] and A. B. Watts[2]

[1]*Southampton Oceanography Centre, Empress Dock, Southampton SO14 3ZH, UK*
[2]*Department of Earth Sciences, University of Oxford, Parks Road, Oxford OX1 3PR, UK*

Catastrophic landslides have played an important role in the evolution of many volcanic islands, such as the Hawaiian Islands and Reunion, although in the Canary Islands, the precise role of landsliding has been a controversial subject. The deep coastal embayments and straight-sided valleys with arcuate headwalls characteristic of the Canary Islands have, in the past, been cited as evidence for both landsliding and caldera collapse. However, examination of the submarine flanks of the islands provides conclusive evidence, in the form of huge fields of blocky volcanic debris, that large-scale landsliding is the dominant mechanism in the formation of these valleys and embayments.

On the northwest flank of El Hierro Island, sidescan sonar images provide evidence for a large debris avalanche which originated in the El Golfo embayment. Angular blocks, up to 1.2 km across and 200 m high, cover the debris avalanche surface. The total volume of avalanche deposits is in the order of 250 km^3. On the north flank of Tenerife, landslide deposits related to the formation of the onshore Orotava and Icod valleys cover at least 5500 km^2 of seafloor. Here, the volume of landslide deposits is estimated at 1100 km^3.

The El Golfo Debris Avalanche is related to both the Canary Debris Flow and a volcaniclastic turbidite found in the Madeira Abyssal Plain 600 km west of the Canaries. Dating of the turbidite and the failure scarp onshore indicates that the failure probably occurred between 13 and 17 thousand years ago. The youngest landslide on the north flank of Tenerife also correlates with a volcaniclastic turbidite in the abyssal plain sequence. This leads us to suggest a general correlation between volcaniclastic turbidites in the abyssal plain sequence and landslides in the Canaries. Tentatively, this correlation suggests that seven major landslides have affected the Canaries during the last 750 thousand years.

Acknowledgement

Financial support from the Europoean Commission Marine Science and Tecnology (MAST II) programme is gratefully acknowledged (Sediment Transport on European Atlantic Margins [STEAM] project; grant MAS2-CT94-0083).

The El Golfo Debris Avalanche, Canary Debris Flow and b turbidite - the result of a single slope failure west of the Canary Is.

D.G.Masson and P.P.E. Weaver

Southampton Oceanography Centre, Empress Dock, Southampton SO14 3ZH, UK

Detailed analysis of sidescan sonar data, high resolution seismic profiles and sediment cores shows that the El Golfo Debris Avalanche, Canary Debris Flow and the 'b' turbidite in the Madiera Abyssal Plain (MAP) are all parts of a complex deposit resulting from a single slope failure on the northwest flank of El Hierro Island in the western Canaries. This event occurred between 13 and 17 thousand years ago, involved some 800 km^3 of rock and sediment, and affected over 100,000 km^2 of seafloor (somewhat larger the area of Portugal).

The El Golfo Debris Avalanche is a blocky avalanche deposit covering 1500 km^2 of seafloor and with an estimated volume of 250-350 km^3, corresponding to an average thickness of 250-350 m over the avalanche deposit area. The avalanche headwall is the 900 m onshore scarp of the El Golfo depression on El Hierro and the avalanche deposit extends to waterdepths of 3000 to 4000 m. The surface of the avalanche is covered by angular blocks of volcanic rock up to 1.2 km across and 200 m high. The Canary Debris Flow originated at about 4000 m waterdepth on the western slopes of the islands of El Hierro and La Palma and travelled 600 km to the edge of the MAP. It produced a thin (average 10 m thick) debris flow sheet over an area of 40,000 km^2, and has a volume of some 400 km^3. The b turbidite in the MAP has a volume of about 100 km^3 and a geochemical signature that shows derivation from the western Canary Islands. Interaction with shallow channels on the continental rise resulted in the coarse and fine fractions of the turbidite following different paths to the MAP, and gave rise to complex depositional patterns on the plain.

Sediment cores from the eastern MAP show that the Canary Debris Flow deposit occurs within the b turbidite, unequivocally demonstrating that the two flow phases are parts of one sedimentation event. However, divergence of the b turbidite and debris flow paths across the rise, controlled by subtle changes in bathymetric trends, suggests that the turbidite was not continuously generated from the debris flow as it crossed the slope, but that both turbidite and debris flow were a consequence of emplacement of the debris avalanche on the upper slope. The debris flow originated from the toe region of the El Golfo Debris Avalanche, although no clear debris flow headwall is visible on sidescan sonar data. The debris flow and avalanche appear to be simultaneous events, with failure of the slope sediments occurring while the avalanche deposits were still mobile enough to fill and disguise the topographic expression of the debris flow headwall. Loading of the slope sediments by the debris avalanche most probably triggered the Canary Debris Flow.

Acknowledgement

Financial support from the Europoean Commission Marine Science and Tecnology (MAST II) programme is gratefully acknowledged (Sediment Transport on European Atlantic Margins [STEAM] project; grant MAS2-CT94-0083).

Genesis of the Roque Nublo Ignimbrites, Gran Canaria, Canary Islands.

Francisco José Pérez-Torrado[1], Joan Martí [2], Simon Day[3,4] & José Mangas[1].

1: Dept. Fisica-Geologia, Universidad de Las Palmas de Gran Canaria, Spain.
2: Institut de Ciencies de la Tierra "Jaume Almera", Barcelona, Spain.
3: Dept. of Geography & Geology, Cheltenham & Gloucester CHE, Cheltenham, U.K..
4: Greig Fester Centre for Hazard Research, University College London, U.K.

The Roque Nublo group (Pliocene, ca. 5,5 to 2,7 Ma) is the product of one of the main episodes in the subaerial construction of Gran Canaria. This is characterised by the construction of a central volcanic complex, the Roque Nublo stratovolcano, which reached a height of at least 2500 m in the central area of the island. The evolution of this stratovolcano involved magmas of alkali basalt-basanite to trachyte-phonolite compositions and a great variety of eruptive mechanisms. The most distinctive lithology in the Roque Nublo volcanic sequence are pyroclastic breccia deposits, the Roque Nublo ignimbrites. These are especially abundant in the Tirajana and El Montañon formations, which represent most of the later activity of the volcano (see Pérez-Torrado et al., *Growth and destruction by lateral collapse of the Roque Nublo oceanic island stratovolcano, Gran Canaria, Canary Islands*, this volume).

The Roque Nublo ignimbrites show a number of distinctive lithological features. They are highly-indurated, matrix - supported breccias with a polymict clast assemblage. Two main types of clast are present: lithic clasts derived from near - surface volcanic formations within the Roque Nublo Group (35-55% of the total rock volume) and juvenile fragments (15-30%). The lithic clasts are unusually abundant for rocks of pyroclastic origin. The juvenile clasts include abundant pumice fragments with irregular, angular to ragged outlines, high crystal content and low vesicularity (< 50%) compared to pumices of comparable composition produced in normal magmatic eruptions. The rest of the rock is composed of crystal fragments (5-7%) and an intergranular, cryptocrystalline devitrified ashy matrix (20-30%). This matrix is strongly zeolitized (in contrast to interbedded airfall and epiclastic units, implying syn - eruptive alteration) but melt inclusions in juvenile phenocrysts indicate a parent magma of trachytic - phonolitic composition. Random magnetic polarities of the clasts indicate low emplacement temperatures, below 300 °C.

The ignimbrites are normally massive, but some units show normal grading (in size and / or abundance) of lithics and, more rarely, reverse grading of the pumice fragments. A large number of vegetable remains occur close to the bases of some units. The bases are normally sharp and planar, without erosive features even where they overlie weakly - indurated ash deposits, except in distal areas where slight erosion occurs at the base of some units.

The ignimbrites show strong facies variations from proximal regions in the centre of the island to distal regions in the coastal areas. They occur in the main palaeovalleys and have lenticular cross - sections in proximal and medial areas, but spread out into sheet - like bodies at the mouths of the palaeovalleys in distal areas of the volcano. The number and thickness of depositional units also varies with distance from the source region near the summit of the volcano. In addition, significant lithological variations occur with distance from the source: a) increase in the proportion (by volume) of lithic clasts, but a marked decrease in the sizes of the largest clasts (from metres to less than 50 cm); b) an increase in the proportion of Miocene lithics; c) a decrease in proportion and size of pumice fragments. Degassification pipes and red thermal alteration of the underlying deposits are rare and limited to the proximal areas. In the proximal facies the ignimbrites are sometimes associated with subordinate, thinly-laminated ash fall and surge deposits (with accretionary lapilli) a few centimetres thick and of restricted lateral extent. In contrast, in the distal facies the ignimbrites are associated with epiclastic conglomerates and lahar deposits.

Certain features of the Roque Nublo ignimbrites are highly unusual: the inferred eruption mechanism must account in particular for the high lithic content; the unusual pumice morphology; the low emplacement temperature; and the syn - eruptive alteration. On the basis of these features and the other characteristics noted above we propose that the Roque Nublo ignimbrites were emplaced in high - magnitude phreatomagmatic-vulcanian eruptions with the following characteristics, shown diagrammatically in Fig. 1.

1) Eruptions involved breaching of an initially closed vent and intense erosion of the vent walls by violent explosions originating from a level close to the surface: these features account for the high abundance and near - surface origin of the lithic clasts.

2) The erupting magma was of trachytic - phonolitic composition with a high crystal content, resulting in high magma viscosities and thus explosive degassing.

3) The explosivity of the eruption was further enhanced by magma - water interaction. Ingress of water into the magma at or below the water table is strongly implied by the ragged to angular, low - vesicularity pumices; the presence of pyroclastic surge deposits, some with accretionary lapilli, at the bases of some of the ignimbrites; the strong syn - emplacement zeolitization of the glass components; and the transition from pyroclastic flows to lahars in the distal facies of some of the flow units. The high rate of erosion of the vent walls, inferred from the high lithic content, may also be related to steam explosions in the heated region around the vent.

4) The lack of plinian fallout deposits associated with these ignimbrites suggest that positively buoyant eruption columns never developed in the Roque Nublo eruptions, and that instantaneous column collapse resulted from the high density of the eruption mixture, which was in turn due to its high lithic content, to the abundance of water vapour and by relative large vent radii. The particular characteristics of the ignimbrites suggest tephra fountaining after initial pyroclastic surge development, followed by development of high - density, rapidly sedimenting pyroclastic flows as the most plausible transport and deposition mechanism.

5) The high - density pyroclastic flows were channelised following the radial network of paleovalleys at the flanks of the Roque Nublo stratovolcano during the main part of their emplacement, but expanded laterally when they arrived at the mouth of the valleys close to the coast. This expansion caused a decreased in the velocity of the flows and their subdivision in different flow units. This explains the existence of a higher number of thin depositional units in distal facies rather than in medial facies.

It is not possible to estimate the frequency of ignimbrite - forming eruptions within the Roque Nublo Group (especially in the ignimbrite - rich Tirajana and El Montañon formations) but the presence of conglomerates interbedded with these ignimbritic deposits, indicate the existence of periods of quiescence between the active episodes. Furthermore, the lava flows interbedded with these ignimbrites suggest the existence of similar episodes of activity, each one including a transition from hydrovolcanic (Roque Nublo ignimbrites and associated pyroclastic surges) to dry conditions (lava flows).

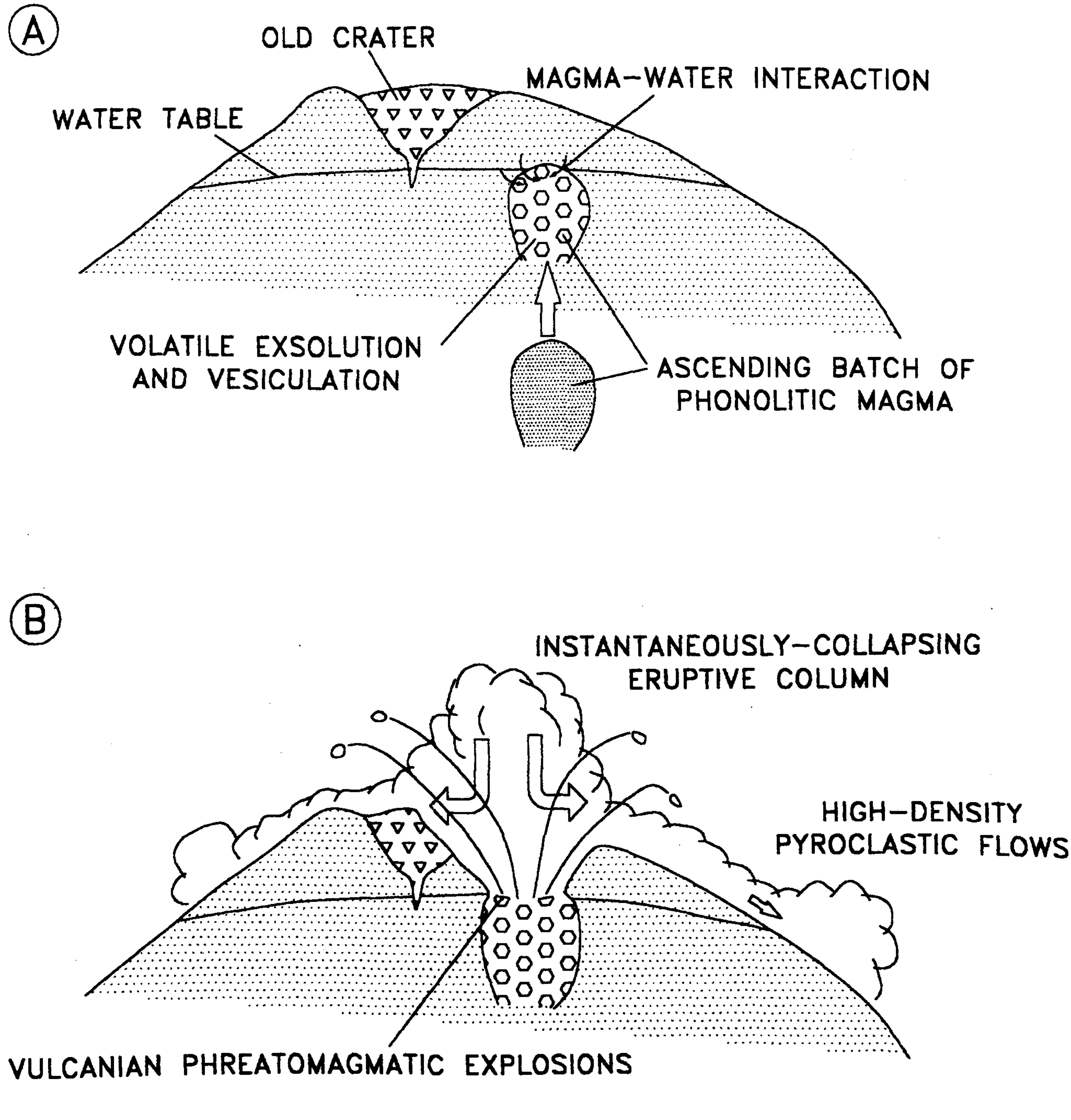

Figure 1.- Proposed eruption mechanism for the production of the Roque Nublo ignimbrites.

A possible tsunami breccia deposit on Fuerteventura, Canary Islands.

S.J. Day[1] and J.C. Carracedo[2]

[1]*Greig Fester Centre for Hazards Research. Dept. of Geological Sciences. University College London*
[2]*Estación Volcanológica de Canarias. Consejo Superior de Investigaciones Científicas*

Reef limestone - bearing breccias deposited by giant tsunami waves up to 400 m above contemporary sea level have previously been identified in the Hawaiian islands and have been associated with giant lateral collapses (Moore & Moore 1984). Similar deposits emplaced high above sea level should be expected to occur in other oceanic island archipelagoes with young, unstable volcanoes, but have not yet been identified outside the Hawaiian archipelago. Here we describe a possible giant tsunami deposit from Fuerteventura in the eastern part of the Canarian archipelago.

The Jandía peninsula in the south of Fuerteventura is the eroded remnant of a subaerial shield volcano of probable late Miocene age, and rises to a maximum of 800 metres above sea level. Extensive arid - climate alluvial fan, scree and aeolian sand deposits occur on both flanks of the peninsula and form a gently -inclined apron around outcrops of the Miocene bedrock. Intercalated with these deposits at a number of locations on the south flank of the peninsula, at between about 35 and 75 metres above present sea level, is a bed containing very well - rounded boulders and pebbles, typical of mature high - energy beach and littoral shoreface facies, and a marine molluscan fauna in many exposures (Fig. 1). For a number of reasons, we interpret this as a recent tsunami deposit rather than as a Messinian (Uppermost Miocene - Pliocene) marine littoral deposit, such as occurs at a number of locations elsewhere in Jandía and in Fuerteventura as a whole:

1. At all but one locality, the deposit is overlain and underlain, without development of unconfomities, by terrestrial deposits, generally scree breccias ith highly angular basalt clasts and a partial interstitial sand matrix or caliche cement, in addition to much empty pore space. The exceptional locality, at Morro Jable, unconformably overlies a marine carbonate sand with shelly fauna (identified as Messinian by Meco & Stearns 1981) and is itself overlain by an aeolian sand layer. The cover on top of the deposit consist of no more than 1 - 2 metres of scree breccia, again except at Morro Jable where a palaeo -dune is present.

2. The deposit is conformable to the moderately inclined (5 - 15 dip) underlying breccia layers (except at Morro Jable) and extends for as much as 40 metres vertically and 300 metres horizontally in the dip direction without development of an underlying abrasion surface or of a coastal palaeocliff at the upslope limit of the deposit. This lack of evidence for in - situ erosion is in strong contrast to the extended abrasion experienced by the well - rounded basalt clasts, of boulder to cobble size, within the deposit. Abrupt transport of these clasts from their environment of formation is implied.

3. The deposit is entirely massive, with no internal stratification, clast imbrication or other structures typical of beach facies. Overall, the deposit has a very simple sheet - like geometry.

4. The fauna consists primarily of Ostrea spp. (oysters) and Conus spp. (benthic gastropods). Preservation varies from extremely good to freshly -fractured angular fragments to highly abraded fragments. None of the oysters are in life position and the fauna is more typical of a moderate - energy shallow marine rather than coastal environment, with a firm sandy substrate rather than littoral boulders. Abrupt transport of these fossils from their life environment is implied. The fauna is much less diverse than the Miocene faunas described by Meco & Stearns (1981) and Meco et al. (1995). An intensely bored and abraded shell of Gryphaea Virleti, most probably reworked from the Messinian deposits, was found: in contrast, the other material contained few if any borings and seems to be of recent origin. Further palaeontological investigations and U - series dating of the shelly fauna is planned.

5. The clast population in the deposit is strongly mixed: in addition to the abundant, very well rounded beach boulders and pebbles, and the bioclastic shells and shell fragments, there are angular clasts of basalt, interpreted as originating from subaerial scree deposits, and abundant interstitial calcareous sand in fresher

exposures in quarries and barranco walls; the carbonate sand and shells have been reprecipitated as caliche in more weathered exposures.

The deposit therefore seems to have been the product of deposition in a single, transient event rather than having produced at a stable shoreline over an extended period. Catastrophic transport and mixing of clasts from shallow marine, beach and terrestrial environments seems to have taken place prior to very rapid deposition as a single sheet. We interpret this as the result of a giant wave scouring loose and weakly - attached material from the offshore and coastal environments before running - up onto the coast of the Jandía peninsula and depositing its load extremely rapidly before draining back into the ocean.

The absence of the deposit at altitudes of less than 30 m above present sea level suggests that considerable scouring of the land may have taken place during this backwash phase. The highest observed altitude of the deposit, 75 metres above present sea level, implies maximum runup of the wave by at least this amount: it should also be noted that these exposures are up to 1 km inland. Furthermore, depending on the age of the deposit, contemporary sea level may have been lower than at present; but it is unlikely to have been higher unless the deposit is pre - Quaternary. Runup heights could have been as much as 130 -200 m if the tsunami occurred during a period of low sea level stand.

Although confirmation awaits palaeontological and radiometric dating of the shelly fauna, we suspect that the deposit is young (late Pleistocene?). The most plausible correlation is with one or other of the several giant lateral collapses that have affected the western Canarian islands of Tenerife, La Palma and El Hierro in the past 1 Ma. These are 300 to 400 km from Jandía: although detailed modelling of the tsunami generated by these collapses is required, the occurrence of 75 m + wave runups in Jandía, if confirmed by further studies of these deposits, would imply wave runups of at least a few hundred metres on islands closer to the wave source. We suggest that, although searches for tsunami deposits should be carried out elsewhere in the Canarian archipelago, they may not be widespread because of powerfully erosive backwashes on the steep slopes of the younger islands.

REFERENCES

Meco, J. & Stearns, C.E. (1981). Emergent littoral deposits in the eastern Canary Islands. Quaternary Research 15, 199 - 208.

Meco, J., Petit - Maire, N., Fontugne, M., Shimmield, G. & Ramos, A.J. (1995). The Quaternary deposits in Lanzarote & Fuerteventura (Eastern Canary Islands, Spain): an overview. In: Meco, J. & Petit - Maire, N. (eds.) Climates of the Past: Proceedings of the CLIP meeting, 2-7 June, 1995, Lanzarote & Fuerteventura, Spain. Publ. Universidad de Las Palmas de Gran Canaria. p. 123 -136.

Moore, J.G. & Moore, G.W. (1984). Deposit from a giant wave on the island of Lanai, Hawaii. Science, 226, 1312 -1315.

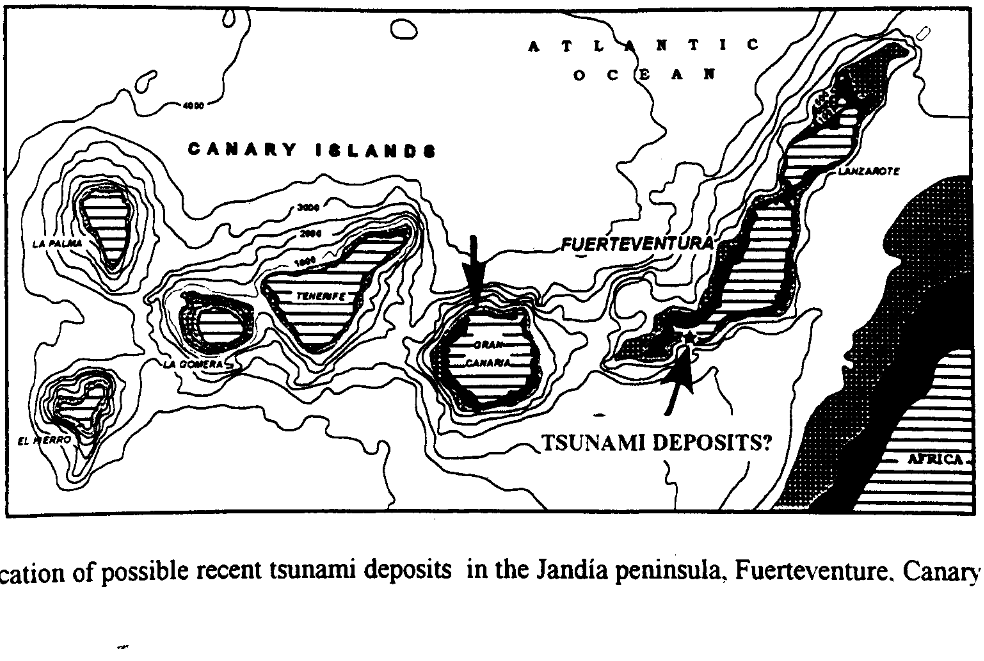

Fig. 1.- Location of possible recent tsunami deposits in the Jandía peninsula, Fuerteventure, Canary Islands .

Geophysical Monitoring of the Fogo Volcano, Cape Verde Islands

Fonseca, J.F.B.D.[1], Heleno, S.I.N.[1], Barros, I.J.[2], Berberan, A.L.[3] and Ramos, M.S.[2]

[1]*Physics Department, Instituto Superior Técnico, Lisboa, Portugal.*
[2]*Laboratorio de Engenharia de Cabo Verde, Praia, Republic of Cape Verde.*
[3]*Laboratorio Nacional de Engenharia Civil, Lisboa, Portugal.*

The geophysical monitoring of the Fogo Volcano, Cape Verde Islands, is the object of a.current joint effort by IST, Lisbon, and LECV, Praia. Exploratory fieldwork was carried out between 1992 and 1995, and included the seismic monitoring of the April 95 Fogo eruption (Fonseca et al., 1996; Heleno et al., this volume). Making use of the knowledge thus gained, a permanent geophysical and geodetic monitoring programme is now under implementation. This paper will summarise the main results so far? and discuss the chosen monitoring strategy.

The Cape Verde Islands are located in the N. Atlantic, on a broad positive bathymetric anomaly (the Cape Verde Rise) in the interior of the African Plate. Courtney and White (1986) modelled the heat flow and geoid anomalies associated with the swell as the result of dynamic uplift over an ascending thermal plume. Fogo is the only island of the archipel with a record of volcanic events since the settlement (early 16th century), but the neighbouring Brava Island (the youngest of the archipelago judging from the sense of motion of the African plate) is more unstable seismically.

Pico do Fogo Volcano, reaching 2829 metres, is the highest point of the roughly conical Fogo Island. The volcano is surrounded by a flat zone, the Chã das Caldeiras which in turn is encircled by a vertical cliff of semi-circular shape, openned towards the E. This configuration was generated by gravity-driven lateral collapse of the eastern flank of an older volcano (Day? unpublished report; Heleno et al., this volume).

The Fogo Volcano has been poorly studied with respect to its internal structure and eruptive mechanism. A temporary network of seismic stations was deployed in early 94 (about a year before the last eruption) in Fogo and Brava Islands, in order to study the background seismicity. The pattern that emerged suggests an E-W trend of seismic activity linking Fogo and Brava Islands, with some of the events evocative of magma movements: "gas-piston" type microearthquakes? seismic swarm activity and harmonic tremor were observed during the 4 months of the survey. The tremor was recorded at a site 3 Km from the locus of the future eruption.

Tilt observations were carried out for several months at a site inside Chã das Caldeiras between August 93 and February 94, at 30 minute intervals. Four tiltmeters were used, of which two were radial with respect to Pico do Fogo Volcano and the other two were tangential. The data reveal a complex non-linear response to temperature variations and tides, and the implications for data correction will be discussed.

Temperature measurements at the bottom of a 16 meter deep borehole were conducted regularly at 24 hour intervals, between February 92 and April 95 (occurrence of the last eruption). Although the borehole was only 3 Km distant from the locus of the eruption, the measurements did not reveal any anomalous trend on the temperature values over that period. This negative result indicated that any success in detecting thermal precursory signals will have to relay on fluids such as fumarolic gases.

The adopted monitoring routine will consist of:

- permanent seismic obsetrvation in 8 short-period 3-component stations; data will be radio-linked in real time from Fogo and Brava islands to the processing/analysis laboratory in Praia, Santiago Island.

- permanent seismic obsetrvation in 2 broad-band 3-component stations, one in Chã das Caldeiras? Fogo, and one in Brava; these stations will allow the monitoring of volcanic tremor and low-frequency seismic events.

- tilt measurements from 2 tilt stations, equipped with 4 tiltmeters each (2 pairs of olthogonal horizontal sensors per station); these stations will be located at the basis of the slope of Pico do Fogo, where most eruptions have taken place during the last few centuries; tilt (and temperature) values will be transmitted to the laboratoly in Praia by radio, at 30 minute intervals.

- infrared temperature measurements from the interior of the Pico do Fogo crater; this is a region of permanent filmarolic activity, and 3 infrared sensors will be used, pointed at different zones of the crater? in order to be able to detect anomalous temperatures of the gases.

A geodetic network was designed with the purpose of detecting deformations associated with inflation or deflation underneath or near Pico do Fogo (Berberan, 1997), thus complementing the tilt measurements. As the next step, the network will be expanded to control also the movements associated with the tendency for lateral collapse of the volcanic edifice. Survey repetitions should take place on a yearly basis, with a more expedite version being carried out at shorter intervals to control ongoing slab sliding.

The preliminaly field work in Fog and Brava islands was supported by ICP (Portuguese Cooperation Agency), JNICT, FLAD and the Gulbenkian Foundation, and equipment was loaned from NERC and BGS, Edinburgh. The Fogo permanent network implementation is funded by JNICT (Programme PRAXIS XXI) and ICP.

References

Berberan, A., 1997. Preliminary design for the geodetic monitoring network of Fogo Volcano Technical paper 13/97-NMG/DB, LNEC Lisbon.

Courtney, RC. and White, RS., 1986. Anomalous heat flow and geoid across the Cape Verde Rise: evidence for dynamic support from a thermal plume in the mantle, (Geoph. J. of the R. astron. Society, **87** pp. 815 - 867.

Day, S.J., unpublished report. Stmctural analysis of Pico do Fogo and Monte Amarelo Volcanoes Fogo Island Cape Verde Archipelago and implications for future lateral collapse and volcanic hazards, IST Lisbon, 1997.

Fonseca, J.F.B.D., Heleno, S.I.N., Walker, A.B., Barros, I.J., Quental, L.M.A.R, Stewart, D. and Ramos, M.M., 1996. Seismic Monitoring of the Fogo Eruption, April 95, *in* B. Thorkelson (De.), Seismology in Europe, IMO Reykjavik, 1996.

Heleno, S.I.N., Fonseca, J.F.B.D. and Day, S.J., this volume. Volcano-tectonic interpretation of the seismicity associated with the 1995 eruption of Fogo, Cape Verde Islands (extended abstract).

Volcano-tectonic interpretation of the seismicity associated with the 1995 eruption on Fogo, Cape Verde Islands

Heleno, S.I.N.[1], Fonseca, J.F.B.D.[1] and Day, S.J.[2,3]

[1]*Instituto Superior Técnico, Lisbon, Portugal.*
[2]*Centre for Volcanic Research, CGCHE, Cheltenham, UK*
[3]*Greig Fester Centre for Hazard Research, University College London, UK*

This paper presents preliminary results of the seismic monitoring carried out during the Fogo eruption of April 1995 (Fonseca et al., 1996). Between April 14 (day 12 after the eruption onset) and July 11, five telemetric stations equipped with short-period (4.5 Hz) geophones were installed inside the 8-Km wide summit depression of the volcano (fig. 1) and the data were recorded continuously onto magnetic tape. So far, about 100 hypocentres have been computed to which a small group of joint focal mechanism solutions were fitted. Due to the scarcity of published work on the structure of Fogo volcano, a reconnaissance study was carried out in early 97 (Day, unpublished report). Here we combine results from this study and from the seismic monitoring.

The current topography of Fogo island clearly suggests the existence of an east-facing lateral collapse structure (Silveira et al., 1996): this was confinned by the reconnaissance study. This collapse structure has been partly filled in by recent volcanic rocks which form the Pico do Fogo volcano and the plain of the Chã das Caldeiras (fig. 1). The vertical cliffs surrounding Chã das Caldeiras provide excellent exposures of the older Monte Amarelo volcano, which contains abundant pre-collapse dykes. The main pre-collapse dyke swarms have bearings of 030°, 150°, 240° and 300°, in a variation of the triple volcanic rift geometry which is typical of oceanic islands (Carracedo, 1996). This radial pattern is cross-cut by a swarm of N-S dykes, suggesting eastward displacement of the eastern flank of the Monte Amarelo volcano prior to collapse. Post-1760 AD historic volcanic vents around the Pico do Fogo volcano show a similar N-S alignment. The 1995 eruption, however, took place along a fissure system bearing 240°, SW of Pico do Fogo itself.

The seismic events were separated in groups according to i) the evolutionary stage of the eruption to which they correspond, ii) spatial clustering and iii) consistency of joint focal mechanism solution. Four phases in the eruption were distinguished: 1) the syn-eruptive phase, from the beginning of the eruption (day 0) to the end of the effusive activity (day 53); 2) the transition phase, from day 54 to day 59, which included a conspicuous episode of strong volcanic tremor; 3) the swarm activity phase, days 60 and 61; and 4) the post-eruptive phase, from day 61 till the end of the monitoring (day 100).

The events of the syn-eruptive phase (fig. 2A) were divided into four groups using the criteria mentioned above, and it was possible to fit a joint focal mechanism solution to each group. Preferred fault planes were selected taking into consideration the elongation of the clusters (when adequate) as well as known structural trends. Therefore, focal solutions A2 and A3 were interpreted as oblique slip along SE-dipping planes striking nearly at 240°, with opposite directions of vertical motion. For solutions A1 and A4 it is not clear which focal plane should be chosen. The events from this phase are deeper, on average, (mostly between 2 Km and 6 Km) than those of the later phases.

During the transition phase the events clearly define two clusters (fig. 2B), one elongated in a nearly N-S direction, and the other undemeath the eruptive fissure and reproducing its 240° strike. The adjusted focal mechanism solutions for both clusters (Bl and B2) show oblique strike-slip with a normal component of vertical motion. The focal plane striking near 350° was chosen for both solutions. The events of this phase are shallower, the typical depths being close to 1.5 Km for the south-eastern cluster and around 2 Km for the north-western cluster.

The episode of strong volcanic tremor, which occurred towards the end of this phase, lasted about 45 minutes and seems to originate in the region between the two clusters.

During the swarm activity phase, of which the present data (fig. 2C) is only a small sample, a clear picture of the 240° strike is given by the elongation of the main cluster, which is also along the direction of the eruptive fissure, but this time at larger depths (between 2 Km and 4 Km). A second group of events further to the NW seem to define a subparallel direction, and have deeper foci (between 3 Km and 6 Km), reproducing the pattern described above for the transition phase. It was not possible to fit joint focal plane solutions to these events.

Finally, in the post-eruptive phase, an elongated cluster of events striking at about 120° (fig. 2D) suggests a new trend, which was not observed before. Although a joint focal mechanism for the entire cluster was not found, its south-eastern sector admits a solution D3 (albeit poorly constrained) of sinistral strike-slip along a vertical plane striking at 120°, which was preferred. The events of the north-western sector are compatible with oblique strike-slip along a plane striking at 030° (solution Dl), one of the structural trends observed in the field. Focal depths for this cluster range between 1 Km and 3 Km. A second cluster (D2) with deeper events, typically between 2 Km and 5 Km, show a N-S elongation along the western limit of the Chã das Caldeiras.

In general the seismicity highlights the structural trends at the surface, both in terms of cluster elongation and interpreted focal planes. This is particularly true for the 240° trend (eruptive fissure and one of the dyke swarms): clusters A2 and A3 are interpreted as the result of deformation associated with the intrusion of a feeder dyke with that strike, and cluster C2 (swarm activity) may correspond to the interaction of groundwater with the top of the dyke durin~ ma~ma drain-back.

Most of the seismicity surrounding the region of inferred dyke intrusion is shallower than that directly related to the emplacement, and consistent with an E-W direction of minimum compression at shallow depths: this is true for clusters A4 and Dl, and to a certain extent to clusters B1 and B2 (NE-SW in this cases). We interpret this as indicating that the euption triggered E-W extension associated with incipient instability of the eastem flank of the volcano. The focal solution A4 may be interpreted as the downward movement of the eastem block in a south-easterly direction, as a result of the push of the dyke intrusion, in which case the slip could be accommodated by one of the main dyke swarms (strike 150°). Similar instability during the post-eruptive phase is suggested by solution Dl on the opposite side of the surface fissure, this time exploiting an alternative direction of weakness (dyke swarm striking 030°). Simultaneously, in the south-eastem region of Chã das Caldeiras, magma drain-back seems to have led to a reversal of the earlier deformation (solution D3). Extensional reactivation of en-echelon N-S structures along the 240° trend during the transition phase may be the explanation for cluster B2, and this extension could have allowed fluid percolation leading to the swarm activity along the same trend immediately after. The ocurrence of instability-related deformation after the end of the eruption may be explicable in terms of pore-fluid pressurization effects (Elsworth et al., this volume).

Field work in Fogo island had the collaboration of BGS, UK, and was financially supported by ECHO, Brussels, ICP, Lisbon and the Gulbenkian Foundation, Lisbon.

References

Day, S.J., unpublished report, Structural analysis of Pico do Fogo and Monte amarelo volcanoes, Fogo island, Cape Verde archipelago; and implications for future lateral collapse and volcanic hazards, IST, Lisbon, 1997

Fonseca, J F.B.D. et al., 1996, in B. Torkelsson (ed.), Seismology in Europe, IMO, Reykjavik.

Silveira, A.s. et al., 1996, Protecção Civil, 7, 3-14.

Carracedo, J.C., 1996, in W.J McGuire, A.P. Jones and J. Neuberg (eds.), S. Publ. 110, Geol. Soc., London.

Figure 1. Orientations of volcanic vent axes, Pico do Fogo and Chã das Caldeiras, Fogo Island. Contour intervals 50m above 1500m (except in old volcanic edifice and collapse scar cliffs), 100m below 1500m.

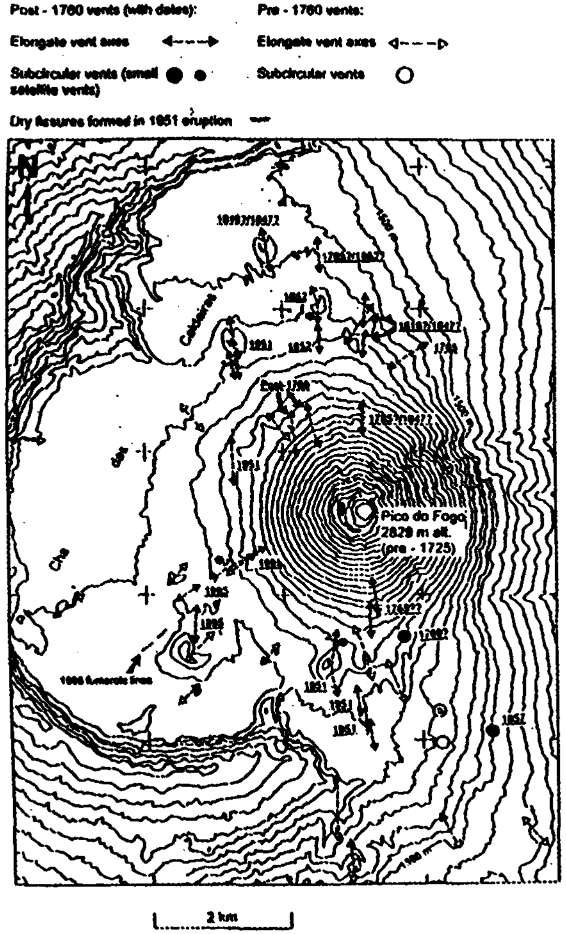

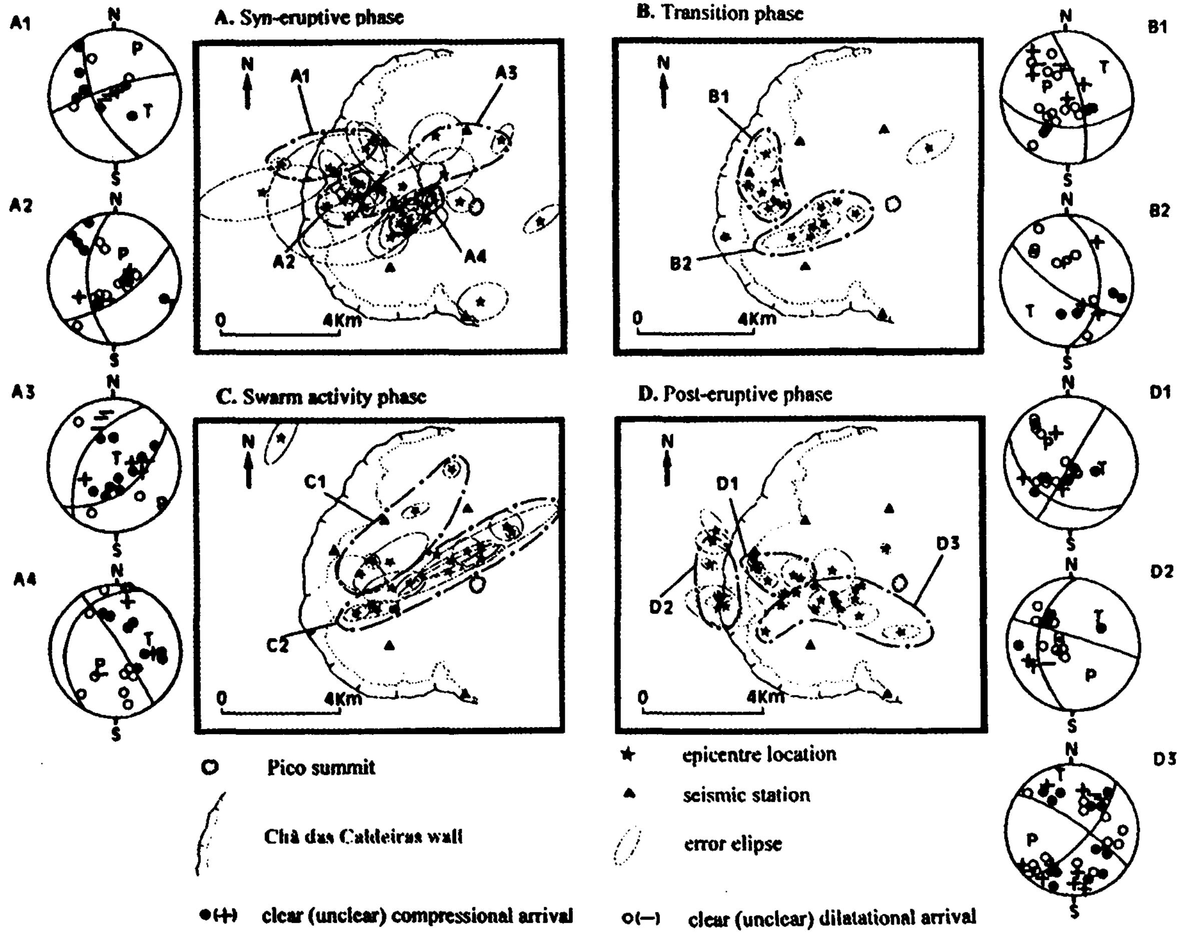

Figure 2. Spatial distribution of the epicentres recorded during the four phases of activity discussed in the text. The groups of events used to construct the joint focal mechanism solutions are depicted. The focal spheres are represented in lower hemisphere stereographic projection.

Time and Spatial Clustering Properties of the Etna Region Seismicity During 1981 - 1991

Valerio De Rubeis, Patrizia Tosi, Alexandro Zenari, Maria Serafina Barbaro

Istituto Nazionale di Geofisica, Via di Vigna Murata 605
00143, Rome, Italy.
++39-6-51860215. e-mail: derubeis@marte.ingrm.it

and Sergio Vinciguerra

Istituto di Geologia e Geofisica, Universit'88 di Catania
256 Catania - Italy
++39-6-51860225. e-mail: vinciguerra@marte.ingrm.it

Time and spatial properties of seismic activity of the Etna Volcano (Italy) are investigated with the fractal dimension analysis, over a specific period (years from 1981 to 1991), inside which a very interesting volcanological (seven major flank eruptions) and seismic activity occurred. A test of completeness on the etnean seismic data performed by following the procedure of Tinti and Mulargia (1985) has shown as result that the data set can be considered complete from M.

The fractal dimension is evaluated adopting the correlation integral method (Grassberger and Procaccia, 1983) since it gives a weight to the number of elements inside the box considered. The time and spatial evolution oft he temporal fractal dimension calculated on a 40 seismic events moving window, allowed the clarification of the relations between the seismic activity and the occurrence of the eruptions. This kind of analysis evidences the clustered character of seismic sequence at short time ranges, giving at the same time information on the global behaviour. Moreover, the spatial localisation of data allowed the analysis of seismic activity in relation to the main structural systems outcropping on the volcano edifice (sector 1) and in the surrounding areas (sector 2 and 3).

The results show the presence of relations at different time and spatial scales between seismic clusters and eruptions occurrences.

Establishing baseline ground deformation studies on La Palma using GPS.

J. L. Moss

Centre for Volcanic Research, Cheltenham and Gloucester College of Higher Education.

Introduction

The island of La Palma currently has a north-south oriented, active, single concentrated rift-zone called the Cumbre Vieja, which acts as a preferential route for the emplacement of magma from depth in the form of dykes. The steep gradient and high/aspect-ratio of the ridge coupled with the prospect of future magma intrusion suggests that large-scale sector failure, as seen earlier in the history of La Palma and at other Canary islands, could be instigated by the evolution and collapse of this volcanic ridge.

The potentially unstable sector is around 20km long and up to 10km wide. The northern boundary of the potential slip zone is located in the vicinity of the San Juan fissures and the Jedey vents, where in 1949 en echelon fissures opened perpendicular to the N-S alignment of the rift; these fissure eruptions were fed by dykes re-oriented from the principal trend. The southern boundary is at the tip of the island where further dykes were re-oriented from the principal trend to feed the 1971 Teneguia eruption. This re-orientation is thought to be a reflection of the local stress regime which is affected by a deep fault underlying the unstable sector. The 1949 eruption at the summit of the ridge, generated normal faults parallel to the rift-zone, which are downthrown to the west with displacements up to four metres. Future dyke intrusion could cause further westward displacement, culminating in piecemeal or wholesale failure of the western flank of the ridge. The arcuate normal faults indicate that the area of potential collapse is a broadly curving sector.

Baseline Ground Deformation Network

At present the monitoring of the island is minimal: a single seismometer is located to detect the co-seismic magmatic intrusion which could indicate a forthcoming eruption. The establishment of the ground deformation monitoring programme facilitates analysis of the current stability of the ridge. The baseline network will ascertain the level of inter-eruptive ground deformation occurring on the island, such that in the event of a future intrusion of magma or the dislocation of the western flank the deviation from the background levels would be accurately assessed. In October 1994 a baseline ground deformation network was established in the central area of the Cumbre Vieja ridge affected by the 1949 faulting, in order to assess if aseismic creep was occurring during the current inter-eruptive period. The faulted area may mark the surface representation of the active precursory slip planes of an impending landslide. If creep continues between eruptive events then failure could not necessarily be solely Linked to magmatic activity and the stability of the western flank could be determined by other topographic and gravitational factors, which would have major implications for the hazard evaluation of the island. The network was established in two stages: firstly an initial small network covering active faults and secondly the expansion to form a broad-scale network encompassing the southern part of the island below the Caldera de Taburiente. The project was conducted in these two stages due to the unavailability of Global Positioning System (GPS) hardware at the start of the project and the requirement of a minimum of three occupations over the fissured area of the ridge to assess the activity of the faults.

The initial network comprised 11 survey stations including two existing Spanish survey pillars, re-occupation of which in 1996 completed the initial baseline survey. For the first set of measurements a Total Station incorporating Electronic Distance Measurement (EDM) and a theodolite was used to measure the slope distance and vertical angle between survey stations. The co-ordinate vector changes recorded reflect changes in the ground surface relative to a fixed survey station (HB07); the field application of this method is accurate to 5mm ± 5ppm. Although the baseline ground deformation network was successfully established, the method used had many limitations. Firstly, vector changes were only determined relative to a single survey station and since they were all located along the apex of the rift it could not be assumed that at any one time all the survey stations would be stable. Secondly, the location of a stable survey station on the Cumbre Vieja ridge is severely Limited by the maximum measurable distance of the EDM method which is Limited to about 2.5km. There are no clear stable Line-of-sight locations suitable for installing survey stations off the ridge, with the distances either being too great or the line-of-sight being restricted by vegetation. The method is also Limited due to the frequent obscuring of the survey stations in cloud, restricting the use of the Total Station as the signals are blocked. The size of the potentially unstable area of the western flank is also problematic; to cover this area using EDM would be logistically unacceptable in terms of the number of survey stations needed and the time it would take to occupy the sites.

The 1997 GPS Campaign

Due to these factors another technique was sought which is not limited by Line-of-sight, distance and the weather. The successful transition to using GPS on the active volcanoes of Etna and Piton de la Fournaise, prompted this technique to be applied on La Palma. GPS is an all-weather surveying system accurate in the field to around 2-4mm + 3-5ppm, since the co-ordinates are calculated by the reception of signals from GPS satellites the line-of-sight between survey stations is no longer required. The transition to this technique enables forward planning of new survey stations in strategic non-line-of-sight locations and since the weather ceases to be provide a problem more reliable daily occupation plans could be devised.

The March 1997 field campaign aimed to re-occupy the EDM ridge network and to complete the broad-scale Cumbre Vieja baseline network which encompasses the fault-bounded Western flank of the Cumbre Vieja. The complete baseline comprises 28 survey stations, providing tight clusters of survey stations around the northern and southern boundaries and at the apex of the sector where the 1949 fault is situated. The survey stations extend past these areas in an effort to identify the boundaries of the sector in the event of future activity. A permanent GPS benchmark on Gran Canaria was used to fix the network, providing absolute rather than relative positioning. Figure 1 shows the locations of the survey stations.

Results and Implications

The results from the EDM surveys and the GPS surveys indicate that distance changes between the survey stations are in the order of 4-l0mm; with changes of 8-l0mm indicating large height differences over long lines. The estimated error for the EDM method is 5mm ± 5ppm. This error value is taken for the GPS data, since although the estimated error for the GPS technique is less, when the two data sets are compared, the greater error is taken.

Expected displacement values for active dyke intrusion are in the magnitude of 500mm and above, and the values for deeper magmatic or tectonic influences are 25mm and above. These values are estimated from the amount of displacement recorded during the 1949 eruption and the background values recorded at Mount Etna when magma is rising in the system. Aseismic creep is estimated to be between 0.8-1.5mm and can only be detected over a number of years. However, evidence of such long term movement can also detected in the surrounding geomorphology, but this has not been recorded at the Cumbre Vieja. In the absence of any evidence for a recent magmatic intrusion the data indicate that the steep western flank of the Cumbre Vieja is stable during the current inter-eruptive period and that future movement would most likely be restricted to intrusive or eruptive periods.

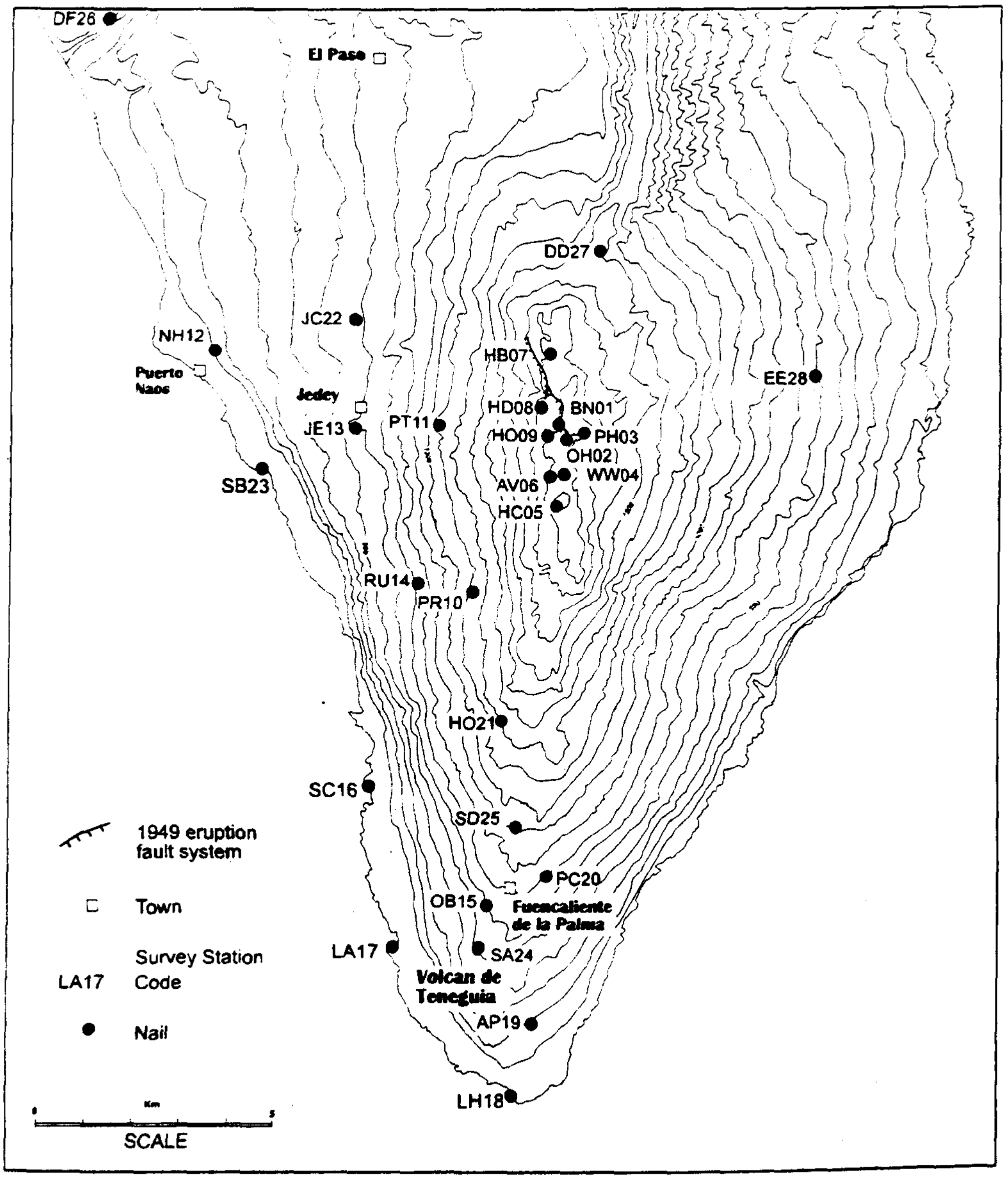

Figure 1. The GPS network of La Palma

The 1990-95 eruption of Unzen volcano, Japan, and its products

Yasuo Miyabuchi and Akira Shimizu
Kyushu Research Center, Forestry and Forest Products Research Institute, Kurokami 4-11-16, Kumamoto 860, Japan.

Abstract

After lying in repose for 198 years, Unzen volcano in western Kyushu, southwestern Japan, began a series of eruptions on November 17, 1990. Activity started with phreatic eruptions, but shifted to magmatic eruptions characterised by lava dome growth and pyroclastic flows triggered by dome collapse in May 1991. A pyroclastic flow on June 3, 1991, killed 43 people, including French and American volcanologists. Repeated pyroclastic flows and debris flows distributed a vast quantity of sediment that devastated much of the area surrounding Unzen volcano. Major deformation of the lava dome has not occurred since 1995, indicating that supply of magma to the dome has stopped.

Although the risk of major pyroclastic flows may now be reduced, the risk of small rockfalls and debris flows persists. We examined the distribution and characteristic features of deposits associated with its eruption. The products of the 1990-95 eruption were divided into pyroclastic flows, ash-cloud surges and pyroclastic fall deposits.

Dome-collapse type pyroclastic flow (block-and-ash flow) deposits, which buried valleys and broadly altered original landforms, are massive, poorly-sorted, and matrix supported with large boulders. Ash-cloud surge deposits, which spread over the surroundings of pyroclastic flow deposits, consist mainly of well sorted sand and are fines-depleted. Pyroclastic fall (co-ignimbrite ash fall) deposits are fine grained and well sorted. Grain size characteristics suggest that particles finer than 2 mm are elutriated from pyroclastic flows into ash-cloud surges and that particles finer than 1/2 mm (mainly 1/16 mm) are further segregated, forming a more dilute ash cloud that results in fall deposits.

Intrinsic and scattering seismic wave attenuation in the Canary Islands

J. A. Canas[1], A. Ugalde[2], L. G. Pujades[2], J. C. Carracedo[3], V. Soler[3] and M.J. Blanco[4]

[1]Instituto Geográfico Nacional. General Ibañez de Ibero, 3, 28003-Madrid, Spain.
[2]Universitat Politécnica de Cataluña. Jordi Girona Salgado, s/n, Modul D-2 08034-Barcelona, Spain.
[3]Estación Volcanológica de Canarias (CSIC). Apdo. de Correos, 195 38206-La Laguna (Tenerife), Spain.
[4]Instituto Geográfico Nacional (Servicio Regional en Canarias). Av. Anaga, 35, p. 11 38001-Sta. Cruz de Tenerife, Spain.

The Canary Islands volcanic archipielago consist of seven main islands located in the continental African edge. This border is expected to have a stable behaviour, but the passive African margin is an atypical case of passive edges since it possesses strong tectonic and magmatic processes. A significant research on the archipielago has been performed during the last 25 years. A number of geophysical and geological studies have been carried out (e. g., Carracedo, 1984; Mézcua et al., 1991); however, due to the important geodynamical complexity of the region, different theories have been proposed for the genesis of the islands, and a unique model has not been generally accepted, although a hotspot origin hypothesis is gaining wide acceptance. The geophysical studies carried out in this region were directed toward obtaining seismic reflection data, gravity and magnetics. Canas et al. (1995) used the first high quality seismic recordings from earthquakes in the archipielago to determine the attenuation of seismic energy using coda waves.

Coda waves constitute a powerful tool for the calculation of seismic wave attenuation in the Earth's lithosphere. Total anelastic attenuation of a body wave can be characterized by the inverse quality factor, Q,-', defined as the fraction of energy lost during a wave cycle. Two effects contribute to the observed total attenuation, as expressed by the equation: $Q_t^{-1} = Q_i^{-1} + Q_s^{-1}$ (Dainty, 1981). Q_i^{-1} represents the intrinsic bsorption, caused by the conversion of seismic energy into heat, and Q_s^{-1} is the scattering attenuation, due to the redistribution of energy that occurs when seismic waves interact with the heterogeneities of the medium. Many theoretical studies have been developed to model the coda shape. In the present study, the Multiple Lapse Time Window Analysis (MLTWA) (Hoshiba et al., 1991), which gives the temporal change of seismic energy while the wave is propagating, is applied to seismic data from the Canary Islands. The following assumptions are made: scattering is multiple and isotropic, the distribution of scatterers is uniform and the coda is only composed of S to S scattered waves. Two attenuation parameters are calculated (Wu, 1985): the seismic albedo (B_0), defined as the dimensionless ratio of the scattering loss to total attenuation, and the inverse of the extinction length (L_e^{-1}) that is the inverse of the distance (in km) over which the primary S wave energy is decreased by e-' . The multiple lapse time window method allows one to estimate B_0 and L_e^{-1} by comparing the energy density predicted by the multiple isotropic scattering theory, in space and time, with the observations. The inverse quality factors Q_t^{-1}, Q_i^{-1} and Q_s^{-1} are then calculated through the expressions (Hoshiba et al., 1991): $Q_t^{-1} = L_e^{-1} v/\omega$; $Q_i^{-1} = (1 - B_0)\, Q_t^{-1}$; and $Q_s^{-1} = B_0 Q_t^{-1}$. The shear wave velocity v in this region has been considered to be 4 km·s^{-1}.

Seismic activity in the Canary Islands is moderate, with earthquake magnitudes usually less than 5. Volcanic and tectonic earthquakes occur in this area, with the EN-SW reverse fault between the islands of Tenerife and Gran Canaria (Mézcua et al., 1991) being the source of almost all the tectonic seismic activity of the region since 1989.

A total of 87 seismograms with hipocentral distances less than 216 km, magnitudes ranging from 2 to 4 and focal depths less than 54 km were available in this study. They were recorded by the Canarian Seismic Network, that belongs to the *Red Sismológica Nacional of the Instituto Geográfico*

Nacional. This network is composed of 6 short-period seismographic stations that are distributed along the entire archipielago.

The MLTWA method was applied to the Canarian seismic data for two hypocentral distance ranges: from 0 to 80 k and from 0 to 140 km. Results show that in both cases and for all the studied frequency bands (1-2 Hz; 2-4 Hz; 6-8 Hz and 8-10 Hz) intrinsic absorption dominates. The low albedos found in the region indicate the low degree of heterogeneity in the Canarian lithosphere at the scale length of the studied frequencies. On the other hand, the degree of frequency dependence of the attenuation parameters is strong in all cases.

We have found that total attenuation is strong and greater than expected for this oldest part of the Atlantic Ocean, where the seismic activity is very moderate. Moreover, the intrinsic absorption dominates over the scattering attenuation at short and long hypocentral distances. Concluding, the geological evidence relative to a hotspot type islands and the high degree of attenuation, with a dominance of the intrinsic absorption over the scattering effect for all the studied frequency bands and hypocentral distance ranges, favour the hypothesis that a strong astenosphere is present in the region.

Monitoring flank instabilities at active volcanoes

W. J. McGuire[1] and J. L. Moss[2]

[1] *Greig Fester Centre for Hazard Research, University College London, Gower Street, London WC1E 6BT*

[2] *Centre for Volcanic Research, Department of Geography & Geology, Cheltenham & Gloucester College of Higher Education, Cheltenham GL50 4AZ*

Large, long-lived, polygenetic volcanoes are dynamically-evolving structures, the life cycles of which are characteristically punctuated by episodes of flank instability and subsequent collapse. Flank instabilities typically develop in response to one or more of a range of agencies, including magma emplacement, the overloading or oversteepening of slopes, and peripheral erosion. Similarly, the lateral collapse of a destabilised volcano may occur in response to a number of triggers of which seismogenic (e.g. tectonic or volcanic earthquakes) or magmagenic (e.g. pore-pressure changes due to magma intrusion) are common. Flank failure, usually resulting in debris-avalanche formation appears to occur several times a century on Earth, and similar behaviour is recognised at volcanoes on Mars and Venus. The frequency and potential scale of flank-collapse events and associated eruptive activity has major implications for the development of monitoring and hazard mitigation strategies at susceptible volcanoes, which must address the possibility of future collapse events which may be ten times greater than that which occurred at Mount St. Helens in 1980.

In common with many other coastal and island volcanic edifices, Mount Etna (Sicily), Piton de la Fournaise (Reunion Island, Indian Ocean), and La Palma (Canary Islands) reveal evidence of both past lateral collapse and contemporary flank instability. Monitoring current flank deformation using electronic distance measurement (EDM) and Global Positioning System (GPS) techniques permits the characteristics of extant movements to be determined and provides important information on the destabilising factors which may have contributed to earlier lateral-collapse events.

At Mount Etna, pre-historic flank collapse is evidenced by the Valle del Bove, a broadly U-shaped depression (7km long by 5km wide and 1km deep) excavated from the eastern flank of the volcano. The Valle del Bove sits within the intersection of NE- and SE-oriented active rift zones, suggesting that progressive displacement associated with repeated dyking is the likely cause of destabilisation and collapse, probably facilitated by seaward tilting of the sub-volcanic basement. Dyke-induced rifting continues to play a role in flank destabilisation at Etna. Geodetic monitoring of four rifting events on the upper southern flanks of the volcano, during 1983, 1985, 1989, and 1991, has revealed a total of 5m lateral displacement along a 2km rim-segment of the Valle del Bove. Dyke accommodation during these rifting events is locally accomplished by this movement, which is destabilising the upper part of a 1km high cliff wall and leading to periodic rock falls along this part of the Valle del Bove rim. Further dyking events in this sector of the volcano are likely to lead to increased instability, particularly as dyke paths are constrained to parallel the sector collapse rim as a result of the tensional stress regime generated in the vicinity of the depression.

On a larger scale, and over a longer time-frame, persistent dyke-related rifting along three well-defined zones in the eastern half of the volcano are related to the mobility and downslope movement of a 30km wide sector of the edifice together with the immediately underlying basement. By means of a positive feedback mechanism, this sliding process itself appears to permit further preferential dyke emplacement in the eastern part of the edifice by effectively reducing lithostatic pressures in this area. Visual observations, seismic studies, and GPS monitoring of ground displacements, suggest that accommodation of this slower, larger-scale displacement of the eastern flank occurs - at least partly - through displacements along active faults. Such accommodation of accumulating, dyke-induced strains is essential if the rift zones are to continue operating over a long period of time.

Piton de la Fournaise has also experienced lateral sliding of a major sector of its flanks, as evidenced by the large, seaward-facing depression of the Grand Bruli, by eastward-dipping fault scarps known as Ramparts and by hummocky submarine terrain adjacent to the Grand Bruli exit. As at Etna, the mobile sector bisects the apex of two intersecting rift zones, suggesting that repeated and persistent magma emplacement over a long period of time have contributed to past flank instability and failure. Again like Etna, the rift zones at Piton de la Fournaise are aligned NE and SE, and constitute preferential paths for shallow dyke intrusions which feed eruptions either within the Enclos caldera or, more rarely, on the lower flanks of the volcano.

Two infra-red EDM networks were established on the rift zones in 1993 and remeasured in 1994 and 1995; in the latter case using the GPS method. Both networks contain common stations which allow them to be linked to a broader GPS deformation network operated by the IPG (Paris). Lateral displacements determined over the period of the three surveys are small (generally centimetric) and apparently incoherent. It is proposed that observed movements result from local block movement, and that extensional behaviour is temporally constrained to dyke-induced rifting episodes. Significant lateral displacements perpendicular to the rift-zone axes are expected to occur during the next dyke emplacement event.

At La Palma, destabilisation of the western flank of the steep-sided Cumbre Vieja volcano is evidenced by the existence of a seaward-facing normal fault system which developed during the course of the 1949 eruption. Concern about continued movements along the fault - precursive to a major lateral collapse event - led to the establishment of an infra-red EDM network across the faults in 1994 and its remeasurement in 1996. Observed lateral displacements were within the expected error-range of the method, and the faults were determined to be currently inactive. Expansion and upgrading of the network in 1997 using GPS, confirmed the current absence of movement. The future emplacement of fresh magma into the edifice is likely, however, to provide optimum conditions for fault reactivation, during which time observations of ground displacement may prove critical in constraining the likelihood, extent, and nature of a resulting flank collapse event.

CIVIL PROTECTION IN THE FACE OF VOLCANIC CRISES IN SPAIN

José Sansón Cerrato
Superior Technical Expert on Natural and Anthropic Risks
Civil Protection Unit. Government Delegation in the Canaries

VOLCANIC RISK IN THE CANARIES

In Spain, the only region with volcanically active areas is the Canary Archipelago, which throughout its history (five centuries) has suffered about one dozen eruptive crises, two of them in the last fifty years (1949 and 1971, La Palma Island). Although the effects of the historic eruptions have not been too destructive, the volcanic activity has a great devastating potential on these islands, keeping in mind their high density of population and the fragility of their infrastructures.

In spite of this, very little attention is given by society to this kind of phenomena in the Canaries. On one hand, the population's perception of this risk is extremely poor as a consequence of the short historical memory, and on the other, the Canary public administrations tend to be more worried about facing other kinds of hazards which materialize every year more or less severely, such as forest fires or sea and wind storms or torrential rains.

Although on the whole, the volcanic hazard in the Canaries can be classified as moderate as compared to that existing in other regions on the planet, the Archipelago's population surpassing 2.6 million people if we sum up the inhabitants included in the census and the average floating population owing to tourism (8 million in 1996 with an average stay of 8.8 days), settled in a surface area of 7,446 km^2, implies a sufficiently high risk index so that the Spanish Civil Protection systems consider it to be among those that must obligatorily have specific emergency plans.

REGULATION ON VOLCANIC RISK PLANNING

The Civil Protection Act 2/1985 of January 21st, foresees the elaboration of Special Plans for certain risks. These Plans were later specified in the Basic Civil Protection Regulation of 1992 (R.D. 407/1992) and defined as instruments elaborated to meet the specific hazards whose nature requires a technical-scientific methodology appropriate for each of them. These Special Plans must be elaborated according to the requirements of the pertinent Basic Guidelines approved by the national Government.

Among others, the mentioned Basic Regulation regarded the volcanic risk as the object of Civil Protection planning, which can be interpreted as a special sensitiveness of the public authorities towards this kind of phenomena which, although they have not caused victims nor important losses in Spain in the past, must have the guarantee in future of an appropriate answer to a future crisis.

Civil Protection's Basic Planning Guidelines for Volcanic Risk were approved by the Council of Ministers on January 19th, 1996. These Guidelines establish the minimum requisites that must be met by Emergency Plans in presence of this risk, to the purposes of foreseeing a national model allowing the coordination and joint action of the different services and administrations involved in case of volcanic crisis.

CONTROL OF VOLCANIC PHENOMENA IN THE CANARIES

In Spain there is no body officially in charge of controlling the volcanic activity as there indeed is, nevertheless, for seismic activity entrusted to the National Geographic Institute or for meteorological phenomena with the National Meteorological Institute. To remedy this deficiency, the Basic Guidelines provide for the constitution of a Scientific Committee on Volcanic Phenomena Evaluation and Control which, made up of representatives of the Higher Council on Scientific Research (CSIC), National Geographic Institute (IGN), Civil Protection Administration, the Autonomous Community of the Canaries and experts who can be appointed by the CSIC, will have the following functions:

Selection of valid precursors
Evaluation of the information obtained from the instrument networks
Formulation of eruptive crisis forecasts
Setting up of optimum methodologies for surveillance and control of volcanic phenomena
Recommendation of mitigation measures in case of eruptive crises

This Scientific Committee was established on March 26th, 1996 and will hold ordinary meetings annually and special ones when the activity registered could be interpreted as the threat of a new volcanic crisis.

EMERGENCY PLANS IN THE FACE OF VOLCANIC PHENOMENA IN THE CANARIES

As forerunners of the Civil Protection planning for this kind of risks, there are two Emergency Plans elaborated by the State Government of both provinces (Las Palmas and Sta. Cruz de Tenerife) in 1982 and 1989, documents which lack scientific grounds coinciding with current knowledge on Canary volcanism and that were drawn up in accordance with the new distribution of competencies of the Spanish Civil Protection.

According to this distribution of competencies existing for Civil Protection in Spain, the Basic Guidelines foresee for the Canary Islands the elaboration of two Emergency Plans for volcanic hazard: a national one and another by the Autonomous Community. However, far from involving an overlapping of functions, it is provided that they be drawn up under the principle of complementarity. Only if the emergency were declared of national interest, will the national Plan be used as an instrument coordinating the whole of the Administrations. In that case, the direction will be assumed by a Directive Committee.

It is the national Plan's function to provide coordination and support plans in emergencies declared to be of national interest or in support of the Autonomous Community's Plan (evacuation, supplies, shelter and social aid, action on volcanic agents and information coordination), the control and information system of volcanic phenomena, and to have available a national data base of mobilizable means and resources. On its behalf, the Autonomous Community's Plan will establish the zoning of the territory according to its volcanic danger, implement an information system for the population, set up specialized Action Groups (Reconaissance, sanitary aid, rescue and life saving, security, communications, information, etc.) and guarantee the operativeness of the procedures, their updating and maintenance.

Although the National Emergency Plan for Volcanic Risk has virtually begun its existence with the constitution of the Scientific Committee on Volcanic Phenomena Evaluation and Control, a body integrated in said Plan, in the near future the work leading to its complete redaction will be undertaken. Regarding the Autonomous Community's Plan, it is foreseeable that it will also be completed in the near future.

BIBLIOGRAPHY

Sansón Cerrato, J. (1996). *Civil Protection in the face of volcanic eruption risk.* Volcanic Risk. Casa de Los Volcanes Series. Lanzarote Island Gov't., pgs. 197-217.

Sansón Cerrato, J. (1995). *Volcanic Risk and Civil Protection in Spain.* Civil Protection, Administration Magazine, No.26, pgs. 7-15.

Basic Guidelines of Civil Protection Planning for Volcanic Hazard. Resolution of February 21st, 1996, Secretary of State of the Interior on the publication of the Council of Ministers Decision approving same. (BOE No.55 of March 4th, 1996).

AUTOR INDEX

AUTHOR INDEX

NOTES